DOCTOR OF PHILOSOPHY

Regulation of the oncogenic PIM1 kinase by SUMOylation

Iyer, R. Sumanth

Award date:
2016

Regulation of the oncogenic PIM1 kinase by SUMOylation

By

R. Sumanth Iyer

A thesis submitted for the degree of

Doctor of Philosophy

University of Dundee

September 2016

Chapter-2 Materials and Methods

List of figures

Chapter-1

Chapter-2

Chapter-3

Chapter-4

Chapter-5

List of tables

Acknowledgements

I use this space to wholeheartedly thank everyone who helped me either scientifically or morally during the past four years of my research. Firstly, a BIG thank you to my supervisor Dr. David Meek for his valuable research guidance, unceasing support and giving me the opportunity to work in his laboratory. I am very thankful to him for giving me the freedom to work on an 'off the wall' project idea I had, which could have ended up being disastrous, but thankfully culminated into this thesis.

I am indebted to Prof. Ron Hay, and particularly Ellis Jaffray from his lab, without whom this project would not have been possible. I am very thankful for their expert guidance on SUMO, very generous sharing of reagents and allowing me to perform SUMOylation experiments in their lab.

Enormous thanks must also go to Dr. Frances Fuller-Pace for her encouragement, making me feel like an extended part of her lab, and for always being there to clear my doubts, be it scientific or non-scientific. I would also like to thank past and present members of the Fuller-Pace lab – Adam, Judit, Celine and Sam for their technical expertise and sharing their wealth of knowledge with me, which has definitely made me a better scientist. Thank you to members of the Meek lab for being great lab mates, specially Anna for sharing our joint frustrations for experiments that refused to work for no good reason. Many thanks to past and present students and research groups in the CRC and JWCC for their suggestions, sharing reagents and making the environment very friendly.

Special thanks to Lois Paton for her advice both in and out of the lab and for helping me get through thesis writing. More importantly, thank you for being an amazing friend throughout my PhD and keeping me grounded under stressful situations. I would also like to express my sincere gratitude to Medical Research Scotland and CXR Biosciences for their financial contribution and useful feedback. This acknowledgement would be incomplete without the mention of the unwavering support of my parents and my brother. I would not be here without their efforts and sacrifices, so thank you.

Declaration

I hereby declare that the following thesis is based on the results of investigation conducted by myself, and that this thesis is of my own composition. Work other than my own is clearly indicated in the text by reference to the relevant researchers or their publications. This dissertation has not in whole, or in part, been previously submitted for any higher degree in any other institution.

R. Sumanth Iyer September 2016

I hereby declare that R. Sumanth Iyer has carried out his research under my supervision and has fulfilled the relevant Ordinance and Regulations of the University of Dundee, so he is qualified to submit the following thesis in application for the degree of Doctor of Philosophy.

Dr. David Meek September 2016

Abbreviations

ABC	ATP binding cassette
ABL	Abelson tyrosine kinase
Ac	Acetylation
AKT	Ak strain thyoma viral oncogene homolog
ALL	Acute lymphoblastic leukemia
AML	Acute myeloid leukemia
AMPK	AMP-activated kinase
APC	Anaphase promoting complex
APL	Acute promyelocytic leukemia
APS	Ammonium persulfate
AR	Androgen receptor
ARE	AUUUA-rich element
ARF	Alternate reading frame protein
ASK1	Apoptosis signalling kinase 1
ATP	Adenosine triphosphate
BAD	Bcl2-associated death promoter
BARD	BRCA1 associated RING domain protein 1
BCL	B-cell lymphoma
BCR	Breakpoint cluster region
BLM	Bloom syndromw RecQ like helicase
BMAL1	Brain and muscle ARNT-like 1
BRCA1	Breast cancer 1
BRD4	Bromodomain containing 4
BSA	Bovine serum albumin
BZEL	BTB-ZF protein expressed in effector lymphocytes
C-terminal	Carboxy terminal

C. elegans	*Caenorhabditis elegans*
CDC	Cell division cycle
CDK	Cyclin dependent kinase
CDKN	Cyclin dependent kinase inhibitor
cDNA	Complementary DNA
CHX	Cycloheximide
CLL	Chronic lymphocytic leukemia
CML	Chronic myelogenous leukemia
CMV	Cytomegalovirus
COT	Cancer osaka thyroid oncogene
CRISPR	Clustered regularly interspaced short palindromic Repeats
CXCR4	C-X-C motif chemokine receptor 4
DAPI	4,6-Diamidino-2-phenylindole
DAXX	Death domain associated protein
DeSI	DeSUMOylating isopeptidase
DMEM	Dulbecco's modified Eagle's media
DMSO	Dimethyl sulfoxide
DNA	Deoxyribonucleic Acid
dNTPs	Deoxyribunucleotide triphosphate
DTT	Dithiothreitol
DUB	Deubiquitinase
E. coli	*Escherichia coli*
ECL	Enhanced Chemiluminescence
EDTA	Ethylenediamine tetraacetic acid
eIF4E/B	Eukaryotic translation initiation factor 4E/B
EGFR	Epidermal growth factor receptor

ELK1	ETS domain containing protein
ERK	Extracellular signal regulated kinase
ERα	Estrogen receptor alpha
Eμ	Immunoglobulin enhancer element
ETK	Epithelial and endothelial tyrosine kinase
FAT10	Human leukocyte antigen-F adjacent transcript 10
FBS	Fetal bovine serum
FLT3	Fms-like tyrosine kinase 3
FOS	FBJ murine osteosarcoma viral oncogene homolog
FOSL1	Fos-like antigen 1
FOXO	Forkhead box
g	Gram
xg	Times gravity (or Relative centrifugal force)
G-CSF	Granulocyte colony stimulation factor
GATA1	GATA binding protein 2
GFP	Green fluorescent protein
GM-CSF	Granulocyte macrophage colony stimulation factor
GSK3	Glycogen synthase kinase 3
GST	Glutathione S-transferase
GTP	Guanosine triphosphate
HCSM	Hydrophobic cluster SUMO motif
HDAC	Histone deacetylase
HEPES	4-(2-hydroxyethyl)-1-piperazineethanesulfonic acid
HIF	Hypoxia inducible factor
HOXA9	Homoebox protein 9
HP1	Heterchromatin 1
hr	Hour(s)

HSF1	Heat shock factor 1
HSP	Heat shock protein
ID2	Inhibitor of DNA binding 2
IGF1	Insulin growth factor receptor 1
IKK	IκB kinase
IL	Interleukin
IRS1	Insulin receptor substrate 1
ISG15	Interferon-stimulated gene 15
JAK	Janus kinase
JNK	c-Jun N-terminal kinase
K-RAS	Kirsten-Rat sarcoma viral oncogene homolog
kDa	Kilodalton
KID1	Kinase induced by depolarisation 1
KLF5	Kruppel-like factor 5
LB	Lura Bertani (also Lysogeny Broth)
LTR	Long terminal repeat
M	Molar
MAPK	Mitogen activated protein kinase
MARK4	Microtubule affinity regulating kinase 4
MBD1	Methyl-CpG binding domain protein 1
MCAF1	MBD1 containing chromatin associated factor 1
MCL	Myeloid cell leukemia
MDC1	Mediator of DNA checkpoint 1
MDM2	Mouse double minute minute 2
Me	Methylation
MEF	Mouse embryonic fibroblasts
MEF2	Myocyte enhancer factor 2

MEK	Mitogen activated protein kinase kinase
MES	3(N-morpholino)ethanesulfonic acid
Min	Minute(s)
miR	Micro RNA
ml	Millilitre
mLST8	mTOR associated protein 8
mM	Millimolar
MMLV	Moloney murine leukemia virus
MOF	Orthologue of Drosophila males absent on the first
MOPS	3(N-morpholino)propanesulfonic acid
mRNA	Messenger RNA
mTOR	Mammalian target of rapamycin
MWCO	Molecuar weight cut-off
MYB	Avian myeloblastosis viral oncogene homolog
MYC	Myelocytomatosis viral oncogene homolog
MT	Mutant
siNS	Non-targeting siRNA
N-terminal	Amino terminal
NC	Nitrocellulose
NDSM	Negatively charged amino acid dependent SUMO motif
NEDD8	Neural precursor cell expressed developmentally downregulated 8
NEMO	NF-kappa B essential modulator
NES	Nuclear export signal
NF-κB	Nuclear factor kappa-B
NFATc1	Nuclear factor of activated T cell cytoplasmic 1
ng	Nanogram

nM	Nanomolar
Ni^{2+}-NTA	Nickel nitrilotriacetic acid
NLS	Nuclear localisation signal
NO	Nitric oxide
NRF2	Nuclear factor erythroid 2 p45-related 2
NSE2	Non-structural maintenance of chromosomes element 2
NUAK1	NUAK family SNF1-like kinase 1
NuMA	Nuclear mitotic apparatus
OD	Optical density
P-TEFb	Positive transcription elongation factor b
p70 S6K	Ribosomal protein S6 kinase
PAGE	Polyacrylamide gel electrophoresis
PARP	Poly ADP-ribose polymerase
PBS	Phosphate buffered saline
PC2	Polycomb protein 2
PCNA	Proliferating cell nuclear antigen
PCR	Polymerase Chain Reaction
PDSM	Phosphorylation dependent SUMO motif
PIAS	Protein inactivator of activated STATs
PIM	Proviral integration site for murine leukemia virus
PIN1	Peptidyl-prolyl isomerase NIMA-interacting 1
PKA	Protein kinase A
PKC	Protein kinase C
PLK1	Polo-like kinase 1
PMA	Phorbol 12-myristate 13-acetate
PML	Promyelocytic leukemia
POL	Polymerase

PP2A	Protein phosphatase 2A
PPAR	Peroxisome proliferator activated receptor
PRAS40	Proline-rich Akt substrate 40
PTM	Post-translational modification
RanBP2	Ran binding protein 2
RanGAP1	Ran GTP-ase activating protein 1
RARα	Retinoic acid receptor alpha
RE	Response Element
RING	Really interesting new gene
RNA	Ribonucleic acid
RNF	RING finger protein
ROS	Reactive oxygen species
rpm	Revolutions per minute
RPMI	Roswell Park Memorial Institute
RT	Room temperature
RTK	Receptor tyrosine kinase
RUNX	Runt related transcription factor
SAE	SUMO activating enzyme
SAP	Scaffold attachment factor-A/B, Acinus and PIAS
SDS	Sodium dodecyl sulfate
SENP	SUMO protease
SIM	SUMO interaction motif
siRNA	Small-interfering RNA
Ski	Sloan-Kettering Institute protein
SKP2	S-phase kinase associated protein 2
SMC	Structural maintenance of chromosome
SnoN	Ski related oncogene

SOC	Super optimal broth with catabolite repression
SOCS	Suppresor of cytokine signalling
SP100	Speckled protein 100 kDa
SP-RING	Siz-PIAS RING
SRC	Sarcoma viral oncogene
STAT	Signal transducer and activator of transcription
STUbL	SUMO targeted ubiquitin ligase
SUMO	Small ubiquitin-like modifier
SV40	Simian virus 40
TAE	Tris acetate EDTA
Tak1	TGFβ activated kinase 1
TBST	Tris buffered saline Tween
TC45	T cell protein tyrosine phosphatase
TDG	Thymine DNA glycosylase
TEL	ETS translocation variant 6
TEMED	Tetramethylethylenediamine
Tet	Tetracycline
TGFβ	Transforming growth factor beta
TKO	Triple knockout
TNFα	Tumour necrosis factor alpha
TOPORS	TOP1 binding arginine/serine rich protein
TPA	2-O-tetradecanoyl-phorbol-13-acetate
TR2	Testicular receptor 2
TRAF6	TNF receptor associated factor 6
TRIM	Tripartite motif containing
Tris	Tris(hydroxymethyl)aminomethane
TRKA	Transforming kinase receptor A

TSC1/2	Tuberous sclerosis complex 1/2
TTP	Tristetraprolin
U	Units of enzyme
Ub	Ubiquitin
UBC	Ubiquitin conjugating
UBD	Ubiquitin binding domain
Ubl	Ubiquitin-like
UPS	Ubiquitin proteasome system
USPL1	Ubiquitin specific peptidase like 1
UTR	Untranslated region
UV	Ultraviolet
V	Volts
v/v	Volume to volume
w/v	Weight to volume
WT	Wild-type
XPC	Xeroderma pigmentosum
YFP	Yellow fluorescent protein
ZIMP	Zinc finger MIZ-type containing
βME	Beta mercaptoethanol
µg	Microgram
µl	Microlitre
µM	Micromolar
^{0}C	Degree Celcius

Amino acids and their corresponding codons

Amino Acid	Letter	DNA Codon
Isoleucine	I	ATT, ATC, ATA
Leucine	L	CTT, CTC, CTA, CTG, TTA, TTG
Valine	V	GTT, GTC, GTA, GTG
Phenylalanine	F	TTT, TTC
Methionine	M	ATG
Cysteine	C	TGT, TGC
Alanine	A	GCT, GCC, GCA, GCG
Glycine	G	GGT, GGC, GGA, GGG
Proline	P	CCT, CCC, CCA, CCG
Threonine	T	ACT, ACC, ACA, ACG
Serine	S	TCT, TCC, TCA, TCG, AGT, AGC
Tyrosine	Y	TAT, TAC
Tryptophan	W	TGG
Glutamine	Q	CAA, CAG
Asparagine	N	AAT, AAC
Histidine	H	CAT, CAC
Glutamic acid	E	GAA, GAG
Aspartic acid	D	GAT, GAC
Lysine	K	AAA, AAG
Arginine	R	CGT, CGC, CGA, CGG, AGA, AGG
Stop codons	-	TAA, TAG, TGA

where, A (adenine), T (thymine), G (guanine), C (cytosine) are DNA bases

Summary

PIM1 (Proviral Integration site for Murine leukemia virus site 1) is a constitutively active serine/threonine protein kinase that is induced physiologically by the JAK-STAT and NF-κB pathways. PIM1 mediates survival signalling in cells, and contributes to the development of resistance towards chemotherapy and radiotherapy. It is also overexpressed in a wide range of haematological malignancies, and in solid tumours of the prostate, colon, breast and lung among others, which makes it an attractive drug target. However, the mechanisms regulating PIM1 kinase activity and protein levels have remained largely unexplored.

Based on PIM1 protein sequence analysis, I identified the presence of a conserved motif ($IK_{169}DE_{171}$) in the active site of PIM1 that is recognised by the Small ubiquitin-like modifier (SUMO). By site-directed mutagenesis of individual lysine residues in PIM1, I showed that PIM1 is covalently modified by SUMO at the consensus K169 site, and also at a second promiscuous site. However, the K169R mutant only abolished SUMOylation at one site, but the E171A mutant abolished SUMOylation at both sites. I also showed that members of the Protein inactivator of activated STATs (PIAS) family could act as E3 SUMO ligases for PIM1. SUMOylated PIM1 showed higher protein kinase activity *in vitro* when Histone H3.3 was used a substrate, indicating that SUMOylation might enhance PIM1 kinase activity. Interestingly, both K169R and E171A displayed substrate specificity *in vitro* and when expressed in cells, suggesting that SUMOylation might govern PIM1 substrate specificity under certain contexts.

Cycloheximide chase analysis revealed that both K169R and K67M (catalytically inactive) mutants of PIM1 were less stable. This can be attributed to the observation that the K169R mutant is incapable of undergoing autophosphorylation similar to the K67M mutant of PIM1. This indicates that both K169 and K67 residues are critical for the intrinsic kinase activity, and may not represent SUMO-specific effects. On the other hand, autophosphorylation of E171A was unaffected, which makes it a better mutant to study effect of SUMOylation on PIM1. The E171A mutant was

more stable than wild-type PIM1 in the cycloheximide assay suggesting that SUMOylation destabilises PIM1. In support of this result, the E171A mutant also showed reduced levels of ubiquitination. Furthermore, expression of RNF4 (a polySUMO targeted E3 ubiquitin ligase) led to degradation of SUMOylated PIM1, and siRNA knockdown of RNF4 increased endogenous levels of PIM1 in cells. Taken together, the data presented here identify a novel mechanism of PIM1 degradation that is, in part, dependent on SUMOylation. SUMOylation of PIM1 also increased PIM1 activity *in vitro* and appears to dictate substrate specificity. Hence, further analysis of this pathway might open avenues for therapeutic intervention.

Chapter 1

Introduction

1.1 The PIM family of oncogenes

Tumorigenesis is a complex multi-step process, which involves activation of oncogenes, and suppression or inactivation of protective tumour suppressor genes, thereby leading to initiation of transformation programme in a cell. The *PIM* family of proto-oncogenes comprises three members named *PIM1*, *PIM2* and *PIM3* encoding serine/threonine protein kinases of approximately 34 kDa of the same name with a broad range of cellular targets. The founding member of this family i.e. *Pim1* was first identified in Moloney Murine leukemia virus (MuLV) induced T-cell lymphomas as a small chromosomal region that frequently displayed proviral insertions associated with transcriptional activation of this gene, hence the name Proviral Integration site for MuLV (Theo Cuypers *et al.*, 1984; Selten *et al.,* 1985). Subsequently *Pim2* was identified as a common proviral integration site in transplanted murine T-cell lymphoma (Breuer *et al.,* 1989). In contrast, *Pim3* was originally identified as Kinase Induced by Depolarisation (*Kid1*) in rat brain cells (Feldman *et al.*, 1998), and later established as a *Pim1* and *2* related kinase overexpressed in lymphomas.

The generation of *Pim* transgenic and knockout mouse models provided interesting information about their oncogenic functions. *Pim1* transgenic mice carrying an upstream immunoglobulin enhancer element (Eμ) and downstream proviral long terminal repeat (LTR) causing increased Pim1 protein expression showed spontaneous development of T-cell lymphomas at low frequency and with long latency showing that Pim1 is a weak oncogene by itself (van Lohuizen *et al.*, 1989). Interestingly, it was observed that a large number of MuLV-induced lymphomas with proviral integrations near *Myc* also showed integration in *Pim1*

locus leading to a speculation that Pim1 might cooperate with Myc in the transformation process (Theo Cuypers *et al.*, 1984). Transgenic mice coexpressing both *Eμ-Pim1* and *Eμ-Myc* succumbed to lymphomas prenatally confirming their strong oncogenic partnership (Verbeek *et al.*, 1991). As second evidence, transgenic mice carrying *Eμ-Myc* but deficient in either *Pim1* or all three *Pim* showed delayed development of lymphomas suggesting that levels of Pim expression might be rate-limiting for Myc-driven tumours. Furthermore, the dependency of Myc on Pim expression was demonstrated in transgenic *Eμ-Myc* mice deficient in *Pim1* where almost 90% tumours showed proviral integrations near *Pim2* locus, and in *Eμ-Myc Pim1:Pim2* double knockout mice where *Pim3* was activated by insertional mutagenesis (van der Lugt *et al.*, 1995; Mikkers *et al.*, 2002). This also indicates that members of *Pim* family have overlapping functions and can compensate for each other in tumorigenesis.

1.2 Structural features of PIM kinases

The human *PIM* genes are located at different chromosomal locations (*PIM1* on chr.6p21.2, *PIM2* on chr.Xp11.23 and *PIM3* on chr.22q13.33) each containing six exons and five introns with large 5' and 3' untranslated regions (UTRs). *PIM* mRNAs are particularly unique in that the 3'UTR contains five copies of the RNA destabilising AUUUA motif, leading to a short half-time in the cells (Saris *et al*., 1991; Wingett *et al*., 1991). A stem-loop pair sequence called eIF4E sensitivity element is also present in the 3' UTR for specific binding of eukaryotic translation initiation factor (eIF4E), which allows nuclear export of *Pim* transcripts for enhanced translation. The 5' UTR, on the other hand, contains long GC-rich regions making *PIM* mRNAs weak transcripts requiring cap-dependent translation (Hoover *et al.*, 1997; Culjkovic *et al.*, 2006).

PIM1 in both mice and humans encodes two protein isoforms of 34 kDa and 44 kDa arising from two alternate translation initiation sites (Saris, Domen and Berns, 1991). Interestingly, only the 34 kDa PIM1 (or PIM1S) is widely reported and studied. Figure 1.1 shows a general representation of *PIM1* gene products. The human 44 kDa PIM1 (or PIM1L) was identified in prostate cancer cells where it was shown to contribute towards resistance to drugs and chemotherapy (Xie *et al.*, 2006, 2008). Both isoforms show comparable kinase activity, but exhibit differences in localisation and protein stability. The 44 kDa isoform is relatively more stable and is specifically localised to the cell membrane, whereas the 34 kDa isoform is nucleo-cytoplasmic. *PIM2* encodes three protein isoforms while no isoforms are reported for PIM3. Pim kinases are highly evolutionarily conserved showing >90% sequence similarity across

different species. For example humans, cows, dogs, cats, rats, mice, zebrafish and *C. elegans* all contain the 313 amino acid long PIM1. Multiple sequence alignment of human Pim kinases suggest that PIM1 is 67.2% and 79.9% similar to PIM2 and PIM3 respectively, whereas Pim2 and Pim3 are 64.4% similar to each other at the protein level (Figure 1.2).

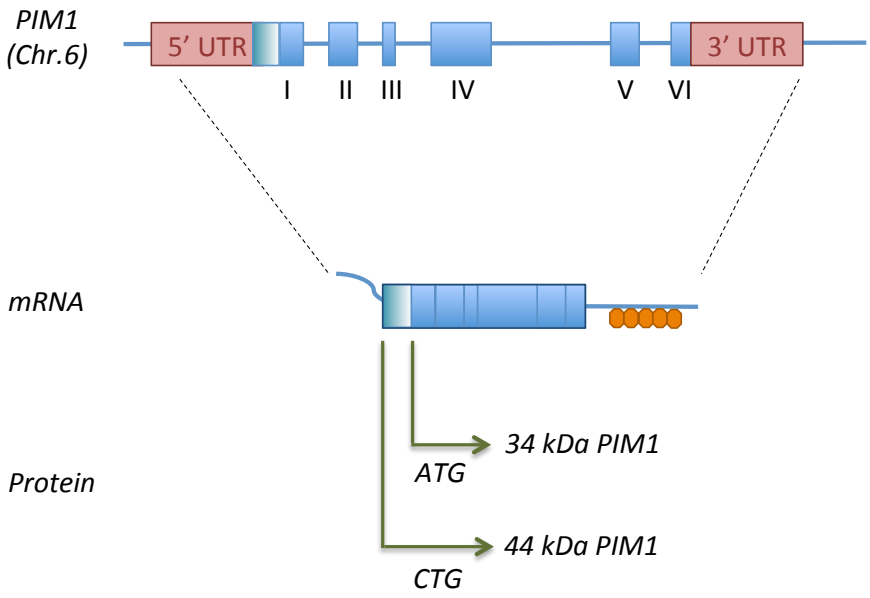

Figure 1.1 *PIM1* gene, transcript and protein

The *PIM1* gene contains 6 exons (blue boxes) and 5 introns with large 5' and 3' untranslated regions (UTRs). The mRNA transcript contains a GC-rich 5' UTR (lariat) and five copies of destabilising AUUUA motif (orange circles) at 3' UTR. ATG is the common or predominant translation site, giving rise to a 34 kDa PIM1 protein. An alternative translation initiation site CTG gives rise to a 44 kDa PIM1 isoform with 90 extra amino acids, which is localised to the cell membrane.

```
PIM1 MLLSKINSLAHLRAAPCNDLH-ATKLAP-GKEKEPLESQYQVGPLLGSGGFGSVYSGIRV
PIM2 MLTK------PLQGPPAPPG--TPTPPPGGKDREAFEAEYRLGPLLGKGGFGTVFAGHRL
PIM3 MLLSKFGSLAHLCGPGGVDHLPVKILQPAKADKESFEKAYQVGAVLGSGGFGTVYAGSRI

PIM1 SDNLPVAIKHVEKDRISDWGELPNGTRVPMEVVLLKKVS--SGFSGVIRLLDWFERPDSF
PIM2 TDRLQVAIKVIPRNRVLGWSPLSDSVTCPLEVALLWKVGAGGGHPGVIRLLDWFETQEGF
PIM3 ADGLPVAVKHVVKERVTEWGSLG-GATVPLEVVLLRKVGAAGGARGVIRLLDWFERPDGF

PIM1 VLILERPEPVQDLFDFITERGALQEELARSFFWQVLEAVRHCHNCGVLHRDIKDENILID
PIM2 MLVLERPLPAQDLFDYITEKGPLGEGPSRCFFGQVVAAIQHCHSRGVVHRDIKDENILID
PIM3 LLVLERPEPAQDLFDFITERGALDEPLARRFFAQVLAAVRHCHSCGVVHRDIKDENLLVD

PIM1 LNRGELKLIDFGSGALLKDTVYTDFDGTRVYSPPEWIRYHRYHGRSAAVWSLGILLYDMV
PIM2 LRRGCAKLIDFGSGALLHDEPYTDFDGTRVYSPPEWISRHQYHALPATVWSLGILLYDMV
PIM3 LRSGELKLIDFGSGALLKDTVYTDFDGTRVYSPPEWIRYHRYHGRSATVWSLGVLLYDMV

PIM1 CGDIPFEHDEEIIRGQVFFRQRVSSECQHLIRWCLALRPSDRPTFEEIQNHPWMQDVLLP
PIM2 CGDIPFERDQEILEAELHFPAHVSPDCCALIRRCLAPKPSSRPSLEEILLDPWMQTPAED
PIM3 CGDIPFEQDEEILRGRLLFRRRVSPECQQLIRWCLSLRPSERPSLDQIAAHPWMLGADGG

PIM1 -QETAEIHLHSLSPGPSK--------- 313
Pim2 VPLNPS----KGGPAPLAWSLLP---- 311
Pim3 VPESCDLRLCTLDPDDVASTTSSSESL 326
```

Figure 1.2 Protein sequence alignment of PIM kinase family members

Multiple sequence alignment of PIM kinases was performed using Clustal Omega software. The sequences for alignment were retrieved from Ensembl genome browser. The accession numbers for PIM1, PIM2 and PIM3 proteins are ENST00000373509, ENST00000376509 and ENST00000360612 respectively. Identical residues are shown in red and the hinge region is highlighted in grey.

Several groups have crystallised PIM1 in complex with nucleotide analogs or small molecule ATP-competitive inhibitors revealing distinctive conformational features of PIM proteins (Bullock *et al.*, 2005; Jacobs *et al.*, 2005; Kumar *et al.*, 2005; Qian *et al.*, 2005). Unlike most protein kinases, PIM kinases are constitutively active and do not require any phosphorylation events for the activation of their kinase activity. Structurally, they adopt the typical two-lobe kinase fold structure with a hinge region (residues 121-126) joining the N- and C-terminal lobular domains. The PIM kinases also share the consensus hinge region sequence of ERPXPX consisting of proline-123 and proline-125 (non-hydrogen bond donor) residues (Figure 1.2), which is not seen in any other kinases known so far. The presence of two proline residues in the hinge region is rather surprising since a proline residue is incapable of forming the conventional hydrogen bonds with the adenine of ATP, which is crucial for maintaining kinases in their active conformation. They also lack the salt bridge between Lys169, a conserved residue in kinases, and the nucleotide phosphate group of ATP. Most notably, the conformation of hinge region in PIM1 produces a wider and larger ATP binding pocket than other kinases. The active conformation of PIM kinases is suggested to be stabilised by two main forces i.e. the salt bridge and hydrogen bond between Arg166 and Asp200, and hydrophobic clusters between the activation loop and catalytic loop of the protein (Qian *et al.*, 2005). The unique structure of PIM1 (Figure 1.3) thus allows us to design highly specific and potent inhibitors of PIM kinases for the treatment of malignancies.

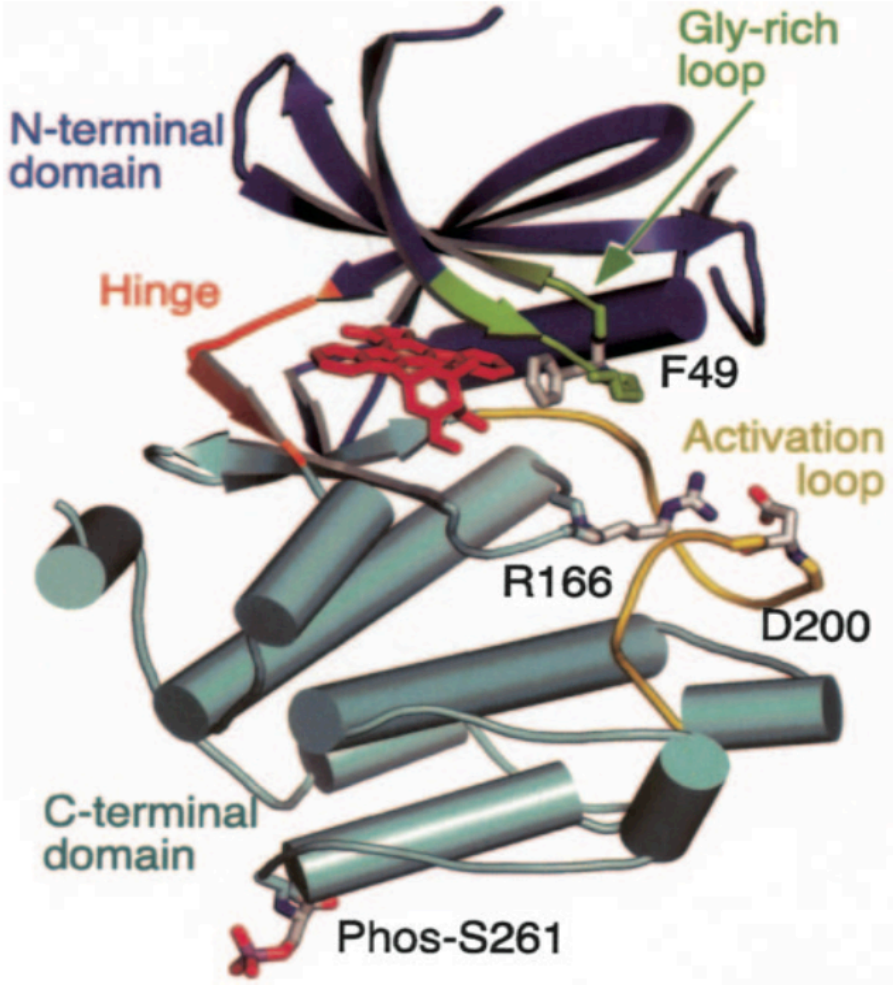

Figure 1.3 Crystal structure of PIM1 with Staurosporine

The structure is shown with β-sheets as arrows and α-helices as cylinders. The N-terminal domain (dark blue) is shown with the glycine rich loop drawn in green. The hinge connecting the two domains is shown in orange. The C-terminal domain is shown in light blue and the activation loop in yellow. The salt-bridge stabilising the active conformation of the activation loop is formed by residues Asp200 and Arg166 drawn as grey carbon-atoms. The autophosphorylation site (S261) was suggested to be an artefact of expression in *E. coli*. The inhibitor staurosporine in red, is shown in the active site of PIM1 (Jacobs *et al.*, 2005).

1.3 Regulation of PIM1

PIM kinases are broadly expressed, although at varying levels, in haematopoietic, neuronal, vascular smooth muscle, cardiomyocyte, endothelial and epithelial cell lineages and in embryonic stem cells (Nawijn *et al*., 2011). Given that PIM kinases are constitutively active and lack regulatory domains, it is conceivable that their enzymatic activity is regulated by their overall protein level in a cell (Shay *et al.*, 2005). PIM kinase activity is largely regulated at the transcriptional level and via protein stabilisation. *PIM* genes display features of early response genes that are induced primarily, although not exclusively, by activation of transcription factors downstream of growth factor signalling pathways such as the Janus kinase-signal transducer and activator of transcription (JAK-STAT) pathway and nuclear factor-κB (NF-κB) pathways. Because PIM kinases show high structural similarity and exhibit overlapping functions (as discussed later), the regulation of only PIM1 has been studied in great detail.

1.3.1 Transcriptional regulation

The JAK-STAT pathway is activated following cytokine receptor stimulation by interleukins (IL-2, 3, 5, 6, 9 7, 11, 12, 15), interferons (IFN-α, γ) and growth factors such as granulocyte colony-stimulating factor (G-CSF), granulocyte-macrophage (GM)-CSF, prolactin, erythropoietin among others (Blanco-Aparicio *et al.*, 2014). Upon ligand-receptor binding, JAK kinases are activated and catalyse trans-autophosphorylation of their cytoplasmic receptor domain. This generates binding sites for STATs and other signalling proteins.

Phosphorylation of STATs (STAT3, 5) through JAK leads to dimerisation of STAT molecules and subsequent translocation to the nucleus, where they bind directly to *PIM1* promoter and activate its transcription. In addition, PIM1 can negatively regulate the JAK-STAT pathway by interacting with suppressor of cytokine signalling (SOCS1, SOCS3) proteins, which inhibits STAT5 activity (Chen *et al.*, 2002; Peltola *et al.*, 2004).

There are a few noticeable examples where cytokines do not appear to be involved in the upregulation of *PIM1*. For instance, the BCR-ABL fusion protein in chronic myelogenous leukemia (CML) activates STAT5 leading to expression of PIM1 (Nieborowska-Skorska *et al.*, 2002). Also, the constitutively active Fms-like tyrosine kinase 3 (FLT3) oncoprotein expressed in acute myeloid leukemia leads to strong upregulation of PIM1 in cells via STAT5 (Kim *et al.*, 2005). Interestingly, PIM1 appears to maintain the activation of mutant FLT3 by phosphorylating only the mutant receptor protein, and enhancing its binding to chaperones such as Hsp90, thus protecting it from proteasomal degradation (Natarajan *et al.*, 2013a).

CD40 receptor, a member of tumour necrosis factor receptor (TNFR) superfamily, upon activation by CD40 ligand leads to upregulation of PIM1 protein levels, and also kinase activity via the NF-κB pathway in B-cells (Zhu *et al.*, 2002). Other receptors like B-cell receptors that activate NF-κB can also upregulate PIM1 levels in B-cells. Conversely, PIM1 also regulates NF-κB signalling by phosphorylating or stabilising a key component of this pathway - RelA/p65 (Nihira *et al.*, 2010).

A transcription factor called Kruppel-like factor 5 (KLF5) was also shown to induce PIM1 expression in response to DNA damage independently of p53 in HCT116 colon cancer cells. KLF5 is recruited to a Sp1 consensus site on the *PIM1* promoter which activates expression of PIM1, and protects the cells from apoptosis (Zhao *et al.*, 2008). The oncogenic K-Ras signalling also upregulates the expression of PIM1, probably through transcription in pancreatic cancer cells. PIM1 expression in this model served as a marker for K-RAS activity conferring anchorage-independent growth and resistance to radiotherapy (Xu *et al.*, 2011).

A recently published report identified *PIM1* as a target of estrogen-receptor-α (ERα) in MCF7 breast cancer cells (Malinen *et al.*, 2013). *PIM1* expression can also be induced by ERα regulated enhancers located distally from *PIM1* gene in response to estrogen. This highlights the involvement of additional pathways converging to induce *PIM* expression other than JAK-STAT or NF-κB pathways. Similarly HOXA9, a homeodomain transcription factor with roles in embryonic development and haematopoiesis, directly targets *PIM1* at the transcriptional level. HOXA9 binds to a distal region of the *PIM1* promoter such that transcription of *PIM1* is upregulated by its overexpression (Hu *et al.*, 2007). Since a previous study identified that HOXA9 interacts with eIF4E, it was also suggested that HOXA9 might also regulate PIM1 via the eIF4E pathway. However, this idea is still not established. But it is now known that PIM2 can directly phosphorylate eIF4E to increase cap-dependent of itself and other oncogenic proteins (Hammerman *et al.*, 2005).

The role of two large 5' and 3' UTRs in *PIM* mRNA, mentioned earlier, is now becoming clear in post-transcriptional control. The 3' UTR contains two AUUUA-rich elements (ARE1 and ARE2), which enhance the decay of the *PIM1* transcript. Tristetraprolin (TTP) is an ARE-binding protein that can recognise AREs and promote the decay of transcripts. Overexpression of TTP in LNCaP prostate cancer cell was shown to significantly reduce *PIM1* expression levels and growth of cancer cells (Kim *et al.*, 2012). Surprisingly, it was also found that TTP-mediated reduction in p21 (target of PIM1) phosphorylation increased p21 levels, which explains the effect of TTP on cell growth. In another study, the induction of TTP was shown to occur rapidly following mitogenic stimulation of *PIM1* by agents such as 12-O-tetradecanoyl-phorbol-13-acetate (TPA) in various non-haematopoietic cells (Mahat *et al.*, 2012).

HuR (Hu antigen R) is another mRNA-binding protein that binds to the 3'-UTR of *PIM1* during hypoxia, resulting in stabilisation of the transcript in pancreatic cancer cells (Blanco *et al.*, 2015). Finally, various microRNAs (miR) miR1 (Nasser *et al.*, 2008), miR33a (Thomas *et al.*, 2012), miR206 (Zhang *et al.*, 2016), miR328 (Eiring *et al.*, 2010) and miR486-5p (Pang *et al.*, 2014) have been shown to bind *PIM1* 3'UTR, resulting in decreased *PIM1* mRNA levels. Figure 1.4 summarises the transcriptional regulation mechanisms of *PIM1*.

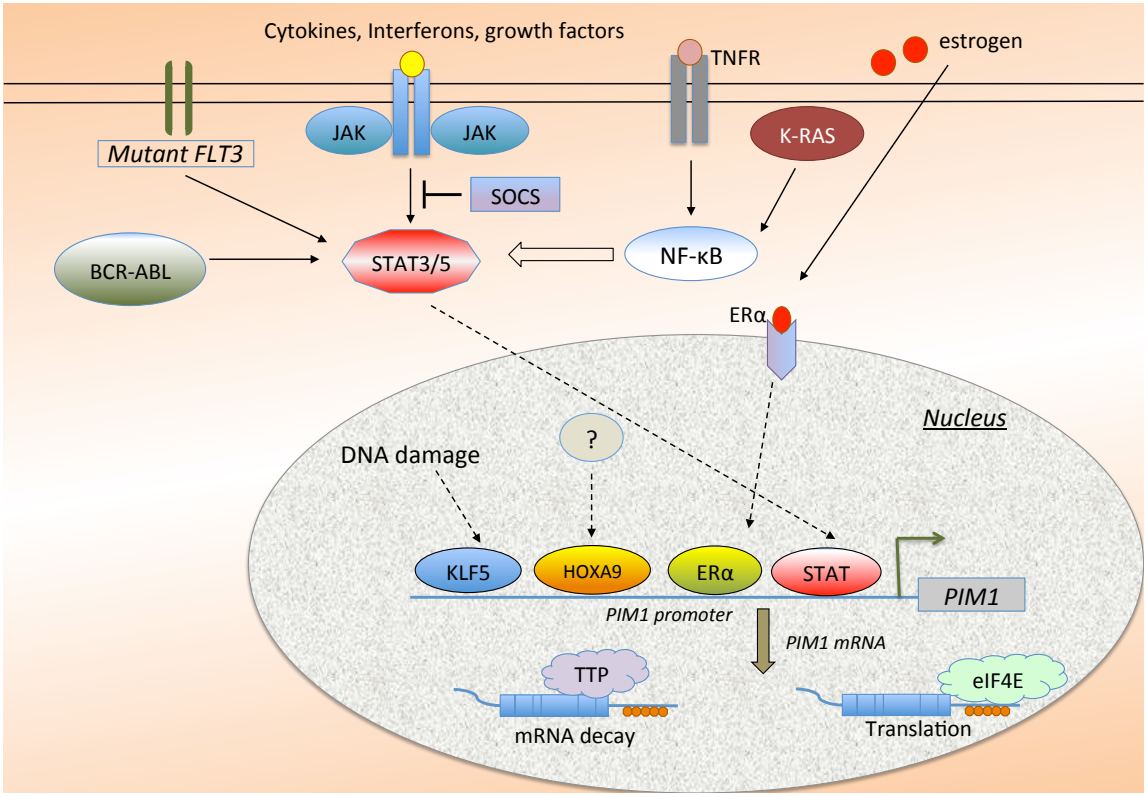

Figure 1.4 Overview of transcriptional regulation of *PIM1*

Stimulation of membrane receptors by cytokines and growth factors stimulates the JAK-STAT and NF-κB pathway, which activates transcription of *PIM1*. Other factors like K-RAS, BCR-ABL, ERα, KLF5 and HOXA9 also stimulate expression of *PIM1* in various tumours. eIF4E leads to enhanced translation of *PIM1* mRNA, while Tristetrasporin (TTP) leads to mRNA decay.

1.3.2 Post-translational regulation

The half-life of PIM1 varies between 5 to 15 minutes in primary cells (Amson *et al.*, 1989) and can be increased up to 100 minutes in certain tumour cells like chronic myelogenous leukemia (CML) cells K562 and BV173 expressing the BCR-ABL fusion protein (Shay *et al.*, 2005). In these cells, heat shock protein HSP90 interacts with and stabilises PIM1 (Mizuno *et al.*, 2001) by protecting it from ubiquitylation and subsequent degradation by the proteasome (Shay *et al.*, 2005). In contrast, binding of ubiquitinated PIM1 with HSP70 favours its degradation via the proteasome (Shay *et al.*, 2005). Treatment with Geldanamycin (Hsp90 inhibitor) prevented accumulation of PIM1 with increased HSP70 binding, while treatment with PS-341 (inhibitor of 26s subunit of the proteasome) caused a build-up of PIM1 with increased HSP90 binding. The dynamics of how HSP70 and HSP90 might change the conformation or affect the shuttling of PIM1 to the proteasome remains a subject of investigation. This study delineates the major post-translational regulation of PIM1 and gives insights into how PIM1 could be efficiently targeted for degradation in cancer therapy.

Hypoxia was recently shown to induce PIM1 expression in solid tumours, but in a hypoxia-inducible factor 1α (HIF1α)-independent manner. Interestingly, inhibition of PIM1 in hypoxic cells resensitised them to chemotherapy, whereas forced expression of PIM1 contributed to resistance to cisplatin, even under normoxia (Chen *et al*., 2009b). Hypoxia leads to nuclear accumulation of HSP90 and decrease in PP2A levels, which prevents degradation of PIM1 by the ubiquitin-proteasome system. Hypoxia was also suggested to promote nuclear

translocation of PIM1, the mechanism and function of which is still not clear (Chen *et al*., 2009a).

Like MYC, all three PIM kinases can be destabilised by the serine/threonine protein phosphatase 2A (PP2A) by dephosphorylation or partial inactivation of kinase activity (Losman *et al.*, 2003; Ma *et al.*, 2007). PP2A can interact with PIM1 substrate through its B56β subunit, as evident by co-immunoprecipitation experiments, and promote its ubiquitination. Knockdown of PP2A or B56β was shown to increase PIM1 stability, and consequently cell viability. On the other hand, overexpression of PP2A led to a decrease in PIM1 protein expression. In one study, it was suggested that PP2A dephosphorylates SOCS1 first to form a complex, which then binds to PIM1 and targets it for degradation (Losman *et al.*, 2003). In another study, it was suggested that the prolyl-isomerise PIN1 binds phosphorylated PIM1 and enhances the ability of PP2A holoenzyme to bind to the complex through the B56β protein (Ma *et al.*, 2007). Figure 1.5 summarises the discussed post-translational regulatory mechanisms of PIM1.

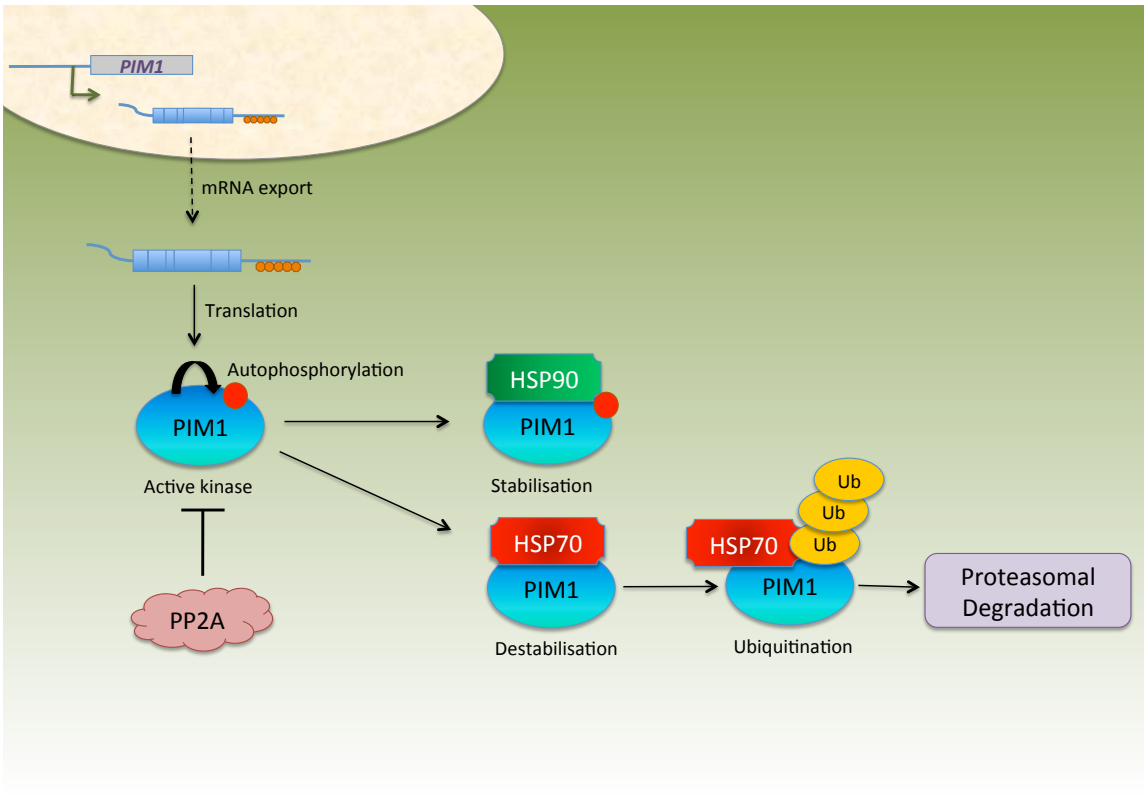

Figure 1.5 Post-translational regulation of PIM1

The PIM1 protein is degraded by the ubiquitin-proteasome system. Binding of PIM1 to HSP90 protects it from proteasomal degradation, while binding to HSP70 promotes degradation. PP2A can directly or indirectly promote destabilisation of PIM1.

1.4 Targets and functions of PIM1 kinase

The serine/threonine kinase PIM mediates its effects by phosphorylating various substrates involved in regulation of important physiological activities such as cell proliferation and cell survival. PIM kinases are largely redundant in function (exceptions exist) with strong affinity for substrates containing the $(K/R)_3$-X-S/T-X consensus motif, where K-lysine, R –arginine, X- is neither a basic nor a large hydrophobic residue, S-serine and T-threonine (Friedmann *et al.*, 1992). However, the sequence K/R-X-R-H-X-S/T, present in Insulin receptor substrate 1 (IRS1) is phosphorylated 20-fold times more efficiently by PIM kinases (Song *et al.*, 2016). Interestingly, the PIM substrate sequence is similar to that of other kinases like AKT, protein kinase A and protein kinase C leading them to share some substrates. Some noteworthy targets of PIM1 and their functions are described below.

1.4.1 Transcriptional regulation

PIM1 regulates the activity of transcriptional co-activator p100 and factors such as c-MYB, RUNX1, RUNX3 and nuclear factor of activated T cell cytoplasmic 1 (NFATc1) by direct phosphorylation (Brault *et al.*, 2010). PIM1 has recently been shown to phosphorylate androgen receptor (AR) at Ser213 leading to transcription of AR-regulated genes in absence of androgen in prostate cancer cell model (Ha *et al.*, 2013).

Both PIM1 and PIM2 increase c-MYC protein stability and transcriptional activity by phosphorylating Ser62 (main site) and Ser329 residues (Zhang *et al.*, 2008a). The dependency of the E-box (CACGTG) transcription factor, c-MYC,

on PIM1 or vice versa in mediating gene transcription and cellular transformation is well known. c-MYC interacts with and recruits PIM1 to E-box located in the enhancer region of c-MYC-target genes *FOSL1* and *ID2* leading to phosphorylation of histone H3 at Ser10 (H3S10) (Zippo *et al.*, 2007). This is followed by the recruitment of 14-3-3 and histone acetyltransferase MOF leading to acetylation (Ac) of Histone 4 at Lys16, which creates a H3K9AcS10P-H4K16Ac nucleosome platform for BRD4 binding. This is ensued by binding of Positive Transcription Elongation Factor b (P-TEFb), which promotes looping of the enhancer towards the promoter causing phosphorylation of RNA POL II on Ser2, and releases the stalled POL II to drive transcription (Zippo *et al.*, 2009). Figure 1.6 illustrates the role of PIM1 in transcription.

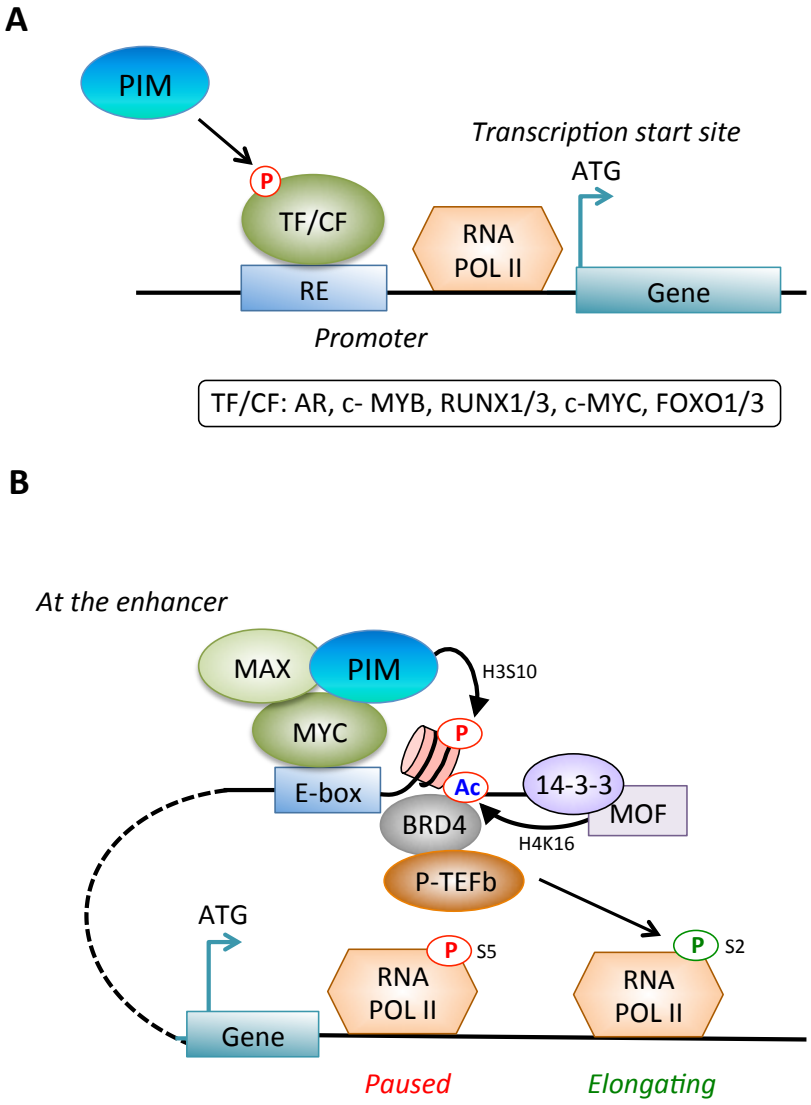

Figure 1.6 Transcriptional regulation by PIM1

(A) PIM1 phosphorylates various transcription factors (TF) and co-factors (CF) on the target gene promoter, and enhances their transcriptional activity. **(B)** PIM1 is recruited to enhancer regions by MYC, where it phosphorylates H3 at S10 and induces concomitant H4K16 acetylation (Ac) by MOF. This is followed by binding of BRD4 and P-TEFb, initiating looping of enhancer towards the promoter (dashed line), phosphorylation of RNA POL II at S2, and release of stalled POL II (Adapted from Nawijn *et al.*, 2011).

1.4.2 Cell Survival

In human malignancies, PIM promotes cell survival as well as chemoresistance through BAD phosphorylation (Figure 1.7)**.** The BCL2-associated death promoter (BAD), a pro-apoptotic member of B-cell lymphoma 2 (BCL2) family, is a target of all PIM kinases (Yan *et al.*, 2003; Aho *et al.*, 2004; Macdonald *et al.*, 2006). Both PIM1 and 2 phosphorylate BAD at Ser112 (predominant site), Ser136 and Ser155, while PIM3 mostly phosphorylates at Ser136 and Ser155. Phosphorylation of Ser112 (a known gate-keeper site for BAD inactivation) by PIM1 disrupts its association with BCL-XL, which promotes anti-apoptotic activity. Furthermore, Ser112 phosphorylated BAD binds to 14-3-3 proteins, and is retained in the cytosol instead of the mitochondria. Interestingly, phosphorylation of BAD at Ser155 has been shown to increase glycolysis in hepatocytes, pancreatic β-cells and B-lymphocytes (Nawijn *et al*., 2011). This suggests a novel role for PIM kinases in glycolysis as they can also phosphorylate BAD at Ser155, however there is no direct evidence to support this hypothesis so far.

PIM1 has also been reported to phosphorylate Apoptosis signalling kinase 1 (ASK1) at Ser83 in H1299 cells upon treatment with hydrogen peroxide. Ser83 phosphorylation of ASK1 impairs the activation of the downstream substrates, JNK and p38, which is associated with decreased Capase3 activation, and reduced cell death (Gu *et al.*, 2009). Other mechanisms of cell survival functions of PIM1 maybe mediated indirectly by c-MYC at the transcriptional or protein levels.

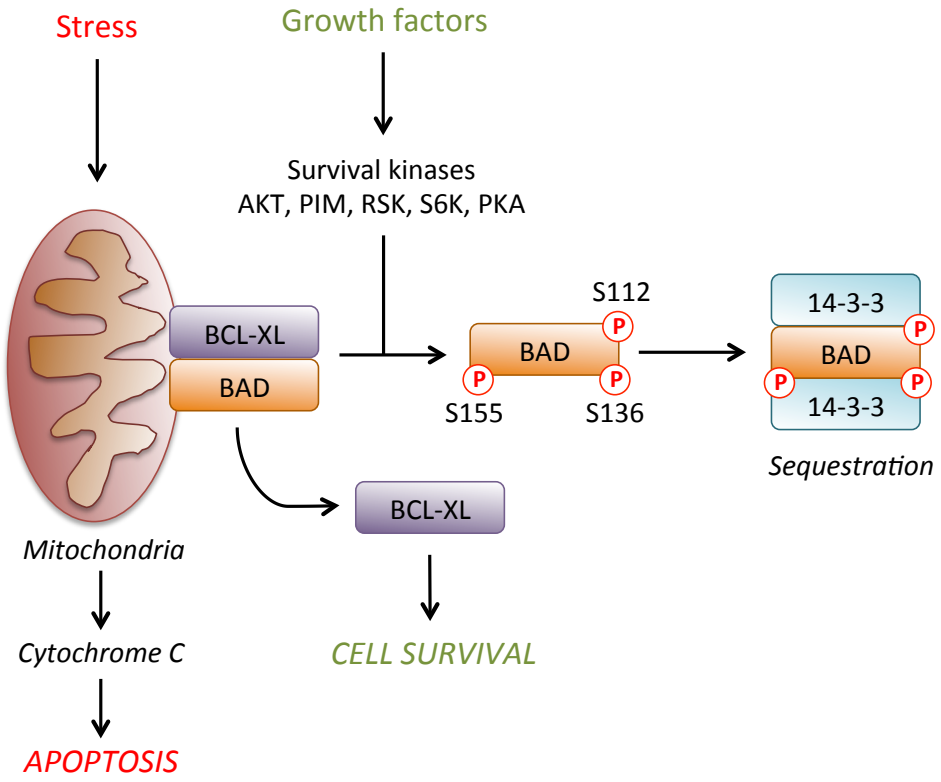

Figure 1.7 Survival signalling through BAD phosphorylation

The pro-apoptotic protein BAD promotes apoptosis by binding and inhibiting BCL-2 family of anti-apoptotic proteins. Growth factors activate a number of downstream kinases such as PIM1, which can then phosphorylate BAD at three sites (S112, S136 and S155) leading to dissociation of BAD from BCL-XL. Phosphorylated BAD is then recognised by 14-3-3 proteins, which sequesters it in the cytoplasm, thereby inhibiting apoptosis.

1.4.3 Cellular senescence

PIM1 can have a tumour suppressive role in certain contexts. Activation of PIM1 has also been shown to induce cellular senescence through the p53 pathway. Our lab previously showed that PIM1 can stabilise MDM2 by phosphorylating it at Ser166 and Ser186 (predominant) residues, (Hogan *et al.*, 2008). Furthermore, co-expression of MDM2 and PIM1 induced expression of p14 (or ARF) in early passage mouse embryonic fibroblasts (MEFs) leading to cellular senescence, as evidenced by an increase in β-galactosidase staining. Consistent with our report, another study showed that PIM1 overexpression inhibited cell growth by inducing senescence in prostate cancer cells (22Rv1) with an intact p53-p21 pathway (Zemskova *et al.*, 2010). Induction of PIM1 by IL6 in human diploid fibroblasts has also been suggested to induce senescence, by direct phosphorylation of heterochromatin protein 1 (HP1γ) at Ser93. PIM1 phosphorylated HP1γ promoted the formation of heterochromatin foci and silencing of proliferative genes (Jin *et al.*, 2014).

1.4.4 Cell Cycle regulation

PIM1 phosphorylates various proteins involved in the regulation of the cell cycle such as CDC25A, p21 and p27 during G1/S, and CDC25C, c-TAK1 during G2/M phase (figure. 6). Phosphorylation by PIM1 enhances the phosphatase activity of CDC25A, a positive G1-specific cell cycle regulator, allowing cells to transit through the G1 and S phases (Mochizuki *et al.*, 1999). Similarly, PIM1 can also enhance CDC25C phosphatase activity by two ways i.e. by direct phosphorylation of CDC25C (Bachmann *et al.*, 2006), and by inactivation of CDC25C-associated kinase 1 (c-Tak1), which is a negative regulator of CDC25C, ensuring cell cycle progression (Bachmann *et al.*, 2004).

PIM mediated phosphorylation of p21 (CDKN1A) at Thr145 was shown to stabilise p21, and result in nuclear to cytoplasmic relocalisation (Wang *et al.*, 2002). Cells expressing p21 in the cytoplasm exhibit increased rate of proliferation, which is most likely due to the dissociation of nuclear p21 from the proliferating cell nuclear antigen (PCNA) (Zhang *et al*., 2007).

PIM1 regulates the expression of p27 at both the transcriptional and protein levels (Morishita *et al.*, 2008). Firstly, phosphorylation of p27 (CDKN1B) at Thr157/Thr198 by PIM1 creates binding sites for 14-3-3 proteins, resulting in the cytoplasmic localisation and subsequent degradation of p27. Secondly, PIM1 also inactivates the forkhead transcription factors FOXO1 and FOXO3, which upregulate the expression of p27 mRNA. Interestingly, PIM1 has also been shown to phosphorylate SKP2 at Thr417, the putative E3 ubiquitin ligase for p27, which stabilises SKP2, enhancing proteasomal degradation of p27 (Cen *et al.*, 2010).

During mitosis, PIM1 has been shown to phosphorylate the nuclear mitotic apparatus (NuMA) protein, and associate in a complex with motor proteins dynein, dynactin and heterochromatin protein 1β (HP1β) maintaining the mitotic apparatus (Bhattacharya *et al.*, 2002). A recent study suggested that both PIM1 and Polo-like kinase 1 (PLK1) colocalise in the centrosome and midbody during mitosis, where they might phosphorylate each other (Van Der Meer *et al.*, 2014). However, the precise role played by PIM1 in the mitotic complex is still unknown. Figure 1.8 illustrates the role of PIM1 in regulating cell cycle.

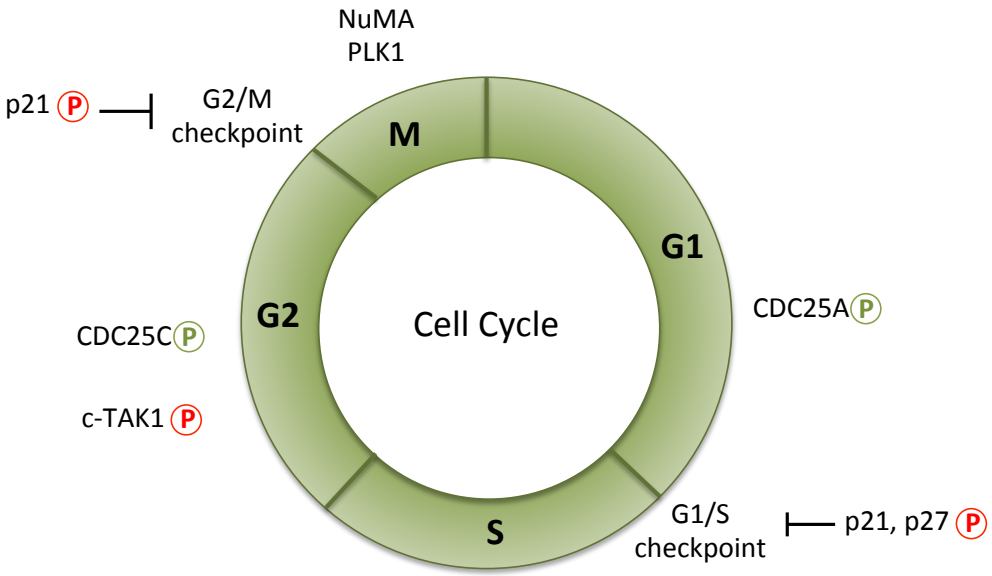

Figure 1.8 Regulation of the cell cycle by PIM1

PIM1 phosphorylates various proteins involved in the regulation of the cell cycle. Phosphorylation of p21, p27 and c-TAK1 by PIM1 (shown in red) inhibits their activity, while phosphorylation of CDC25A and CDC25C by PIM1 (shown in green) promotes their activity to drive the cell cycle.

1.4.5 Translation

PIM kinases have been shown to regulate protein translation by controlling the activity of both upstream and downstream regulators of the mTOR (mammlian target of rapamycin) pathway (Figure 1.9). The mTOR complex 1 (mTORC1) comprises five proteins namely the kinase mTOR, and the regulatory subunits RAPTOR, DEPTOR, mLST8 and PRAS40 (Laplante and Sabatini, 2009). PRAS40 is a negative regulator of mTORC1 kinase activity, and upon phosphorylation at Thr246 by PIM1, dissociates from the mTORC1 complex (Zhang *et al.*, 2009). This increases mTORC1 activity leading to phosphorylation of downstream proteins 4E-BP1 and p70 S6K. Phosphorylation of 4E-BP1 and p70 S6K activates downstream proteins eIF-4E (eukaryotic initiation factor 4E) and eIF-4B (eukaryotic initiation factor 4B) respectively, which initiates cap-dependent translation of weak mRNA transcripts such as *c-MYC, CYCLIN D* and *PIM* itself (Schatz *et al.*, 2011). Interestingly, PIM2 can promote protein translation even in the presence of rapamycin (mTOR inhibitor) or growth factor withdrawal by directly phosphorylating 4E-BP1 and eIF-4E (Hammerman *et al.*, 2005). Moreover, PIM1 can also directly phosphorylate eIF-4B on Ser406 which contributes to the increase in protein levels of the receptor tyrosine kinases such as MET, suggesting that PIM kinases can control protein translation in an mTOR-independent manner (Cen *et al.*, 2014). The mTORC1 complex activity is negatively regulated by the upstream tuberous sclerosis complex (TSC), comprising TSC1 and TSC2. In multiple myeloma cells, PIM2 was shown to directly phosphorylate TSC2 at Ser1798, relieving suppression of mTORC1 signalling and promoting cell proliferation (Lu *et al.*, 2013)

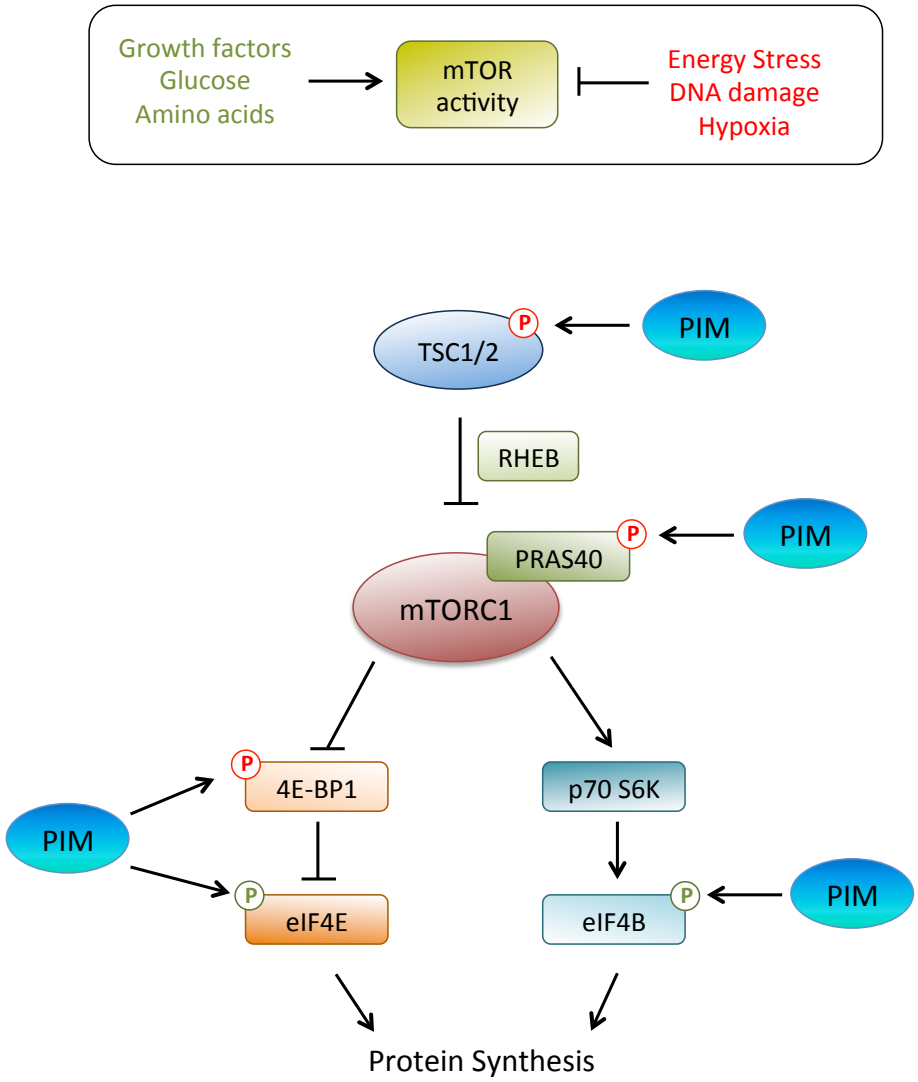

Figure 1.9 Regulation of mTOR pathway by PIM kinases

The mTORC1 complex integrates growth and stress signals, and accordingly activates or inhibits protein synthesis in cells. PIM kinases promote protein synthesis required for cell growth and proliferation by phosphorylating various substrates of the mTOR pathway. Phosphorylations that inhibit activity of a protein are shown in red, whereas activating phosphorylations are shown in green. PIM kinases inhibit the activity of TSC1/2, the upstream negative regulator of mTORC1 complex, in addition to PRAS40. Both of these phosphorylations promote the kinase activity of mTOR. Activated mTOR activates p70 S6K, which further activates eIF4B to promote protein translation. mTOR also inhibits the negative regulator of protein synthesis 4E-BP1 by direct phosphorylation. Inactivation of 4E-BP1 activates eIF4E, which also promote protein translation. Interestingly, PIM kinases can also directly phosphorylate 4E-BP1, eIF4E and eIF4B independently of the mTOR pathway, and upregulate protein translation in cells.

1.4.6 Cellular metabolism

The master sensor of intracellular energy status, AMP-activated kinase (AMPK), is an indirect target of Pim kinases. Under energy stress, AMPK becomes activated, which then phosphorylates RAPTOR and TSC2 in such a way that inhibits the activity of mTORC1, resulting in the inhibition of translation and proliferation (Hardie, 2007). Deletion of all three *Pim* kinases in mouse embryonic fibroblasts (MEF) was shown to cause energy deficiency, reduced cap-dependent translation and persistent AMPK activation. Interestingly, expression of *Pim3* alone rescued the phenotype, most likely due to an increase in *c-Myc* and peroxisome proliferator-activated receptor gamma coactivator 1α (*Pgc1α*) protein levels (Beharry *et al.*, 2010).

Furthermore, PIM kinases also play a crucial role in K-Ras mediated cellular transformation, as *Pim* triple knockout MEF (TKO MEF) undergo cell death in response to activated K-Ras^{G12V} (Song *et al.*, 2014). Activated K-Ras is known to increase the cellular levels of reactive oxygen species (ROS) (Weinberg *et al.*, 2010), and Pim kinases appear to be required for the transcription of genes such as superoxide dismutase (Sod1, 2, 3), glutathione peroxidase 4 (Gpx4), and peroxiredoxin 3 (Prdx3) involved in scavenging ROS. Deletion of all three *Pim* kinases also altered the intracellular concentration of 178 metabolites involved in glycolysis and mitochondrial oxidative phosphorylation. Interestingly, forced expression of c-Myc overcame the defects associated with the deletion of *Pim* kinases, suggesting an important role for Pim kinases in regulating cellular metabolism, in part through c-Myc.

The transcription factor, nuclear factor erythroid 2 p45-related factor 2 (NRF2), is a master regulator of cellular redox homeostasis, and is required for the induction of a battery of cytoprotective genes, in response to environmental stress conditions such as ROS (DeNicola *et al.*, 2011). A recent study indicated that under hypoxic conditions, Pim kinases promote nuclear localisation and activity of NRF2 to induce expression of antioxidant genes (Warfel *et al.*, 2016). Inhibition of PIM kinase in hypoxic cells by small molecular inhibitors prevented nuclear localisation of NRF2 and an increase in intracellular ROS concentrations, which induced cell death. Since there is no direct evidence of PIM kinases phosphorylating NRF2, these effects are most likely mediated by another PIM interacting oncogene.

1.4.7 Some unique functions of PIM2 and PIM3

The regulation of cap-dependent protein translation is one of the important functions of PIM2, as mentioned earlier. In addition, PIM2 activates NF-κB by inducing phosphorylation of COT (Hammerman *et al.*, 2004) which was proposed to be crucial for anti-apoptotic function of PIM2. Interestingly, functions of PIM2 seem to be context-dependent as the 34 kDa isoform promotes G1 arrest by elevating levels of Thr14/Tyr15 phosphorylation of Cyclin-dependent kinase 2 (CDK2), and increases apoptosis in HeLa cells by a pathway involving p73 (Levy *et al.*, 2012).

PIM3 is a positive-regulator of β-catenin dependent transcription and is suggested to regulate β-catenin mRNA, hence a regulator of WNT-pathway (Isaac *et al*., 2011). Only PIM3 was shown to phosphorylate STAT3 at Tyr705 in prostate cancer (DU145) and pancreatic cancer (MiaPaCa2) cell lines. These cells exhibit constitutive expression of the survival protein pSTAT3 via PIM3 contributing to drug resistance (Chang *et al.*, 2010). Interestingly, c-MYC directly induces expression of PIM3 in B-cell lymphomas, and induces survival signalling through phosphorylation of BAD (Forshell *et al.*, 2011). PIM3 was recently found to promote endothelial cell sprouting and migration in response to TNFα. Hence PIM3 plays an important role in TNFα-induced angiogenesis (Yang *et al.*, 2011).

1.5 PIM kinases in cancer and their inhibition

Elevation of PIM1 found in tumours is generally considered not to be due to genetic rearrangement, but a result of dysregulated transcriptional regulation and protein stability, to some extent associated with MYC expression. Mutations in PIM1 are rare, but point mutations have been reported in 43% of B-cell diffuse large cell lymphomas (Pasqualucci *et al.*, 2001). PIM kinases are overexpressed in a significant proportion of haematological malignancies such as acute myeloid leukemia (AML), chronic myelogenous leukemia (CML), mixed-lineage lymphoma (MLL), chronic lymphocytic leukemia (CLL), Mantle-cell lymphoma (MCL) and Burkitt's lymphoma where its expression level correlates with poor prognosis. In case of solid tumours of epithelial origin, PIM is overexpressed in prostate cancer (almost 50%), squamous cell carcinoma, pancreatic cancer, gastric cancer, colorectal cancers and others where its expression correlates with high-tumour grade (Brault *et al.*, 2010; Nawijn *et al*., 2011).

1.5.1 PIM1 and therapeutic resistance

PIM kinases confer therapeutic resistance in multiple cancer types through several mechanisms. The 44 kDa isoform of PIM1 has been shown to negatively affect drug transport into the cells by phosphorylating the P-glycoprotein ATP-binding cassette G2 (ABCG2) at Thr362, promoting its activity. ABC proteins have been shown to function as efflux pumps for chemotherapeutic drugs, and their expression is linked to drug resistance (Xie *et al.*, 2008). PIM1 also phosphorylates ABCB1 at Ser683 which protects it from ubiquitin mediated degradation, as well as enhancing its glycosylation and cell

surface expression (Xie *et al.*, 2010). PIM kinase inhibitors have also been shown to reduce surface expression of ABCB1 and ABCG2 in breast cancer (Natarajan *et al*., 2013b) suggesting that PIM kinase inhibitors can be used to sensitize tumours to chemotherapy.

PIM kinase inhibitors were shown to sensitise cells towards the BCL-2 inhibitor ABT-737, by reducing the expression of MCL1 (Song and Kraft, 2012). A study showed that inhibition of AKT leads to activation of a compensatory survival signalling pathway by upregulating expression of PIM1, and several other receptor tyrosine kinases such as MET. Inhibition of PIM1 not only induced apoptosis but also reduced expression of RTK by downregulation of cap-dependent translation in AKT-inhibitor resistant cells (Cen *et al.*, 2013).

1.5.2 PIM kinase inhibitors in development

PIM kinases are increasingly being considered as targets for new drug development because of their important roles in regulating cancer-specific pathways, such as cell survival, cell cycle progression and cellular migration. The crystal structure of PIM kinases, as discussed earlier, shows the unique mode of ATP binding, which indicates that highly specific inhibitors can be identified for use in cancer therapy with least off-target effect on other kinases. Due to functional redundancy, simultaneous targeting of all three PIM kinases can be advantageous in treating cancer. Supporting this view is the fact that the PIM kinases are dispensable in normal cells as *Pim* triple knockout mice are viable and fertile with normal life span, although they display reduced body size

(Mikkers *et al.*, 2004). This makes PIM kinase a useful target for cancer therapy without affecting the normal tissues severely.

Several small-molecule inhibitors of PIM1/2/3 have been designed, some of which have already undergone clinical trials, or are in preclinical stages at the moment. Most PIM inhibitors are ATP-competitive compounds that form polar interactions with the active site residues in PIM kinases (for example Lys67 in PIM1), and appear to display a common mechanism of action. PIM kinase inhibitors target translation by reducing levels of phospho 4E-BP1 and phospho S6K, and induce apoptosis by reducing phospho BAD, concomitant with a G0/G1 cell cycle arrest (Keane *et al.*, 2015). Some clinically relevant PIM kinase inhibitors have been described below with clinicaltrial.gov identifier numbers (NCT) mentioned in brackets.

a) SGI-1776 (Supergen)

It was the first ATP-competitive inhibitor of PIM kinases to enter Phase I clinical trails for the treatment of refractory prostate cancer, refractory non-Hodgkin's lymphoma and leukemia (NCT00848601 and NCT01239108). Unfortunately, the study had to be terminated prematurely because of cardiotoxicity. It is possible that this side effect could be associated with the reported cardioprotective role of PIM1 (Muraski *et al.*, 2007). The *in vitro* IC50 values for PIM1, 2 and 3 are 7, 363 and 69 nM respectively. Although it is highly selective for Pim kinases, it also inhibits FLT3 and TRKA (Chen *et al.*, 2009c).

b) AZD1208 (Astrazeneca)

It is a second generation ATP-competitive inhibitor of PIM kinases with IC50 values in the low nanomolar range, and a more potent inhibitor than SGI-1776. The sensitivity of AZD1208 in AML cell lines was reported to correlate with PIM1 expression and STAT5 activation (Keeton *et al.*, 2014). It was tested in Phase I clinical trails for the treatment of acute myeloid leukemia (AML) and advanced lymphomas and other solid cancers (NCT01489722 and NCT01588548). Unfortunately, the AML trial had to be terminated and the results have not been made public.

c) LGH447 (Novartis)

It was first tested as a single agent for the treatment of refractory/relapsed multiple myeloma. The results were promising, and a further Phase I/II clinical trial is currently underway as a single agent in AML/high risk myelodysplastic syndromes, and in combination with PI3K inhibitor BYL719 in multiple myeloma (NCT01456689, NCT02160951, NCT02144038 and NCT02078609).

d) LGB321 (Novartis)

It is an ATP-competitive inhibitor of PIM kinases, and structurally related to LGH447 with IC50 in picomolar range. It is currently being tested in preclinical models, where it demonstrated limited activity in solid tumours, but good activity in haematological malignancies, especially against those overexpressing PIM2 (Garcia *et al*., 2014).

e) AZD1897 (Astrazeneca)

This ATP-competitive pan-PIM kinase inhibitor has not yet reached clinical trials. However, published data from *in vitro* and *in vivo* settings showed >50% synergistic cytotoxicity when combined with AKT inhibitor AZD5363 (Meja *et al.*, 2014).

1.6 The Ubiquitin System

Ubiquitination (or ubiquitylation) is the process by which the 76 amino acid long polypeptide, called ubiquitin, is covalently attached to one or more lysine residues in target proteins. This is achieved by an enzymatic cascade consisting three main steps namely activation, conjugation and ligation respectively (Figure 1.10). In the first step, ubiquitin (Ub) is transferred to an Ubiquitin activating enzyme (or E1) in an ATP-dependent manner, to form an E1-Ub complex linked by a thioester bond. In the second step, the activated ubiquitin is transferred to ubiquitin conjugating enzyme (UBC or E2), again forming an E2-Ub thioester bond. In the third step, a Ubiquitin ligase (or E3), which binds both E2-Ub and substrate, allows the formation of an isopeptide bind between the carboxy terminal of ubiquitin and the amino group of a lysine residue on the target protein. Similar to phosphorylation, ubiquitination is also a reversible modification, which can be edited and/or erased by a set of enzymes called Deubiquitinases (or DUBs). Presently, it is estimated that the human proteome contains two E1s (UBA1 and UBA6), about 40 E2s, over 600 E3 ubiquitin ligases and over 90 DUBs (Heride *et al.*, 2014). The discovery of ubiquitin sparked the identification of several ubiquitin-like (Ubl) proteins or modifiers such as NEDD8, SUMO, ISG15, FAT10 and others. All members of the ubiquitin-like family of proteins contain the conserved ubiquitin β-fold, and target the substrate lysine residue by a pathway similar to ubiquitin (Kerscher *et al.*, 2006). Since SUMO is the topic of discussion of this thesis, other ubiquitin-like modifications have not been described here.

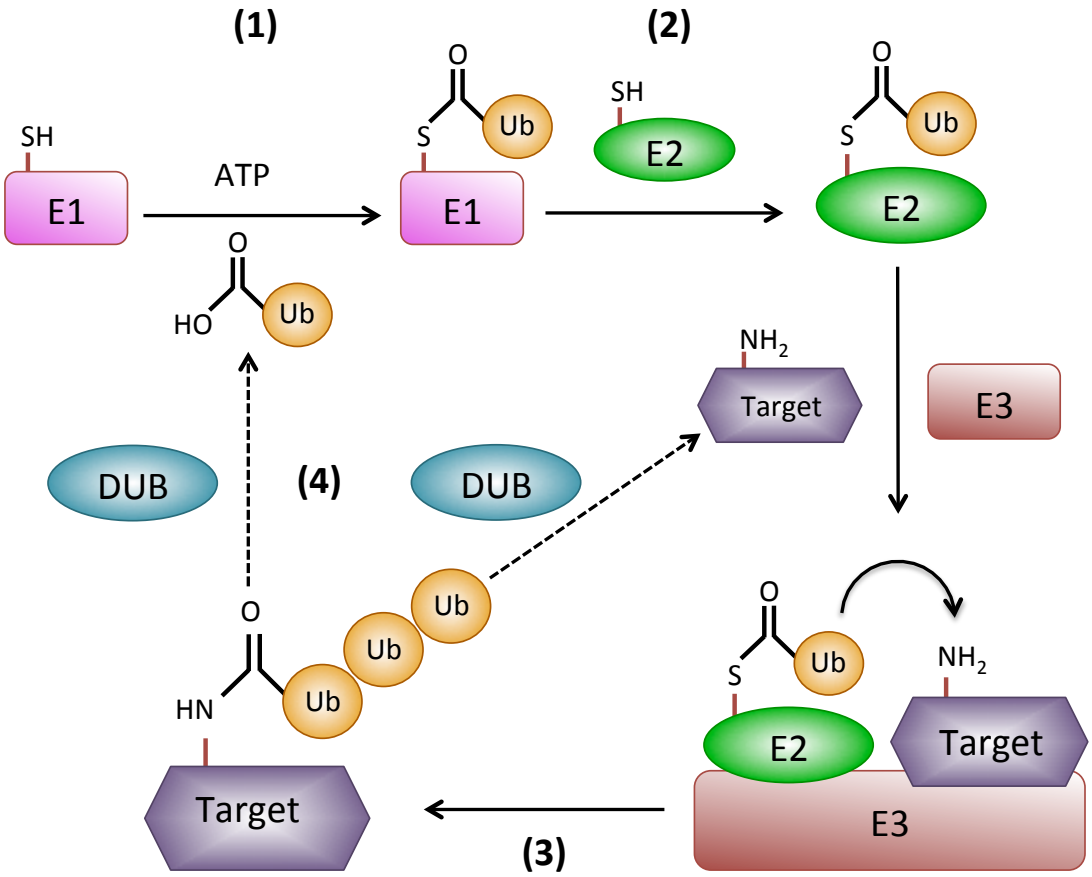

Figure 1.10 The ubiquitin conjugation cycle

The enzymatic cascade describing the covalent attachment of ubiquitin (Ub) to lysine residues of a target protein are shown in this figure. In the first step, a ubiquitin activating enzyme (E1) forms a thioester bond with ubiquitin. In the second step the activated ubiquitin is transferred to a ubiquitin conjugating enzyme E2. In the third step, a ubiquitin E3 ligase binds the ubiquitin loaded E2 and the substrate, and catalyses transfer of ubiquitin to a lysine residue on the target protein. Multiple copies of ubiquitin can be attached to the substrate leading to formation of polyubiquitin chains. Enzymes called deubiquitinating enzymes (DUB) can cleave the ubiquitin chain from the target freeing the ubiquitin and the substrate.

1.6.1 The Ubiquitin code and its functions

The N-terminal methionine (M1) and the seven lysine residues (K6, K11, K27, L29, K33, K48 and K63) present within ubiquitin act as further sites of attachment by ubiquitin itself, thereby allowing formation of polymeric chains (Kulathu and Komander, 2012). The process of addition of polymeric ubiquitin chains to proteins is called polyubiquitination, whereas the addition of a single ubiquitin moiety is called monoubiquitination. About 10% of total histone H2A population in cells is monoubiquitinated. Monoubiquitination of histones is mediated by the Polycomb repressive complex, and is therefore implicated in gene silencing (Wang *et al.*, 2004).

When a ubiquitin chain is formed of the same type of lysine or methionine linkages, it is called a homotypic ubiquitin chain. On the other hand, a heterotypic ubiquitin chain is a chain that is formed of mixed linkages within the same chain. The type of the linked chain formed on a substrate is dictated by a specific combination of the E2 and E3 enzymes involved in the process. Different linkages are conformationally distinct from each other, and therefore serve as binding platforms for other proteins containing ubiquitin binding domains (UBD). This interaction mediates downstream events associated with protein degradation, trafficking and cellular signalling (Komander and Rape, 2012).

The most widely studied and abundant form of homotypic ubiquitin chain found in eukaryotic cells is K48-linked chain. Proteins conjugated with K48-linked ubiquitin chains are specifically recognised and degraded by the 26S

proteasome, which is composed of one 20S core and two 19S regulatory subunits (Chau *et al.*, 1989; Thrower *et al.*, 2000). However, this does not mean that other homotypic linkages are not recognised by the proteasome. For example, in addition to K48-linked chains, K11- and K29-linked conjugates also accumulate when the proteasome is inhibited. Interestingly, K11-linked chains synthesised by the anaphase promoting complex (APC/C) result in the proteolysis of substrates, such as Aurora-B, involved in mitosis (Jin *et al.*, 2008; Matsumoto *et al.*, 2010; Min *et al.*, 2015).

Another well-studied homotypic chain, after K48-linked chain, is K63-linked chain. In contrast to K48-linked chains, K63-linked chains are generally involved in non-proteolytic functions such as DNA repair and cell signalling pathways (Chen and Sun, 2009). K63-linked chains play a crucial role in cytokine (TNFα, IL-1R) induced activation of NF-κB pathway. Binding of cytokines to their membrane receptors initiates the recruitment of multi-protein complexes inside the cell including the E3 ubiquitin ligase TRAF6, which catalyses the formation of K63-linked chains on itself and other substrates. The K63-linked chains act as a scaffold for a protein kinase called TGFβ activated kinase 1 (TAK1), which can then phosphorylate the downstream kinase, IκB kinase (IKK) resulting in its activation (Deng *et al.*, 2000; Wang *et al.*, 2001).

The functions of M1, K6, K27, K29 and K33-linked chains are still largely unknown, but recent discoveries point to a diverse range of functions. In brief, K6-linked chains were shown to recruit a cofactor UBXN1, which inhibits the activity of BRCA1-BARD1 complex during the DNA damage response (Wu-Baer *et al*., 2010). Polyubiquitination of several mitochondrial proteins by K27-linked

chains upon mitochondrial damage was shown to recruit the autophagy adaptor protein p62, leading to clearance of damaged mitochondria by a process called mitophagy (Geisler *et al.*, 2010). Of note, polyubiquitination of kinases such as NUAK1 and MARK4 by K29- and K33-linked chains has been shown to inhibit their kinase activity without leading to degradation (Al-Hakim *et al.*, 2008). Lastly, similar to K63-linked chains, both M1- and M1/K63-hybrid chains are involved in the activation of immune signalling and NF-κB activation (Rahighi *et al.*, 2009; Emmerich *et al.*, 2013). Figure 1.11 illustrates the crystal structure of ubiquitin with internal site of modification, and their associated functions.

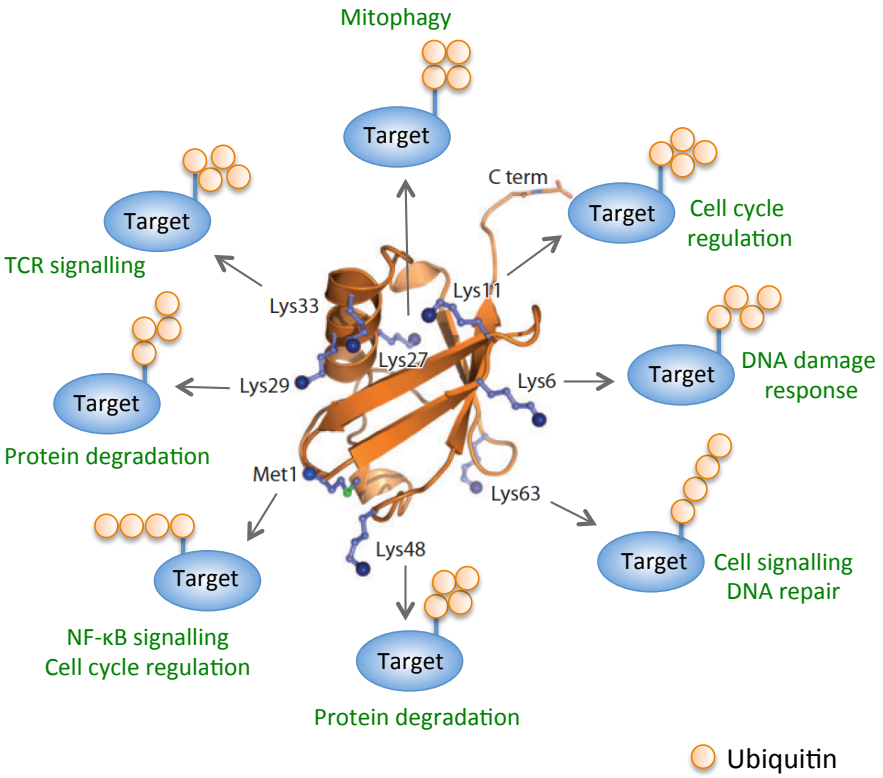

Figure 1.11 Types and function of different ubiquitin linkages

Crystal structure of ubiquitin (centre) showing the seven internal lysine residues and methionine residue. Ubiquitin can form links with other ubiquitin molecules through these residues, leading to formation of different chains. Different conformations of polyubiquitin chains with different linkages are illustrated here. (Adapted from Komander 2009; Komander and Rape 2012)

1.7 Small Ubiquitin-like Modifier (SUMO)

The Small Ubiquitin-like Modifier (SUMO) is a member of the ubiquitin-like family of proteins, which shares similarities with ubiquitin at the structural level (Martin *et al.*, 2007). Figure 1.12 shows similarity between SUMO and ubiquitin at the protein, structural and mechanistic level. Yeast contains only one SUMO isoform called Smt3 (Shen *et al.*, 1996b), while humans express five different SUMO isoforms – SUMO1, SUMO2, SUMO3 (Melchior, 2000), SUMO4 (Owerbach *et al.*, 2005) and SUMO5 (Liang *et al.*, 2016). Only SUMO1, SUMO2 and SUMO3 have been extensively studied in the literature, and described in this thesis. SUMO4 is defective in substrate conjugation as a Pro90 residue in its C-terminal domain prevents its maturation and activation (Owerbach *et al.*, 2005). However, another study showed that SUMO4 is rapidly degraded under 'normal' conditions, but stabilised under stress conditions like starvation. During this period, SUMO4 was suggested to be processed by endogenous hydrolases, and covalently conjugated to its substrates (Guo *et al.*, 2005; Wei *et al.*, 2008). SUMO5 was only recently identified as a regulator of PML nuclear bodies, similar to SUMO2/3 (Liang *et al.*, 2016). Other SUMO5 substrates are yet to be identified.

SUMO2 and SUMO3 differ from each other by only 3 amino acids at their N-terminus, and are functionally indistinguishable. Moreover, the SUMO2 antibody also recognises SUMO3, hence in the literature they are commonly referred to as SUMO2/3. On the other hand, SUMO1 is only 46% identical to SUMO2/3 at the sequence level (Martin *et al.*, 2007). An important feature that distinguishes SUMO2/3 from SUMO1 is its ability to form polymeric chains on

itself. SUMO2/3 contain an internal consensus SUMO modification site, which allows conjugation of other SUMO molecules. SUMO1 does not contain this motif but is still able to recognise the site in SUMO2/3 for SUMO modification. Attachment of SUMO1 to a chain hence results in termination of the poly-SUMO chain (Tatham *et al.*, 2001). A sequence alignment of the protein sequences of SUMO1, SUMO2 and SUMO3 is shown in figure 1.12A.

Although most SUMO targets can be modified by all SUMO isoforms, some substrates display SUMO-paralogue specificity i.e. they can only be modified by one SUMO isoform (Vertegaal *et al.*, 2006). For instance, the Ran GTP-ase Activating Protein 1 (RanGAP1), the first identified SUMO substrate, is modified exclusively by SUMO1 (Matunis *et al.*, 1996; Saitoh and Hinchey, 2000). Although it seems that SUMO2/3 can compensate for the loss of SUMO1 as mice deficient for SUMO1 are viable (Evdokimov *et al.*, 2008; Zhang *et al.*, 2008b). Examples of substrates that are preferentially modified by SUMO2/3 in cells include Topoisomerase II, BMAL1 and p68 (Jacobs *et al.*, 2007; Agostinho *et al.*, 2008; Lee *et al.*, 2008).

Interestingly, there is a larger pool of unconjugated SUMO2/3 in cells than SUMO1, with most of SUMO1 being conjugated to RanGAP1 (Saitoh and Hinchey, 2000). Various studies have shown that the levels of SUMO2/3 modified proteins in a cell increase dramatically in response to stress such as heat shock and DNA damage (Enserink, 2015), suggesting that the free pool of SUMO2/3 is conjugated under physiological conditions of stress.

SUMO1 and SUMO2/3 also display differences in their cellular localisation. In interphase HeLa cells stably expressing YFP-tagged SUMO

isoforms, SUMO1 was found to localise to the nuclear envelope, nucleolus and cytoplasmic foci, whereas SUMO2 and 3 were predominantly present in the nucleoplasm and nuclear bodies. During mitosis, however, SUMO1 was localised to the spindle, and SUMO2/3 to the centromeres and condensed chromosomes (Ayaydin and Dasso, 2004).

A

```
Ub        ----------------------MQIFVKTLTGKTITLEVEPSDTIENVKAKIQDKE
SUMO1     MSDQEAKPSTEDLGDKKEGEYIKLKVIGQDSSEIHFKVKMTTHLKKLKESYCQRQ
SUMO2     MADEKPKE----GVKTENNDHINLKVAGQDGSVVQFKIKRHTPLSKLMKAYCERQ
SUMO3     MSEEKPKE----GVKTE-NDHINLKVAGQDGSVVQFKIKRHTPLSKLMKAYCERQ

Ub        GIPPDQQRLIFAGKQLEDGRTLSDYNIQKESTLHLVLRLRGG 76
SUMO1     GVPMNSLRFLFEGQRIADNHTPKELGMEEEDVIEVYQEQTGG 97
SUMO2     GLSMRQIRFRFDGQPINETDTPAQLEMEDEDTIDVFQQQTGG 93
SUMO3     GLSMRQIRFRFDGQPINETDTPAQLEMEDEDTIDVFQQQTGG 92
```

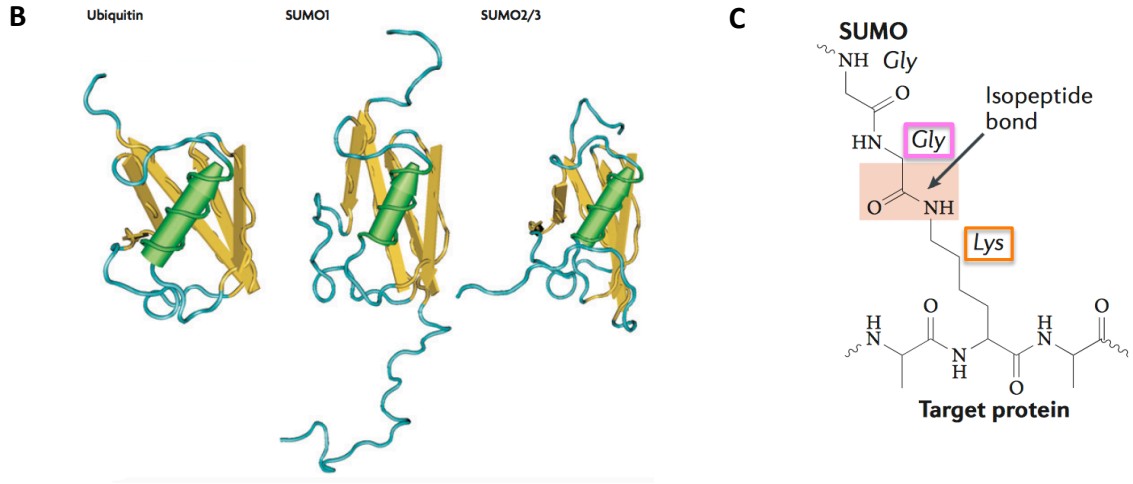

Figure 1.12 Structural relationship between SUMO and ubiquitin

(A) Multiple sequence alignment of ubiquitin, SUMO1, 2 and 3 was performed using Clustal Omega software. The sequences for alignment were retrieved from http://www.ncbi.nlm.nih.gov/protein/. The accession numbers are CAA44911.1 (ubiquitin), NP_001005781.1 (SUMO1), AAH716545.1 (SUMO2) and NP_008867.2 (SUMO3). Identical residues present in all four proteins are shown in red, and identical residues present in all SUMO family members are shown in green. **(B)** Crystal structures of ubiquitin, SUMO1 and SUMO2/3 showing structural similarity (Martin *et al.*, 2007). **(C)** Both ubiquitin and SUMO form a covalent isopeptide bond with the lysine on the target protein through their C-terminal diglycine motif (Hickey *et al.*, 2012).

1.7.1 SUMOylation pathway

SUMOylation is the process by which SUMO1/2/3 is covalently attached to one or more lysine residues on a target protein. The modified lysine residue is usually part of a consensus SUMO motif (described in the next section). The enzymatic process is similar to that of the ubiquitin pathway, with a few exceptions. All SUMO isoforms are synthesised as inactive precursors, which are first cleaved at their C-terminus by SUMO specific proteases (or SENP) to expose the di-glycine motif. A hetero-dimeric SUMO E1 enzyme (SAE1/2) then activates SUMO proteins in an ATP-dependent manner resulting in the formation of a thioester bond between SUMO and SAE1/2. The activated SUMO is then transferred to an E2 SUMO conjugating enzyme UBC9, again through the formation of a thioester bond. Lastly, in the presence of an E3 SUMO ligase, UBC9 catalyses the formation of an isopeptide bond between the di-glycine motif of SUMO and the substrate lysine residue. SUMOylation can also be reversed by the isopeptidase activity of SENP resulting in substrate deSUMOylation (Hay, 2005). The process of SUMOylation has been summarised in figure 1.13.

Modification by SUMO is a highly dynamic process where substrates undergo rapid SUMOylation and equally rapid deconjugation cycles (Hay, 2005). The highly labile nature of this modification is reflected in the co-localisation of the proteins involved in SUMO addition or removal. Additionally, requirement of ATP for activation of SUMO pathway may be a rate-limiting factor affecting steady state levels of SUMOylation. Another long-standing observation in the SUMO system is that only a small proportion of a particular substrate is post-

translationally modified relative to the total pool of the protein in the cell. While this is true in most situations, proteins involved in the DNA repair process (such as PARP and PCNA) are thought to be SUMOylated to a greater degree. Furthermore, almost 100% of all cellular RanGAP1 is modified by SUMO1 in cells. Hence, these observations indicate that the concept of only 1% of a substrate being SUMOylated at a given point (Johnson, 2004) is probably not true, and needs to be validated experimentally. Nevertheless, even a small proportion of SUMOylated protein is still important as mutation of the SUMOylated lysine in substrates can have large functional defects. For example, a small pool of SUMOylated ELK1 is still fully able to repress transcription (Yang *et al*., 2003). In this case, it has been proposed that SUMO is required for initiation but not maintenance of repression. Accordingly, SUMO conjugation may promote recruitment of factors necessary to form a repressive complex. Once the complex is formed and the SUMOylated protein is locked in the complex, SUMO is no longer required and is removed by the action of SENP. This further raises the possibility that a previously SUMOylated protein molecule may have different properties compared to an identical protein molecule with no history of SUMOylation. This has been observed in the case of Thymine-DNA glycosylase (TDG), where SUMOylated TDG shows increased rate of enzymatic activity (Hardeland *et al*., 2002).

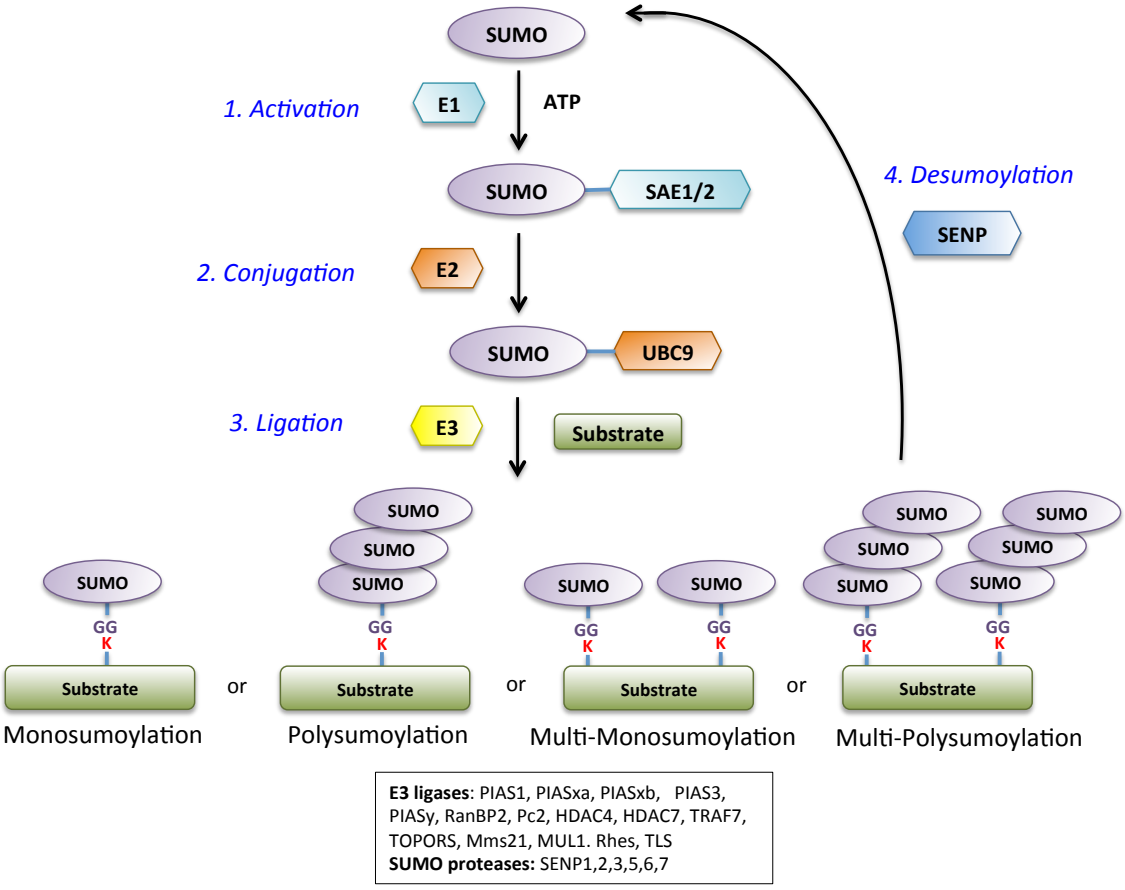

Figure 1.13 The SUMOylation pathway

The mature form of SUMO is first activated by the formation of a thioester bond with the active site of the SUMO E1 enzyme, SAE1/2, in the presence of ATP. The activated SUMO is then passed to the active site of the SUMO E2 enzyme, Ubc9, which then catalyses transfer of SUMO to the target protein, often in the presence of an E3 SUMO ligase. SUMO can be conjugated to one or more lysine on the substrate in a number of ways. SUMO monomers or polymers can be cleaved by the action of SUMO proteases (SENP), releasing free SUMO which can undergo further rounds of conjugation to target proteins.

1.7.2 SUMO Recognition Motifs

Generally, SUMO conjugation of substrates occurs on lysine residues present within a core consensus motif ψKxE/D, where ψ (psi) is a hydrophobic residue (usually I/V/L/F/M) and x is any amino acid (Rodriguez *et al*., 2001). However, not all proteins containing this motif are SUMOylated, and in some cases the modified lysine does not conform to the consensus motif. Therefore, additional residues surrounding the SUMO motif and/or other structural features guiding SUMO modification of a substrate have also been suggested. For example, some proteins such as p53 and IκBα require a nuclear localisation signal for efficient SUMO1 modification in cells (Rodriguez *et al*., 2001). Other proposed SUMO recognition motifs are described below.

1. A patch of acidic residues present immediately downstream of the consensus SUMO-motif ψKxE/Dxx$(E/D)_4$xxxx, termed NDSM (negatively charged amino acid-dependent SUMOylation motif), was suggested to enhance UBC9 binding to ELK1, thus promoting SUMOylation (Yang *et al.*, 2006).
2. In some cases, phosphorylation of residues adjacent to the SUMO-motif was suggested to be required for SUMOylation. This motif ψKxE/DxxSP called PDSM (phosphorylation dependent SUMOylation motif) is present in many transcription factors such as heat-shock factor1 (HSF1), GATA1 and MEF2 (Hietakangas *et al.*, 2006).
3. The voltage gated potassium channel Kv 1.5 protein is SUMOylated at a Synergy control motif, characterised by the consensus sequence [P/G]-x-(0-4)-ψKxE/D-x-(0-4)-[P/G] (Benson *et al.*, 2007).

4. Recently, a mass-spectrometry-based proteomics study identified substrates containing an inverted SUMO-motif E/DxKψ, and another extended SUMO-motif called hydrophobic cluster SUMOylation motif (HCSM). The HCSM motif consists of at least three hydrophobic amino acids preceding the SUMOylated lysine residue, and is involved in SUMOylation of proteins such as RanGAP1, BRD4 and ZBTB1 (Matic *et al.*, 2010).

1.7.3 SAE1/SAE2

The SUMO activating enzyme (SAE), or the SUMO E1 enzyme, is a heterodimer comprising two subunits SAE1 and SAE2 in human (Desterro *et al.*, 1999), or Aos1 and Ubs2 respectively in yeast (Johnson *et al.*, 1997). Structurally, SAE1 resembles the N terminus, and SAE2 the C terminus of a ubiquitin E1 enzyme UBA1 (Gong *et al.*, 1999). While both SAE1 and SAE2 contain a nuclear localisation signal (NLS), only SAE2 contains the ubiquitin-like (UbL) domain that interacts with SUMO1 (Lois and Lima, 2005). Mechanistically, the SUMO E1 activates SUMO and transfers it to the SUMO E2 enzyme Ubc9. This is achieved in three steps. Firstly, SAE1/2 binds ATP and magnesium, and catalyses adenylation of the C-terminal di-glycine motif of SUMO1. This adenylated glycine in SUMO is then attacked by an active site cysteine (Cys173) present in SAE2 resulting in the release of AMP and formation of the SUMO E1-SUMO thioester bond. Lastly, The charged E1 is then recruited to UBC9, where SUMO is transferred to the active cysteine (Cys93) of UBC9 (Olsen *et al.*, 2010).

1.7.4 UBC9 or UBE2I

The SUMO E2 enzyme, Ubc9, was first identified in *S. cerevisae* based on its sequence similarity with other known ubiquitin E2 enzymes, where it was shown to be critical for cell cycle progression (Seufert *et al*., 1995). Human UBC9 (or UBE2I) was discovered later in a yeast-two hybrid system using human RAD52 protein as “bait”. In the same study, UBC9 was found to interact with other proteins such as RAD51, p53 and SUMO1, suggesting a role in the DNA damage/repair pathway (Shen *et al.*, 1996a). It was initially thought that Ubc9 conjugated ubiquitin, but it was later demonstrated that it was a SUMO specific, not ubiquitin, conjugating E2 enzyme (Desterro *et al*., 1997).

Unlike the ubiquitin system where specific combinations of E2 and E3 enzymes are required for substrate specificity and conjugation, the SUMO E2 alone can recognise and modify substrates with SUMO in the absence of an E3 SUMO ligase, at least *in vitro* (Gareau and Lima, 2010). Structural biology has provided mechanistic insights into the mechanism of this unique interaction between the substrate and the E2. The crystal structure of a charged UBC9 (UBC9 conjugated to SUMO) in complex with its substrate showed that the residues in the SUMO consensus motif are directly recognised by and bound to UBC9, and the target lysine fits into a hydrophobic groove on UBC9 (Bernier-Villamor *et al.*, 2002; Lin *et al.*, 2002). UBC9 also contains a patch of basic residues which can interact with the acidic residues present downstream of the core SUMO-motif, such as in negatively charged amino acid dependent SUMOylation motif (NDSM). Since most validated SUMO motifs are often

present in extended loops or unstructured domains of a substrate protein, this could be a crucial factor in determining the ability or the extent to which the substrate can be modified by SUMO.

1.7.5 SUMO E3 ligases

The SUMO E3 ligases can be broadly divided into following two classes:

1.7.5.1 SP-RING containing E3 SUMO ligases

So far, five functional E3 SUMO ligases containing the SP-RING (Siz/PIAS-RING) domain have been identified in humans. These include members of the Protein Inactivator of Activated STATs (PIAS) family (PIAS1, PIAS2/x, PIAS3 and PIAS4/y) and NSE2 (or MMS21). The PIAS family is described in detail in the next section.

NSE2 is a dedicated and essential subunit of the human SMC5-SMC6 DNA repair complex. Upon DNA damage, NSE2 stimulates SUMOylation of SMC6, which protects the cell from apoptosis, most likely by promoting homologous recombination (Potts and Yu, 2005). In addition, two novel PIAS-like proteins containing the SP-RING domain, ZIMP7 and ZIMP10, have also been identified, but the SUMO E3 ligase activity of these proteins has not yet been explored in detail (Huang *et al.*, 2005; Lee, Beliakoff and Sun, 2007).

Both PIAS1 and PIAS3 were initially identified as potent repressors of the transcription factors STAT1 and STAT3 respectively, thus acting as negative regulators of JAK-STAT signalling pathway (Chung *et al.*, 1997; Liu *et al.*, 1998). Structurally, all PIAS proteins contain five distinct domains or motifs in the

following order: an N-terminal SAP (Scaffold attachment factor-A/B, Acinus and PIAS) domain, a PINIT motif, an SP-RING domain, a SIM (SUMO-Interaction Motif) and a serine/threonine rich C-terminal region. The SAP domain is responsible for binding A/T rich DNA sequences that are usually present near enhancer regions on the chromatin, and can also interact with proteins such as p53 (Okubo *et al.*, 2004). The SAP domain also contains the typical nuclear receptor interacting motif LxxLL (where x is any amino acid and L is leucine) that mediates protein-protein interactions with nuclear receptors and transcriptional co-regulators (Heery *et al.*, 1997). The PINIT motif, at least for PIAS3, is involved in its nuclear retention (Duval *et al.*, 2003). Other studies suggest that it may be required for substrate specificity. In case of Siz1 (the yeast homologue of PIAS), the PINIT motif is required for binding and SUMO modification of the proliferating cell nuclear antigen (PCNA) (Yunus and Lima, 2009).

The SP-RING domain of PIAS proteins is functionally similar to the RING (Really Interesting New Gene) domain present in E3 ubiquitin ligases. However, the SP-RING domain does not contain the two zinc-binding cysteine residues found in the canonical RING domain consensus sequence. Instead, other conserved residues present in the SP-RING domain coordinate to bind one Zn^{2+} ion. The SP-RING domain is crucial for the E3 ligase activity of PIAS proteins. Unlike the ubiquitin RING domain, they do not form thioester intermediates with SUMO, but simply acts as a scaffold, to bring a SUMO charged Ubc9 in close proximity to the target lysine on the substrate (Johnson and Gupta, 2001; Yunus and Lima, 2009).

The SIM motif is a cluster of hydrophobic residues composed of ψxψψ or ψψxψ (where ψ is I/V/L and x is any amino acid) followed by a patch of negatively charged residues, which interacts non-covalently with SUMO (Geoffroy and Hay, 2009). Although its exact function in the context of E3 ligase activity remains unclear, it is proposed that SIMs may promote interactions with other SUMO-conjugated proteins, and may direct PIAS proteins to specific sub-cellular structures or complexes (Gareau and Lima, 2010). The C-terminal tail of PIAS (except PIASy) contains the serine/threonine rich region, and is the least conserved region amongst different PIAS family members. Their function is presently unknown. Figure 1.14 shows the structure of PIAS family of E3 SUMO ligases.

1.7.5.2 Non-SP-RING containing E3 SUMO ligases

Several other proteins in humans have been reported to have E3 SUMO ligase activity despite lacking any obvious similarity to other E3 ligases. Some examples include Ran-binding protein 2 (RanBP2), Polycomb protein 2 (PC2), and Histone deacetylases 4 and 7 (HDAC4, HDAC7) (Wilkinson and Henley, 2010). Interestingly, some ubiquitin E3 ligases have also been shown to possess SUMO ligase activity, which include TOPORS, MDM2 and TRIM proteins (Weger *et al*., 2005; Chu and Yang, 2011; Stindt *et al.*, 2011).

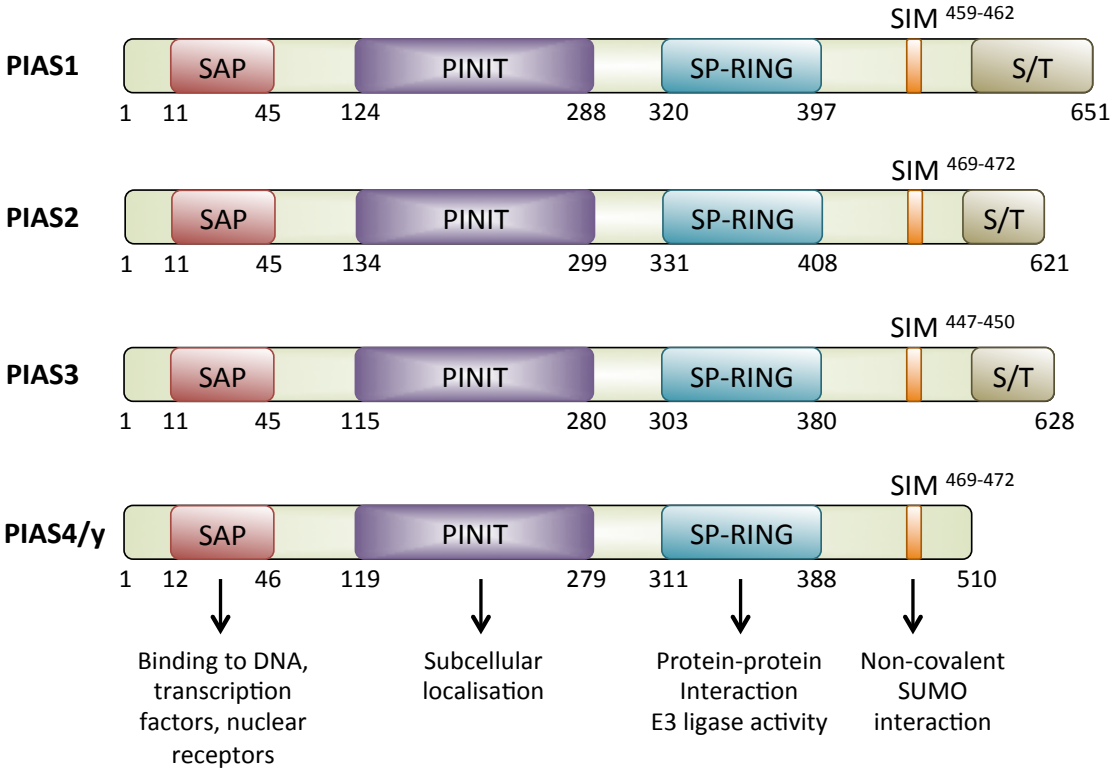

Figure 1.14 PIAS family of SUMO E3 ligases

Schematic showing the conserved structural domains of the four PIAS family members (Adapted from Jentsch and Psakhye, 2013). SAP-Scaffold Attachment factor-A/B; Acinus and PIAS; PINIT- motif composed of proline, isoleucine, asparagine, isoleucine and threonine; SP-RING-Siz/PIAS Really Interesting New Gene domain; SIM-SUMO Interaction Motif; S/T-serine/threonine rich domain

1.7.6 SENP

Sentrin specific proteases (or SENP) are a class of enzymes that perform two important functions in the SUMO pathway. Firstly, they are involved in the maturation of newly synthesised SUMO in cells, by cleaving their C-terminus to expose the di-glycine motif required for SUMO conjugation. Secondly, they catalyse removal of SUMO monomers and polymers from target substrate, thus maintaining the balance of global SUMOylation in cells. The high activity of SENP in cells makes detection of SUMOylated proteins very difficult in cell lysates. Humans express six SENP family members, designated SENP1-3 and SENP5-7 (Wilkinson and Henley, 2010). It should be noted that there is another SENP called SENP8 (or DEN1) in humans, but it acts on another ubiquitin-like protein NEDD8, instead of SUMO (Wu *et al.*, 2003).

The SENP family members can be broadly divided on the basis of their function, localisation and SUMO paralogue specificity. Interestingly, only SENP1, SENP2 and SENP5 are capable of processing SUMO precursors to active SUMO (Yeh, 2009). SENP1 and SENP2 are capable of deconjugating all three SUMO isoforms, and are localised to the nuclear pore complex and nucleoplasm. Both contain a nuclear localisation signal (NLS) and nuclear export signal (NES), which allows them to shuttle between the cytoplasm and the nucleus. Senp1 appears to be the main SUMO1 C-terminal hydrolase as *Senp1* -/- embryos cannot process SUMO1 (Cheng *et al.*, 2007). SENP3 and SENP5 are mostly localised to the nucleolus, and preferentially deconjugate SUMO2/3. SENP6 and SENP7 are localised in the nucleoplasm, and also prefer SUMO2/3 chains to SUMO1. In addition, SENP6 and SENP7 possess SUMO

chain editing activity, meaning they can remove individual SUMO moieties from the chain, without cleaving the whole chain (Hickey, Wilson and Hochstrasser, 2012).

More recently, two additional SUMO proteases were identified. These include DeSI1 and DeSI2 (Shin *et al.*, 2012) and USPL1 (Schulz *et al.*, 2012). DeSI1 and DeSI2 appear to be specifically deSUMOylate the transcriptional repressor BZEL. On the other hand, USPL1 is unique among SUMO proteases as it localise to cajal bodies in the nucleus, with preference for SUMO2/3.

1.7.7 SUMO targeted Ubiquitin ligases (STUbLs)

SUMO and ubiquitin have been shown to target the same proteins with different outcomes, and were therefore considered functionally antagonistic. However, emerging evidence suggests that the two pathways are not completely distinct, but may function in cooperation, under certain contexts. The SUMO targeted ubiquitin ligase (or STUbL) links the SUMO pathway with the ubiquitin system. A STUbL is a RING-domain containing E3 ubiquitin ligase that has a strong binding affinity towards proteins that are polySUMOylated. Binding of STUbL to a polySUMOylated protein recruits a ubiquitin-charged E2 enzyme, leading to ubiquitination of the polySUMOylated protein, and subsequent degradation by the proteasome. An important feature of STUbL that distinguishes it from other E3 ubiquitin ligases is the presence of multiple functional SUMO-interaction motifs (SIMs), that mediates non-covalent interactions with polySUMO chains attached on proteins (Geoffroy and Hay, 2009). Currently, only two functional STUbL, RNF4 (or SNURF) and RNF111 (or Arkadia) have been identified in humans, and described below.

1.7.7.1 RNF4

RNF4 was first discovered as a novel RING finger protein that interacted with androgen receptor (AR) and was shown to increase steroid receptor mediated gene transcription (Moilanen *et al.*, 1998; Poukka *et al.*, 2000). It was later shown to colocalise with SUMO1 in PML nuclear bodies (Häkli *et al.*, 2005). The first evidence of RNF4 acting as a STUbL came from studies performed in yeast. Yeast lacking Slx8-Rfp (yeast homologue of RNF4) showed accumulation

of SUMOylated proteins and genomic instability, which could be reversed by expression of human RNF4 (Prudden *et al.*, 2007). This led to the identification of PML as the first physiological substrate of RNF4 in human cells (Lallemand-Breitenbach *et al.*, 2008; Tatham *et al.*, 2008). RNF4 contains four N-terminal SIM and a RING domain at the C-terminal (Figure 1.15A).

Acute promyelocytic leukemia (APL) is a type of blood cancer characterised by the presence of the driving oncogenic fusion protein called PML-RARα. The chemical, arsenic trioxide (As_2O_3) is used for the treatment of APL as it specifically induces degradation of the PML-RARα protein. It was found that arsenic induces polySUMOylation of PML on K160 residue (and also PML nuclear bodies) in cells, which recruits RNF4 leading to its ubiquitination and degradation (Lallemand-Breitenbach *et al.*, 2008; Tatham *et al.*, 2008). This is illustrated in figure 1.15. Interestingly, depletion of RNF4 in human cells caused an increase in levels of SUMOylated proteins suggesting that SUMOylation plays a bigger role in targeting proteins for ubiquitin-mediated proteolysis (Tatham *et al*., 2008).

Apart from regulating PML, RNF4 also plays an important role in the DNA damage response. RNF4 mediates clearance of several SUMOylated proteins such as MDC1 during DNA damage, which facilitates DNA double strand break repair (Luo *et al.*, 2012). RNF4 has also been shown to regulate transcriptional activity of PARP1 by mediating its degradation during heat-shock (Martin *et al.*, 2009), and of Hypoxia Inducible Factor 2α (HIF2α) during hypoxia and normoxia (van Hagen *et al.*, 2009). This suggests a broader role of SUMOylation and RNF4 in regulating important cellular processes. A recent study showed that

Ubiquitin-specific protease 11 (or USP11) could counteract the effects of RNF4 by deubuiquitinating ubiquitin-SUMO hybrid chains, upon DNA damage induced by methyl methanesulfonate (Hendriks *et al.*, 2015).

1.7.7.2 RNF111

RNF111 was identified through a bioinformatic search of proteins that shared sequence homology with RNF4 (Sun and Hunter, 2012). Like RNF4, RNF111 can also trigger ubiquitination and degradation of SUMOylated PML in response to As_2O_3 (Erker *et al.*, 2013) and requires the presence of all three SIM and RING domain (Figure 1.15B). Interestingly, a study showed that in the presence of the E2 UBC13-MMS2, RNF111 catalysed the formation of the non-proteolytic K63 chains on SUMOylated Xeroderma Pigmentosum (XPC) protein (Poulsen *et al.*, 2013). The association of RNF4 with UBC13 was not found in this study, which suggests that RNF111 is capable of interacting with a wider range of E2 enzymes than RNF4, which explains the formation of K63-linked chains by RNF111. It should be noted that RNF111 mediated ubiquitination of SnoN/Ski does not require the presence of SIMs, suggesting that it can also function as a SUMO-independent ubiquitin ligase (Erker *et al.*, 2013).

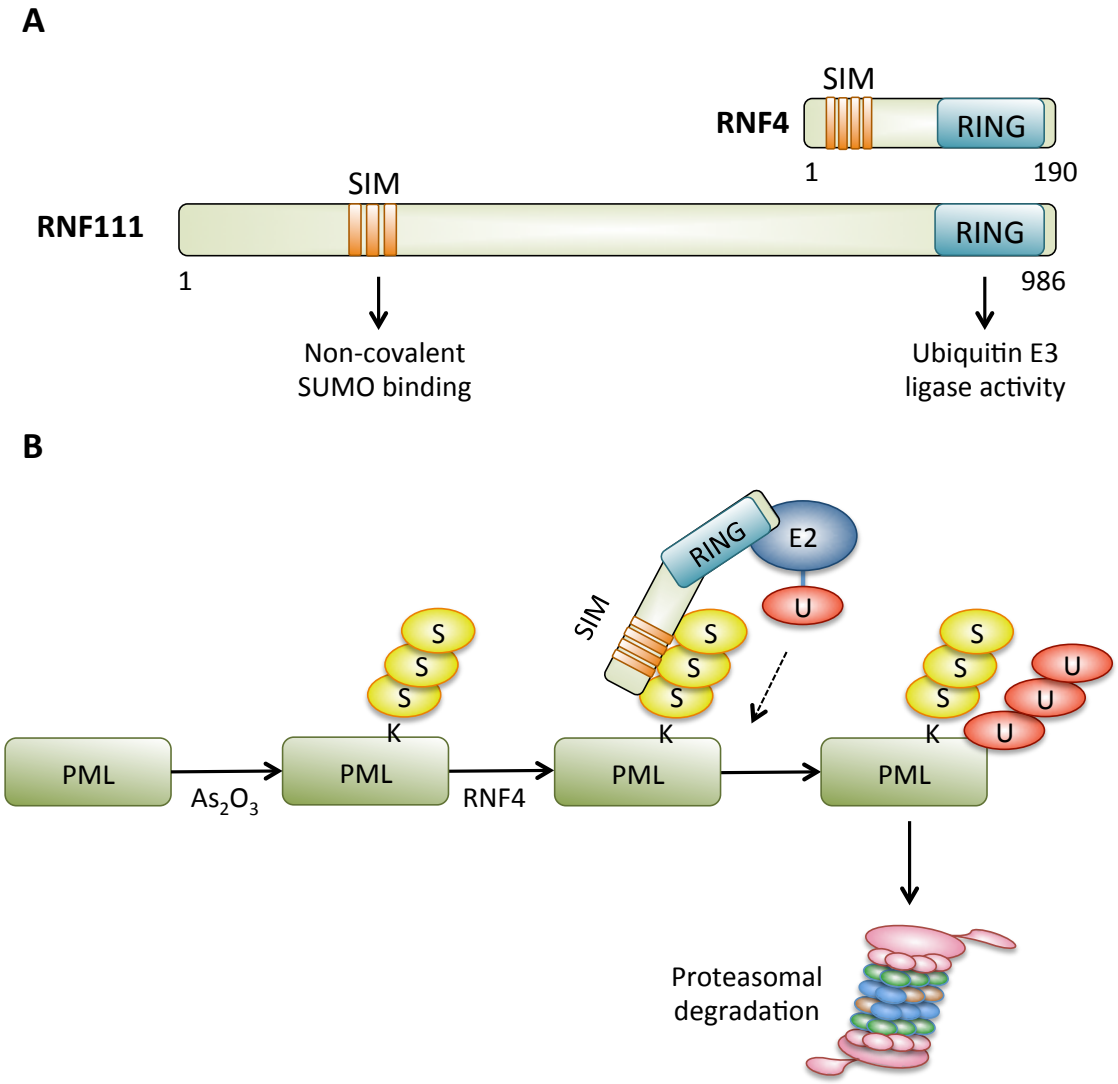

Figure 1.15 SUMO targeted ubiquitin ligases

(A) Schematic showing the SUMO targeted E3 ubiquitin ligases, RNF4 and RNF111 with their functional domains. RING (Really New Interesting Gene) recruits a ubiquitin loaded E2 enzyme to the SUMOylated protein. SIM (SUMO Interaction motif) is required for the recognition and binding of polySUMO chains on the target protein. **(B)** Arsenic trioxide induces formation of polySUMO chains on the promyelocytic leukemia (PML) protein. RNF4 binds to these SUMO chains and recruits a ubiquitin E2, and together they form polyubiquitin chains on PML, leading to its degradation by the proteasome.

1.8 Regulation of global SUMOylation by cellular stress

Numerous stimuli have been reported to cause alteration in the global levels of SUMOylation, which is consistent with the role of SUMO in mediating a stress response. However, there is a significant increase in SUMO2/3 conjugates rather than SUMO1 conjugates in cells upon heat shock (Saitoh and Hinchey, 2000). It is also important to emphasise that specific substrates are differentially SUMOylated under these conditions, as opposed to a general increase or decrease of all substrates. Although heat shock results in a global increase of SUMO modification in cells, SUMOylation of some substrates remains unchanged (eg. DNA Topoisomerases), while SUMOylation of some substrates is increased (eg. Heat shock proteins) (Golebiowski *et al.*, 2009). Stress-dependent increase in conjugation of both SUMO1 and SUMO2/3 has also been observed under conditions of oxygen and glucose deprivation (or ischemia) in hippocampal neurons (Cimarosti and Henley, 2008).

Reactive oxygen species such as hydrogen peroxide (H_2O_2) and nitric oxide (NO) are constantly produced during metabolic reactions in the human body, and also in response to external factors such as UV radiation and chemotherapeutic agents, resulting in oxidative stress in cells. While high levels of oxidative stress cause global hyperSUMOylation, low doses result in a global decrease of SUMO conjugation (Bossis and Melchior, 2006). Mechanistically, at low doses of H_2O_2, a disulphide bond is formed between UBA2 (E1) and UBC9 (E2), which impairs the activity of both E1 and E2. Interestingly, SUMO isopeptidases are not affected unless exceedingly high concentrations of ROS are present (Bossis and Melchior, 2006). In contrast, NO induced oxidative

stress also results in hypoSUMOylation, but by a different mechanism, involving proteasomal degradation of the SUMO E3 ligase PIAS3 (Qu *et al.*, 2007). Products of infectious pathogens also negatively affect SUMOylation. The adenoviral protein Gam1 causes proteasomal degradation of the SUMO E1 enzyme, while the toxin Lysteriolysin O produced by *Lysteria monocytogenes* leads to proteasome-independent degradation of UBC9 (Boggio *et al.*, 2004; Ribet *et al.*, 2010).

1.9 Regulation of SUMOylation by phosphorylation and acetylation

Regulation of SUMOylation is largely controlled at the substrate level by the concerted action of E3 ligases, SENP and the stimuli involved. Other PTMs such as phosphorylation, ubiquitination and acetylation also play an important in the regulation of SUMOylation. However, these effects are more substrate specific rather than a global change in SUMOylation. Some important examples have been discussed here.

Phosphorylation of a substrate can also enhance or inhibit its SUMOylation. Upon DNA damage, PML gets phosphorylated by HIPK2 and other kinases, which further enhances PML SUMOylation (Gresko *et al.*, 2009). Similarly, phosphorylation of the nuclear receptor TR2 in response to retinoic acid by ERK2 leads to its SUMOylation and association with PML bodies (Gupta *et al.*, 2008). Furthermore, prior phosphorylation of MEF2 and HSF1 enhances their SUMOylation (Guo *et al.*, 2007). Both MEF2 and HSF1 contain a phosphorylation dependent SUMO motif (PDSM), whereas the phosphorylation site in PML and TR2 does not lie within a PDSM. In PDSM, the additional

negative charge of the phosphate group enhances substrate and UBC9 binding, thus promoting SUMOylation (Hietakangas *et al.*, 2006). In the latter case, it can be speculated that phosphorylation might lead to a change in cellular localisation and/or changes in protein structure, which favour SUMO modification of the substrate. On the other hand, phosphorylation of substrates can also inhibit SUMOylation, such as in the case of IκBα (Desterro *et al*., 1998), c-JUN/c-FOS (Bossis *et al.*, 2005), p53 (Lin *et al*., 2004) and ELK1 (Yang *et al.*, 2003).

Another way of regulating SUMOylation is by competing for the same target lysine residue, such as in the case of SP3 and p300, where SUMOylation and acetylation have antagonistic effects on the substrate activity (Sapetschnig *et al.*, 2002; Bouras *et al.*, 2005). Recently, acetylation of some proteins such as Histone H3 was shown to promote SUMOylation, which has prompted the existence of a SUMO-acetylation dependent SUMO motif (Hendriks *et al.*, 2014). However, in this case acetylation and SUMOylation of the substrate occur at two different lysine residues. The functional consequence of H3 SUMOylation remains unknown.

Interestingly, SUMO itself can be acetylated at a key lysine residue (SUMO1 at K37, SUMO2 at K33 and SUMO3 at K32), which controls SUMO-SIM interaction in a selective manner (Ullmann *et al*., 2012). SUMO chains on a substrate typically act as recognition or binding platforms for other proteins containing SIMs. These interactions are crucial in regulating a number of SUMO-associated functions such as targeting RanGAP1 to the nuclear pore complex, recruitment of PML into nuclear bodies and activation or repression of various transcription factors. While acetylation of SUMO does not seem to

impair binding of RanGAP1-SUMO1 to RanBP2, it negatively affects its interaction with PML, PIAS and DAXX proteins. This adds another layer of complexity to the regulation of substrate-specific SUMOylation.

1.10 Crosstalk between SUMOylation and ubiquitination

Lysine is a versatile amino acid as it is amenable to multiple PTMs such as ubiquitination, SUMOylation, methylation and acetylation among many others. This section highlights scenarios in which SUMO and ubiquitin target the same residue, but have antagonistic effects.

The first evidence showing that ubiquitin and SUMO compete for the same acceptor lysine residue for modification in proteins came from studies performed on Inhibitor of NF-κB α (or IκBα). Nuclear factor κB (or NF-κB) is a group of transcription factors involved in growth factor signalling and cell survival. Under steady state, NF-κB is bound to its negative regulator IκBα, which sequesters it into the cytoplasm. In response to cytokines or DNA damage, Ser32/36 phosphorylated IκBα is ubiquitinated on K21 and is rapidly degraded. This allows NF-κB to translocate to the nucleus and activate transcription of NF-κB target genes. It was shown that IκBα is also SUMOylated on K21, which blocks its ubiquitination, stabilises IκBα and represses NF-κB (Desterro *et al*., 1998). Moreover, activation of IκB kinase (IKK) is achieved through the sequential modification of its regulatory subunit NEMO (NF-κB essential modulator) by SUMO and ubiquitin. SUMOylation of NEMO at K277 and K309 results in its nuclear accumulation, where upon DNA damage it is phosphorylated by ATM. This phosphorylation allows modification of K277 and

K309 by ubiquitin, which allows it to translocate to the cytoplasm and associate with other IKK subunit forming an active kinase (Huang *et al.*, 2003).

Another example where SUMO and ubiquitin target the same lysine residue is yeast PCNA (Proliferating Cell Nuclear Antigen). PCNA acts a sliding clamp, and a processivity factor for DNA polymerases, and other proteins involved in DNA replication and repair (Ulrich, 2009). Since PCNA is a homo-trimer, individual subunits can be modified simultaneously by SUMO and ubiquitin. Yeast PCNA is SUMOylated at K164 during the S-phase, which recruits the helicase Srs2. This prevents homologous recombination during DNA replication. During DNA damage, K164 can be monoubiquitinated or polyubiquitinated at K164. Monoubiquitinated PCNA triggers an error-prone DNA repair process called translation synthesis, by recruiting the DNA Polymerases Polη and Rev1. Interestingly, the monoubiquitination on PCNA can be extended to form a K63-linked polyubiquitin chain, which activates an error-free repair pathway (Denuc and Marfany, 2010). Thus, the same lysine can be modified in three different ways leading to distinct outcomes.

1.11 Consequences of SUMOylation

The functional consequences of SUMOylation depend entirely on the target protein and its associated cellular process, and are thus difficult to predict or generalise. However, consequences of SUMOylation at the molecular levels can be broadly divided into three main categories, and illustrated in figure 1.16 (Everett *et al*., 2013).

First, the covalent attachment of SUMO to the substrate may lead to

conformational or structural changes in the target protein, directly modifying its function. This has been seen in the case of Thymine DNA glycosylase (TDG). The function of TDG is to recognise and remove mismatched base pairs. SUMOylation of TDG at the C-terminus induces a conformation change of its N-terminus, which reduces it DNA binding ability without affecting the catalytic activity. This results in dissociation of TDG from the DNA, allowing the next cycle of base excision repair to take place (Hardeland *et al.*, 2002; Steinacher and Schär, 2005).

Second, SUMOylation may block a binding site for another protein on the substrate, which can lead to decrease in protein activity. For example, SUMOylation of the ubiquitin conjugating enzyme E2-25k blocks its interaction with E1 ubiquitin enzyme, leading to decrease in its ability to conjugate ubiquitin to target proteins (Pichler *et al.*, 2005). Similar observation has also been made in the Mitogen activated protein kinase (MAPK) pathway, where the MEK specific E3 ligase, MEKK1, promotes SUMOylation of MEK1/2. MEK1/2 SUMOylation hinders its interaction with a downstream kinase called ERK1/2, preventing ERK1/2 phosphorylation and activation of the MAPK pathway (Kubota *et al.*, 2011).

Third, the covalently attached SUMOylation may promote formation of protein complexes by recruiting proteins that interact directly with the substrate or through non-covalent SUMO binding. The classical example is the nuclear protein RanGAP1. Unmodified RanGAP1 is localised to the cytoplasm, whereas SUMOylated RanGAP1 is localised to the nuclear pore. The localisation is strictly SUMO dependent as it promotes the interaction of RanGAP1 with the

nuclear pore associated protein RanBP2 (Mahajan *et al.*, 1997). SUMOylation also regulates assembly of complexes involved in DNA methylation (or silencing) by covalently modifying Methyl-CpG binding domain protein MBD1. SUMOylation of MBD1 promotes the formation of heterochromatin foci by recruiting MCAF1 and HP1 by non-covalent SUMO-SIM interaction (Uchimura *et al.*, 2006).

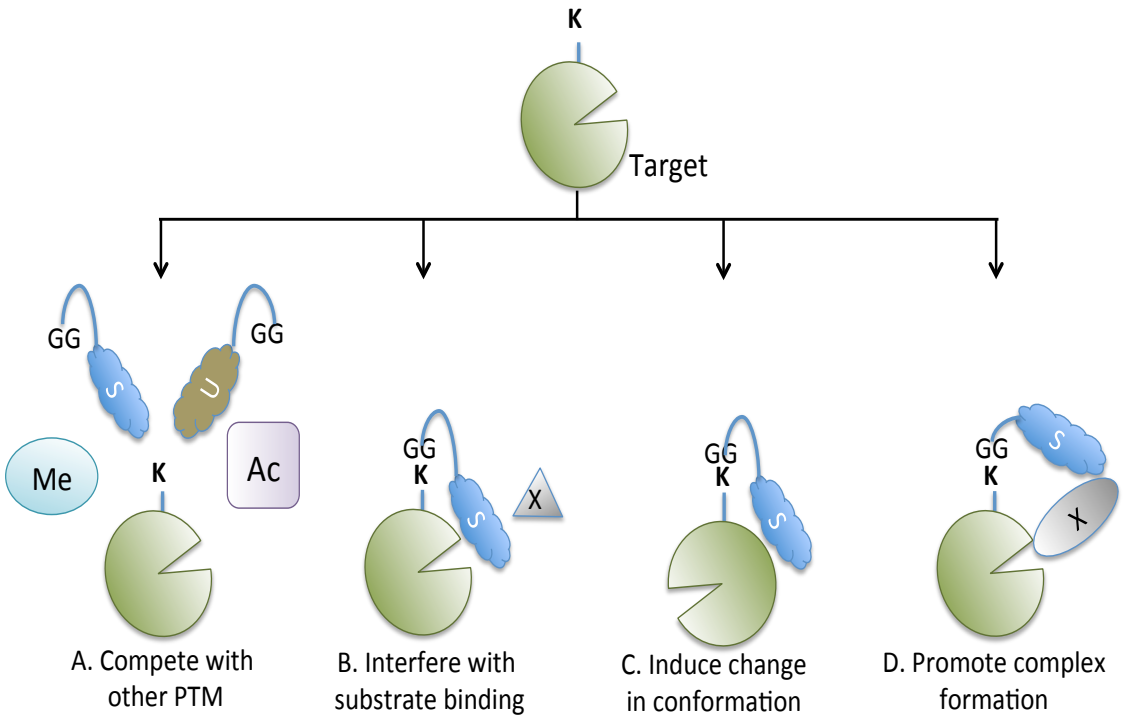

Figure 1.16 Consequences of SUMOylation on the target protein

SUMOylation can affect the substrate protein in many ways. Different kinds of post-translational modifications (PTM) occurring on the same lysine such as ubiquitination, acetylation (Ac) or methylation (Me) can have distinct functional consequences on the substrate. SUMO might compete with these PTM, and hence affect the function of the protein. SUMOylation can interfere with protein-protein interactions by masking binding sites for other proteins. It can also create novel binding platforms that promote interaction with other proteins in a SUMO-dependent manner. SUMOylation can also induce a change in conformation of the substrate protein, altering its activity (Adapted from Everett *et al*., 2013)

1.12 Aims of the project

Oncogenic proteins, particularly kinases, which promote survival and proliferation of cancer cells, have remained sought after drug targets. While many inhibitors such as Imatinib (an inhibitor of BCR-ABL fusion protein in CML) and Vemurafenib (an inhibitor of V600E mutant of B-RAF in melanomas) have been approved for use in the clinic, resistance remains a major obstacle. PIM kinases have been found to play a role in the development of resistance to various forms of cancer therapy, and as mentioned previously various small molecule inhibitors are currently undergoing clinical trials. Unfortunately, the first two PIM kinase inhibitors, SGI-1776 and AZD1208, to enter Phase-I clinical trials failed due to cardiotoxicity. So, presently there are no clinically approved PIM kinase inhibitors on the market.

Considerable research has been conducted on identifying targets of PIM1 kinase, and studying the effects of PIM1 inhibition in preclinical settings, but there is very little information on how PIM1 protein itself is regulated in normal or cancer cells. This can prove to be a drawback in realising the complete potential of existing drugs, and can have a significant impact on how PIM kinase inhibitors work or can be improved in terms of efficacy or sensitivity. In the present study, I wished to fill in the crucial gaps in our understanding of PIM1, and so the research aims were

- To identify mechanism(s) that regulate or control PIM1 levels in cells
- To identify novel therapeutic or alternative strategies to target PIM1 in cancer

CXR Biosciences, a Dundee based small biotech company, identified a novel inhibitor of PIM kinases named CXR1002, which also underwent Phase I clinical trial (Personal communication). However, the IC50 values of this drug in cell lines is in high micromolar range, and so this project was set up, in collaboration, to identify strategies to improve the sensitivity of CXR1002 (or other PIM kinase inhibitors) by modulating cross-talking pathways. At the beginning of my PhD, I attempted to validate CXR1002 as a PIM kinase inhibitor, however, with time the focus of the project shifted from CXR1002 to studying mechanisms regulating PIM1. Therefore, results of the CXR1002 study have been presented in appendix, as they do not directly relate to the main topic of this thesis.

Chapter 2

Materials & Methods

2.1 Reagents and buffers

2.1.1 Stock solutions

All chemicals were purchased from Sigma, and dissolved in autoclaved Milli-Q water, unless stated otherwise.

Chemical	Concentration
Tris buffer (pH 7.5, 8, 8.5)	1 M
Sodium chloride (NaCl)	5 M
Ethylenediaminetetraacetic acid (EDTA) pH 8	0.5 M
Magnesium chloride ($MgCl_2$)	1 M
Dithiothreitol (DTT)	1 M
Ammonium persulfate (APS)	10% (w/v)
Sodium dodecyl sulfate (SDS)	10% (w/v)
Tris buffer pH 6.8	1.25 M
Tris buffer pH 8.8	1.25 M
Potassium chloride (KCl)	3 M
Ampicillin	100 mg/ml
KanaMYCin	50 mg/ml
Chloramphenicol	34 mg/ml in ethanol
Doxycycline hyclate	1 mg/ml
Polybrene	10 mg/ml in PBS
HygroMYCin B Readymade (Thermo Fisher Scientific)	50 mg/ml
Triton X-100	10% (v/v)

Puromycin Readymade (Thermo Fisher Scientific)	10 mg/ml
Cycloheximide	100 mg/ml Dimethyl sulfoxide (DMSO)
Calcium chloride ($CaCl_2.2H_2O$)	1 M
Morpholinepropanesulfonic acid (MOPS) pH 6.8	0.5 M
Manganese chloride ($MnCl_2.4H_2O$)	1 M
Potassium acetate (CH_3COOK) pH 7.5	1 M
Sodium hydroxide (NaOH)	5 M
Imidazole	1 M
Protease inhibitors EDTA-free (Roche)	25X
Phosphatase inhibitor (Roche)	10X
Adenosine triphosphate (ATP)	20 mM
Sodium dihydrogen phosphate ($NaH_2PO_4.2H_2O$)	1 M
Disodium hydrogen phosphate ($Na_2HPO_4.2H_2O$)	1 M
Luminol	90 mM in DMSO
p-Coumaric acid	250 mM in DMSO
Hydrogen peroxide (H_2O_2) Readymade	30%
Isopropyl β-D-1-thiogalactopyranoside (IPTG)	1M
MG132 (Selleckchem)	100 mM in DMSO

2.1.2 Buffers

Bacterial culture

Luria Broth (LB) broth

10 g LB mix per 400 ml water

(1% w/v Bacto-tryptone, 0.5% w/v Bacto-yeast extract, 171 mM NaCl)

LB agar

9.25 g per 250 ml water (same as LB broth plus 1.5% w/v Bacto agar)

Transformation Buffer-1

10 mM $CaCl_2.2H_2O$

15% (v/v) Glycerol

30 mM CH_3COOK pH 7.5

50 mM $MnCl_2.4H_2O$

100 mM RbCl

pH adjusted to 5.8 using 0.2 M acetic acid

Transformation Buffer-2

75 mM $CaCl_2.2H_2O$

0.15% (v/v) Glycerol

10 mM MOPS pH 6.8

10 mM RbCl

Western Blotting

10X Tris buffered saline (TBS)

200 mM Tris

1.368 M NaCl – final pH adjusted to 7.6

1X TBS-Tween (TBST)

1 part 10X TBS

9 parts water

0.1% (v/v) Tween-20

Blocking buffer

5% (w/v) non-fat dry milk (Marvel) in 1X TBST

Antibody dilution buffer

5% (w/v) milk/TBST or 5% (w/v) Bovine Serum Albumin (BSA)/TBST

Enhanced Chemiluminescence (ECL) Solution-1

2.5 mM Luminol

396 µM p-Coumaric acid

100 mM Tris pH 8.5

ECL Solution-2

0.0192% (v/v) Hydrogen peroxide

100 mM Tris pH 8.5

10X SDS-Polyacrylamide gel electrophoresis (PAGE) Running buffer

250 mM Tris base

1.92 M Glycine

34.67 mM SDS

10X Wet-Transfer buffer

250 mM Tris base

1.92 M Glycine

1X Transfer buffer

1 part 10X transfer buffer

7 parts water

2 parts methanol

2X SDS sample buffer

125 mM Tris-HCl (pH 6.8)

20% (v/v) glycerol

4% (w/v) SDS

0.04% (v/v) Bromophenol blue

Ponceau S solution

0.1% (w/v) Ponceau S

5% Acetic acid

Gel staining

Coomassie stain

0.2% (w/v) Coomassie Brilliant Blue R250

50% (v/v) ethanol

10% (v/v) acetic acid

Destainer-I

40% (v/v) ethanol

7% (v/v) acetic acid

Destainer-II

10% (v/v) ethanol

7% (v/v) acetic acid

Agarose Gel Electrophoresis

1% Agarose Gel

1 g Agarose in 100 ml 1X Tris acetate EDTA (TAE)

Agarose Gel Running Buffer (50X TAE)

2 M Tris acetate

0.05 M EDTA

Ni^{2+}-NTA Pulldown

2X Sodium phosphate buffer pH 8

47.35 ml - 200 mM $Na_2HPO_4.2H_20$

2.65 ml - 200 mM $NaH_2PO_4.2H_2O$

2X Sodium phosphate buffer pH 6.3

11.25 ml - 200 mM $Na_2HPO_4.2H_20$

38.75 ml - 200 mM $NaH_2PO_4.2H_2O$

Denaturing lysis buffer (pH 8)

6 M Guanidium-HCl

10 mM Tris-HCl (pH 8)

100 mM sodium phosphate buffer (pH 8)

5 mM Imidazole

5 mM β-mercaptoethanol (β-ME)

Lysis buffer wash (pH 8)

6 M Guanidium-HCl

10 mM Tris-HCl (pH 8)

100 mM sodium phosphate buffer (pH 8)

5 mM β-mercaptoethanol

0.1% (v/v) Triton X-100

Urea wash buffer (pH 8)

8 M Urea

10 mM Tris-HCl (pH 8)

100 mM sodium phosphate buffer (pH 8)

5 mM β-mercaptoethanol

0.1% (v/v) Triton X-100

Urea Wash Buffer (pH 6.3)

8 M Urea

10 mM Tris-HCl (pH 8)

100 mM sodium phosphate buffer (pH 6.3)

5 mM β-mercaptoethanol

0.1% (v/v) Triton X-100

Ni^{2+}-NTA Elution buffer

200 mM Imidazole

5% (w/v) SDS

150 mM Tris-HCl (pH 6.7)

30% (v/v) glycerol

720 mM β-mercaptoethanol

0.0025% (v/v) Bromophenol blue

6XHis Protein purification

Wash buffer

50 mM Tris pH 7.5

500 mM NaCl

20 mM Imidazole

Elution buffer

50 mM Tris pH 7.5

500 mM NaCl

1 mM DTT

200 mM Imidazole

Dialysis buffer

50 mM Tris pH 7.5

500 mM NaCl

1 mM DTT

Immunofluorescence (IF)

Blocking buffer/Antibody dilution buffer

5% (w/v) BSA

0.1% (v/v) Triton

1X TBS

Fixation buffer

4% (w/v) p-formaldehyde in 1X PBS

Wash buffer

1X PBS or 1X TBS

Permeabilisation Buffer

0.1% (v/v) Triton

1X PBS

Other buffers

Co-immunoprecipitation buffer

50 mM Tris-HCl pH7.5

150 mM NaCl

1% (v/v) NP-40 (Igepal)

Protease Inhibitors (EDTA free)

Phosphatase inhibitors

Cytoplasmic extraction buffer

50 mM Tris-HCl pH 7.5

10 mM KCl

5 mM MgCl2

0.5% (v/v) NP40 (Igepal)

1 mM DTT

Protease inhibitor (EDTA-free)

Phosphatase inhibitors

Cell freezing buffer

90% Fetal Bovine Serum (FBS)

10% Dimethyl sulfoxide (DMSO)

2.1.3 Antibodies

2.1.3.1 Primary antibodies

Antibody	Species	Company (Cat. No.)	Dilution for Western blot (WB)
PIM1 (12H8)	Mouse monoclonal	Santa Cruz (sc-13513)	1:200 (endogenous) 1:1000 (transfected) 1:50 (for IF)
PIM1	Rabbit polyclonal	Bethyl (A300-313)	1:1000
ACTIN	Mouse monoclonal	Abcam (ab-6276)	1:10,000
ACTIN	Rabbit polyclonal	Sigma (A2066)	1:10,000
GAPDH	Mouse monoclonal	Sigma (G8795)	1:10,000
GFP	Rabbit polyclonal	Santa Cruz (sc-8334)	1:800
MYC tag (9E10)	Mouse monoclonal	In-house (hybridoma)	1:3
HA tag (12CA5)	Mouse monoclonal	Sigma	1:1000
FLAG tag M2	Mouse monoclonal	Sigma (F1804)	1:1000

His tag	Mouse monoclonal	GE Healthcare (27471001)	1:5000
GST tag	Rabbit polyclonal	Santa Cruz (sc-459)	1:1000
Phospho Ser62 c-MYC	Rabbit monoclonal	Cell Signalling (13748)	1:1000
Total c-MYC	Rabbit monoclonal	Cell Signalling (5605)	1:1000
Phospho Ser10 Histone H3	Rabbit polyclonal	Millipore (06-570)	1:1000
Total Histone H3	Rabbit monoclonal	Cell Signalling (4499)	1:1000
Phospho Ser112 BAD	Rabbit monoclonal	Cell Signalling (5284)	1:1000
Total BAD	Rabbit monoclonal	Cell Signalling (9239)	1:1000
Phospho Thr37/46 4E-BP1	Rabbit monoclonal	Cell Signalling (2855)	1:1000
Total 4E-BP1	Rabbit monoclonal	Cell Signalling (9644)	1:1000
Phospho Thr389 p70 S6 Kinase	Rabbit monoclonal	Cell Signalling (108D2)	1:1000
Total p70	Rabbit	Cell Signalling	1:1000

S6 Kinase	monoclonal	(49D7)	
Ubiquitin	Mouse monoclonal	Cell Signalling (3936)	1:1000
SUMO2	Rabbit polyclonal	Thermo Fisher Scientific (51-9100)	1:1000
UBC9	Sheep polyclonal	Ron Hay Lab, Dundee	1:1000
RNF4	Chicken polyclonal	Ron Hay Lab, Dundee	1:1000
Phospho Ser473 Akt	Rabbit Monoclonal	Cell Signalling (D9E)	1:1000
Total AKT	Mouse monoclonal	Cell Signalling (40D4)	1:1000
Total ERK1/2	Mouse monoclonal	Transduction Lab (ER16)	1:1000
Phospho Thr202/204 ERK1/2	Mouse monoclonal	Cell Signalling (9106)	1:1000
MDM2 (SMP14+4B2)	Mouse monoclonal	Moravian Biotech	1:1000 (SMP14)+ 1:2000 (4B2)
Phospho-Tyrosine	Mouse monoclonal	Cell Signalling (9411)	1:1000

2.1.3.2 Secondary antibodies

Secondary antibody	Company	Dilution
HRP-anti mouse	Biorad	1:2000 for WB
HRP-anti rabbit	Biorad	1:2000 for WB
HRP-anti sheep	Jackson ImmunoResearch	1:10,000 for WB
HRP-anti chicken	Jackson ImmunoResearch	1:10,000 for WB
Anti-mouse Alexa Fluor 488	Thermo Fisher Scientific	1:1000 for IF
Anti-mouse Alexa Fluor 568	Thermo Fisher Scientific	1:1000 for IF
Anti-rabbit Alexa Fluor 488	Thermo Fisher Scientific	1:1000 for IF
Anti-rabbit Alexa Fluor 568	Thermo Fisher Scientific	1:1000 for IF

2.1.4 siRNA

A SMART-pool consisting of 4 individual siRNAs was purchased from Dharmacon at 5 nM pack size. Upon receipt, the siRNA was resuspended in 250 µl of sterile Nuclease-free water (Thermo Fisher Scientific) to get a stock concentration of 20 µM. It was then aliquoted (to reduce the number of freeze-thaw cycles) and stored at -80 ^{0}C for long-term storage.

Target protein	Oligo name	siRNA sequence (5'-3')
Non-targeting control	siNT	Pool of 4 siRNAs UGGUUUACAUGUCGACUAA UGGUUUACAUGUUGUGUGA UGGUUUACAUGUUUUCUGA UGGUUUACAUGUUUUCCUA
Human PIM1	siPIM1	Pool of 4 siRNAs GAUGGGACCCGAGUGUAUA GAUAUGGUGUGUGGAGAUA UCGAGAGGCCCGACAGUUU GGGGAGAGCUGCCUAAUGG
Human UBC9 (UBE2I)	siUBC9	Pool of 4 siRNAs GGGAAGGAGGCUUGUUUAA GAAGUUUGCGCCCUCAUAA GGCCAGCCAUCACAAUCAA GAACCACCAUUAUUUCACC

Human RNF4	siRNF4	Pool of 4 siRNAs GCUAAUACUUGCCCAACUU GAAUGGACGUCUCAUCGUU GACAGAGACGUAUAUGUGA GCAAUAAAUUCUAGACAAG

2.1.5 Plasmids

Description	Vector	Lab No.	Source
MDM2 WT	pCMV	1127	Published (Hogan *et al.*, 2008)
PIM1 cDNA	pOTB7	1347	Geneservice Ltd. UK
PIM1 cDNA	pCR2.1	1350	Meek Lab stock
GST-PIM1 WT	pGEX-4T-1	1352	Published (Hogan *et al.*, 2008)
PIM1 WT	pSG5-MYC tag	1354	Published (Hogan *et al.*, 2008)
PIM1 K67M (kinase dead)	pSG5-MYC tag	1359	Published (Hogan *et al.*, 2008)
PIM1 K5R	pSG5-MYC tag	1692	Mutagenesis of 1354
PIM1 K24R	pSG5-MYC tag	1693	Mutagenesis of 1354
PIM1 K29, 31R	pSG5-MYC tag	1676	Mutagenesis of 1354
PIM1 K67R	pSG5-MYC tag	1694	Mutagenesis of 1354
PIM1 K71R	pSG5-MYC tag	1677	Mutagenesis of 1354
PIM1 K94, 95R	pSG5-MYC tag	1657	Mutagenesis of 1354
PIM1 K169R	pSG5-MYC tag	1645	Mutagenesis of 1354
PIM1 E171Q	pSG5-MYC tag	1748	Mutagenesis of 1354
PIM1 K183R	pSG5-MYC tag	1678	Mutagenesis of 1354
PIM1 E181A	pSG5-MYC tag	1679	Mutagenesis of 1354

PIM1 K194R	pSG5-MYC tag	1655	Mutagenesis of 1354
PIM1 K313R	pSG5-MYC tag	1695	Mutagenesis of 1354
6Xhis-SUMO1	pcDNA3	1681	Published (Jacobs *et al.*, 2007)
6Xhis-SUMO2	pcDNA3	1682	Published (Jacobs *et al.*, 2007)
6Xhis-SUMO3	pcDNA3	1648	Published (Jacobs *et al.*, 2007)
6Xhis-Ubiquitin	pcDNA3	1432	Published (Hogan *et al.*, 2008)
HA-UBC9	pcDNA3	1680	R. Hay Lab, Dundee
YFP-PIM1 WT	pEYFP-C1	1675	Cloning
YFP-PIM1 WT	pcDNA5/FRT/TO	1715	Cloning
YFP-K169R	pcDNA5/FRT/TO	1724	Mutagenesis and cloning
YFP-E171A	pcDNA5/FRT/TO	1725	Mutagenesis and cloning
YFP-K67M	pcDNA5/FRT/TO	1726	Mutagenesis and cloning
YFP alone	pcDNA5/FRT/TO	1728	Mutagenesis and cloning
Flp recombinase	pOG44	1714	A. Saurin Lab, Dundee
HA-PIAS1	pKW2T	1651	Published (Jacobs *et al.*, 2007)
Flag-PIAS3	pCMV	1649	Published (Jacobs *et al.*, 2007)

HA-PIASy	pKW2T	1652	Published (Jacobs *et al.*, 2007)
Flag-RNF4 (rat)	pcDNA3	1706	Published (Tatham *et al.*, 2008)
Flag-RNF4 (rat) mSIM	pcDNA3	1707	Published (Tatham *et al.*, 2008)
Flag-RNF4 (rat) mRING	pcDNA3	1708	Published (Tatham *et al.*, 2008)
Flag-SENP1 WT	pcDNA3	1698	de la Vega Lab, Dundee
Flag-SENP1 MT	pcDNA3	1699	de la Vega Lab, Dundee
6Xhis-PIM1 WT	pcDNA3	1730	Cloning
PIM1	pBABE-puro	1755	Cloning
K169R	pBABE-puro	1760	Mutagenesis of 1755
E171A	pBABE-puro	1761	Mutagenesis of 1755
K67M	pBABE-puro	1762	Mutagenesis of 1755
6Xhis-PIM1	pHAT2	1754	Cloning
6Xhis-K169R	pHAT2	1756	Mutagenesis of 1754
6Xhis-E171A	pHAT2	1757	Mutagenesis of 1754
6Xhis-K67M	pHAT2	1758	Mutagenesis of 1754
6Xhis-E171Q	pHAT2	1759	Mutagenesis of 1754

2.2 DNA manipulation and analysis

2.2.1 Preparation of competent cells

A 5 ml overnight culture was set up using a previous stock of competent *Escherichia coli* (*E. coli*) cells in LB. No antibiotics were used for preparation of competent DH5α cells. However, chloramphenicol was added at 34 µg/ml for preparation of competent Rosetta2 (DE3) pLys cells. The following day, 200 ml LB was inoculated with 1 ml from overnight culture and cultured in a 37 ^{0}C incubator-shaker until optical density (OD) at 600 nm reached 0.3-0.4. The culture was split into four 50 ml tubes and incubated on ice for 30 min. Cells were pelleted by centrifugation at 2000 xg for 5 min at 4 ^{0}C. The pellets were resuspended in 16 ml of Transformation buffer-1 per 50 ml of original culture and incubated on ice for 15 min. The cells were pelleted again as before and resuspended in 4 ml of Transformation buffer-2 per 50 ml of original culture. The cells were finally aliquoted in desired amounts and stored at -80 ^{0}C until use.

2.2.2 Transformation of plasmid DNA into competent cells

Transformation of competent *E. coli* cells was carried out by mixing 50-100 µl competent cells with 10-100 ng plasmid DNA or 10 µl ligation mix. The transformation reaction was incubated on ice for 20 min followed by heat shock at 42 ^{0}C for 30 seconds. The tube was quickly returned on ice for 2 min. SOC media (Thermo Fisher Scientific, 500 µl) was added immediately to the reaction mix, and the tube further incubated for 1 hour at 37 ^{0}C with gentle agitation. The transformation mix (50 µl) was spread evenly over an LB plate with the appropriate antibiotic and incubated overnight at 37 ^{0}C.

2.2.3 Plasmid Miniprep

Three to six random individual bacterial colonies from the plate were screened for the plasmid of interest by inoculating a mini-culture (5 ml LB supplemented with antibiotics) and incubating it overnight. Next day, 1.5 ml of overnight culture was transferred to fresh eppendorf tubes and centrifuged at 12,000 xg for 2 min at RT. The plasmid DNA was then purified using the QIAprep Miniprep Kit (Qiagen) according to manufacturer's instructions and reagents supplied in the kit.

The bacterial pellet was first resuspended in Buffer P1 (250 µl) followed by addition of Buffer P2 (250 µl). After 5 min incubation at RT, Buffer N3 (350 µl) was added, and centrifuged at 12,000 xg for 10 min at RT. The supernatant was carefully removed and applied to QIAprep spin column (provided with the kit) and centrifuged for 1 min at 12,000 xg at RT. The column was washed successively by adding Buffer PB (500 µl) and Buffer PE (750 µl). The QIAprep column was placed in a fresh eppendorf tube. The DNA was eluted by adding 50 µl of sterile water to the centre of the column, and centrifuging it for 1 min at 12,000 xg. Positive colonies were then identified on the basis of plasmid size by agarose gel electrophoresis and DNA sequencing. An overnight culture (500 ml) of the positive colony was set up and a bacterial glycerol stock was obtained for future use.

2.2.4 Plasmid Maxiprep

Large-scale purification of plasmid DNA was done using PureLink HiPure Plasmid Maxiprep kit (Thermo Fisher Scientific) according to manufacturer's

instructions and reagents supplied in the kit. An overnight culture of *E. coli* (500 ml) was first centrifuged at 4000 xg (Jouan CR412 centrifuge) for 10 min at RT, and the pellet was resuspended in Resuspension Buffer (10 ml). The cell suspension was transferred to a 50 ml centrifuge tube followed by addition of Lysis Buffer (10 ml) and incubated for 5 min at RT. Precipitation Buffer (10 ml) was added immediately to the cell suspension, gently mixed and centrifuged at 15,000 xg (Eppendorf Centrifuge 5804 R) for 10 min at RT. The supernatant was then carefully loaded onto an equilibrated column and allowed to drain by gravity flow to allow binding of the DNA to the column. The column was then washed with Wash Buffer (60 ml) and a sterile 30 ml centrifuge tube was placed under the column after the column was completely drained. Elution buffer (15 ml) was added to the column to elute the DNA, followed by the addition of isopropanol (10.5 ml) to the eluted DNA. The elution tube was centrifuged at 15,000 xg for 30 min at 4 ^{0}C and the pellet was resuspended in 70% ethanol (5 ml), centrifuged again at 15,000 xg for 5 min at 4 ^{0}C. The pellet was then air-dried for 10-15 min and resuspended in 500 µl sterile water. The concentration of isolated DNA was determined by measuring its absorbance at 260 nm using Nanodrop 2000 spectrophotometer (Thermo Fisher Scientific). The DNA was diluted with sterile water to a final concentration of 1 µg/µl and stored at -20^{0}C until further use.

2.2.5 Colony PCR

The colony PCR method was used for screening large number of colonies when the miniprep method failed to identify positive bacterial colonies.

A PCR master mix (220 µl) for 10 reactions was prepared consisting of 2 µl of forward primer (10 µM), 2 µl of reverse primer (10 µM), 4 µl dNTPs (25 mM), 40 µl of 5X Taq Polymerase Buffer (Promega), 6 µl of $MgCl_2$ (25 mM, Promega), 164 µl of sterile water and 2 µl of Taq DNA polymerase (5U/µl, Promega). 20 µl of master mix was aliquoted out into 10 sterile labelled PCR tubes. A single bacterial colony was carefully picked from the plate was subsequently dipped into the PCR mix and subjected to DNA amplification reaction in a thermal cycler using the conditions described below. The bacterial colonies were simultaneously streaked on an ampicillin plate and incubated overnight at 37 ^{0}C. The positive colony was identified by agarose gel electrophoreses of the samples on a 1% agarose gel. A large-scale culture (500 ml) of the positive colony from the ampicillin plate was eventually set up and DNA purified as previously described.

PCR setup

1. Initial Denaturation at 94 ^{0}C for 5 min
2. Denaturation at 94 ^{0}C for 30 seconds
3. Annealing at 60 ^{0}C

} 30 cycles

4. Extension at 72 ^{0}C for 2 min
5. Final Extension at 72 ^{0}C for 10 min

2.2.6 Agarose gel electrophoresis and PCR purification

An aliquot of PCR or plasmid DNA was run on a 1% agarose gel (with 0.5 µg/ml ethidium bromide) alongside a DNA ladder (Fermentas Generuler) as a

reference at 120 V for 40-50 min in 1X TAE running buffer, and viewed under a UV-transilluminator. The amplified product was subsequently purified using QIAquick PCR Purification kit (Qiagen) using reagents supplied in the kit. Five volumes of Buffer PB was added to one volume of the PCR sample, mixed and applied to the QIAquick spin column. To bind DNA, the column was centrifuged at 16,000 xg for 1 min and the flow through was discarded. The column was washed by adding Buffer PE (750 µl) and centrifuged twice as done previously and discarding the flow through. The column was then placed in a sterile labelled eppendorf tube, and 50 µl of sterile water was added to the centre of the QIAquick membrane and centrifuged again to obtain purified PCR product.

2.2.7 Gel extraction

This was performed following restriction digestion of plasmid DNA. The desired DNA fragment (of the right size) was excised carefully from the gel and purified using QIAquick Gel Extraction Kit (Qiagen) according to manufacturer's instructions. In a tube, three volumes of Buffer QG was added to one volume of gel and incubated at 50 ^{0}C for 10 min to dissolve the gel completely. The sample was applied to the column after mixing it with one gel volume of isopropanol and centrifuged for 1 min at 16,000 xg. The column was washed sequentially with Buffer QG (500 µl), Buffer PE (750 µl) respectively and centrifuged 1 min between each wash with the flow through being discarded. The QIAquick column was placed in a fresh tube and the DNA was eluted in 50 µl sterile water by centrifugation at 16,000 xg for 1 min.

2.2.8 A-tailing and TA-cloning of the PCR product

PCR products generated using Taq Polymerase contain adenine base (A) overhangs at the 5' and 3' ends, which can be directly used to ligate into a vector containing thymine (T) overhangs. However, high-fidelity DNA Polymerases such as Pfu, Pfx and KOD generate blunt ended PCR products without any overhangs. Therefore, A-tails or overhangs were added to these PCR products prior to TA-cloning procedure.

The PCR products were A-tailed using NEBNext dA-Tailing module (NEB, UK) to enable ligation into TA Cloning plasmid vector pCR 2.1 (Thermo Fisher Scientific). The A-tailing reaction (25 µl) consisted of 15 µl purified PCR product (~2 µg DNA), 2.5 µl 10X dA-tailing reaction buffer, 1.5 µl Klenow fragment (3'→5' exo$^-$) and 6 µl sterile water. The reaction was incubated in a thermal cycler for 30 min at 37 ^{0}C.

The A-tailed PCR product was ligated into pCR®2.1 vector in a reaction mixture (10 µl) containing 3 µl of A-tailed PCR, 1 µl of 10X Ligation Buffer (Thermo Fisher Scientific), 2 µl of 25 ng/µl pCR2.1 vector (Thermo Fisher Scientific), 1 µl of T4 DNA Ligase (4U/µl, Thermo Fisher Scientific) and sterile water (3 µl). The ligation mixture was incubated overnight at RT.

2.2.9 Restriction digestion and ligation

Restriction digestion of the plasmid was carried out using Type-II Restriction enzymes (New England Biosciences, UK). A restriction digestion reaction (20 µl) was set up containing plasmid DNA (up to 5 µg), 10X NEB Buffer (2 µl), EcoRI (1 µl of 10,000 U/ml) or KpnI (1 µl of 10,000 U/ml) and sterile

water. The reaction was incubated at 37 ^{0}C for 1-2 hours. The reaction was supplemented with 100 µg/ml BSA in case of KpnI digestion. 10X NEB buffer-1 was used for KpnI, and 10X ECoRI buffer for EcoRI enzyme digestions. The restriction enzyme digested products were viewed on a 1% agarose gel.

The insert DNA was ligated into the desired plasmid vector, both cut with the same restriction enzyme, using 1:3 (vector:insert) molar ratio. The vector and insert were incubated overnight at RT with 1X T4 ligase buffer supplied with the kit, and 1 unit T4 DNA ligase (Thermo Fisher Scientific) in a total reaction volume of 20 µl.

2.2.10 Site-directed mutagenesis

Mutagenesis was performed using Quikchange Lightning Site-Directed Mutagenesis kit (Agilent Technologies) according to manufacturer's instructions. Primer pairs used to insert a mutation were designed using the primer design tool available online (http://www.genomics.agilent.com/primerDesignProgram) and purchased from Sigma. The primer pairs have been listed in table 2.1.

Reaction setup and thermal cycling conditions are described below. Following the PCR cycles, 2 µl of DpnI restriction enzyme (from the kit) was added directly to the reaction and incubated at 37 ^{0}C for 10-15 min to digest the methylated, non-mutated parental template DNA. The DNA (2 µl) was then transformed using standard procedure as described in section 2.2.2 into XL-10 Gold-ultracompetent cells (45 µl, kit component) supplemented with β-ME (2 µl, kit component). Several colonies of transformed cells were cultured in

appropriate antibiotic containing media, the DNA was purified and the insert was sequenced to identify a clone with the desired mutation.

Component (stock conc.)	Volume
10X Quikchange Lightning Buffer	5 µl
dNTP mixture	1 µl
QuikSolution reagent	1.5 µl
125 ng/µl Forward primer	1 µl
125 ng/µl Reverse primer	1 µl
100 ng/µl Template DNA	1 µl
Quikchange Enzyme mix	1 µl
Sterile nuclease free water	38.5 µl
Total	**50 µl**

The conditions followed for PCR were as follows:

1. Initial denaturation at 95 ^{0}C for 2 min
2. Denaturation at 95 ^{0}C for 20 seconds
3. Annealing at 60 ^{0}C for 10 seconds
4. Extension at 68 ^{0}C for 30 seconds/kb of plasmid length

(2–4: 18 cycles)

5. Final extension at 68 ^{0}C for 5 min

Table 2.1 Primers used for mutagenesis

Primer name	Sequence (5'-3')
PIM1 K5R For	TTC AAT GCT CTT GTC CAG AAT CAA CTC GCT TTG CCC
PIM1 K5R Rev	GGG CAA GCG AGT TGA TTC TGG ACA AGA GCA TTG AA
PIM1 K24R For	GGG CGC CAG CCT GGT GGC GTG CA
PIM1 K24R Rev	TGC ACG CCA CCA GGC TGG CGC CC
PIM1 K29, 31R For	AGG GGC TCC CTC TCC CTG CCG GGC GCC
PIM1 K29, 31R Rev	GGC GCC CGG CAG GGA GAG GGA GCC CCT
PIM1 K67R For	CTC CAC GTG TCT GAT GGC CAC CGG CAA GTT
PIM1 K67R Rev	AAC TTG CCG GTG GCC ATC AGA CAC GTG GAG
PIM1 K67M For	GTC CTT CTC CAC GTG CAT GAT GGC CAC CGG CA
PIM1 K67M Rev	TGC CGG TGG CCA TCA TGC ACG TGG AGA AGG AC
PIM1 K71R For	AAA TCC GGT CCC TCT CCA CGT GTT TGA TGG CCA
PIM1 K71R Rev	TGG CCA TCA AAC ACG TGG AGA GGG ACC GGA TTT
PIM1 K94, 95R For	CCG AGC TCA CCC TCC TCA GCA GGA CCA CTT CCA TGG

PIM1 K94, 95R Rev	CCA TGG AAG TGG TCC TGC TGA GGA GGG TGA GCT CGG
PIM1 K169R For	GTG CTC CAC CGC GAC ATC AGG GAC GAA AAC ATC
PIM1 K169R Rev	GAT GTT TTC GTC CCT GAT GTC GCG GTG GAG CAC
PIM1 E171A For	CCG CGA CAT CAA GGA CGC AAA CAT CCT TAT CGA CC
PIM1 E171A Rev	GGT CGA TAA GGA TGT TTG CGT CCT TGA TGT CGC GG
PIM1 E171Q For	GAG GTC GAT AAG GAT GTT CTG GTC CTT GAT GTC GCG GTG
PIM1 E171Q Rev	CAC CGC GAC ATC AAG GAC CAG AAC ATC CTT ATC GAC CTC
PIM1 E181A For	CGA TGA GCT TGA GCG CGC CGC GAT TGA GG
PIM1 E181A Rev	CCT CAA TCG CGG CGC GCT CAA GCT CAT CG
PIM1 K183R For	GAA GTC GAT GAG CCT GAG CTC GCC GCG ATT G
PIM1 K183R Rev	CAA TCG CGG CGA GCT CAG GCT CAT CGA CTT C
PIM1 K194R For	GAC GGT GTC CCT GAG CAG CGC CCC C
PIM1 K194R Rev	GGG GGC GCT GCT CAG GGA CAC CGT C
PIM1 K313R For	GAA AGG CTG CTA TCT GCT GGG CCC CGG
PIM1 K313R Rev	CCG GGG CCC AGC AGA TAG CAG CCT TTC

2.2.11 DNA sequencing

Following ligation or mutagenesis, the insert was sequenced to confirm the correct nucleotide sequence and to rule out any unwanted incorporation or deletion of bases in the insert. DNA sequencing was carried out by the Genetics Core Services at Ninewells Hospital and Medical School.

Table 2.2 Sequencing primers

Vector/Insert	Primer name	Sequence (5'-3')
pcDNA3	T7 Forward	TAA TAC GAC TCA CTA TAG GG
pcDNA3	SP6 Reverse	CAT TTA GGT GAC ACT ATA G
pcDNA5/FRT/TO	CMV Forward	CGC AAA TGG GCG GTA GGC CTG
pcDNA5/FRT/TO	BGH Reverse	TAG AAG GCA CAG TCG AGG
pSG9M	T7 Forward	TAA TAC GAC TCA CTA TAG GG
pCR 2.1	M13 Forward	TGT AAA ACG ACG GCC AGT
pCR 2.1	M13 Reverse	CAG GAA ACA GCT ATG ACC
pHAT2	T7 Forward	TAA TAC GAC TCA CTA TAG GG
pBABE-puro	pBABE Forward	CTT TAT CCA GCC CTC AC
PIM1 internal	Seq Reverse-1	GAC TCC AGG GGC TCC TTC TC
PIM1 internal	Seq Reverse-2	GCC AAG CAC CAT CTA ATG AGA
PIM1 internal	Seq Forward	TCT CAT TAG ATG GTG CTT GGC

2.3 Plasmid construction

2.3.1 Generation of 6Xhis tagged PIM1 mammalian expression vector

To allow purification of PIM1 under denaturing conditions using Ni^{2+}-NTA beads, a hexa-histidine tagged PIM1 plasmid was generated in pcDNA3 mammalian expression vector. Full-length human *PIM1* cDNA sequence was PCR amplified from Mammalian Gene Collection (MGC) clone (available as glycerol stock DWM 1347) using primer pair described below. The forward primer was designed to insert a 5' EcoRI restriction site followed immediately by transcription start site (ATG) with six histidine tag codons to be in frame with *PIM1* coding sequence. The reverse primer contained a SalI restriction site. EcoRI and SalI sites were chosen for two main reasons. Firstly, they are absent from the *PIM1* coding sequence. Secondly, presence of these sites allows cloning into the multiple-cloning site (MCS) of commonly used expression vectors such as pcDNA3.

The PCR product was then purified and A-tailed using the procedure described in section 2.2.6 and 2.2.8 respectively. The A-tailed PCR product was ligated directly into pCR2.1 by means of TA-cloning. Ligated plasmid was transformed into DH5α cells and minipreps from randomly selected colonies were sequenced to verify the DNA sequence. The pCR2.1 vector itself contains EcoRI site at 5' and 3 ends; hence EcoRI digestion alone released the 6Xhis-*PIM1* fragment, which was then ligated into EcoRI digested pcDNA3 vector

Component (stock conc.)	Volume
10X PfX Buffer	5 µl
10 mM dNTP	1.5 µl
25 mM $MgSO_4$	2 µl
10 µM Forward primer	1 µl
10 µM Reverse primer	1 µl
10 ng/µl Template DNA (1347)	1 µl
Pfx Polymerase	1 µl
Sterile nuclease free water	37.5 µl
Total	**50 µl**

The conditions followed for PCR were as follows:

1. Initial denaturation at 94 ^{0}C for 5 min
2. Denaturation at 94 ^{0}C for 30 seconds
3. Annealing at 56 ^{0}C for 1 min
4. Extension at 72 ^{0}C for 2 min

} 30 cycles

5. Final extension at 72 ^{0}C for 10 min

Primer name	Sequence (5' – 3')
6Xhis-*PIM1* Forward primer	AGA ATT CAT GGC TCA TCA TCA TCA TCA TCA TGG GAT GCT CTT GTC CAA AAT C
6Xhis-*PIM1* Reverse primer	AGT CGA CAG AAA CTA TTT GCT GGG CCC CGG CGA CAG GCT GTG

2.3.2 Generation of YFP-tagged PIM1 mammalian expression vector

Full-length human *PIM1* cDNA sequence was PCR amplified from Mammalian Gene Collection (MGC) clone (available as glycerol stock DWM 1347) using primer pair described below and the same PCR conditions as described in 2.3.1. The forward primer was designed to insert a 5' EcoRI restriction site and the reverse primer contained a 3'-XbaI restriction site to be in frame with the pEYFP-C1 vector (containing a 5'-Yellow Fluorescent Protein tag).

Primer name	**Sequence (5' – 3')**
***PIM1* PCR Forward primer**	AGA ATT CCA TGC TCT TGT CCA AAA TCA ACT CGC
***PIM1* PCR Reverse primer**	ATC TAG AGC CAG AAA GGC TGC TAT TTG C

The PCR product was then purified and A-tailed using the procedure described previously. The A-tailed PCR product was ligated directly into pCR2.1 by means of TA-cloning. Ligated plasmid was transformed into DH5α cells and minipreps from randomly selected colonies were sequenced to verify the DNA sequence. Although the insert contained both EcoRI and XbaI sites, EcoRI digestion was sufficient to release the desired *PIM1* fragment as the pCR2.1 vector contains internal EcoRI sites flanking the ligated insert. The vector pEYFP-C1 was hence also digested with only EcoRI, and the *PIM1* fragment was ligated directly into it. Positive clones were identified by DNA sequencing.

2.3.3 Generation of tet-inducible YFP-tagged PIM1 mammalian expression vector

A cDNA encoding YFP-PIM1 was PCR amplified from pEYFP-PIM1 (DWM 1675) using a forward primer containing 5' KpnI site and a reverse primer with 3' SalI site as described in the table below. As control, *YFP* alone was also PCR amplified. The amplified fragments were PCR purified, A-tailed and ligated into pCR2.1 vector by TA-cloning procedure. Site-directed mutagenesis was performed with the YFP-PIM1/pCR2.1 plasmid to generate the K169R, E171A, and K67M mutants.

Primer name	**Sequence (5' – 3')**
YFP-*PIM1* Forward primer	AGG TAC CAT GGT GAG CAA GGG CGA GGA G
YFP-*PIM1* Reverse primer	AGT CGA CGC CAG AAA GGC TGC TAT TTG C
***YFP* only PCR Forward primer**	AGG TAC CAT GGT GAG CAA GGG CGA GGA G
***YFP* only PCR Reverse primer**	TGG TAC CCT AGA AGC TTG AGC TCG AGA TCT G

Sequencing of the pCR2.1/YFP-PIM1 plasmid showed that the insert had ligated in the opposite orientation such that it now had KpnI site on both 5' and 3' (internal site present in pCR2.1) ends. Therefore, KpnI digest alone was

sufficient to release the *YFP-PIM1* fragment. The vector containing tet-inducible elements pcDNA5/FRT/TO was also digested with only KpnI, and both the insert and the plasmid ligated to obtain YFP-PIM1/pcDNA5/FRT/TO plasmid. Following transformation, colonies were grown and minipreps done. Plasmids were sequenced and checked for YFP expression following transfection under a fluorescent microscope (EVOS FLoid Cell Imaging platform, Thermo Fisher Scientific).

2.3.4 Generation of 6Xhis tagged PIM1 bacterial expression vector

The plasmid vector for generating 6Xhis-PIM1 fusion protein for protein production and purification, pHAT2, was a kind gift from Dr. Marko Hyvonen, University of Cambridge (UK). The *PIM1* insert was obtained by EcoRI restriction digestion of DWM 1350, and ligated into EcoRI digested pHAT2 vector. The resulting ligation was transformed into competent cells and a 5 ml overnight culture was set up to isolate plasmid DNA. Positive clones were identified by sequencing using T7 Forward and SP6 reverse primers. Site-directed mutagenesis was performed with DWM 1754 plasmid to generate the K169R, E171A, K67M and E171Q mutants.

2.3.5 Generation of PIM1 expression vector for retrovirus production

PIM1 cDNA was obtained by EcoRI restriction digestion of plasmid DWM 1350. The fragment was then cloned into the EcoRI site of pBABE-puro vector using standard cloning procedure, and mutagenesis was performed to generate K169R, E171A and K67M mutants.

2.4 Protein expression, purification and analysis

2.4.1 Recombinant protein expression in *E. coli*

The *E. coli* strain Rosetta 2 (DE3) pLys (Novagen) was used for the expression of GST and 6Xhis fusion proteins. This strain of bacteria was chosen as it supplies tRNAs for the seven codons rarely used in *E. coli* (AUA, AGG, AGA, CUA, CCC, GGA and CGG) on a compatible chloramphenicol-resistant plasmid pRARE, thus allowing efficient translation of eukaryotic proteins.

For GST-PIM1 expression, cells were transformed with the desired pGEX-4T-1 derivative plasmids (DWM 1352). For 6Xhis-PIM1 protein expression, cells were transformed with pHAT2 derivative plasmids (DWM 1754, 1756, 1757, 1758, 1759). Approximately 50 µl of transformation mix was plated on LB-agar plates containing 100 µg/µl ampicillin, and incubated overnight at 37 ^{0}C. The following day, a single colony was picked and grown overnight in 5-10 ml LB selection media at 37 ^{0}C in an incubator-shaker.

For protein expression, 400 ml LB selection media was inoculated with 10 ml of starter culture and grown at 37 ^{0}C in an incubator-shaker until OD at 600 nm reached between 0.4-0.6 (usually in 3-4 hours). An aliquot (1 ml) was taken at this point to analyse as pre-induction sample for later analysis, after which IPTG was added to a final concentration of 0.2 mM. The culture was then incubated at 30 ^{0}C with shaking at 225 rpm for a further 3 hours, after which another 1 ml aliquot (post-induction) was taken to analyse on gel. The cells were pelleted by centrifugation at 4000 xg for 20 min at 4 ^{0}C, supernatant was discarded and the pellet was stored at -80 ^{0}C once prior to protein extraction.

It is necessary to check protein induction before performing the next protein purification step. To do this, the pre- and post-induction samples were centrifuged at maximum speed for 2 min at RT and the pellet was lysed in 50 µl 2X sample buffer. The lysate was then sonicated once or twice at 30% amplitude for 20 sec, centrifuged at maximum speed for 10 min at RT, quantified as described under section 2.4.4, and ran on an 8% SDS-polyacrylamide gel. The gel was then stained with coomassie as described under 2.4.7 to visualise the protein bands. The desired recombinant protein appears as a clearly distinguishable band running at the correct molecular weight in the post-induction sample, but is absent in the pre-induction sample.

2.4.2 GST-PIM1 protein purification

Once protein induction was successfully confirmed, the pellet was thawed on ice, lysed in 20 ml of B-PER Complete Bacterial Protein Extraction Reagent (Thermo Fisher Scientific). It was then incubated for 30 min at RT on a tube rotator. Since B-PER lysis buffer contains a non-ionic detergent in a Tris-buffer with lysozyme and universal nuclease, it eliminates the need of sonicating the bacterial lysate. Following incubation, the lysate was centrifuged at 10,000 xg for 20 min at 4 ^{0}C and the pellet discarded.

The GST-fusion protein was then affinity-purified using Glutathione Sepharose 4B (GST) beads (Amersham). GSH beads were prepared by washing them extensively with 10 volumes of PBS to remove any residual ethanol (preservative) and stored as 50% slurry in PBS at 4 ^{0}C until use.

Approximately 1 ml of GST beads was then added to the lysate in a 15 ml falcon tube, placed on a tube rotator and incubated at 4 ^{0}C for 2 hours to allow binding of GST-fusion protein to the beads. The beads were pelleted gently by centrifugation at 400 xg for 2 min, and then washed three times (10 min each) with 10 ml of 50 mM Tris pH 7.5 on a tube rotator at 4 ^{0}C. The GST-fusion protein was eluted by incubating the beads with 500 µl of 10 mM reduced glutathione in 50 mM Tris (final pH readjusted to 7.5) for 30 min on a rotator at RT. The beads were centrifuged as before and the supernatant was collected (elution 1). The elution process was repeated again (elution 2) and stored at 4 ^{0}C until further analysis by SDS-PAGE.

A dialysis was set up to remove the reduced glutathione from the elutions. The positive fraction (elution 1 or 2, or both pooled together) was carefully injected into a Slide-A-Lyzer Dialysis cassette (10 K MWCO, Thermo Fisher Scientific) and placed in a beaker containing dialysis buffer (50 mM Tris pH 7.5, 20% glycerol) and a magnetic stirrer overnight at 4 ^{0}C. The concentration of the purified protein was estimated by SDS-PAGE, using known amounts of BSA as standards, aliquoted and stored at -80 ^{0}C until further use.

2.4.3 Purification of 6Xhis-PIM1 and mutants

Protein induction was first confirmed by SDS-PAGE of the pre and post-induction samples. The pellet was thawed on ice, lysed in 20 ml of B-PER Complete Bacterial Protein Extraction Reagent (Thermo Fisher Scientific) and incubated for 30 min at RT on a tube rotator. Following incubation, the lysate was centrifuged at 10,000 xg at 4 ^{0}C for 20 min and the pellet discarded.

Imidazole was added to the clarified lysate at 10 mM final concentration. The 6Xhis-fusion protein was then affinity-purified using Ni^{2+}-NTA agarose beads (Qiagen). The beads were prewashed extensively with 10 volumes of PBS to remove any residual ethanol (preservative) and stored as 50% slurry in B-PER reagent at 4 ^{0}C until use. The following steps were performed in a cold room. Approximately 1 ml of Ni^{2+}-NTA beads was added to a Poly-prep column (Biorad) with the lysate, and allowed to flow through by gravity. The flow-through was re-loaded on the column twice to maximise protein binding. The column was then washed thrice with 20 ml cold wash buffer. Approximately 3-4 ml of fresh elution buffer was added to the column, and elutions were collected in 500 µl fractions. Ten microliters of each eluted protein fraction was run on a gel and stained with coomassie to identify the positive fractions. The desired elutions were pooled and dialysis was set up to remove the imidazole. The elution was carefully injected into a Slide-A-Lyzer Dialysis cassette (10 K MWCO, Thermo Fisher Scientific) and placed in a beaker containing dialysis buffer and a magnetic stirrer overnight at 4 ^{0}C. The concentration of the purified protein was estimated by SDS-PAGE, using known amounts of BSA as standards, aliquoted and stored at -80 ^{0}C until further use.

2.4.4 Protein extraction and quantification

Cells were washed twice in PBS and lysed directly in 2X SDS sample buffer without reducing agent, and transferred to labelled eppendorf tubes. Lysates were then sonicated once at 30% amplitude for 20-30 sec using a SONICS Vibra-Cell sonicator (model VCX 130). Sonicated lysates were

centrifuged for 10 min at 12,000 xg at RT to pellet the insoluble particles. Total protein concentration in the cell lysates was determined using BCA-DC protein assay kit (Biorad) in a 96-well plate format. In brief, Reagent A and Reagent S were first combined in a ratio of 50:1 (v/v), and 25 µl of this solution was transferred per well of a 96-well plate. This was followed by addition of 17 µl water and 3 µl of cell lysate or protein sample per well of a 96-well plate. 200 µl of Reagent B was then added per well, and the plate was incubated in the dark for 15 min. At this point, the absorbance of each sample was measured at 750 nm using a GloMax-Multi detection system (Promega). To obtain protein concentration (in mg/ml), the absorbance values were plotted on MS Excel against a pre-determined standard curve generated with BSA. The cell lysates were diluted to the desired concentration using 2X SDS sample buffer and DTT was added at a final concentration of 100 mM. Samples were heated to 95 ^{0}C for 5 min, allowed to cool and ran on a polyacrylamide gel for western blotting.

2.4.5 SDS-PAGE using hand made gels

Protein samples were separated based on their molecular weight on a sodium dodecyl sulfate-polyacrylamide gel (SDS-PAG) of the desired percentage. 5 µl of protein marker (PageRuler, Fermentas) was loaded as a reference on the gel. The composition of polyacrylamide gel used is given in table 2.3. The gels were run at 120 V until the samples had stacked properly and began to separate. The gel was then run at 170 V till the dye front had almost reached the bottom of the gel.

Table 2.3 Composition of SDS-PAGE gels

STACKING GEL	**Volume for 1 gel**
Sterile water	2.15 ml
1.25 M Tris pH 6.8	300 µl
30% (w/v) Acrylamide (Severn Biotech Ltd)	500 µl
10% SDS	30 µl
10% APS	25 µl
TEMED	2.5 µl

SEPARATING GEL	**8%**	**10%**	**12.5%**
Sterile water	3.95 ml	3.3 ml	2.475 ml
1.25 M Tris pH 8.8	3 ml	3 ml	3 ml
30% (w/v) Acrylamide	2.65 ml	3.3 ml	4.125 ml
10% SDS	100 µl	100 µl	100 µl
10% APS	100 µl	100 µl	100 µl
TEMED	7.5 µl	7.5 µl	7.5 µl

2.4.6 SDS-PAGE using precast gels

Novex NuPAGE Precast gels (4-12% Bis-Tris) were used in conjugation with XCell SureLock Mini Cell Electrophoresis system using 1X MOPS or 1X MES running buffer at 180 V till the dye front reached the bottom of the gel. The gel was then either transferred onto a nitrocellulose membrane for western blotting or stained with coomassie. All the above-mentioned reagents and equipment were purchased from Thermo Fisher Scientific.

2.4.7 Coomassie staining of gels

The gel was incubated with 20-30 ml coomassie stain for 1 hour at RT with gentle shaking. Following this, the gel was washed with Destainer-I for 1 hour at RT on a shaker. The gel was further washed with Destainer-II overnight or until the background was clear and the protein bands became visible. The washing buffer was changed frequently during the procedure.

2.4.8 Western Blotting

The protein samples (on SDS-PAG) were transferred onto a nitrocellulose membrane (Hybond, GE Healthcare) using a wet transfer blotting unit (Mini Trans-Blot Cell, Bio-Rad). The gel sandwich was prepared as follows: one pre-wetted filter paper was placed on a pre wetted fibre pad placed on the cassette, and the gel gently placed over it. Next, a pre wetted NC membrane was placed on top of the gel and stacked on top with a filter paper and a fibre pad (both pre wetted) respectively. The cassette was placed in the electrophoresis tank module filled with transfer buffer and ran at 100 V constant for 1 hour.

Nitrocellulose membranes were routinely stained with Ponceau S solution after protein transfer to check transfer efficiency and equal protein loading.

For protein detection, the membranes were first blocked in 5% non-fat dry milk in TBST (Marvel) for 1 hour at RT (30 min for endogenous PIM1), following overnight incubation with primary antibodies either in 5% milk or 5% BSA (as recommended by the antibody manufacturer). Next day, the membranes were washed thrice, 5 min each, in TBST on a roller. The membranes were incubated for one hour at RT in secondary antibodies diluted in 5% milk/TBST. Excess antibody was removed by washing as done previously. Equal volume of ECL solution-1 and ECL solution-2 were mixed in a tube and added to the membranes for chemiluminescent detection of proteins on the membranes. Images were acquired either on a film (Konica Monolta) using an X-ray film processor (SRX-101A, Konica Minolta) or using the ChemiDoc MP Imaging system (Biorad).

2.5 Cell culture and other methods

2.5.1 Cell lines

Cell lines described in the table 2.4 were cultured in a humidified 5% CO_2 incubator (Heraeus, HeraCell) at 37 ^{0}C. Cell lines were maintained in Dulbecco's Modified Eagle Medium (DMEM, Thermo Fisher Scientific) supplemented with 10% (v/v) fetal bovine serum (FBS, Biosera) and 2 mM L-glutamine (Thermo Fisher Scientific). HeLa-FRT cells expressing YFP-PIM1 were maintained in media containing 200 µg/ml hygroMYCin B. U2OS-FRT cells expressing YFP-PIM1 were maintained in media containing 100 µg/ml hygroMYCin B. DU145 cells stably expressing PIM1 were maintained in media containing 0.25 µg/ml puroMYCin.

H1299 and COS7 cells were from Meek Lab liquid nitrogen stocks (originally purchased from ATCC). HeLa-FRT cells were a kind gift from Prof. Stephen Taylor (University of Manchester) and U2OS-FRT cells were a kind gift from Prof. Kevin Hiom (University of Dundee). DU145 cells were a kind gift from Dr. Ghulam Nabi (University of Dundee) and Phoenix-AMPHO cells were a kind gift from the Skin tumour Laboratory (University of Dundee).

Table 2.4 Cell lines

S. No	Cell Line	Description	Media
1.	H1299	Human non-small cell lung cancer; derived from metastatic lymph node	DMEM
2.	COS7	African green monkey kidney cells; SV40 transformed	DMEM
3.	HeLa-FRT (Parental)	Human cervical cancer; HPV positive	DMEM
4.	U2OS-FRT (Parental)	Human osteosarcoma (bone cancer)	DMEM
5.	DU145	Human prostate cancer; derived from brain metastatic site	DMEM
7.	Phoenix-AMPHO	Human embryonic kidney cells; adenovirus E1a and SV40 transformed HEK293T cells	DMEM

2.5.2 Subculturing cells

Cell lines were maintained in growth phase by subculturing them every 2-3 days or when they reached 80-90% confluency in a Laminar flow hood (Scanlaf). Cells were washed twice in pre-warmed sterile 1X PBS before the addition of 1-2 ml 0.25 % Trypsin-EDTA (Thermo Fisher Scientific), following which they were placed back in the incubator for 2-3 min to allow the cells to detach from the plate. Detached cells were re-suspended in medium containing FBS, and the desired percentage of cells was transferred to a new dish containing fresh media, and placed back in the CO_2 incubator.

2.5.3 Cell Seeding

Cells were trypsinised and resuspended in an appropriate volume of medium. A small aliquot of cell suspension was added to each end of an Improved Neubauer Haemocytometer (1/400m^2, Hawksley UK) and cells within four corner square grids were counted by a microscope. The average number of cells recorded in the grids represented: number of cells x10^4 per ml in the cell suspension. The suspension was then diluted as required for the experiment.

2.5.4 Cryopreservation of cells

Cells from a confluent T75 flask were trypsinised and resuspended in 10 ml of complete growth media. The cells were pelleted gently by centrifugation at 1000 xg for 3 min at RT, prior to aspirating the growth media. The cell pellet was then resuspended in 5 ml or 10 ml (depending on pellet size) cold freezing

media. A total of 1 ml cell suspension was transferred to individual cryogenic vials (Corning), and incubated on ice for 15 min. The vials were placed in a Cryo 1 ^{0}C Cool box (VWR) to ensure slow freezing and transferred to a -80 ^{0}C freezer for 2 days. The frozen vials were subsequently transferred to a liquid nitrogen tank for long-term preservation.

2.5.5 Revival of cryopreserved cells

A frozen vial of the desired cell line was removed from the liquid nitrogen tank, and thawed rapidly in a 37 ^{0}C water bath. The thawed cells were transferred to a 15 ml tube and 9 ml of pre-warmed media was added before cell centrifugation at 1000 xg for 3 min at RT. The media was aspirated and the cell pellet was resuspended in 10 ml fresh media and transferred to a T75 flask containing 10 ml media. The cells were placed in a humidified CO_2 incubator at 37 ^{0}C. Cells were also tested for MYCoplasma contamination prior to using them for experiments.

2.5.6 Mycoplasma testing

Cell lines were tested for the presence of MYCoplasma using the MycoAlert Mycoplasma detection kit (Lonza) according to manufacturer's instructions. Cell lines to be tested were grown for 4-7 days in the same growth media, and an aliquot of growth media was then used in the test. The growth media (around 1 ml) was centrifuged at 1000 xg for 3 min at RT to pellet any cells, and 100 µl of the supernatant was added to a well of white-bottom 96-well microplate. A total of 100 µl MycoAlert reagent was added to the sample and

incubated for 5 min at RT following which luminescence was detected on a GloMax-Multi detection system (Promega). This reading was designated as A. Next, 100 µl of MycoAlert substrate was added to the same sample and incubated for 10 min at RT, followed by reading luminescence as before. This reading was designated B. The value determining the Mycoplasma status was obtained by dividing reading B by reading A (or B/A). A value of <0.9 is indicative of no Mycoplasma contamination (negative), 0.9-1.2 indicative of borderline contamination and >1.2 indicative of Mycoplasma contamination (positive).

2.5.7 Transient transfection using Lipofectamine 2000

Cells were seeded 24 hours prior to transfection to achieve a confluence of ~70% on the day of transfection. Plasmid transfection was performed using DNA (µg) to Lipofectamine 2000 (µl) ratio of 1:3 according to manufacturer's instructions. Firstly, the plasmid DNA to be transfected was diluted in OptiMEM in a tube. In a second tube, the required amount of Lipofectamine 2000 was diluted in the same volume of OptiMEM as the plasmid mix and incubated for 5 min at RT. The transfection mixes were combined 1:1 (v/v), and incubated for 15-20 min at RT (see table below for volumes). After this, the mix was added dropwise to the cells, the media in the plates mixed and the cells returned to the CO_2 incubator. The cells were usually harvested 24-72 hours post transfection depending on the nature of the experiment.

Plate	Final volume of transfection mix	Maximum amount of plasmid used	Maximum volume of Lipofectamine 2000 used
6-well (per well)	200 µl	6 µg	18 µl
10 cm^2	1000 µl	15 µg	45 µl

2.5.8 Transient transfection using Fugene HD

Cells to be transfected were seeded in a 6-well plate 24 hours before transfection at 60-70% confluency. In general, cells were transfected using a DNA (µg) to Fugene HD (µl) ratio of 1:6 according to manufacturer's instructions. Prior to transfection, both serum free media and Fugene HD were equilibrated to RT. For each well to be transfected, the required amount of DNA was diluted in 100 µl serum free media in a tube. In another tube, the calculated amount of Fugene HD was diluted in 100 µl serum free media. After 5 min incubation at RT, the diluted Fugene HD was mixed with DNA and allowed to sit for 15 min at RT. Transfection mixes were then added dropwise to cells, mixed by gentle swirling, and incubated for at least 24 hours in a CO_2 incubator before checking protein expression.

2.5.9 siRNA knockdown using Lipofectamine RNAiMAX

The optimal seeding density of cells for a successful siRNA transfection experiment was first determined by plating cells at varying densities ranging from $0.25x10^5$ to $2x10^5$ cells/well in a 6-well plate. The cell number that gave 80-90% confluent cells 72 hours (for a 48 hour siRNA treatment) or 96 hours (for a 72 hour siRNA treatment) post seeding was chosen as the optimum seeding density.

All siRNA transfections were performed using Lipofectamine RNAiMAX reagent and 20 μM siRNA stocks as listed under 2.1.4. The method described here is for one well of a 6-well plate. Briefly, 3 μl of siRNA was first added to 100 μl OptiMEM in an eppendorf tube and mixed gently by pipetting up and down. In another eppendorf tube, 4 μl of RNAiMAX was added to 100 μl OptiMEM, mixed by pipetting and incubated for 5 min at RT. Following incubation, the diluted RNAiMAX solution was mixed with the siRNA solution, mixed by pipetting, and incubated for 15-20 min at RT. During this time, the media on the 6-well plate was replaced by adding 2.8 ml of fresh media. Finally, The siRNA-RNAiMAX mix was added to the cells in a dropwise manner, and incubated further for 48 or 72 hours at 37 ^{0}C in a CO_2 incubator. Final siRNA concentration used was 20 nM.

2.5.10 Generation of tet-inducible cell lines

Stable cell lines expressing WT PIM1 or different mutants were created using the Flp-In TRex system (Thermo Fisher Scientific). This system was chosen as it enables targeted integration of gene of interest into a single FRT (Flp Recombination Target) site present in Flp-In cells using Flp-recombinase

mediated DNA recombination. The resulting cell lines are hence ‘isogenic’ and prevent spurious effects observed with random integration of plasmid DNA into host cell line. The Flp-In cells also stably express the Tet-repressor protein (from pcDNA6/TR plasmid) that allows us to modulate levels of expression of our gene of interest in a tetracycline-inducible manner. A schematic diagram illustrating the process of creating a cell line by this method is shown in figure 2.1.

HeLa-FRT (parental) or U2OS-FRT (parental) cells were used to generate tetracycline inducible YFP-PIM1-expressing cell lines. Cells ($1x10^5$) were seeded in a 6-well dish and transfected the following day with 0.1 µg pcDNA5/FRT/TO (encoding YFP-PIM1 or YFP alone) and 0.3 µg pOG44 (encoding Flp-recombinase) using Fugene HD. Two days post transfection, cells were trypsinised and reseeded in 10 cm^2 plates in complete DMEM media containing 200 µg/ml hygromycin B (for HeLa-FRT) or 100 µg/ml hygromycin B (for U2OS-FRT). The cells were allowed to grow, with media being changed every 2-3 days, until colonies began to appear (usually 2 weeks). Colonies that survived hygromycin B selection were considered positive for the integration of pcDNA5/FRT/TO. All colonies for each plasmid were pooled, expanded and frozen before testing them for expression. Cell lines were tested for expression of protein by the addition of doxycycline at 1 µg/ml, in the first instance, 24 hours prior to lysis for western blotting or checking under a fluorescence microscope. Hereafter, the resulting cell lines were maintained in complete DMEM with 200 µg/ml or 100 µg/ml hygromycin B to ensure propagation of positive clones. Hygromycin B was not used in actual experiments.

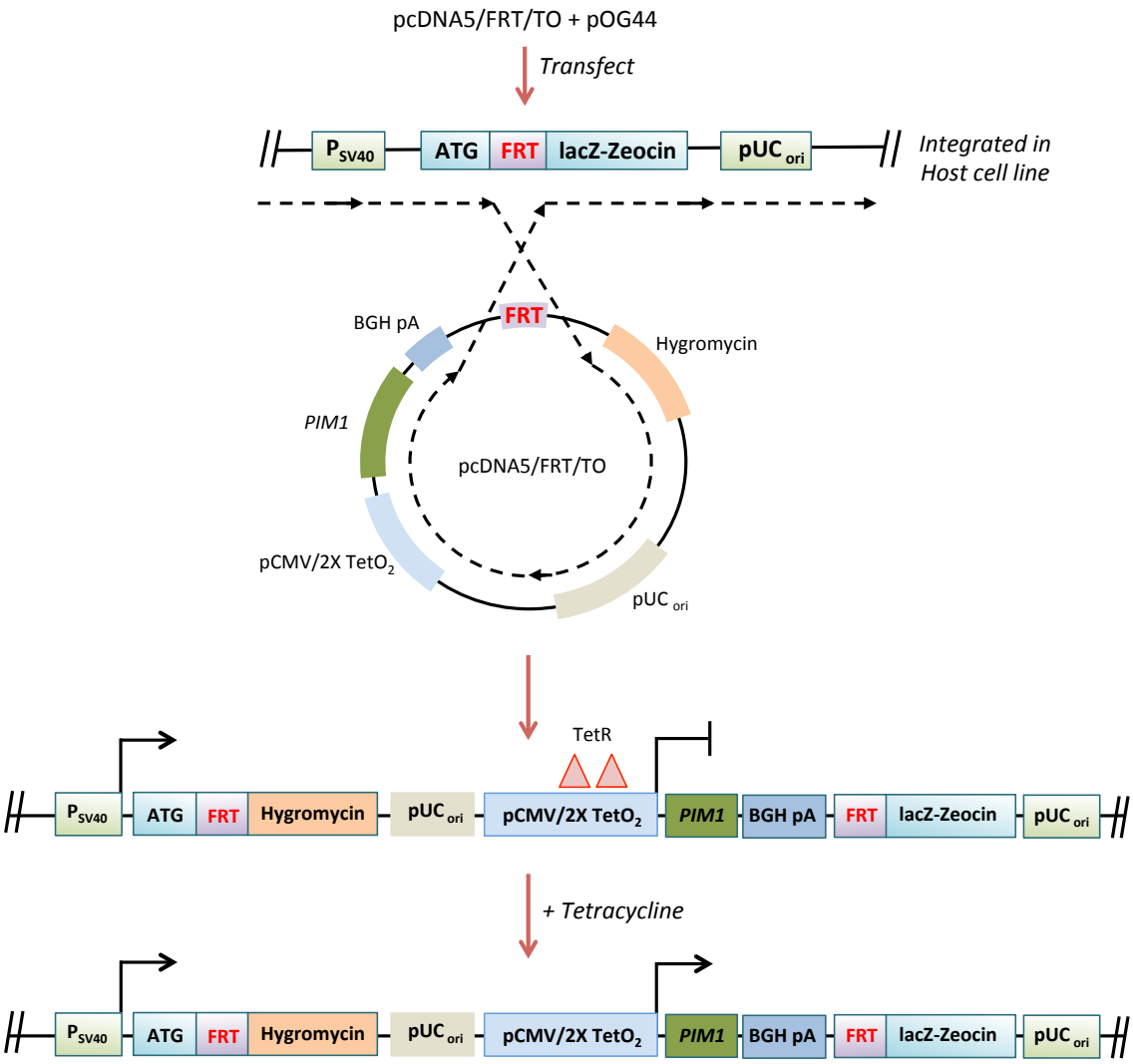

Figure 2.1 Generation of tet-inducible cell lines using Flp-In system (Adapted from Flp-In TRex manual) The HeLa-FRT or U2OS-FRT cells used here already contain a stably integrated copy of the FRT gene locus, which allows us to insert a gene of interest in this locus by homologous recombination. In the first step, pcDNA5/FRT/TO vector containing the gene of interest (YFP-PIM1) is cotransfected with pOG44 plasmid in these cells. The Flp recombinase expressed from the pOG44 plasmid catalyses a recombination event between the FRT sites in the host cell line and the pcDNA5/FRT/TO vector. Successful integration confers hygromycin resistance to the cells. The host cell lines used here also stably express the Tet repressor protein (TetR), which binds to the 2X Tet operator ($TetO_2$) sequences and inhibits expression of gene of interest. Tetracycline addition results in a change in conformation of TetT and its dissociation from the $TetO_2$, thus activates expression of the gene of interest in these cells.

2.5.11 Generation of DU145-PIM1 cell lines using retroviral transduction

The retroviral packaging cell line, Phoenix-AMPHO, expressing the viral gag-pol and envelope proteins was used for the production of replication-incompetent retroviral particles. The viral package signal, transcription initiation and other processing elements, along with the gene of interest (*PIM1*) were expressed from the pBABE-puro vector, derived from the Moloney murine leukemia virus (MMLV). The following procedure was carried out in accordance with Biosafety Level-2 protocols.

Phoenix cells were seeded at $4x10^6$ cells in T25 flasks and transfected the following day with 5 µg pBABE-puro plasmid (expressing WT PIM1 or mutants) using Lipofectamine 2000 as described previously. After 48 hours, the cells were expanded into a T175 flask and further incubated till the cells reached 80-90% confluency. At this point, the media was replaced with 20 ml fresh DMEM media and the flask was transferred to a 32 ^{0}C incubator for production of viral particles. The target cells to be infected (DU145) were seeded at $4x10^4$ cells per T25 flask and incubated overnight at 37 ^{0}C prior to first round of retroviral transduction.

After 24 hours incubation at 32 ^{0}C, the conditioned media (containing viral particles) from the Phoenix cells was collected and filtered through a 0.45 µm non-pyrogenic filter to remove any Phoenix cells from the media. Fresh media (20 ml) was added to the flask and again placed in the 32 ^{0}C incubator for further 48 hours. The conditioned media was mixed 1:1 with fresh DMEM media, and polybrene was added at 10 µg/ml final concentration. The media on target cells (DU145) was replaced with the above-mentioned media and the flasks

were placed overnight at 32 ^{0}C for efficient transduction. The following day, media on target cells was replaced with fresh DMEM and the flask was placed back in the 37 ^{0}C incubator for 24 hours to allow cell recovery. The cells were transduced a second time using the 48 hour conditioned media from Phoenix cells as done previously. The target cells were allowed to recover for 48 hours after the second round of transduction at 37 ^{0}C, and puroMYCin was added at 0.25 µg/ml final concentration for selection of transduced cells. After one week of puroMYCin selection i.e. when there were no viable cells present in the non-transduced flask of DU145, the surviving colonies in the transduced flaks were pooled, expanded and the expression of PIM1 was examined by western blotting.

2.5.12 Co-immunoprecipitation

H1299 cells (6-8x10^5) were seeded in 10 cm^2 dish and transfected 24 hours later with the indicated plasmids for 36-48 hours. Cells were washed twice in cold PBS and lysed directly by scraping in 500 µl of cold CO-IP buffer. The lysate was incubated in the cold room for 30 min on a tube rotator, sonicated once at 30% amplitude for 20 secs, and centrifuged at maximum speed for 20 min at 4 ^{0}C to remove cell debris. The supernatant was carefully transferred to a new-labelled tube and the pellet was discarded. The lysate were then pre-cleared by addition of 50 µl of Protein-A/G sepharose beads (50% slurry in PBS) and kept rotating in the cold room for 45 min. The bead-lysate mixture was centrifuged at 2000 xg for 2 min and the supernatant was again transferred to a new-labelled tube. Approximately 10% volume of the lysate was kept aside, as

input, to check protein expression later. The remaining lysate was divided into two or three equal parts (one for IgG negative control, and others for test antibody) and 2 µg of the appropriate antibody was added. The total volume of lysate in each tube was made up to 600 µl using CO-IP buffer and incubated overnight on a tube rotator in the cold room. Next day, 50 µl of Protein-A/G sepharose beads (previously washed and stored as 50% slurry in CO-IP buffer) was added to the lysate-antibody mixture and incubated for 1-2 hours on a tube rotator in the cold room. The beads were then pelleted by centrifugation at 800 xg for 2 min, and washed three times in CO-IP buffer on a tube rotator for 5 min per wash in the cold room, and supernatant discarded after each wash. After the last wash, 50 µl of 2X SDS sample buffer (with DTT) was added to the beads and boiled for 5 min to elute the proteins before analysing them by western blotting.

2.5.13 Nuclear-Cytoplasmic protein fractionation

Cells from one confluent 10 cm^2 dish were washed twice in cold PBS, scraped in 1 ml PBS and transferred to a new eppendorf tube. The cells were pelleted by centrifugation, lysed in 350 µl of cytoplasmic extraction buffer and incubated on ice for 10 min with gentle vortexing every 2-3 min. The lysates were then centrifuged at 1000 xg for 5 min at 4 ^{0}C. The supernatant (cytoplasmic extract) was collected in a fresh tube. The remaining cell pellet was washed three times in 0.5-1 ml of cytoplasmic extraction buffer and centrifuged as before. The pellet was lysed in 100 µl of 2X SDS sample buffer, sonicated once at 30% amplitude for 20 sec, and centrifuged at 12, 000 xg for 15 min to

pellet cell debris. The supernatant (nuclear extract) was collected and the pellet discarded. The protein concentration of the cytoplasmic and nuclear extracts was determined and equal amounts were loaded on a gel for analysis of protein of interest by western blotting.

2.5.14 Immunofluorescence

Cells (2-5x10^4) were seeded on 13 mm coverslips in a 24-well dish for at least 24 hours prior to staining. The cells were washed twice in PBS to remove excess media, and fixation buffer (prewarmed to 37 ^{0}C) was added for 10 min at RT. Following two washes with PBS, the cells were then permeabilised for 5 min at RT by adding permeabilisation buffer. The cells were washed three times, 5 min each, in PBS and blocked in blocking solution for 15-20 min at RT with gentle shaking. The coverslips were incubated with the primary antibody (diluted in blocking buffer) for 1 hour at RT or overnight at 4 ^{0}C in a humidified chamber. The coverslips were then washed thrice in TBS, 5 min each with gentle shaking. Next, the coverslips were incubated with the desired combination of secondary antibodies for 1 hour at RT in a dark-humidified chamber. After a further three washes in TBS, the coverslips were incubated for 5 min with DAPI (1:10,000 in blocking buffer) at RT, and washed five times with TBS. Excess liquid from the coverslips was carefully removed with filter paper, and the coverslips were mounted with ProLong Gold antifade reagent (Thermo Fisher Scientific) on microscopic glass slides. The slides were allowed to dry overnight in the dark. The next day, the edges of the coverslip were sealed using nail-polish and let to

dry at RT. The stained cells were visualised using an SP5 confocal microscope (Leica microsystems).

2.5.15 SUMOylation and Ubiquitination assay

Affinity purification of hexa-histidine (6Xhis) tagged SUMOylated or ubiquitinated proteins was done under denaturing conditions using Ni^{2+}-NTA agarose beads (Qiagen) and procedure described in Tatham *et al*., 2009.

COS7 ($1x10^6$) or H1299 ($8x10^5$) cells were seeded in 10 cm^2 dishes overnight and transfected with plasmids encoding either 6Xhis tagged SUMO (for SUMOylation assay) or 6Xhis tagged Ubiquitin (for ubiquitination assay) along with other plasmids as indicated in respective figures. After 36-48 hours, cells were washed twice in PBS and scraped in 1 ml of PBS. Ten percent of the cell suspension was lysed directly in 2X SDS buffer (input), and the remaining was lysed in 5 ml 6M Guanidium-HCl lysis buffer (pH 8). The samples were sonicated once at 35% amplitude for 30 sec and centrifuged at maximum speed for 20 min at RT. The supernatant was transferred to a new tube with the addition of 5mM imidazole and 5 mM β-ME. 70 µl of Ni^{2+}-NTA beads (50% slurry in lysis buffer) was then added to the lysate and left on a tube rotator for 2 hours at RT. The beads were gently centrifuged at 400 xg for 1 min and washed successively, once with 4 ml of Guanidium-HCl wash buffer (pH 8), once with 8M Urea wash buffer (pH 8) and thrice with 8M Urea wash buffer (pH 6.3). The proteins were eluted by incubating in 50 µl of Ni^{2+}-NTA elution buffer for 30 min at RT on a tube rotator, boiled for 5 min before running on a gel.

2.5.16 Anchorage-independent growth assay

DU145 cells stably expressing WT PIM1 or mutants were assessed for their ability to grow as colonies in soft-agar. First, the base layer was prepared by mixing equal volumes of 2X RPMI media with 1.8% agarose. About 0.8 ml of this solution was quickly added (avoiding any air bubbles) per well in a 12-well plate. The base layer was allowed to set for 2 hours at RT inside the hood. During this time, cells were trypsinised and diluted to $1.6X10^4$ cells/ml in 2X RPMI media. Equal volume of cell suspension was then mixed with equal volume of 0.9% agarose to obtain the cell layer. Around 0.9 ml of the cell layer was carefully pipetted on top of the base layer. The plates were then allowed to set for one hour at RT in the hood, following which they were placed in a CO_2 incubator. Cells were fed with 200 µl of 1X RPMI media twice each week until colonies began to appear.

2.6 In vitro assays

2.6.1 Kinase assay by western blotting

PIM1 kinase assays were carried out using recombinant 6Xhis-PIM1 (wild-type and mutants) with histone H3.3 (NEB, UK) or c-MYC (DSTT, University of Dundee) as substrate. Reactions were carried out in a total volume of 20 µl containing 50 mM Tris-HCl pH 7.5, 10 mM $MgCl_2$, 0.5 mM ATP, 1 µg substrate and approximately 0.5-1 µg PIM1 kinase. Appropriate negative control reactions without any substrate or kinase were also set up simultaneously. Reactions were incubated in a 30 ^{0}C water bath for 30 min, and terminated by addition of 2X SDS sample buffer (with DTT). The reactions were boiled for 5

min followed by either coomassie staining of the gel or SDS-PAGE and western blotting using a phospho-specific antibody.

2.6.2 *In vitro* SUMOylation assay

The following recombinant proteins were purified and kindly provided by the Hay lab (University of Dundee): untagged SAE1/2, untagged UBC9, GST-SUMO1/2, untagged SUMO1/2, Creatine kinase, SENP1, PIAS1 and IR1+M fragment.

2.6.2.1 Using ^{35}S-methionine labelled PIM1

This procedure was performed with Ellis Jaffray from Prof. Ron Hay's laboratory at the School of Life Sciences, University of Dundee. ^{35}S-methionine labelled PIM1 was generated using a wheat germ lysate coupled *in vitro* transcription/translation system (Promega) from 1 µg MYC-PIM1 plasmid or 1 µg SP100 (positive control) according to manufacturer's procedure. The reaction (25 µl) containing wheat germ lysate (12.5 µl), 25X reaction buffer (1 µl), T7 RNA Polymerase (0.5 µl), amino acid mix without methionine (0.5 µl), RNAsin ribonuclease inhibitor (0.5 µl), DNA template (1 µl), ^{35}S methionine (1.25 µl) and nuclease free water (1.25 µl) was incubated for 2 hours at 30 ^{0}C.

SUMOylation of ^{35}S-methionine labelled substrate was performed in a 20 µl reaction mix containing an ATP-regeneration system (50 mM Tris pH 7.5, 5 mM $MgCl_2$, 2 mM ATP, 10 mM creatine phosphate, 3.5 U/ml creatine kinase, 0.6 U/ml inorganic pyrophosphatase), 120 ng SAE1/2, 750 ng UBC9, 500 ng SUMO1 or SUMO2, EDTA-free protease inhibitor (Roche) and 5 mM DTT. The

reaction was incubated for 4 hours at 37 ^{0}C and terminated by adding SDS-sample buffer. Proteins were separated by standard SDS-PAGE, transferred on a PVDF membrane. The film was exposed overnight on the membrane and visualised on a phosphorimager (Fuji BAS 1500, MacBAS software, Fuji Film, Tokyo, Japan).

2.6.2.2 Using recombinant GST-PIM1

SUMOylation of recombinant GST-PIM1 was performed in 25 µl reaction mix containing 50 mM Tris pH 7.5, 5 mM $MgCl_2$, 2 mM ATP, 5 mM DTT, 900 ng GST-PIM1, 150 ng SAE1/2, 1.5 µg UBC9, 6.25 µg SUMO1 or SUMO2. The reaction was incubated for 4 hours at 37 ^{0}C and terminated by adding SDS-sample buffer. Proteins were separated by SDS-PAGE, subjected to western blotting, and probed with anti-GST antibody.

2.6.3 Kinase assay using SUMOylated PIM1

2.6.3.1 *In vitro* SUMOylation and affinity purification of SUMOylated-PIM1

In vitro SUMOylation of 6Xhis-PIM1 was carried out overnight at 37 ^{0}C in 100 µl reaction containing 50 mM Tris pH 7.5, 3 mM ATP, 5 mM $MgCl_2$, 5 mM DTT, 20 µg 6Xhis-PIM1, 50 µg GST-SUMO2, 5 µg UBC9, 0.9 µg SAE1/2 and 1.5 µg IR1+M fragment of RanBP2. The reaction was diluted 5-fold with 50 mM Tris pH 7.5 and SUMOylated proteins were captured by adding 400 µl (50% slurry) GST beads (GE Healthcare) overnight at 4 ^{0}C. The beads were washed three times in wash buffer (50 mM Tris pH 7.5 and 150 mM NaCl) and eluted by

adding 400 µl elution buffer (20 mM reduced glutathione, 50 mM Tris pH 8, 150 mM NaCl and 1 mM DTT) for 2 hours at 4 ^{0}C on a rotating mixer.

2.6.3.2 DeSUMOylation assay and kinase assay

Elutions from *in vitro* SUMOylation reactions were divided into two equal parts. Active SENP1 (aa 415-643) was added to one of them at 20 nM final concentration. First, the reactions were incubated at 30 ^{0}C for 1 hour for deSUMOylation to occur, following which 5 µg Histone H3.3 (substrate) and kinase buffer (50 mM Tris pH 7.5, 10 mM $MgCl_2$, 0.5 mM ATP final concentration) was added. The reactions were further incubated at 30 ^{0}C for kinase assay with aliquots (40 µl) being collected at 0, 15, 30 and 45 min. The samples were subjected to SDS-PAGE and western blotting was performed using indicated antibodies.

2.6.4 Lambda phosphatase treatment

Dephosphorylation of PIM1 was carried out using lambda protein phosphatase kit from NEB, UK. Reactions were carried out in 10 µl final volume containing up to 1 µg 6Xhis tagged PIM1 (WT and mutants), 1 mM $MnCl_2$, 400 U lambda phosphatase and 1X PMP buffer (50 mM HEPES, 100 mM NaCl, 2 mM DTT, 0.01% Brij-35, buffer pH 7.5). The reactions were incubated at 30 ^{0}C for 1 hour, and terminated by addition of 2X SDS sample buffer with DTT. Reactions were boiled for 5 min and ran on a gel followed by coomassie staining.

Chapter 3

Identification and mechanism of PIM1 SUMOylation

3.1 Introduction

Signal transduction by protein kinases is a complex process that involves rapid activation, deactivation or degradation of other proteins, including the kinases themselves. Small fluctuations in the activity of a single kinase can have profound effects on the cells, and lead to the development of diseases such as cancer. Hence, the activity of a kinase in a cell is tightly controlled by various post-translational modifications (PTM) such as phosphorylation, acetylation and ubiquitination, to name a few. In contrast to most kinases, PIM kinases naturally adopt a catalytically active conformation, and do not rely on any external phosphorylation events for their activity. Nevertheless, in one report the tyrosine kinase, ETK, was shown to increase the kinase activity of PIM1 by phosphorylating PIM1 at Tyr218 (Kim *et al.*, 2004). Additionally, PLK1 and PIM1 were also shown to phosphorylate each other *in vitro*, but the functional consequence remains unclear (Van Der Meer *et al.*, 2014).

As mentioned earlier, PIM1 has a very short-half life in primary cells (5-10 min), which indicates that under physiological conditions, the levels of PIM1 mRNA and protein are strictly maintained at very low levels. However, in cancer cells the mechanisms controlling the stability of PIM1 are dysregulated leading to hyperactivation of PIM1. This observation also suggests that the absolute levels of PIM1 in a cell determine the level of its activity. Therefore, it is important to identify the mechanisms that regulate the levels or activity of PIM1 in cancer cells, so that they can be exploited therapeutically.

To date, there is only one published study on the regulation of PIM1 protein levels in cells (Shay *et al.*, 2005). Here, it was shown that the ubiquitin-proteasome system regulates PIM1 turnover in cells, in a manner that is influenced by the binding of the heat shock proteins - HSP90 and HSP70. However, neither the E3 ubiquitin ligases involved nor the modified lysine(s) in PIM1 were investigated in this study. Since the mechanisms regulating PIM1 kinase activity and stability have remained largely unexplored, I wanted to investigate whether PIM1 undergoes any other PTMs. In this chapter, I will discuss the PTM of PIM1 by the Small Ubiquitin-like Modifier (SUMO) protein, and identify the functional components involved in this PTM.

3.2 Bioinformatics based prediction of potential post-translational modification sites in PIM kinases

In order to identify novel sites of PTM in PIM1, I utilised several bioinformatic tools. One of which, PhosphoSitePlus, is a freely available online database containing PTM site data for human and mouse proteins reported in the published scientific literature, and identified through high-throughput mass-spectrometry by Cell Signaling Technology (Hornbeck *et al.*, 2004). A basic search for the available information on the three PIM kinases revealed several sites of phosphorylation (on serine, threonine and tyrosine) and ubiquitination (on lysine). Since none of these sites were validated experimentally, they were considered as predicted sites of modification. Although many sites of modification were suggested for PIM kinases on the website, only those sites that appeared in more than one mass-spectrometry record were considered for further analysis. Interestingly, this method highlighted sites of ubiquitination and Ser8 as a site of potential phosphorylation. Ser8 was previously shown to be autophosphorylated by PIM1 (Bullock *et al.*, 2005; Jacobs *et al.*, 2005) and therefore not examined further. Table 3.1 lists the predicted sites of modification listed on PhosphoSitePlus (www.phosphosite.org).

Table 3.1 Predicted sites of PTM in PIM kinases by PhosphoSitePlus

Protein	Site	Modification	Sequence	No. of records
PIM1	Ser8	Phosphorylation	MLLSKIN**S**LAHLRAA	7
	Lys169	Ubiquitination	GVLHRDI**K**DENILID	2
	Lys183	Ubiquitination	DLNRGEL**K**LIDFSG	2
	Lys194	Ubiquitination	FGSGALL**K**DTVYTDF	10
PIM2	Lys40	Ubiquitination	RLGPLLG**K**GGFGTVF	23
	Lys61	Ubiquitination	DRLQVAI**K**VIPRNRV	26
	Lys89	Ubiquitination	LEVALLW**K**VGAGGGH	4
	Lys132	Ubiquitination	LFDYITE**K**GPLGEGP	4
	Lys165	Ubiquitination	GVVHRDI**K**DENILID	14
	Lys179	Ubiquitination	DLRRGCA**K**LIDDFGSG	11
PIM3	Ser8	Phosphorylation	MLLSKFG**S**LAHLCGP	4
	Lys38	Ubiquitination	ADKESFE**K**AYQVGAV	2
	Lys172	Ubiquitination	GVVHRDI**K**DENLLVD	4
	Lys186	Ubiquitination	DLRSGEL**K**LIDFGSG	4
	Lys197	Ubiquitination	FGSGALL**K**DTVYTDF	10

As mentioned previously, PIM kinases share a high level of homology at the amino acid level, and hence some of the PTMs predicted for PIM1 were also present in PIM2 and PIM3. These were assumed to be of high importance as not only do they suggest evolutionary conservation, but point towards a common mechanism of regulation of the three kinases. Of note, all four sites listed for PIM1 were also found in PIM3. However, only two sites were found in common amongst the three family members i.e. K169 and K194 in PIM1, K165 and K179 in PIM2 and K172 and K186 in PIM3 respectively.

Interestingly, the amino acid sequence surrounding K169 of PIM1, K165 of PIM2 and K172 of PIM3 resembles a consensus SUMO-recognition motif. The classic SUMO consensus motif is ψKxE/D, where ψ (psi) is a hydrophobic residue (usually I/V/L/F/M) and x is any amino acid (Rodriguez *et al*., 2001). In addition, the SUMO-motif lies in the active site of PIM1 responsible for substrate binding as evidenced from the crystal structure of PIM1 (Figure 3.1). Hence, it could be speculated that SUMOylation at this site would affect PIM1 kinase activity. Therefore, I wanted to test if PIM kinases could also be SUMOylated, and if this has an impact on its activity and/or stability. PIM1 was chosen for further investigation, as it is the most widely studied member of the PIM kinase family.

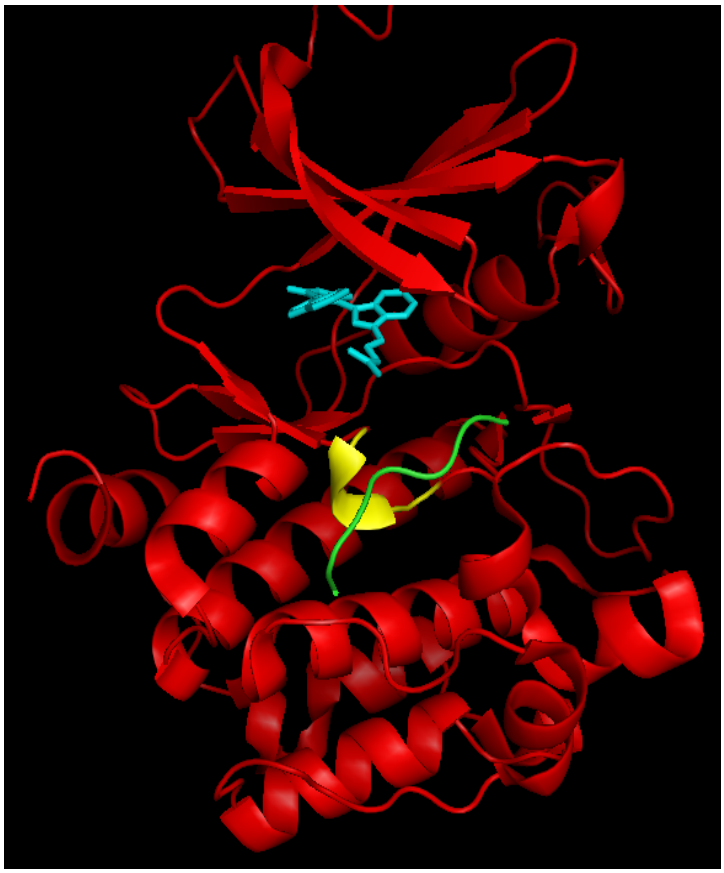

Figure 3.1 Crystal structure of PIM1 highlighting the consensus SUMO motif

Crystal structure was obtained from Protein Data Bank (PDB ID: 2BIL) and edited in PyMOL. PIM1 is shown in red here. An ATP analogue, highlighted in blue, shows the ATP binding site in PIM1. The consensus SUMO motif present in PIM1 is shown in yellow. A PIM consensus peptide (PIMitide), highlighted in green, shows the substrate binding site in PIM1. The overlap between the consensus SUMO site and the substrate binding site can be clearly seen in this figure.

3.3 Modification of PIM1 by SUMO1, 2 and 3 in cultured cells

To determine whether PIM1 can by modified by SUMO in cells, a Ni^{2+}-NTA pull-down experiment was performed under denaturing conditions as described previously (Tatham *et al.*, 2009). Lysis of cells under denaturing conditions has two main advantages. Firstly, it rapidly and irreversibly inactivates the deSUMOylating enzymes, which preserves the otherwise highly labile SUMO modification. Secondly, only covalent modifications such as SUMOylation or ubiquitination are kept intact under these conditions. The protocol relies on the high binding affinity of Ni^{2+}-NTA beads towards proteins carrying a hexa-histidine (6Xhis) tag, usually on SUMO1, 2 or 3. All proteins modified by or covalently attached with SUMO are enriched through this procedure and can be detected by western blotting using an antibody against the protein of interest.

COS7 cells were transfected with plasmids encoding 6Xhis tagged SUMO1, SUMO2 or SUMO3 with MYC-tagged PIM1. PIM1 was also co-transfected with empty pcDNA3 as a negative control. After 42-48 hours, the SUMOylated proteins were captured by Ni^{2+}-NTA beads, separated by SDS-PAGE and western blotted with the anti-MYC tag (clone 9E10) antibody to visualise SUMOylated PIM1. As seen in Figure 3.2A, slowly migrating bands of PIM1 were observed in cells transfected with 6Xhis-SUMO family members but not with empty vector, suggesting that PIM1 can be modified by SUMO1, 2 and 3. The apparent shift in the molecular weight of PIM1 from 34 kDa to 55 kDa is also consistent with the covalent addition of a 15-20 kDa SUMO moiety. Importantly, it was observed that SUMOylated PIM1 runs as a

doublet indicating that there are at least two independent sites of SUMOylation in PIM1..

PIM1 was expressed at equal levels in all samples as determined by western blotting using inputs (whole cell lysate, Figure 3.2B). The SUMOylated PIM1 bands, as expected, were indistinguishable in the inputs even though several bands of higher molecular weight were observed. This is because only a small fraction of any protein is modified at a given time, and unless enriched the SUMOylated proteins are difficult to detect in whole cell lysates.

The expression of the three SUMO isoforms and their purification was also checked using the Ni^{2+}-NTA pull-down samples by western blotting for His-tag antibody. As shown in Figure 3.2C, SUMO1 was expressed at a lower level than SUMO2 and 3 which explains the lower level of PIM1 SUMOylation seen with SUMO1 in Figure 3.2A. It was also observed that unmodified PIM1 itself binds non-specifically to the Ni^{2+}-NTA beads even in the absence of 6Xhis-SUMO. However, this does not affect the results as SUMOylated PIM1 runs at a higher molecular weight than unmodified PIM1.

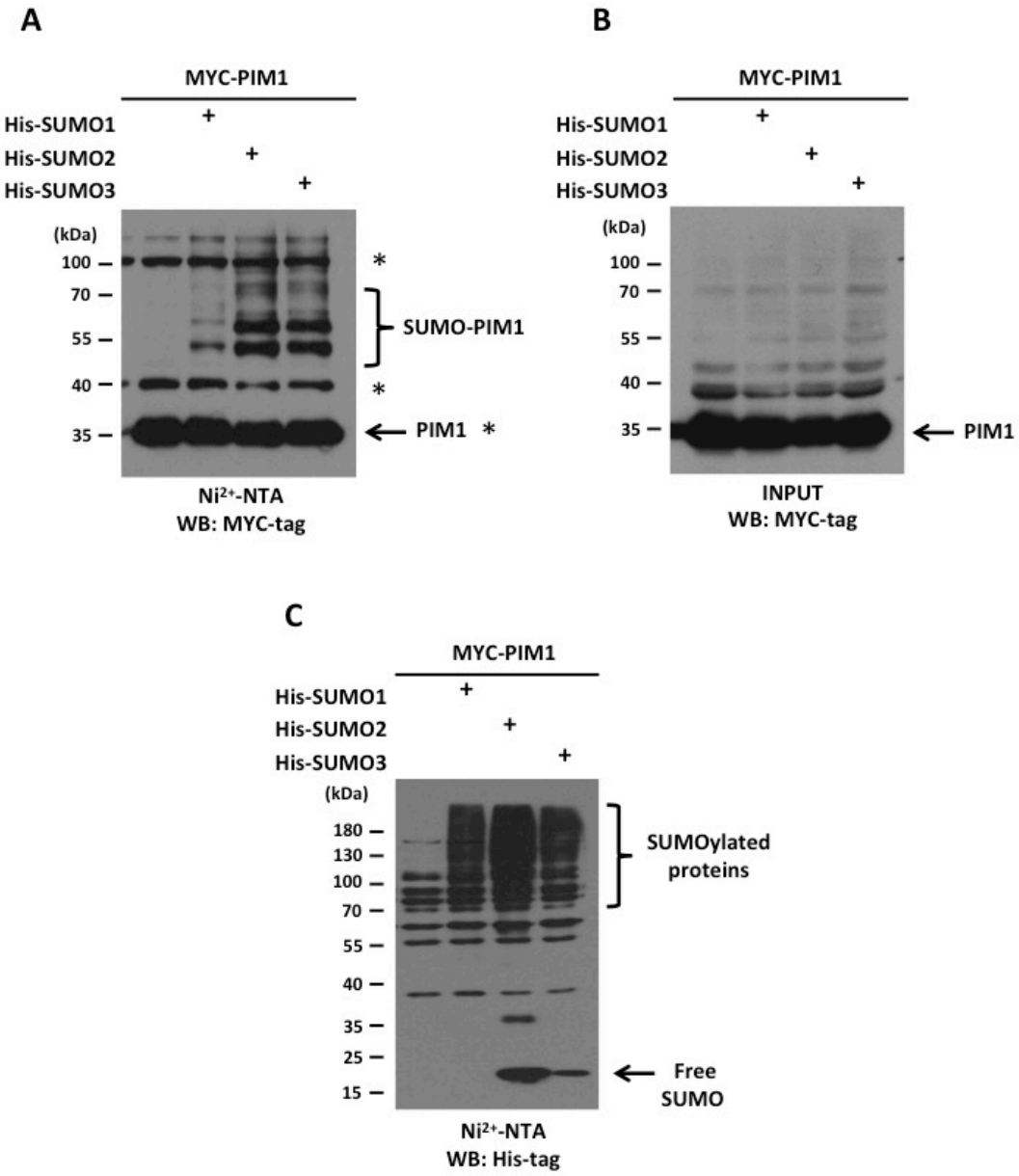

Figure 3.2 Modification of PIM1 by SUMO1, 2 and 3 in cultured cells

COS7 cells were transfected with plasmids encoding MYC-tagged PIM1 with 6Xhis-SUMO1, 2 or 3. Cell lysates were prepared 42-48 hours after transfection. An aliquot of whole cell lysate was taken as input, and the remainder subjected to Ni^{2+}-NTA pull-down to capture SUMOylated proteins. Note that unmodified PIM1 binds non-specifically to Ni^{2+}-NTA beads. **(A)** PIM1 SUMOylation was analysed by western blotting of Ni^{2+}-NTA pull-down samples using MYC-tag antibody. **(B)** Total levels of PIM1 expressed under each transfection condition was analysed by western blotting of Input samples using MYC-tag antibody. **(C)** The levels of total SUMOylated proteins under each case was analysed by western blotting of Ni^{2+}-NTA pull-down samples using His-tag antibody. The data shown here is representative of three independent experiments.

3.4 *In vitro* SUMOylation of PIM1

To show that SUMOylation of PIM1 was not an artefact of overexpression, an *in vitro* SUMOylation experiment was performed using two different approaches.

In the first set of experiments, *in vitro* transcribed and translated ^{35}S-methionine labelled MYC-PIM1 was incubated with recombinant SUMO E1 enzyme SAE1/2, SUMO E2 enzyme Ubc9 and SUMO1 or SUMO2, in the presence of an ATP-regeneration system. A PIM1 alone reaction was also set up as a negative control. Additionally, a well-known substrate for SUMOylation, SP100, was used as a positive control to check the efficiency of the *in vitro* SUMOylation reaction. As shown in Figure 3.3A, both SUMO1 and SUMO2 modified PIM1 to the same extent resulting in the shift of PIM1 to a double band running at 55 kDa. The modification was not very efficient when compared with the positive control, SP100. However, this could be because *in vitro* reactions do not recapitulate cellular conditions, and sometimes other factors or E3 SUMO ligases might be necessary for optimal SUMOylation.

In the second experiment, recombinant GST-PIM1 was incubated with recombinant SUMO1 or SUMO2, in the presence of SAE1/2, Ubc9 and ATP. GST-PIM1 alone was used as a negative control. The expression and purification of GST-PIM1 has been described in chapter-2 (section 2.4.1 and 2.4.2). Equal amounts of SUMO1 and SUMO2 were used in these reactions. Figure 3.3B shows that GST-PIM1 can be modified *in vitro* by SUMO1 and 2 to a similar extent. The results obtained with both approaches were identical. Interestingly, the doublet pattern observed for SUMO1 modified PIM1 was different to that of SUMO2 modified PIM1. It is possible that SUMO1 and 2

might target different sites for modification, which could result in different electrophoretic gel mobility. Since SUMO2 is the predominant SUMO isoform found in cells, and the fact that a significantly larger number of proteins are modified by SUMO2/3 than SUMO1 (Saitoh and Hinchey, 2000), subsequent experiments were done using only SUMO2.

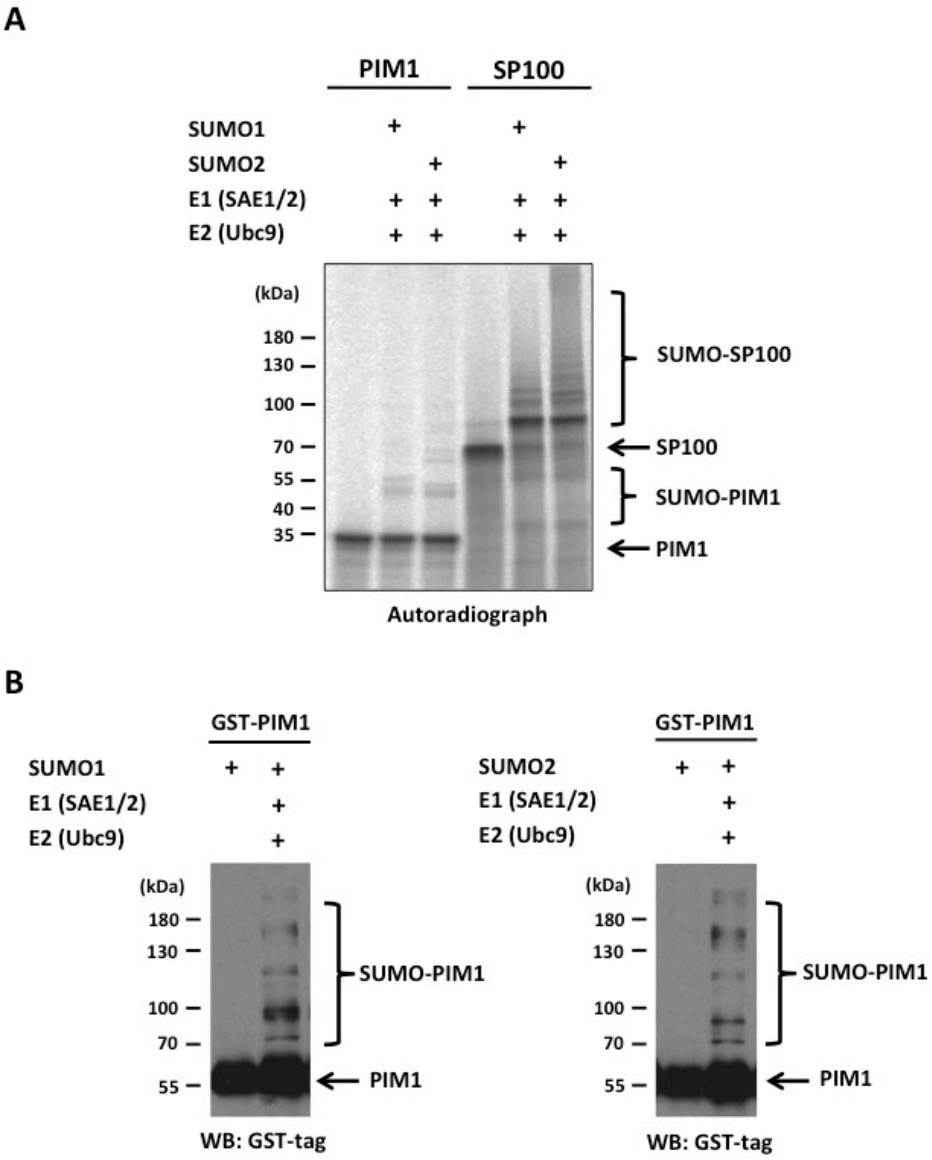

Figure 3.3 *In vitro* SUMOylation of PIM1

(A) *In vitro* transcribed and translated ^{35}S-methionine labelled PIM1 was incubated with recombinant SAE1/2, Ubc9 with SUMO1 or SUMO2 in the presence of ATP-regeneration system. The reactions were terminated and SDS-PAGE was performed. SUMOylation of radiolabelled PIM1 was visualised on a Phosphorimager. SP100 was used as a positive control in the SUMOylation reaction. **(B)** Recombinant GST-PIM1 was incubated in the presence of ATP, recombinant SAE1/2, Ubc9 with SUMO1 (left) or SUMO2 (right). The reactions were terminated and resolved by SDS-PAGE. Western blotting was performed using a GST-tag antibody to detect SUMOylated PIM1. The data shown here is representative of two independent experiments.

3.5 Modification of ectopically expressed PIM1 by endogenous SUMO2

From the experiments described above, it is reasonable to suppose that PIM1 can be SUMOylated. But since the conditions used i.e. ectopic expression and *in vitro* reconstitution are not truly physiological, it is crucial to demonstrate SUMOylation of protein at the endogenous level. Several methods have been proposed in the literature for the detection of endogenous SUMOylated proteins.

The most common method is immunoprecipitation of the endogenous protein followed by western blotting with a SUMO antibody. Inversely, SUMO can be immunoprecipitated from cells, followed by western blotting for the test protein. The latter method, however, is less sensitive as the proportion of SUMOylated protein in the pool will be very small. Another factor to consider is that under native conditions, antibodies might not bind SUMOylated proteins because of issues such as epitope masking. Immunoprecipitation of SUMOylated PIM1 was challenging for various reasons. Firstly, the levels of endogenous PIM1 were found to be very low in all adherent cell lines tested. Secondly, commercially available PIM1 antibodies were found to be not suitable for immunoprecipitation of endogenous PIM1. Thirdly, the IgG heavy chain runs at the same size as SUMOylated PIM1 at 55 kDa on a gel, which makes detection of SUMOylated PIM1 more difficult.

SUMOylated proteins can also be enriched from HeLa cells stably expressing 6Xhis-SUMO1 or 2 by a Ni^{2+}-NTA pull-down experiment, followed by western blotting for the protein of interest. Unfortunately, the results from these cell lines were not reproducible mainly because the PIM1 antibody detected several non-specific bands in the negative control cells that do not

express any 6Xhis-SUMO. Several attempts using other antibodies were also unsuccessful.

In an attempt to resolve the antibody issues and the low levels of endogenous PIM1, I decided to ectopically express only PIM1 in cells and analyse its modification by endogenous SUMO2. To do this, I tagged PIM1 with a 6Xhis-tag, and transfected H1299 cells which express low levels of PIM1, and performed a Ni^{2+}-NTA pull-down experiment under denaturing conditions. The generation of a plasmid expressing 6Xhis-PIM1 has been described under section 2.3.1. H1299 cells transfected with empty vector was used as a negative control. The lysates were resolved by SDS-PAGE, and western blotting was performed using His-tag (PIM1) and SUMO2 (endogenous) antibody. Figure 3.4A shows that PIM1 was efficiently affinity purified from cells expressing 6Xhis-PIM1. Bands of high molecular weight were also observed in both the input and Ni^{2+}-NTA pull-down samples, suggestive of ubiquitinated and SUMOylated forms. Figure 3.4B shows that PIM1 was modified by endogenous SUMO2 in H1299 cells. PolySUMOylated bands were also detected under these conditions. Western blotting was also performed on the Ni^{2+}-NTA samples using an Ubiquitin-specific antibody. Figure 3.4C shows the PIM1 is also polyubiquitinated in H1299 cells.

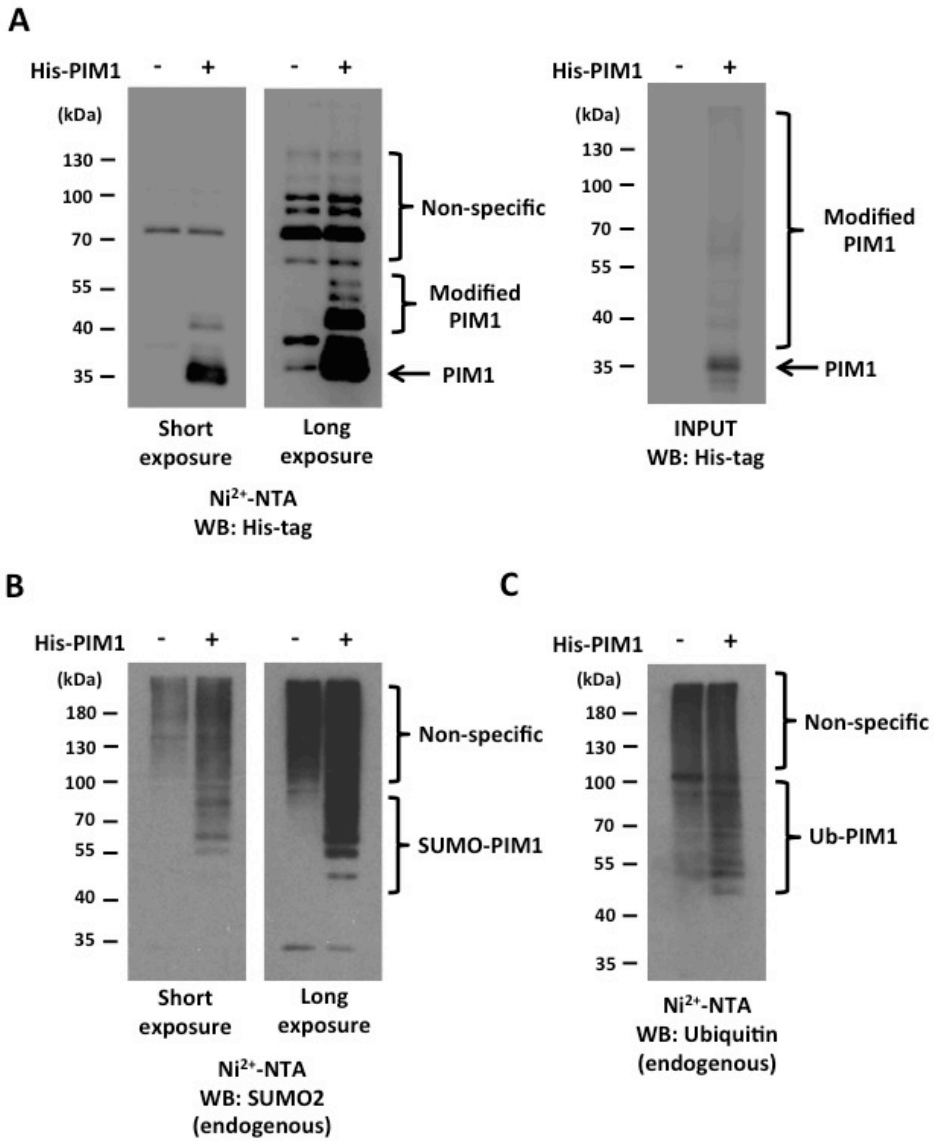

Figure 3.4 Modification of ectopically expressed PIM1 by endogenous SUMO2

H1299 cells were transfected with a plasmid expressing 6Xhis-PIM1, and harvested 48 hours after transfection. An aliquot of whole cell lysate was taken as input, and the remainder subjected to Ni^{2+}-NTA pull-down to capture His-PIM1. **(A)** Western blotting was performed on Ni^{2+}-NTA and input samples to confirm PIM1 expression and purification. The same Ni^{2+}-NTA samples were western blotted for endogenous SUMO2 **(B)** or ubiquitin **(C)** to confirm presence of SUMOylated and ubiquitinated PIM1 in cells. The data shown here is representative of two independent experiments.

3.6 Identification of the sites of SUMOylation in PIM1

The 34 kDa PIM1 protein contains 12 lysine residues (Figure 3.5A). Since only lysine 169 (K169) is present within a consensus SUMO motif (ΨKxD/E, where Ψ is usually I/V/L and x is any amino acid), only one site was expected to be SUMOylated in PIM1. However, result shown in figure 3.2A suggests that PIM1 is modified at multiple sites. In order to identify the sites of SUMO modification in PIM1, all lysine residues were mutated to arginine individually by site-directed mutagenesis. Since other PTMs such as ubiquitination, methylation, acetylation, neddylation etc also occur on lysine residues, therefore any effects observed with the lysine to arginine mutants must be carefully interpreted, as they may be the result of inhibition of other PTM. Mutation of the glutamic acid adjacent to the modified lysine has also been shown to disrupt SUMOylation. Hence, E171 was also mutated to alanine. Glutamic acid E181 was also mutated to alanine as it forms an inverted SUMO motif (D/ExKΨ) with lysine 183 (K183). A kinase dead mutant of PIM1 referred to as K67M, was also included to examine if kinase activity was required for SUMOylation.

Wild-type PIM1 and various mutants were tested for their ability to undergo SUMOylation when co-expressed with 6Xhis-SUMO2 in COS7 by performing a Ni^{2+}-NTA pull-down experiment. All proteins were expressed at near equal levels in this experiment using pre-determined plasmid concentrations for each mutant. In all cases, the total amount of plasmid transfected was normalised with empty vector. Figure 3.5B (left panel) shows that wild-type PIM1 was modified with SUMO2 resulting in a doublet running at 55 kDa. The kinase dead mutant, K67M, was also modified to the same

extent as the wild-type (WT) indicating that SUMOylation of PIM1 occurs independently of its kinase activity. This also rules out that the possibility that the PIM1-SUMO doublet band represents the autophosphorylated and nonphosphorylated form of PIM1, as the K67M mutant is incapable of autophosphorylation (Padma and Nagarajan, 1991). Substitution of lysine residues present in the N-terminal lobe of PIM1 to arginine (K5R, K24R, K29, 31R, K67R, K71R and K94, 95R) did not affect SUMOylation suggesting that these lysines were not individually targeted for SUMOylation. On the other hand, Figure 3.5B (right panel) shows that K169R mutation partially abolished SUMOylation, as evident from the loss of the upper band from the doublet observed with wild-type PIM1, confirming that K169 is one of the main sites of SUMOylation. Interestingly, the E171A mutant completely abolished SUMOylation of PIM1. This result was unexpected, as the K to R and E to A mutants, so far in the literature, have been shown to produce the same effect on SUMOylation. It is possible that E (negatively charged amino acid) to A (nonpolar amino acid) substitution alters the structure of the SUMO-motif in PIM1 significantly such that it is no longer recognised by the enzymes of the SUMO pathway. To investigate this further, E171 was mutated to glutamine (Q), which is a slightly more conservative substitution. As anticipated, the E171Q mutant only partially abolished SUMOylation of PIM1, in a manner identical to the K169R mutant. Mutation of other sites (E181A, K183R, K194R and K313R) also did not affect PIM1 SUMOylation suggesting that they were not involved in SUMOylation. Overall, only K169 was identified as a specific site of SUMO modification, whereas the second (non-consensus) site of modification is promiscuous.

The mutational analysis of PIM1 shown in Fig 3.5B suggests two important things. Firstly, the sites of SUMO modification in PIM1 may be mutually exclusive. This is based on the calculation that covalent attachment of a single 20 kDa SUMO moiety to a 34 kDa PIM1 would result in the formation of a ~55 kDa PIM1 species, whereas attachment of two or more SUMO moieties at distinct sites simultaneously should result in the formation of a ~75 kDa or >75 kDa PIM1 species (Fig 3.5C). Although I detected a doublet of PIM1 at ~55 kDa upon coexpression of SUMO2 consistent with monoSUMOylation, I did not observe any multi-monoSUMOylated (>75 kDa) species of PIM1 on the gel (Fig 3.5B). Secondly, the PIM1 doublet observed at 55 kDa is consistent with PIM1 being SUMOylated at two independent sites. The top band of the ~55 kDa represents PIM1 SUMOylated at K169 as mutation of this site to R169 led to the disappearance to the top band of the PIM1-SUMO doublet at ~55 kDa. Therefore, the bottom band of the doublet may represent PIM1 SUMOylated at the non-consensus site. It appears that PIM1 SUMOylated at K169 runs at a slightly higher mobility compared to PIM1 SUMOylated at the non-consensus lysine.

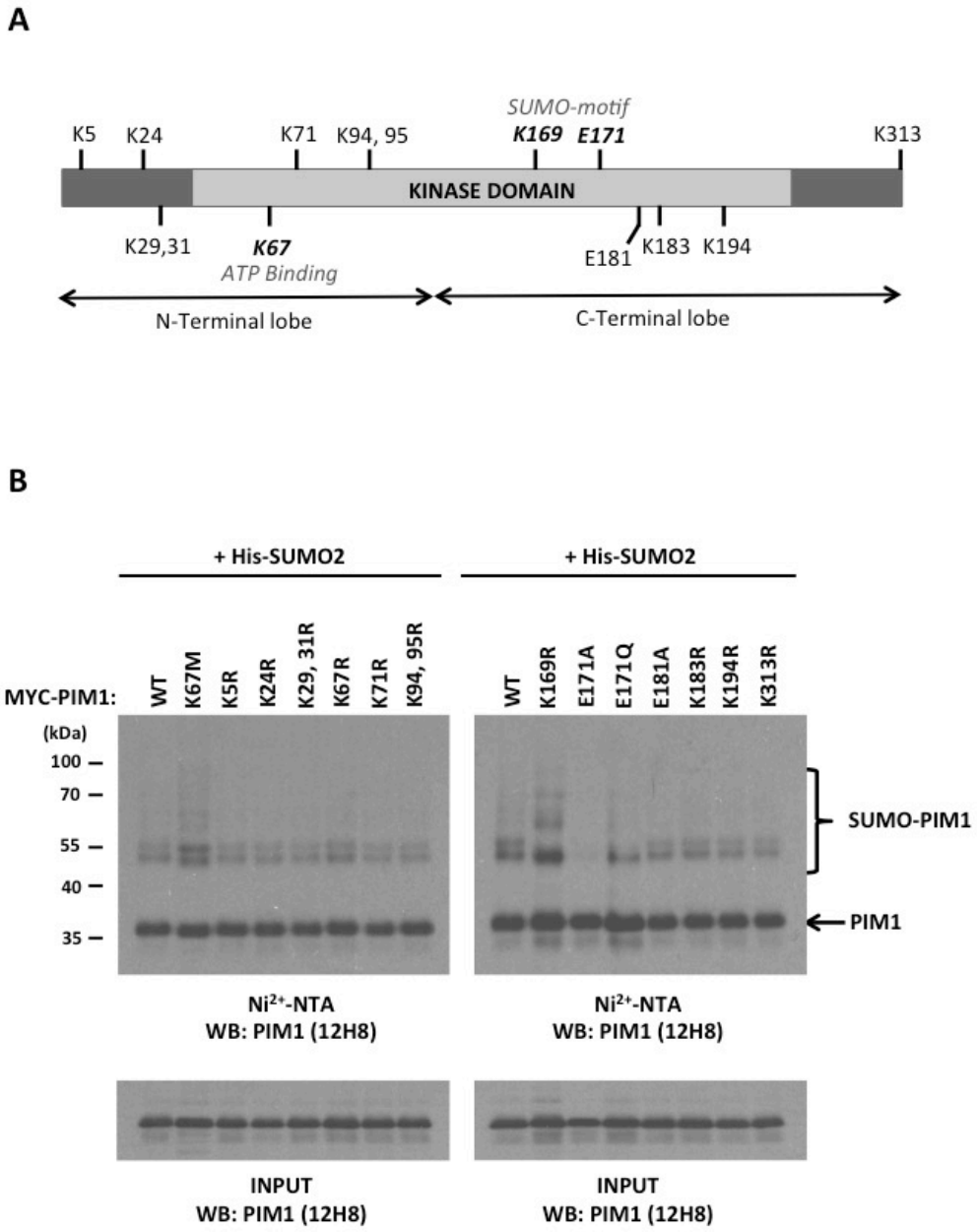

Figure 3.5 Identification of the sites of SUMOylation in PIM1

(A) Schematic showing the functional domains in PIM1, and the position of various lysine residues and glutamic acid predicted to be involved in SUMOylation. **(B)** COS7 cells were transfected with the various PIM1 mutants and 6Xhis-SUMO2. An aliquot of whole cell lysate was taken as input, and the remainder subjected to Ni^{2+}-NTA pull-down to capture SUMOylated proteins. The samples were subjected to SDS-PAGE followed by western blotting using a PIM1 antibody. The data shown here is representative of two independent experiments.

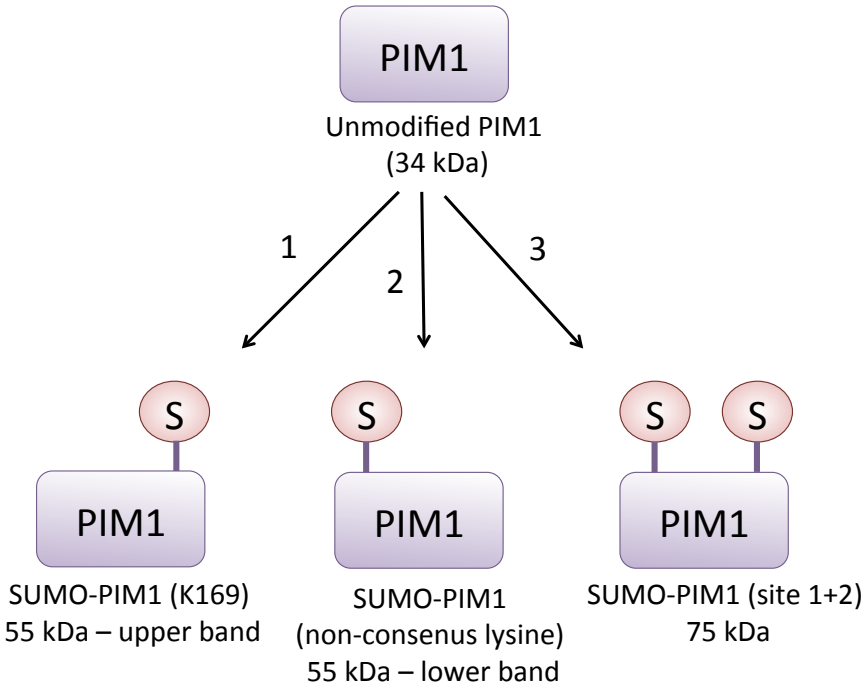

Figure 3.5 (C) Schematic illustrating changes in the electrophoretic gel mobility of PIM1 upon covalent attachment of SUMO at the consensus (K169) and non-consensus site. SUMOylation at these sites may occur in a mutually exclusive manner, as a 75 kDa species of PIM1 is not observed in the SUMOylation assay.

3.7 DeSUMOylation of PIM1 by SENP1

SUMOylation is a reversible process mediated by members of the SUMO protease family (SENP1-3 and SENP5-7). SENPs catalyse removal of SUMO from SUMOylated substrates, and also cleavage of inactive SUMO to yield active SUMO (Hickey *et al*., 2012). SENP1 was used as a representative in this experiments as it shows little specificity towards SUMO1 or SUMO2/3 modified substrates, and thus is a good tool to confirm SUMOylation of a protein.

To demonstrate that SENP1 was capable of deSUMOylating PIM1, COS7 cells were co-transfected with plasmids expressing PIM1, 6Xhis-SUMO2 with either active SENP1 or a catalytically inactive SENP1 (C602S mutant). SUMOylated proteins were captured by Ni^{2+}-NTA pull-down method, and PIM1 SUMOylation was analysed by western blotting. As shown in Figure 3.6 inputs, both active and inactive SENP1 were expressed at equal protein levels. Expression of SUMO2 led to PIM1 SUMOylation (observed as a 55 kDa doublet band), which disappeared upon co-expression of wild-type SENP1 but not the inactive SENP1 mutant. The results shown in figure 3.6 indicates that SENP1 can deSUMOylate PIM1, and also strengthens the observation that the 55 kDa bands are indeed SUMOylated forms of PIM1.

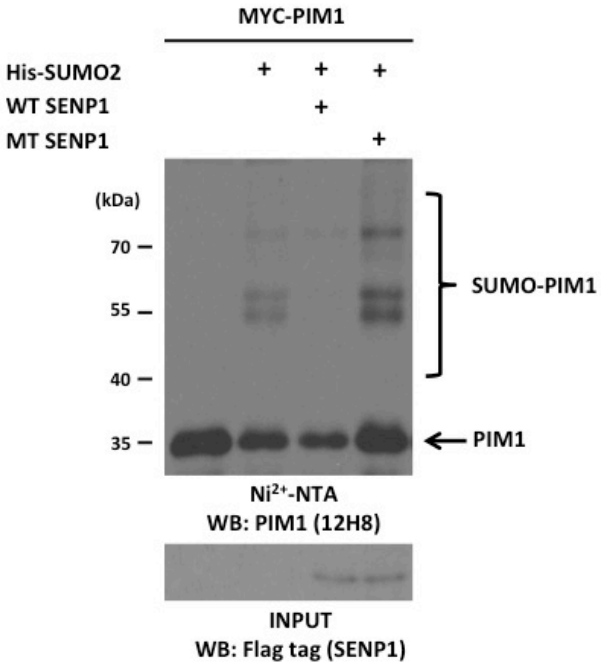

Figure 3.6 DeSUMOylation of PIM1 by SENP1

COS7 cells were transfected with plasmids expressing PIM1 alone, or with 6Xhis-SUMO2 in combination with active Flag-SENP1 (WT) or inactive Flag-SENP1 (MT), and Ni^{2+}-NTA pull-down was performed to isolate SUMOylated proteins, followed by SDS-PAGE and western blotting for PIM1. Western blotting of whole cell lysate or input was done using Flag-tag antibody to show expression of SENP1. The data shown here is representative of two independent experiments.

3.8 Identification of PIAS family members as E3 SUMO ligases for PIM1

SUMO E3 ligases regulate global protein SUMOylation by acting as a platform, which can recruit UBC9, SUMO and substrate in different ways, thus facilitating efficient transfer of SUMO to protein substrates. Unlike the ubiquitin-proteasome system, a large number of proteins can be modified in the absence of an E3 SUMO ligase. They are therefore, thought to mediate substrate and substrate-lysine specificity under specific cellular conditions. Various E3 SUMO ligases have been identified such as the Protein Inactivator of Activated STATs (PIAS) family, TOPORS, PC2, RanBP2 and HDAC4 to name a few. It was not possible to test all identified E3 SUMO ligases for their activity on PIM1. So, as a starting point, I hypothesised that PIAS family members might act as E3 SUMO ligases since, like PIM1, they are themselves regulated by the JAK-STAT pathway. PIAS1 and PIAS3 were shown to inhibit binding of the transcription factors STAT1 and STAT3 respectively to their target gene promoters, thus negatively regulating the JAK-STAT pathway (Chung *et al.*, 1997; Liu *et al.*, 1998).

I tested the ability of three PIAS family members – PIAS1, PIASy (or PIAS4) and PIAS3 for their ability to stimulate PIM1 SUMOylation. PIM1 was transfected in COS7 cells with 6Xhis-SUMO2 alone or in combination with HA-tagged PIAS1, HA-tagged PIASy or Flag-tagged PIAS3, and a Ni^{2+}-NTA pull-down experiment was performed. As shown in Figure 3.7, a small proportion of PIM1 was SUMOylated upon co-expression of 6Xhis-SUMO2 alone. However, this was dramatically increased in the presence of PIAS3 under basal conditions leading to polySUMOylated forms of PIM1, consistent

with the role of an E3 SUMO ligase. PIAS1 and PIASy did not stimulate PIM1 SUMOylation to the same extent as PIAS3. Nevertheless, the stimulation observed was higher when compared with the no E3 ligase sample. To rule out that this difference was simply because of the higher levels of PIM1 observed when co-expressed with PIAS3 (as shown in the inputs), the same set of samples were also treated with the proteasome inhibitor MG132 (20 μM for 6 hours) in an effort to stabilise or equalise PIM1 levels. Under these conditions, PIAS3 was more potent than PIAS1 and PIASy in enhancing PIM1 SUMOylation. Intriguingly, PIAS1 could also stimulate polySUMOylation of PIM1, an effect that was not noticeable under basal conditions. PIASy did not stimulate PIM1 SUMOylation any further when compared with the no E3 ligase sample. Taken together, these results suggest that PIAS1 and PIAS3 might serve as E3 SUMO ligases for PIM1. Although PIAS proteins are highly active in cells, one limitation of this experiment is that the equal levels of E3 SUMO ligases expressed here may not directly correlate with their activity. This difference in the E3 SUMO activity can be identified by western blotting of Ni^{2+}-NTA pull-down samples using a His-tag antibody to detect the total increase in the levels of SUMOylated proteins in the cellular extracts upon expression of the PIAS proteins.

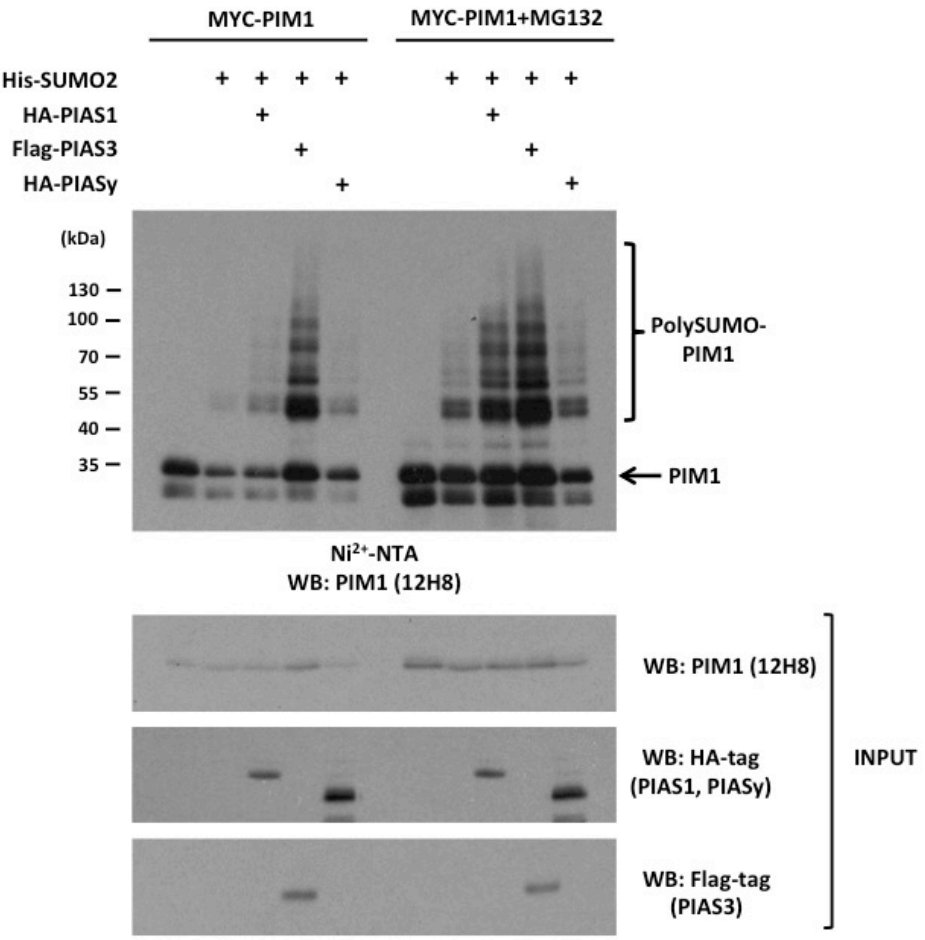

Figure 3.7 Identification of PIAS family members as E3 SUMO ligases for PIM1

Western blots of Ni^{2+}-NTA pull-down samples showing PIM1 SUMOylation, from COS7 cells transfected with plasmids expressing PIM1, 6Xhis-SUMO2 with PIAS1, PIAS3 or PIASy in the absence or presence of MG132 (20 μM for 6 hours). A western blot of whole cell lysate (input) was also performed to confirm the expression PIM1, PIAS1, PIAS3 and PIAS3 using the indicated antibodies. The data shown here is representative of two independent experiments.

3.9 Interaction of PIM1 with PIAS1 and PIAS3

Various studies have shown that SUMO E3 ligases primarily interact with a SUMO bound UBC9, while the Ubc9 itself binds the substrates. However, in some cases, the E3 ligase is required for both substrate and Ubc9 binding acting as a bridge (Gareau and Lima, 2010). To test if PIM1 directly interacted with PIAS3, H1299 cells were transiently transfected with plasmids encoding MYC-tagged PIM1 and Flag-tagged PIAS3, and co-immunoprecipitation was performed using anti-flag antibody or mouse IgG as negative control. The immunoprecipitated proteins were analysed by SDS-PAGE and western blotting. Figure 3.8A shows that PIM1 was detected in the PIAS3 immunoprecipitated sample, showing that the two proteins can indeed interact. No PIAS3 or PIM1 protein was detected in the control IgG samples suggesting that the antibodies were specific.

The ability of PIM1 to interact with PIAS1 was also tested by co-immunoprecipitation. Plasmids encoding MYC-tagged PIM1 and HA-tagged PIAS1 were co-transfected in H1299 and immunoprecipitated using anti-HA antibody or mouse IgG as negative control. Since PIAS1 mediated SUMOylation was clearly seen when the proteasome was inhibited (Figure 3.5), the transfected cells were also treated with MG132 as done previously. The concentration of the protein in the lysate was determined using BCA-DC assay, and equal amount of lysate was used in the experiment to accurately reflect the levels of proteins before and after proteasome inhibition. The inputs from Figure 3.8B show that the levels of PIAS1 remain largely unchanged, however, levels of PIM1 protein increase following MG132 treatment, as expected. No PIM1 or PIAS1 was detected in the IgG negative

control immunoprecipitation reactions. Roughly equal amount of PIAS1 was immunoprecipitated under both conditions. Importantly, interaction of PIAS1 with PIM1 was only observed under conditions of proteasome inhibition suggesting this PIAS1 might target PIM1 for degradation by a SUMO-dependent ubiquitination mechanism.

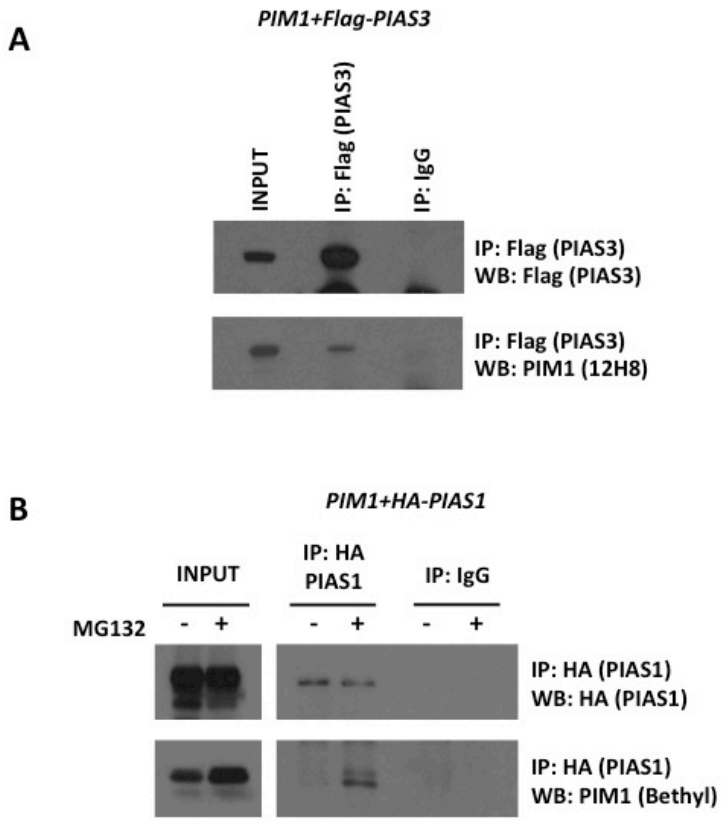

Figure 3.8 Interaction of PIM1 with PIAS1 and PIAS3

(A) H1299 cells were co-transfected with PIM1 and PIAS3 expression plasmids, and co-immunoprecipitation was performed using Flag-antibody to pull-down PIAS3 associated complexes. The immunoprecipitated (IP) samples were western blotted using Flag-tag and PIM1 antibody to show that PIAS3 and PIM1 can form a complex in cells. Mouse IgG was used as a negative control. **(B)** H1299 cells were transfected with plasmids expressing PIM1 and PIAS1 in the presence or absence of MG132 (20 μM for 6 hours), and equal amount of lysate were subjected to immunoprecipitation using HA-tag (PIAS1) antibody. The IP samples were western blotted for the presence of PIAS1 and PIM1 using anti-HA and PIM1 (Bethyl) antibodies. Mouse IgG was used as a negative control. The data shown here is representative of two independent experiments.

3.10 Summary and Discussion

In this chapter, I wanted to identify novel sites of PTM in PIM1. Based on the bioinformatic analysis of the amino acid sequence of PIM kinases, I identified the presence of a conserved SUMO consensus motif in the active site of PIM1. The presence of a consensus SUMO-motif in the active site is quite intriguing as it overlaps with the conserved Ser/Thr kinase domain motif, HRDxKxxN (Hanks and Hunter, 1995). Based on the study of other protein kinases, at least two residues within this motif are directly involved in catalysis: an invariant aspartic acid that acts by accepting a proton from the attacking hydroxyl substrate and a lysine (K169 in PIM1) that is thought to neutralise the negative charge of the γ-phosphate during transfer. However, it is now known that K169 in PIM1 actually does not form the conventional salt bridge with the nucleotide phosphate group of ATP as seen with other kinases (Qian *et al*., 2005). Therefore, the possibility that SUMOylation may occur at K169 is particularly interesting as it may regulate the catalytic activity of PIM1 through a novel mechanism. Moreover, the same motif was shown to be SUMOylated in other kinases such as Aurora B and AKT, and has been described in the final discussion (Fernández-Miranda *et al.*, 2010; Li *et al.*, 2013).

I showed that PIM1 could be modified covalently by SUMO1, SUMO2 and SUMO3 *in vitro* and in cultured cells and appear as a closely migrating doublet around 55 kDa. In a recent study, over one-third of all SUMOylated proteins were predicted to contain more than one SUMOylation site. Also, proteins such as PARP and hnRNPM were found to contain over 10 SUMOylation sites. There is also evidence of multiple SUMOylation sites

being modified simultaneously (Tammsalu *et al.*, 2014). By site-directed mutagenesis of individual lysine residues in PIM1, I showed that K169 is one of the main sites of modification while the second site is promiscuous. Interestingly, mutation of E171 to alanine was sufficient to abolish SUMOylation at both sites. Promiscuity of the modified lysine is not uncommon in the SUMO system, and has been observed previously with other substrates such as PARP, BLM and DAXX (Eladad *et al.*, 2005; Lin *et al*., 2006; Martin *et al*., 2009). Similar effects have also been observed in the ubiquitin system (Danielsen *et al.*, 2011). Why this happens is not very clear, although, it can be speculated that mutation of a lysine residue where the modification usually occurs, forces the modification to occur on an adjacent lysine. Unfortunately, in these cases, mutation of a single lysine is not sufficient to abolish SUMOylation, and different combinations of lysine need to be mutated to arginine simultaneously. A major disadvantage of substituting all the lysine to arginine in a protein is that the SUMO-specific effects become indistinguishable from other modifications such as ubiquitination and acetylation that also occur on lysine residues. However, in case of PIM1, the K169R is SUMOylated at one site, while the E171A mutant is impaired in overall SUMOylated allowing us to ascertain individual effects of SUMOylation at a single site versus SUMOylation at both sites. The functional effects of these mutants are discussed in the next chapter.

I also showed that the SUMO protease, SENP1, could deconjugate SUMO from SUMOylated PIM1. It should be noted that most SENPs have overlapping substrates, so under a cellular condition, one or more SENPs could be involved in deSUMOylation of PIM1. I also identified members of

the PIAS family as E3 SUMO ligases for PIM1. Interestingly, inhibition of the proteasome activity by MG132 not only stabilised unmodified PIM1 but also the SUMOylated form of PIM1, suggesting that SUMO modification and PIM1 turnover could be related. PIAS3 enhanced polySUMOylation of PIM1 under basal conditions and upon proteasomal inhibition. On the other hand, PIAS1 mediated PIM1 polySUMOylation was only observed under conditions of proteasomal inhibition. I further showed that PIAS1 and PIAS3 could directly interact with PIM1 in cells. The interplay of the SUMO and ubiquitin systems in regulating PIM1 levels will be discussed in the next chapter.

Chapter 4

Effect of SUMOylation on PIM1 activity and stability

4.1 Introduction

SUMOylation is a highly dynamic and reversible post-translational modification that is known to affect several biological processes such as transcription, translation, cell cycle progression and DNA repair. Covalent attachment of SUMO to one or more lysine residues on target proteins can alter the structure, and hence the function of the target protein by promoting or inhibiting specific cellular protein interactions under physiological and/or stress conditions. In broad terms, SUMOylation has been shown to affect the activity, cellular localisation and stability of its substrates (Wilkinson & Henley 2012).

The proto-oncogene, PIM1, is induced in response to cytokines and growth factors mainly via the JAK-STAT pathway. While mechanisms regulating the stability of PIM1 mRNA have been studied extensively, there is little information on the regulation of PIM1 protein. Although it is known that the ubiquitin-proteasome pathway degrades PIM1, it is presently unknown how the activity and substrate specificity of PIM1 activity is regulated prior to its destruction. In addition, factors influencing PIM1 stability and localisation are still poorly understood. Given that SUMOylation of PIM1 occurs in the kinase domain, it is plausible that SUMOylation might alter its kinase activity. This would, thus, have an impact on the stability of the protein, and its function altogether. Therefore, in this chapter, I wanted to investigate the functional consequences of SUMOylation on PIM1, and how SUMOylation may impact PIM1 stability or interaction with the ubiquitin pathway.

4.2 Autophosphorylation of PIM1 and SUMO-mutants

PIM kinases are capable of autophosphorylation on serine, threonine and even tyrosine residues. It was suggested that autophosphorylation is required for PIM1 activity (Telerman *et al.*, 1988; Palaty *et al.*, 1997), but there is no substantial evidence to support these claims. Therefore, I wanted to investigate this aspect, and also find out if the SUMO-mutants, K169R and E171A, are capable of undergoing autophosphorylation. To do this recombinant 6Xhis-PIM1 proteins were expressed in bacteria and purified as previously described in chapter-2 (section 2.4.1 and 2.4.3). The generation of a 6Xhis-PIM1 bacterial expression plasmid and its mutagenesis has also been described in chapter-2 (section 2.3.4 and 2.2.10).

Phosphorylation usually results in a small but distinguishable shift in the electrophoretic mobility of a protein on an SDS-polyacrylamide gel. To check if there were any visible differences in the mobility of WT PIM1 and the various PIM1 mutants, the purified proteins were resolved by SDS-PAGE and stained with coomassie to visualise the protein. As shown in figure 4.1A, WT PIM1 runs at a slightly higher molecular weight when compared with the K67M mutant, showing that PIM1 indeed undergoes autophosphorylation in bacteria as the K67M is incapable of autophosphorylation (Padma and Nagarajan, 1991). In terms of gel mobility, the K169R mutant was identical to the K67M mutant, while the E171A and E171Q mutants were identical to WT-PIM1. There are no commercially available antibodies against the sites of autophosphorylation in PIM1, so I used a general phospho-Tyrosine antibody that is capable of detecting phosphorylated tyrosine residues irrespective of the identity of the surrounding residues to detect

autophosphorylation of the purified PIM1 proteins on a western blot. As expected, tyrosine phosphorylation was observed with WT PIM1 but not with the K67M mutant. The E171A and E171Q mutants were also capable of autophosphorylation like WT, but the K169R mutants showed very little to no tyrosine autophosphorylation.

To confirm that the difference in mobility was due to autophosphorylation of PIM1, the proteins were treated with lambda phosphatase and resolved by SDS-PAGE (Figure 4.1B). Lambda phosphatase catalyses dephosphorylation of serine, threonine and tyrosine residues, which should down shift the WT and E171A protein bands to the same level as the K67M and K169R mutants. As expected, phosphatase treatment altered the mobility of the WT and E171A on a gel, but not the K169R and K67M mutants, further confirming the results.

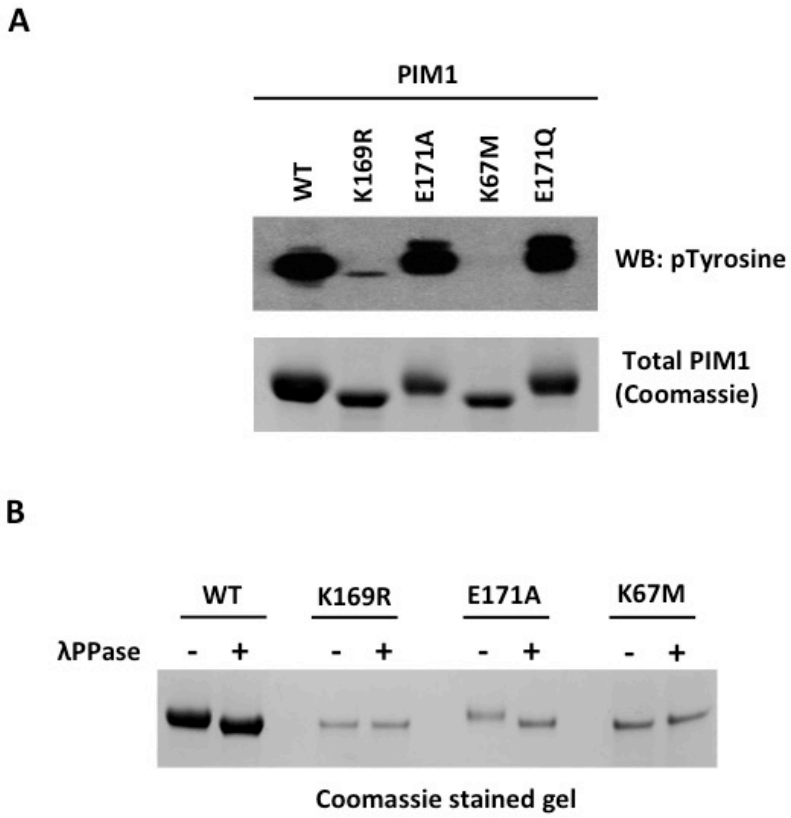

Figure 4.1 Autophosphorylation of WT PIM1 and mutants

6Xhis-PIM1 (WT and mutants) was expressed and purified from bacterial cells, and resolved by SDS-PAGE. Panel **(A)** shows the relative mobility of the purified proteins on a coomassie stained gel. A western blot for the same samples was also performed using a pan-phospho tyrosine antibody to show autophosphorylation. **(B)** The purified PIM1 proteins were treated with lambda phosphatase (+) to remove overall phosphorylation or untreated (-). Samples were resolved by SDS-PAGE, and stained with coomassie to visualise a shift in mobility, which is indicative of dephosphorylation. The data shown here is representative of two independent experiments.

4.3 *In vitro* kinase activity of PIM1 and SUMO-mutants

Next, I wanted to determine if the PIM1 SUMO-mutants, K169R and E171A, were catalytically active or inactive on PIM1 substrates. To do this, I performed *in vitro* kinase assays using purified recombinant 6Xhis-tagged PIM1 (wild-type or mutants) with Histone H3.3 (Zippo *et al.*, 2007) or c-MYC (Zhang *et al.*, 2008) as a substrate. For kinase assays, equal amount of substrate was incubated with WT or mutant PIM1 in the presence of $MgCl_2$ and ATP as described under section 2.6.1. Following 30 min incubation at 30 ^{0}C, the reactions were terminated by addition of 2X SDS lysis buffer and resolved by SDS-PAGE. The gels were either stained with coomassie to check total protein levels, or transferred onto a nitrocellulose membrane for western blotting using phospho-specific antibodies against phospho-Ser10 of H3.3 and phospho-Ser62 of c-MYC, as a read-out of kinase activity.

Wild-type PIM1 was used as a positive control in these reactions, and also as a baseline against which the kinase activity of the K169R and E171A mutants were measured. An E171Q mutant was also generated to verify the effects of mutating E171 on PIM1 kinase activity. A kinase-dead version of PIM1, K67M, was included as a negative control. In addition, a no kinase control reaction was set up to confirm the specificity of the phospho-specific antibody.

The *in vitro* kinase assay performed using Histone H3.3 as a substrate (Fig. 4.2) shows that nearly equal amount of substrate (H3.3) and kinase (PIM1) were used in each reaction. As expected, wild-type PIM1 phosphorylated Histone H3.3 at Ser10 residue, whereas the K67M (kinase-dead) mutant did not. The K169R (to a lesser extent), E171A and E171Q

mutants were also able to phosphorylate Ser10 of Histone H3.3, indicating that these mutants were active, at least *in vitro*. To confirm these results, a second well-known substrate of PIM1, c-MYC, was used in an *in vitro* kinase assay. Again, wild-type PIM1 phosphorylated c-MYC at Ser62 but the K67M mutant did not. Surprisingly, both K169R and E171A mutants showed a similar significant decrease in their ability to phosphorylate c-MYC at Ser62. The E171Q mutant was also incapable of phosphorylating c-MYC, indicating that these PIM1 mutants show reduced kinase activity towards c-MYC as a substrate *in vitro*.

The results obtained here show that the SUMO mutants display reduced kinase activity towards c-MYC but not Histone H3.3. The E171A and E171Q mutants behaved similarly in the kinase assay suggesting the effects were specific to the E171 of PIM1. These results also raise the possibility that these sites may be determinants of PIM1 substrate specificity or are required for protein-protein interactions with some substrates (such as c-MYC) but not others (such as H3.3), which would explain why they could phosphorylate one of them better than the other. Another possibility is that SUMOylation of PIM1 guides substrate specificity, which would depend upon a number of factors such as the site of modification and the biological context under which PIM1 gets SUMOylated.

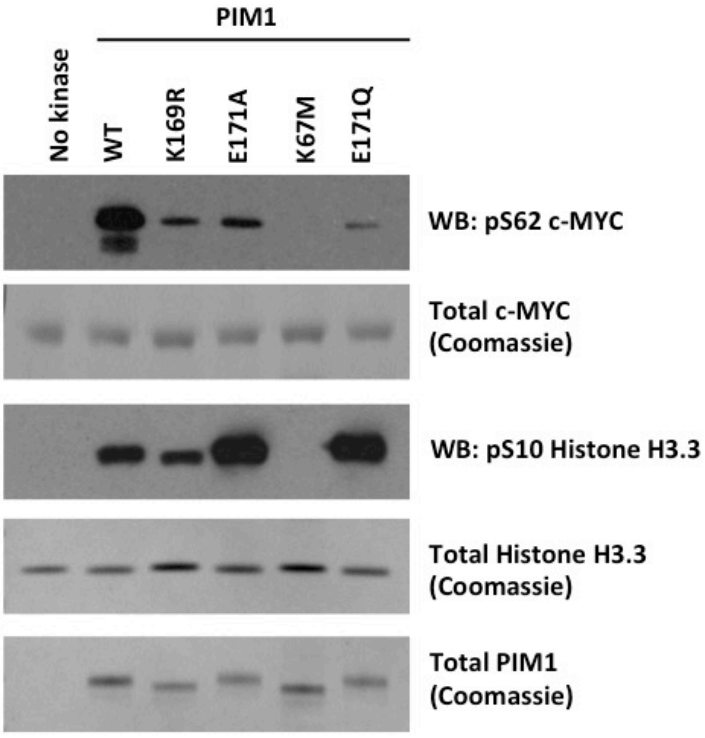

Figure 4.2 *In vitro* kinase assays using WT PIM1 and mutants

In vitro kinase assays were carried out using recombinant c-MYC or Histone H3.3 in the absence or presence of the indicated purified PIM1 protein. The reactions were incubated at 30 ^{0}C for 30 min and terminated by the addition of 2X sample buffer. The samples were resolved by SDS-PAGE, and either stained with coomassie or transferred to a nitrocellulose membrane for western blotting using phospho-specific antibodies. The data shown here is representative of two independent experiments.

4.4 Development of a method to purify SUMOylated PIM1 from *in vitro* SUMOylation reaction

Since the PIM1 SUMO-mutants do not directly mimic the effect of SUMOylation on PIM1 activity, I attempted to purify SUMOylated PIM1 from *in vitro* SUMOylation reactions, for subsequent use in a kinase assay to measure its activity. The experimental steps leading to the final experiment are described first below.

4.4.1 Small scale *in vitro* SUMOylation reactions

Previous *in vitro* SUMOylation experiments performed in chapter-3 using GST-PIM1 and SUMO2 generated a very little amount of SUMOylated PIM1. Therefore, to eliminate the possibility that the GST-tag on PIM1 itself was inhibitory, SUMOylation of 6Xhis-PIM1 was also tested. Addition of an E3 SUMO ligase can also increase the amount of SUMOylated protein *in vitro*. I used purified PIAS1 in the assay as an E3 SUMO ligase since it was readily available from Prof. Ron Hay's lab (University of Dundee). Active recombinant PIAS3 was not available, so I decided to use the IR1+M fragment as a proxy for SUMO E3 ligase to increase the levels of SUMOylated PIM1 in the reactions. The IR1+M fragment is a small portion of the SUMO E3 ligase RanBP2 that exerts complete E3 SUMO ligase activity *in vitro* with little substrate specificity (Pichler *et al.*, 2004). A combination of 6Xhis-PIM1 with GST-SUMO2 or GST-PIM1 with 6Xhis-SUMO2 was used, as I wanted to perform affinity purification of SUMOylated PIM1 using Ni^{2+}-NTA or GST beads.

Figure 4.3 shows the small scale *in vitro* SUMOylation reactions that

were carried out using GST-PIM1 and 6Xhis-SUMO2 with increasing amounts of either IR1+M or PIAS1, to identify the condition under which maximum PIM1 SUMOylation was achieved. Lane-2 of coomassie stained gel shows appearance of multiple higher molecular weight bands consistent with SUMOylated GST-PIM1 (around 75-100 kDa) in the absence of an E3 SUMO ligase. Addition of IR1+M, but not PIAS1, led to a small increase in levels of higher molecular weight bands. To confirm that these bands corresponded to SUMOylated PIM1, a western blot was performed on the same samples using a GST-tag antibody (Fig 4.3B). SUMOylated PIM1 was observed even in the absence of an E3 ligase but increased in the presence of IR1+M. However, addition of PIAS1 did not enhance PIM1 SUMOylation. This might be because PIAS proteins themselves are autoSUMOylated (Kotaja *et al.*, 2002), and this might affect their ability to SUMOylate some substrates *in vitro*.

Figure 4.4 shows the small scale *in vitro* SUMOylation reaction that was carried out using 6Xhis-PIM1 and GST-SUMO2 under the same conditions as described above. As before, higher molecular weight bands corresponding to SUMOylated PIM1 were observed in the presence of GST-SUMO2 alone without any E3 SUMO ligase. IR1+M led to polymerisation of GST-SUMO2 as evidenced by the disappearance of monomeric GST-SUMO2 in the reactions. PIAS1 failed to utilise the free SUMO2 suggesting that once autoSUMOylated PIAS1 was incapable of SUMOylating PIM1 *in vitro*. To check the levels of SUMOylated PIM1, western blotting was performed on the same samples, which showed that the presence of IR1+M slightly increased the levels of polySUMOylated PIM1, whereas PIAS1 did

not affect the levels of total SUMOylated PIM1 (Fig 4.4B). Under the experimental conditions tested, it was not possible to substantially increase the amount of SUMOylated PIM1; therefore, I chose to scale up the reaction containing 6xhis-PIM1 with GST-SUMO2 and IR1+M for further purification experiments. A detailed procedure has been described in chapter-2 (section 2.6.3).

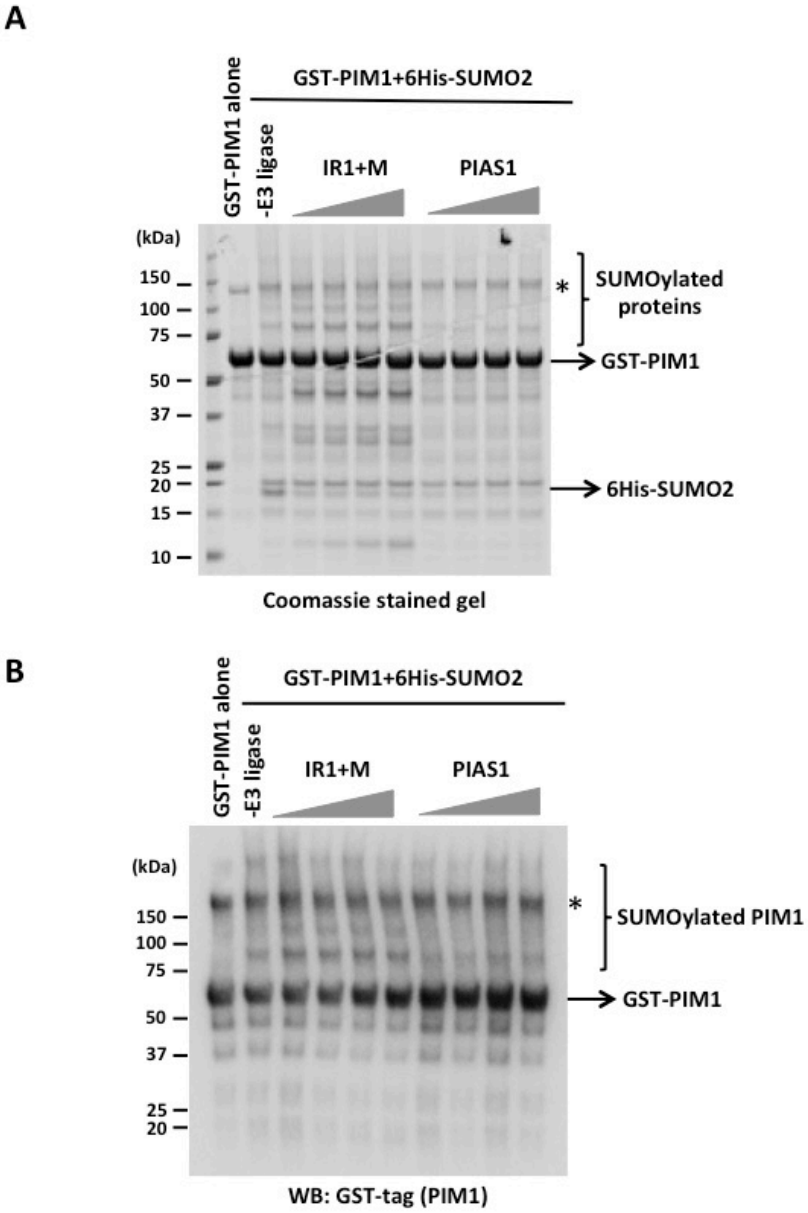

Figure 4.3 *In vitro* SUMOylation using purified GST-PIM1 and 6Xhis-SUMO2

(A) *In vitro* SUMOylation reactions were carried out using GST-PIM1 and 6Xhis-SUMO2 in the absence of an E3 ligase, or in the presence of increasing concentrations of an E3 SUMO ligase (IR1+M or PIAS1). The reactions were incubated overnight at 37 ^{0}C, and terminated by the addition of 2X sample buffer. The samples were resolved by SDS-PAGE and stained with coomassie. **(B)** Western blotting was also performed on the same sample using anti-GST antibody to detect SUMOylated PIM1. This experiment was only performed once.

* indicates an unknown protein (non-specific) co-eluting with GST-PIM1 during protein purification and also cross-reactive with the GST-tag antibody.

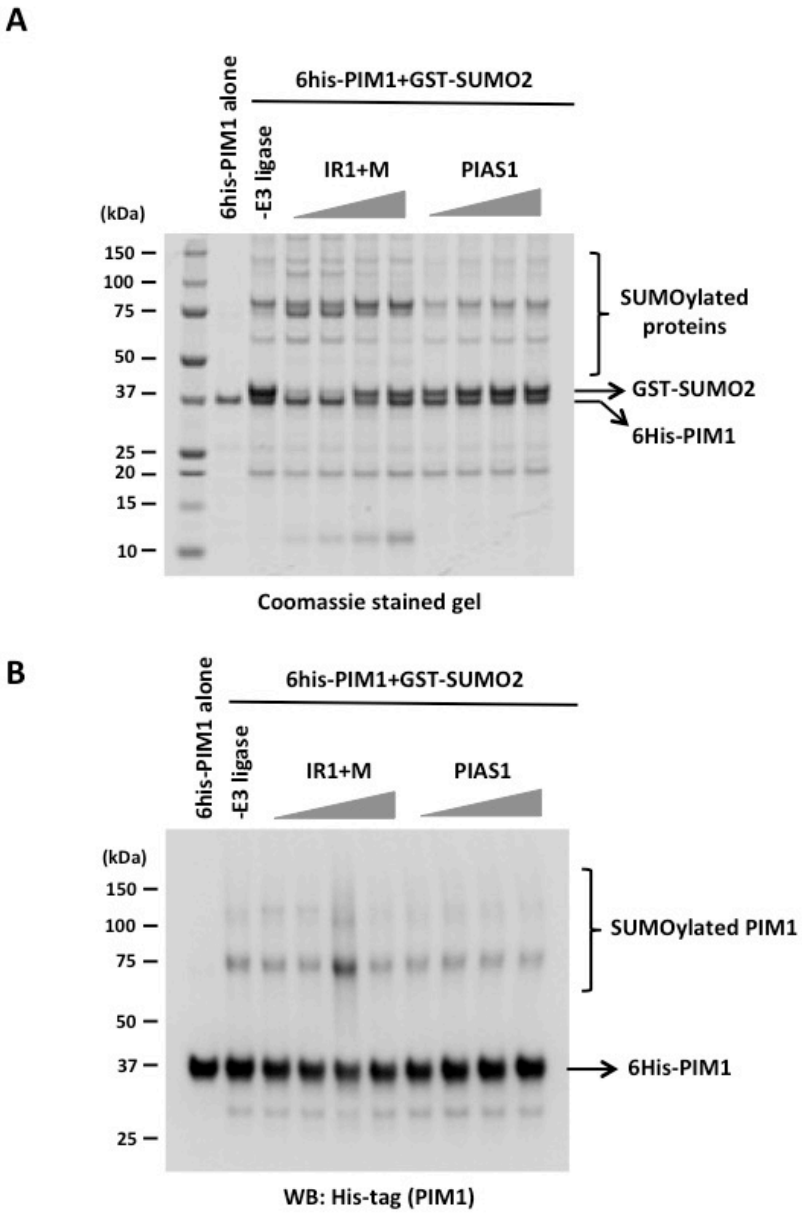

Figure 4.4 *In vitro* SUMOylation using purified 6Xhis-PIM1 and GST-SUMO2

(A) *In vitro* SUMOylation reactions were carried out using 6Xhis-PIM1 and GST-SUMO2 in the absence of an E3 ligase, or in the presence of increasing concentrations of an E3 SUMO ligase (IR1+M or PIAS1). The reactions were incubated overnight at 37 ^{0}C, and terminated by the addition of 2X sample buffer. The samples were resolved by SDS-PAGE and stained with coomassie. **(B)** Western blotting was also performed on the same sample using anti-His tag antibody to detect SUMOylated PIM1. The data shown here is representative of two independent experiments.

4.4.2 Purification of SUMOylated PIM1

The experimental strategy devised for the affinity purification of SUMOylated PIM1 has been shown in figure 4.5A. The washing and dialysis buffers used here contained 50 mM Tris pH 7.5 and 500 mM NaCl because the recombinant 6Xhis-PIM1 was purified under these conditions, and remained active in this buffer. The elution buffer was additionally supplemented with 1 mM DTT. In the first step, 6Xhis-tagged proteins i.e. the total pool of PIM1 (unmodified and SUMO-modified) was captured using Ni^{2+}-NTA beads. The captured proteins were eluted using imidazole and then dialysed to remove any imidazole. Next, GST-beads were added to specifically capture GST-SUMO2 modified PIM1, while getting rid of the unmodified PIM1 from the mix. Finally, SUMOylated PIM1 was eluted from the GST-beads using reduced glutathione, dialysed and concentrated using a spin column concentrator. As shown in figure 4.5B, both SUMOylated and unmodified PIM1 were mostly present in the first elution, showing that the pull-down worked. However, some PIM1 was still bound to the Ni^{2+}-NTA post-elution despite using a high concentration of imidazole (200 mM), suggesting that the protein was getting precipitated on the beads. The same problem was observed with elutions from GST-beads. Unfortunately, neither the concentrated elution nor the flow-through from the GST-beads showed any enrichment of SUMOylated PIM1, indicating that the protein was getting lost at some step during the process. It is possible that the binding of SUMOylated PIM1 with GST-beads was not successful, and hence SUMOylated PIM1 was washed away. Alternatively, some proteins stick to the membranes of the concentrator, which makes their elution quite difficult.

The following changes were made to the protocol in order to circumvent the problems observed above:

1. SUMOylated PIM1 was captured using GST-beads first followed by Ni^{2+}-NTA, to check if this method worked better.

2. To avoid protein precipitation on the beads, the reaction mix was diluted at least five in 50 mM Tris pH 7.5 before adding the beads.

3. The beads were incubated overnight at 4 ^{0}C instead to 1-2 hours to increase the binding of proteins to the beads.

4. The concentration of NaCl was reduced from 500 mM to 150 mM in wash and elution buffers.

5. Dialysis and concentration steps were skipped to avoid loss of protein and activity. This also reduced the time of the procedure by 2-3 days.

The purification experiment was repeated again with the changes described above, and the results are shown in figure 4.6A. The elutions obtained here were named GST elution-1 or Ni^{2+}-NTA-1, denoting the type of beads used in the first affinity purification step. The GST-beads efficiently captured the SUMOylated proteins from the reaction, and unmodified PIM1 was washed away in the flow through as desired. Most of the SUMOylated protein was found in the two elutions and very little was left uneluted from the beads. On the other hand, the Ni^{2+}-NTA beads seemed to pull-down all the protein from the SUMOylation reaction as the flow through did not contain much protein. This was not observed when 500 mM NaCl was used previously (Figure 4.4B), which would suggest that PIM1 might interact non-covalently with SUMO and/or SUMOylated proteins, and a salt concentration of 150 mM used here was insufficient to disrupt these interactions.

In the second affinity-purification step, fresh Ni^{2+}-NTA beads were added to GST-elution-1, or fresh GST-beads were added to Ni^{2+}-NTA elution-1 to purify SUMOylated PIM1. The resulting final elutions were named Ni^{2+}-NTA elution-2 or GST elution-2. Unfortunately, under both conditions the SUMOylated PIM1 failed to elute from the beads as observed in figure 4.6B. The most common way of eluting such proteins is by using a strong denaturing agent such as urea. The disadvantage of this method is that the proteins lose their structural and functional integrity, and can no longer be used in enzymatic assays without successful renaturation of the protein. Because of the limitations of this process, I decided to test the GST elution-1 (containing SUMOylated PIM1 and SUMO2) in a kinase assay, which is described in the next section.

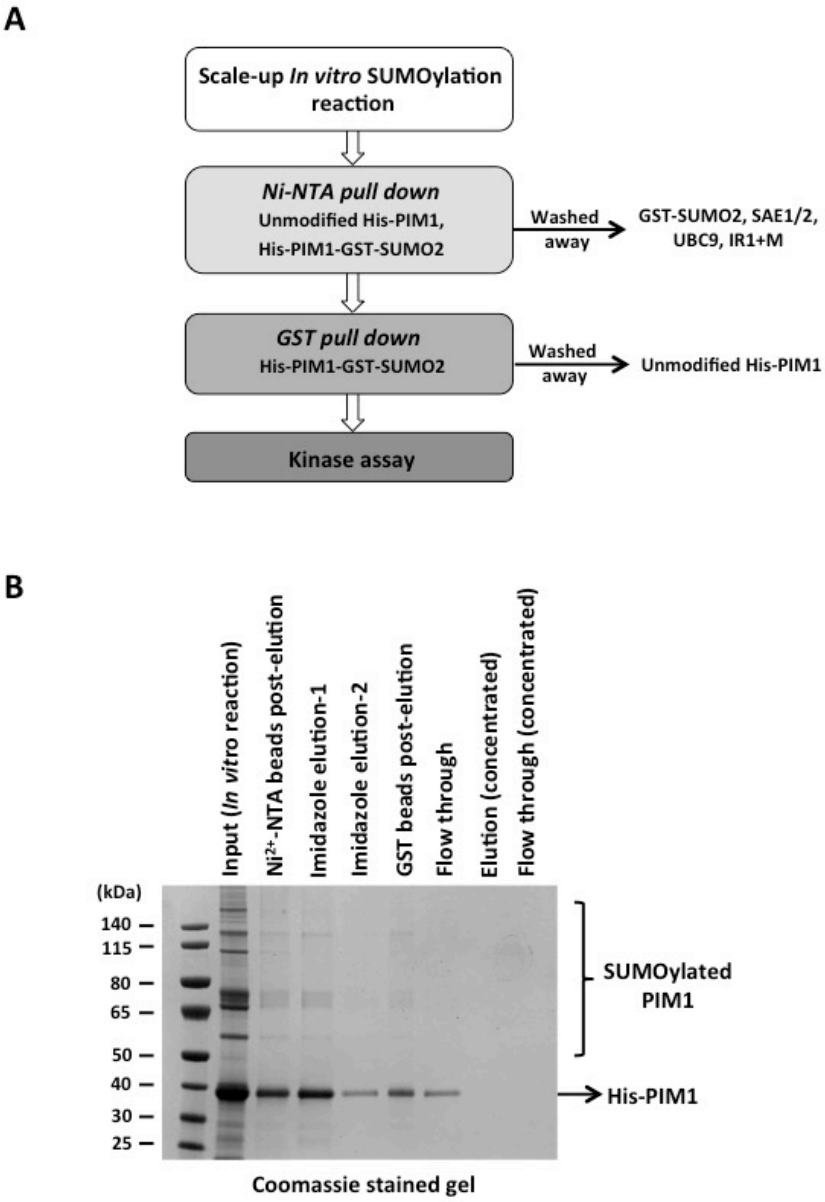

Figure 4.5 Purification of SUMOylated PIM1 from in vitro SUMOylation reaction

(A) Schematic outlining the proposed method of purification of SUMOylated PIM1 from *in vitro* SUMOylation reactions. **(B)** Coomassie stained gel showing the different steps of outlined purification procedure. 6Xhis-PIM1 (unmodified and SUMO modified) was first pulled down using Ni^{2+}-NTA beads, and eluted using imidazole. Eluted proteins were bound to GST-beads to pull down SUMOylated PIM1, and eluted using reduced glutathione. The beads were also boiled post elution to check efficiency and binding of proteins to the beads. This experiment was only performed once.

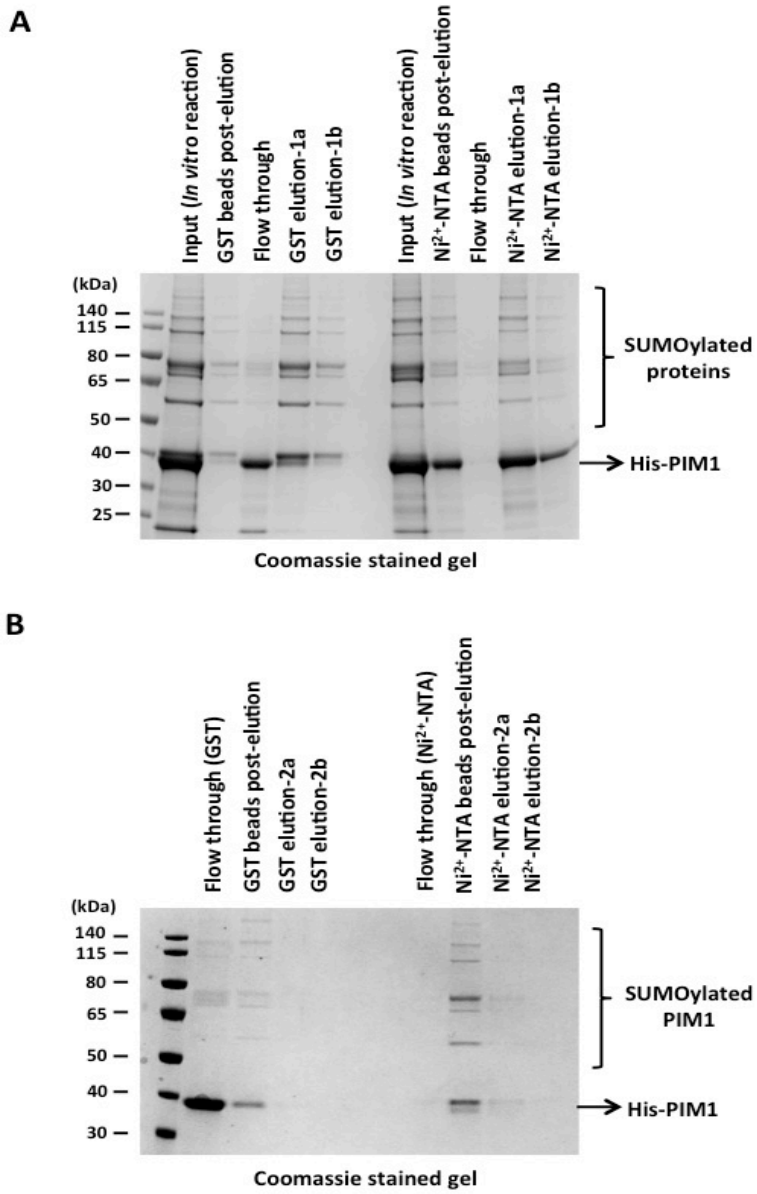

Figure 4.6 Purification of SUMOylated PIM1 from in vitro SUMOylation reaction

(A) Products of the *in vitro* SUMOylation reactions were divided into two equal fractions. The first fraction was bound to GST-beads to pull down all SUMOylated proteins including PIM1. The proteins were eluted from the beads using reduced glutathione. The second fraction was bound to Ni^{2+}-NTA beads to pull down SUMOylated and unmodified PIM1. The proteins were eluted using imidazole. The samples were resolved by SDS-PAGE and stained with coomassie. **(B)** Elutions from GST-beads were bound to Ni^{2+}-NTA beads, and elutions from Ni^{2+}-NTA beads were bound to GST-beads to isolate SUMOylated PIM1. The bound proteins were eluted as done before, and resolved by SDS-PAGE followed by coomassie staining to check purification of SUMOylated PIM1. The data shown here is representative of two independent experiments.

4.5 SUMOylation of PIM1 increases its kinase activity *in vitro*

The main goal of purifying SUMOylated PIM1 was to get rid of the relatively large proportion of unmodified PIM1 from the reactions, as it can mask the effects of the small proportion of SUMOylated PIM1 in a kinase assay. However, this might not be entirely possible as PIM1 interacts with itself, so a proportion of SUMOylated PIM1 interacts and co-purifies with unmodified PIM1, as evident from GST elution-1 shown in figure 4.6A. However, I was able to wash away the majority of unmodified PIM1 through the method described above, and increase the ratio of SUMO-modified PIM1 to unmodified PIM1. Since the GST elution-1 was obtained by affinity purification of the *in vitro* SUMOylation reactions (containing GST-SUMO2, 6Xhis-PIM1, SAE1/2, IR1+M) using GST beads, it contains a mix of SUMOylated PIM1 and SUMO2 itself and some unmodified PIM1.

For an accurate comparison of relative kinase activity, the same amount of unmodified PIM1 and SUMOylated PIM1 was used in each kinase assay reaction. This was achieved by first deSUMOylating an equal amount of GST elution-1 *in vitro* using the catalytic domain (amino acids 415-643) of the SUMO protease SENP1 (Shen *et al.*, 2006). Histone H3.3 was used as a representative substrate in this experiment. Figure 4.7A illustrates the kinase assay performed using SUMOylated and deSUMOylated PIM1. The procedure has been described in detail in chapter-2 (section 2.6.3).

As shown in figure 4.7B, SUMOylated PIM1 was found to be more active in phosphorylating Histone H3.3 at Ser10 when compared with unmodified PIM1 at all the time points. Equal amount of substrate was used in these reactions, which was further confirmed by western blotting for total Histone H3.3. To rule out that presence of SENP1 catalytic domain affected

PIM1 kinase activity, a control kinase assay was set up. Unmodified PIM1 kinase was incubated with increasing concentrations of SENP1 catalytic domain for 1 hour at 30 ^{0}C as done previously, followed by the addition of kinase assay buffer, ATP and Histone H3.3 substrate for further 30 min at 30 ^{0}C. The reactions were terminated by addition of SDS sample buffer, and ran on an SDS-polyacrylamide gel. Coomassie staining of the gel confirmed the presence of equal amount of kinase and substrate in each reaction (Fig 4.7C). Western blotting performed using phospho Ser10 Histone H3.3 antibody showed no obvious difference in the level of phosphorylation in the absence or presence of the SENP1 fragment. These results confirm that, under these conditions, SUMOylated PIM1 shows higher kinase activity towards Histone H3.3 than unmodified PIM1.

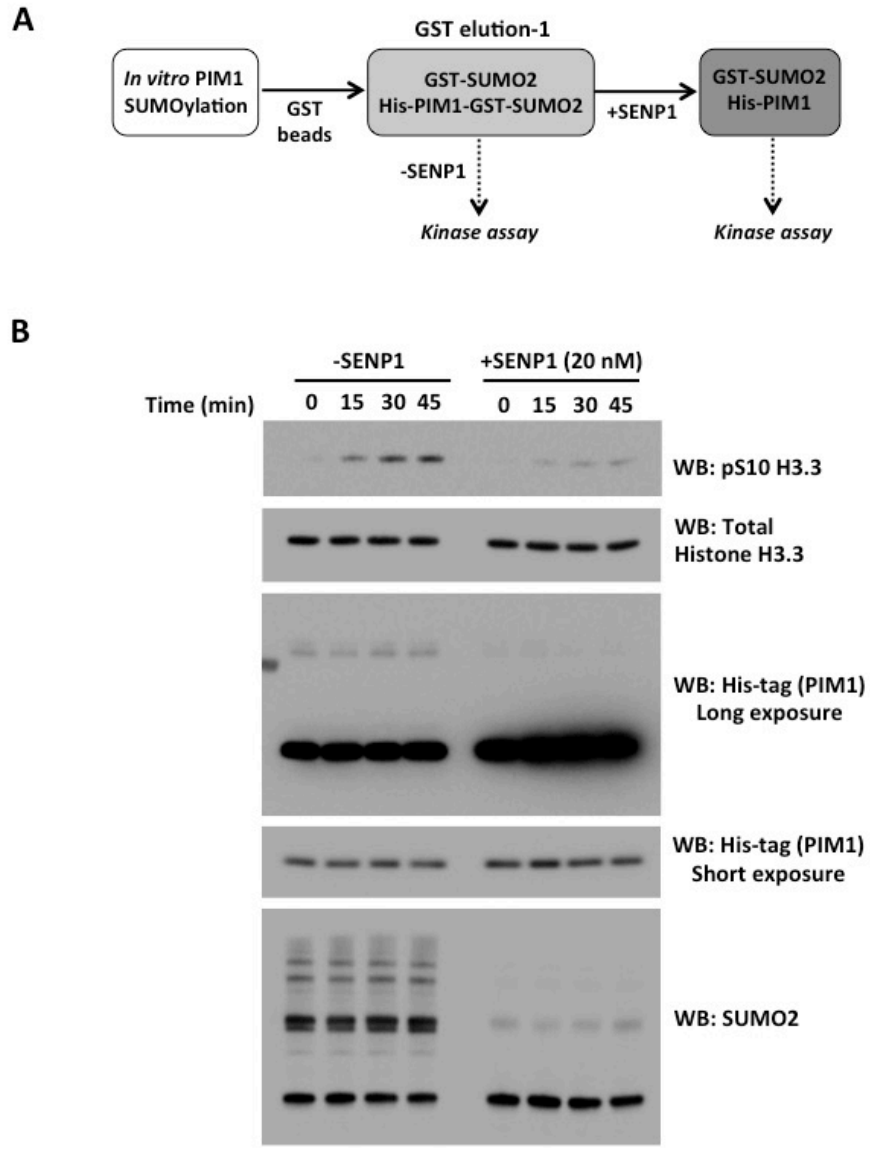

Figure 4.7 DeSUMOylation coupled kinase assay

(A) Schematic outlining the purification of SUMOylated proteins, followed by deSUMOylation and kinase assay to measure the activity of SUMOylated PIM1. **(B)** SUMOylated proteins were captured using GST-beads, and eluted in reduced glutathione. The elutions were divided into two equal parts. The first part was left untreated, and the second part was treated with SENP1 catalytic domain to deconjugate SUMO from proteins. Resulting mix of proteins containing SUMOylated PIM1 or (deSUMOylated) unmodified PIM1 was used in a kinase assay using Histone H3.3 as a substrate. Samples were collected at the indicated time points and terminated by the addition of 2X sample buffer, and resolved by SDS-PAGE.

C

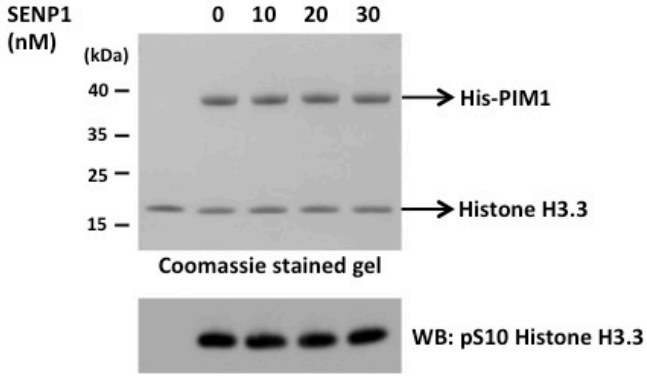

Western blotting was performed using indicated antibodies to measure histone H3.3 phosphorylation. **(C)** Purified WT PIM1 was first incubated with or without SENP1 catalytic domain fragment for 1 hour at 30 ^{0}C, and immediately used in a kinase assay using Histone H3.3 as substrate. The reactions were incubated at 30 0C for 30 min and terminated by adding 2X sample buffer. The samples were resolved by SDS-PAGE and either stained with coomassie to check protein levels. A western blot was also performed to measure histone H3.3 phosphorylation using a phospho-specific antibody. The data shown here is representative of two independent experiments.

4.6 PIM1 protein induction in tetracycline-inducible cell lines

HeLa and U2OS cells expressing YFP-tagged PIM1 (WT and mutants) in a tetracycline-inducible manner were generated to assess PIM1 function under cellular conditions. The generation of these cell lines has been described in chapter-2 (section 2.3.3 and 2.5.10). Once a stable pool of colonies was established, the cells were assayed for the expression of YFP-PIM1 by the addition of doxycycline (a more stable analogue of tetracycline) at a concentration of 1 µg/ml for 24 hours, followed by western blotting with GFP-tag antibody. Since YFP is a mutant form of GFP, the GFP antibody is widely used to detect YFP in western blotting, immunofluorescence, flow-cytometry and also for immunoprecipitation.

Figure 4.8A shows that YFP-PIM1 expression is induced in HeLa-FRT cells only when doxycycline is added to the cells. The blots also show the maximum possible expression levels of WT, K169R, E171A and K67M achievable in HeLa-FRT cells upon addition of a saturating concentration of doxycycline (1 µg/ml). The main advantage of using these cell lines is that by adding varying concentrations of doxycycline to the cells, we can control the level of protein expression. In order to find out the concentrations of doxycycline at which WT PIM1 and mutants were expressed at comparable levels, cells were treated with the indicated concentration of doxycycline for 48 hours, followed by western blotting with GFP-antibody. The results shown in figure 4.8B show that the system works as expected, but it was difficult to determine relative concentrations at which WT, K169R, E171A and K67M were expressed at exactly equal levels. However, WT PIM1 expression at 10 ng/ml seemed comparable to the expression of K169R at 20 ng/ml, E171A at

10 ng/ml or 12 ng/ml and K67M at 50 ng/ml. The first few experiments such as cycloheximide chase assays (described later) were performed with HeLa-FRT cells. However, over time these cells lost their responsiveness to doxycycline, and could not be used any further. Therefore, I also generated new PIM1 inducible cell lines in U2OS background.

Figure 4.9A shows the maximum possible expression levels of WT PIM1 and mutants upon addition of 1 µg/ml doxycycline for 24 hours in U2OS-FRT cells, which is very similar to the expression levels observed in the HeLa-FRT cells. These levels possibly reflect the differences in their protein stability (discussed in the next section). A doxycycline titre was also performed to identify conditions of similar protein expression levels in the different U2OS cell lines. Figure 4.9B shows the increase in levels of protein expression in response to increasing doxycycline concentrations. WT PIM1 expression at 10 ng/ml seemed comparable to that of the expression of K169R at 20 ng/ml, E171A at 10 ng/ml and K67M at 50 ng/ml. Cells expressing K169R showed some protein expression even in the absence of doxycycline. This leakiness is probably because of the presence of tetracycline (tet) in the FBS, and can be eliminated by the use of tet-free FBS.

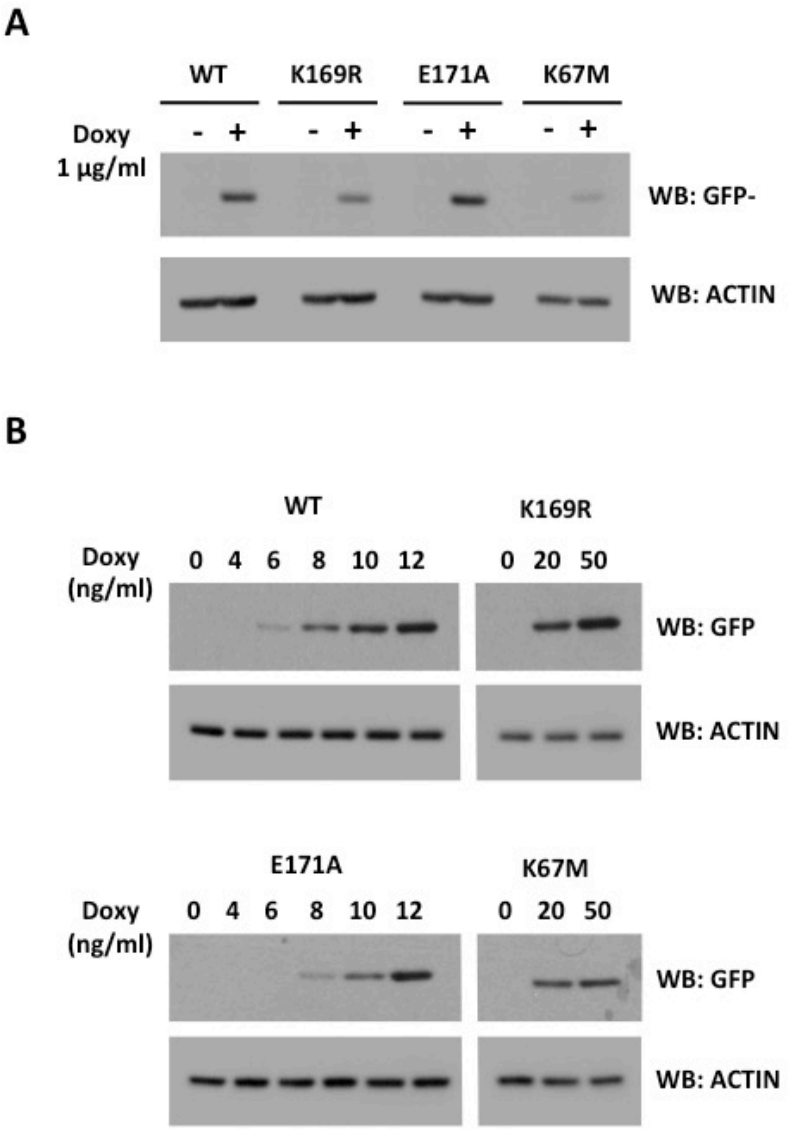

Figure 4.8 Induction of PIM1 proteins in HeLa-FRT cells following doxycycline addition **(A)** The cells were assayed for the expression of YFP-PIM1 in the presence or absence of doxycycline (1 µg/ml) for 24 hours, followed by western blotting with GFP-tag antibody. **(B)** Cells were treated with increasing concentrations of doxycycline for 48 hours, followed by western blotting with GFP-antibody. The data shown here is representative of two independent experiments.

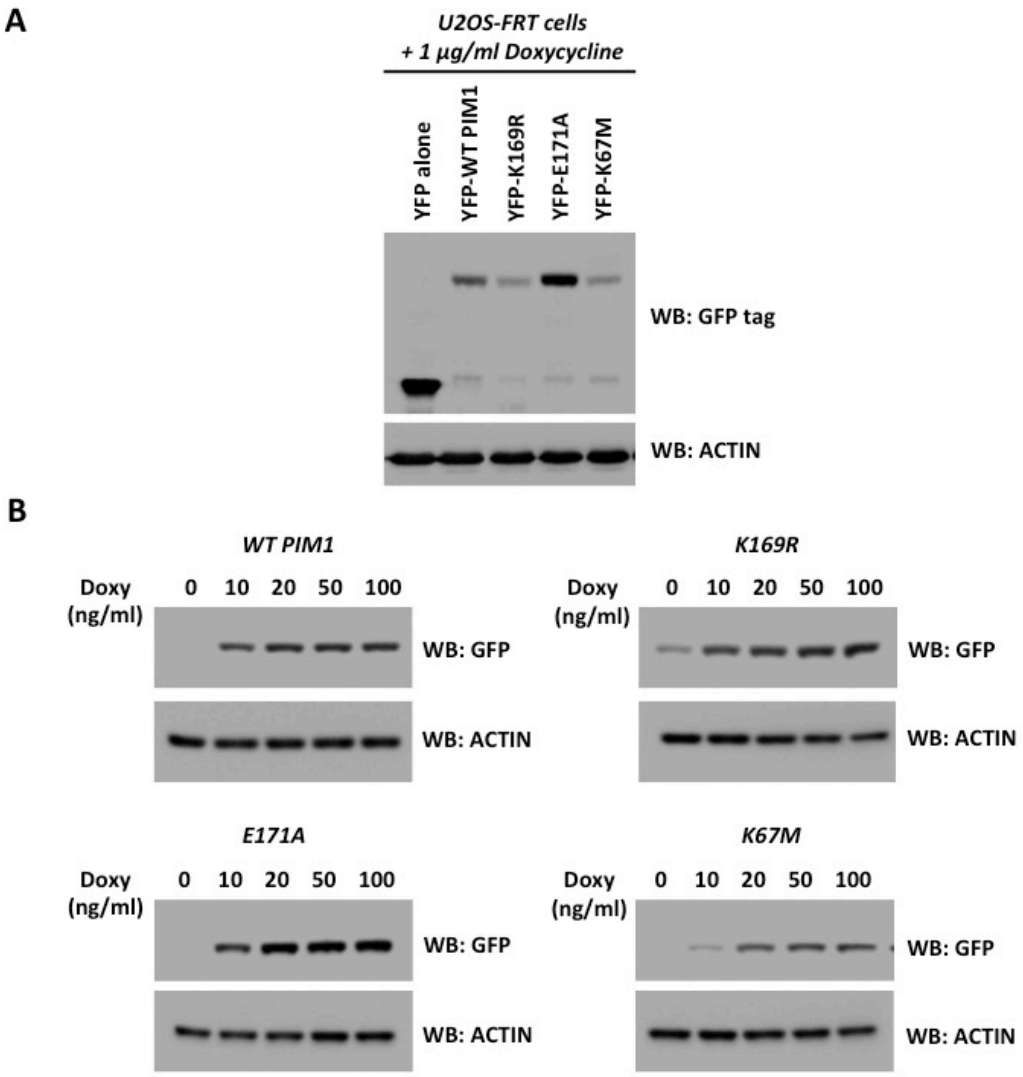

Figure 4.9 Induction of PIM1 proteins in U2OS-FRT cells following doxycycline addition (A) Cells were treated with 1 µg/ml doxycycline for 24 hours, followed by western blotting using anti-GFP antibody. **(B)** Cells expressing PIM1 were treated with increasing concentrations of doxycycline for 48 hours, followed by western blotting using anti-GFP antibody. The data shown here is representative of two independent experiments.

4.7 Phosphorylation of endogenous substrates by PIM1 and mutants

The *in vitro* kinase assays performed using the K169R and the E171A mutants suggested that the SUMOylation might regulate PIM1 substrate specificity. To check if these effects could also be observed under cellular conditions, I used the U2OS-FRT cells expressing YFP-PIM1 in a tet-inducible manner. The expression of PIM1 was induced by addition of the indicated concentration of doxycycline to the cells for 48 hours (Fig 4.10), followed by western blotting for some PIM1 substrates. As shown in the figure 4.10, there was a small but clear increase in Histone H3 phosphorylation at Ser10 in cells expressing WT PIM1. Cells expressing YFP alone or the kinase dead K67M PIM1 did not affect Histone H3 phosphorylation as expected, confirming that YFP-PIM1 was indeed active in U2OS cells. The two PIM1 SUMO-mutants, K169R and E171A, although expressed at higher levels when compared to WT PIM1, phosphorylated Histone H3 to the same extent as the WT PIM1 indicating that these mutants were active against Histone H3, as observed previously in the *in vitro* kinase assays. I next checked the phosphorylation of the classical PIM1 substrate, BAD. As previously published (Aho *et al.*, 2004), WT PIM1 phosphorylated BAD at Ser112, whereas the K67M mutant did not. Interestingly, the PIM1 SUMO mutants were incapable of phosphorylating BAD and thus, in this case, behaved as kinase-dead K67M mutant. Furthermore, a small increase in the total levels of c-MYC protein was observed in cells expressing WT PIM1 but not K67M, suggesting phosphorylation mediated stabilisation of c-MYC as previously reported (Zhang *et al.*, 2008). The K169R and the E171A mutants were also capable of stabilising c-MYC and phosphorylating c-MYC

at Ser62 as the WT PIM1. This is in contrast to the observations from *in vitro* kinase assays performed with c-MYC as a substrate, and could be due to the differences in protein folding between bacterial and mammalian cells, or due to the different environment of cells.

PIM kinase inhibitors such as SGI-1776 and AZD1208 have been shown to exert anti-tumour effects by inhibiting protein translation via decreased phosphorylation of 4E-BP1 and p70 S6K (Yang *et al.*, 2012; Keeton *et al.*, 2014). So I wanted to examine if expression of WT PIM1 or mutants affected protein translation in U2OS cells by looking at phosphorylation of 4E-BP1 at Thr37/46 and p70 S6K at Thr389. However, there was no significant increase in phosphorylation of these proteins, suggesting that protein translation was not affected in these cells upon PIM1 expression.

Additionally, I also looked at signalling pathways activated in response to PIM1 activation in U2OS cells. Small molecule inhibition of AKT in prostate cancers has been shown to activate PIM kinases, indicating the existence of a feedback loop between PIM and AKT kinases (Cen *et al.*, 2013). Therefore, I wanted to investigate if expression of PIM1 has any effect on the levels or activity of AKT in U2OS cells. Western blotting performed using a pan-AKT antibody showed that PIM1 (WT or mutant) does not affect the total levels of AKT. However, expression of WT PIM1 significantly reduced basal phosphorylation of AKT at Ser473. Since phosphorylation of AKT at Ser473 is required for maximal activation of kinase activity, these results suggest that basal activity of AKT is reduced in these cells. The same downregulation of AKT activity was also observed in cells expressing the K169R and the E171A

mutants suggesting that PIM1 SUMOylation may not play a role in the PIM1-AKT feedback mechanism. Also, the K67M mutant did not affect AKT phosphorylation or activity suggesting that kinase activity of PIM1 is important for the downregulation of AKT activity. These results are also supported by a previous study showing that the hearts of PIM1 knock-out mice show higher levels of AKT Ser473 phosphorylation when compared with wild-type mice (Muraski *et al.*, 2007).

Furthermore, I looked at ERK1/2 phosphorylation as inhibition of PIM1 by siRNA or small molecule inhibitors has been shown to decrease ERK1/2 phosphorylation in prostate and CLL cells (Wang *et al.*, 2012; Decker *et al.*, 2014). As observed in figure 4.10, expression of PIM1 in U2OS cells significantly increased the levels of phospho ERK1/2 at Thr202/Tyr204 without affecting the total levels of ERK1/2, while the kinase-dead mutant K67M did not. Intriguingly, the PIM1 SUMO-mutants did not affect ERK1/2 phosphorylation in U2OS cells, suggesting that PIM1 SUMOylation regulates ERK signalling in cancer cells.

Overall, the results shown here, using the PIM1 K169R and E171A mutants, suggest that PIM1 SUMOylation may regulate substrate specificity, and maybe involved in the maintenance of ERK signalling, but not AKT pathway. However, further investigation is required in support of this hypothesis.

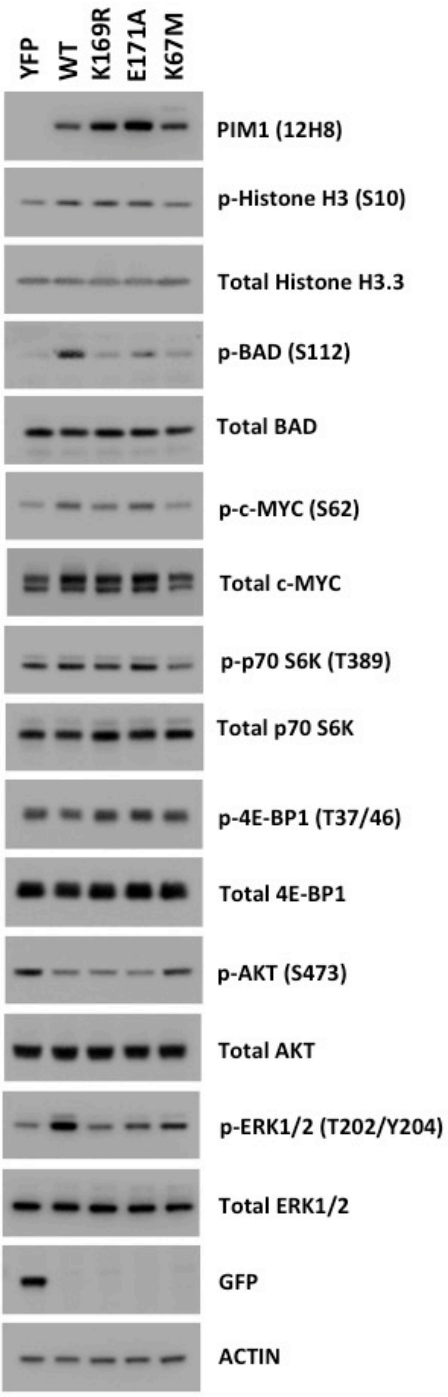

Figure 4.10 Phosphorylation of endogenous substrates by WT PIM1 and mutants in U2OS-FRT cells U2OS-FRT cells expressing YFP alone, YFP-WT PIM1 and YFP-E171A were treated with 10 ng/ml doxycycline; U2OS-FRT expressing YFP-K169R was treated with 20 ng/ml doxycycline and U2OS-FRT expressing YFP-K67M was treated with 50 ng/ml doxycycline for 48 hours, followed by western blotting using indicated antibodies. The data shown here is representative of two independent experiments.

4.8 SUMOylation of PIM1 regulates protein-protein interactions

To investigate if PIM1 SUMOylation promotes or inhibits interaction of PIM1 with its substrates, co-immunoprecipitation experiments were performed using WT PIM1 or mutants. I first tested the interaction of PIM1 with c-MYC since it is an important PIM1 substrate. To do this, H1299 cells were co-transfected with plasmids encoding c-MYC with WT PIM1 or the indicated mutants, and immunoprecipitated using two different PIM1 antibodies as described in chapter-2 (section 2.5.12). The elutions were resolved by SDS-PAGE, followed by western blotting with PIM1 and c-MYC antibodies. As seen in figure 4.11, immunoprecipitation of PIM1 was successful with both antibodies, and no PIM1 was detected when IgG was used as negative control. As expected, c-MYC co-immunoprecipitated with WT PIM1 as previously reported (Zhang *et al.*, 2008), but not in IgG showing specificity of the interaction. c-MYC was also found to co-immunoprecipitate with the K169R and E171A mutants, suggesting that the mutation of these sites or PIM1 SUMOylation does not affect protein-protein interactions with c-MYC.

I also tested PIM1 interaction of another substrate, MDM2, by co-immunoprecipitation experiment. This was performed in H1299 cells transfected with MDM2 and PIM1 plasmids. Since both PIM1 antibodies (12H8 and Bethyl) gave same results with c-MYC co-immunoprecipitation, I only used 12H8 PIM1 antibody for immunoprecipitation here. As shown in figure 4.12A, PIM1 (WT and mutants) were immunoprecipitated efficiently in all cases, and no protein was detected in the IgG negative control as desired. MDM2 co-immunoprecipitated with WT PIM1 and was absent from IgG

samples. A closer look at the immunoprecipitated MDM2 showed two closely migrating bands suggestive of some phosphorylated form of MDM2. The K169R and the K67M mutants also pulled down the modified and unmodified forms of MDM2. Interestingly, the E171A mutant only interacted with the higher molecular weight form of MDM2, but not with the lower molecular weight band. This suggests that the E171 residue in PIM1 is important for interaction with MDM2, or that SUMOylation of PIM1 promotes its interaction with MDM2.

Our lab previously demonstrated that PIM1 increases the stability of wild-type MDM2, in a manner that is not dependent on the PIM1 phosphorylation sites in MDM2 i.e. Ser166 and Ser186 (Hogan *et al.*, 2008), suggesting that interaction of MDM2 with PIM1 alone is sufficient for its stabilisation, or that a PIM1 substrate indirectly regulates MDM2 levels. Therefore, I wanted to investigate if the PIM1 SUMO mutants, K169R and E171A could also stabilise MDM2 levels. For this, H1299 cells were transfected with plasmids expressing MDM2 alone, or in combination with WT PIM1, K169R, E171A or K67M, followed by western blotting for MDM2 and PIM1. As observed in figure 4.12B, expression of WT PIM1, but not K67M, increased the levels of MDM2 when compared with MDM2 alone. The K169R mutant also stabilised MDM2, although to a lesser extent than the WT PIM1. Surprisingly, the E171A mutant seemed to destabilise MDM2 acting as dominant-negative, further suggesting that PIM1 mediated stabilisation of MDM2 might be SUMOylation dependent. It should be noted that double bands for MDM2 are only visible in hand-made gels but not in precast gels, presumably due to the difference in gel composition that can affect protein

mobility and resolution. The samples in figure 4.12B were resolved on a precast gel, so the MDM2 doublets are not observed here. Since the exact nature and site of MDM2 phosphorylation was unknown, I did not follow up on this, but it will be interesting to investigate this aspect in the future.

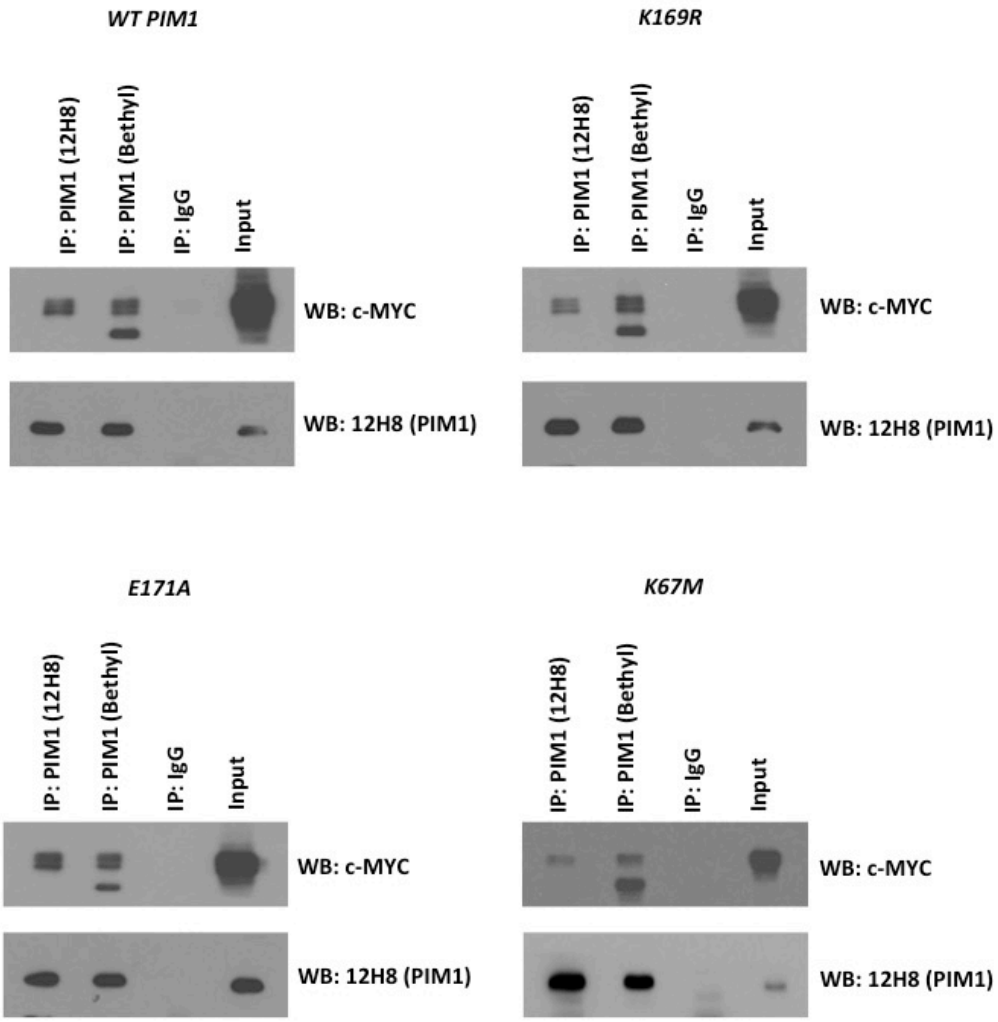

Figure 4.11 Co-immunoprecipitation of PIM1 with its substrate, c-MYC

H1299 cells were transfected with plasmids expressing c-MYC with either WT PIM1 or the mutants. Co-immunoprecipitation was performed using two PIM1 antibodies 12H8 and Bethyl or IgG negative control, and immune complexes were captured on Protein-A beads. Immunoprecipitated proteins were eluted by boiling the beads in 2X sample buffer, followed by western blotting for c-MYC or PIM1. The data shown here is representative of two independent experiments.

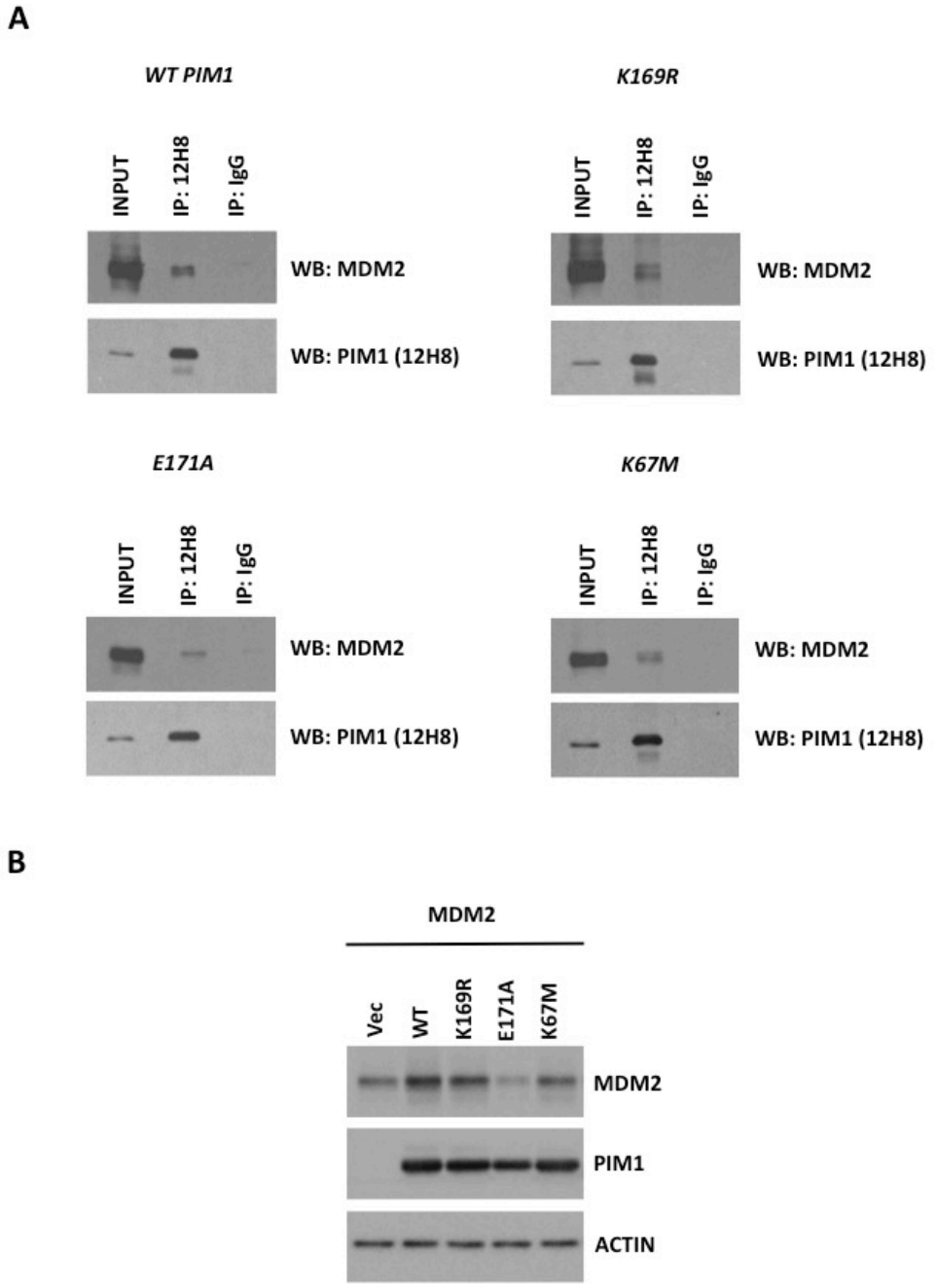

Figure 4.12 Co-immunoprecipitation of PIM1 with its substrate, MDM2

(A) H1299 cells were transfected with plasmids expressing MDM2 with either WT PIM1 or the mutants. Co-immunoprecipitation was performed using 12H8 (PIM1) antibody or IgG negative control, and immune complexes were captured on Protein-A beads. Immunoprecipitated proteins were eluted by boiling the beads in 2X sample buffer, followed by western blotting for MDM2 or PIM1. **(B)** Equal amount of the indicated PIM1 proteins were coexpressed with MDM2 in H1299 cells, and the lysates were subjected to SDS-PAGE using precast gels, followed by western blotting using indicated antibodies. The data shown here is representative of two independent experiments.

4.9 SUMOylation of PIM1 differentially regulates its stability

To determine whether SUMOylation of PIM1 affects its stability, I performed cycloheximide (CHX) chase assays. CHX blocks global protein synthesis in eukaryotic cells, and can therefore be used to measure half-life or relative protein stability in cells. To perform this assay, I transfected H1299 cells with plasmids encoding MYC-tagged WT PIM1, K169R, E171A and K67M. After 24 hours, cells were untreated or treated with 50 µg/ml CHX, and the cells were harvested at 1, 2, 3 or 4 hours post CHX addition. The cell extracts were analysed for expression of PIM1 by SDS-PAGE and western blotting using 12H8 (PIM1) antibody. The relative levels of protein were also quantified using Image Lab software (Biorad). As indicated in figure 4.13, the half-life (T1/2) of WT PIM1 was found to be around 120 min in these cells. The K67M or kinase-dead PIM1 was relatively unstable with a half-life of approximately 70 min, suggesting that kinase activity of PIM1 regulates it stability. On the other hand, the K169R mutant was slightly less stable than the WT with a half-life of 110 min. Interestingly, the E171A mutant was relatively more stable than WT PIM1, K169R and K67M with a half-life of over 240 min. The T1/4 (25% protein remaining) for WT, K169R, E171A and K67M was >240 min, 180 min, >240 min and 160 min respectively.

To further confirm these results, and to show that the results were not affected by transfection efficiency of the different plasmids in H1299 cells, I used HeLa-FRT cells inducibly expressing YFP-PIM1 for the CHX assay. HeLa-FRT-PIM1 cells were treated with doxycycline (50 ng/ml) for 24 hours prior to the addition of CHX (50 µg/ml). Cells were harvested at the given time periods, resolved by SDS-PAGE and western blotting was performed using GFP antibody to detect PIM1. The half-life of YFP tagged WT PIM1

and the mutants in HeLa cells were qualitatively similar to H1299 cells. Contrary to the western blots shown in Fig 4.14 and the results obtained in H1299, the quantification data showed that both WT PIM1 and K169R mutant have a half-life of 80 min in HeLa-FRT cells. However, the T1/4 (25% protein remaining) of WT PIM1 and K169R was 160 min and 135 min respectively suggesting that WT PIM1 was indeed slightly more stable than K169R. This error can be resolved by obtaining an average of quantification data from 2 or 3 independent experiments. As expected, the K67M mutant was again relatively unstable than WT PIM1 (half life around 57 min). The E171A mutant was most stable with half-life over 360 min (Figure 4.14). The T1/4 of E171A was >360 min and that of K67M was 115 min.

The western blot data and their quantification performed here suggest that the relative protein stabilities of WT PIM1 and its mutants are in the following order: E171A>WT>K169R>K67M, indicating that SUMOylation differentially regulates PIM1 stability in the cells. Since the K169R mutant is less stable than the WT, this would suggest that SUMOylation at K169 stabilises PIM1. On the contrary, PIM1 SUMOylation at K169 and a second unknown lysine together might negatively regulate PIM1 stability, as the E171A mutant (incapable of SUMOylation at both sites) is more stable than WT PIM1.

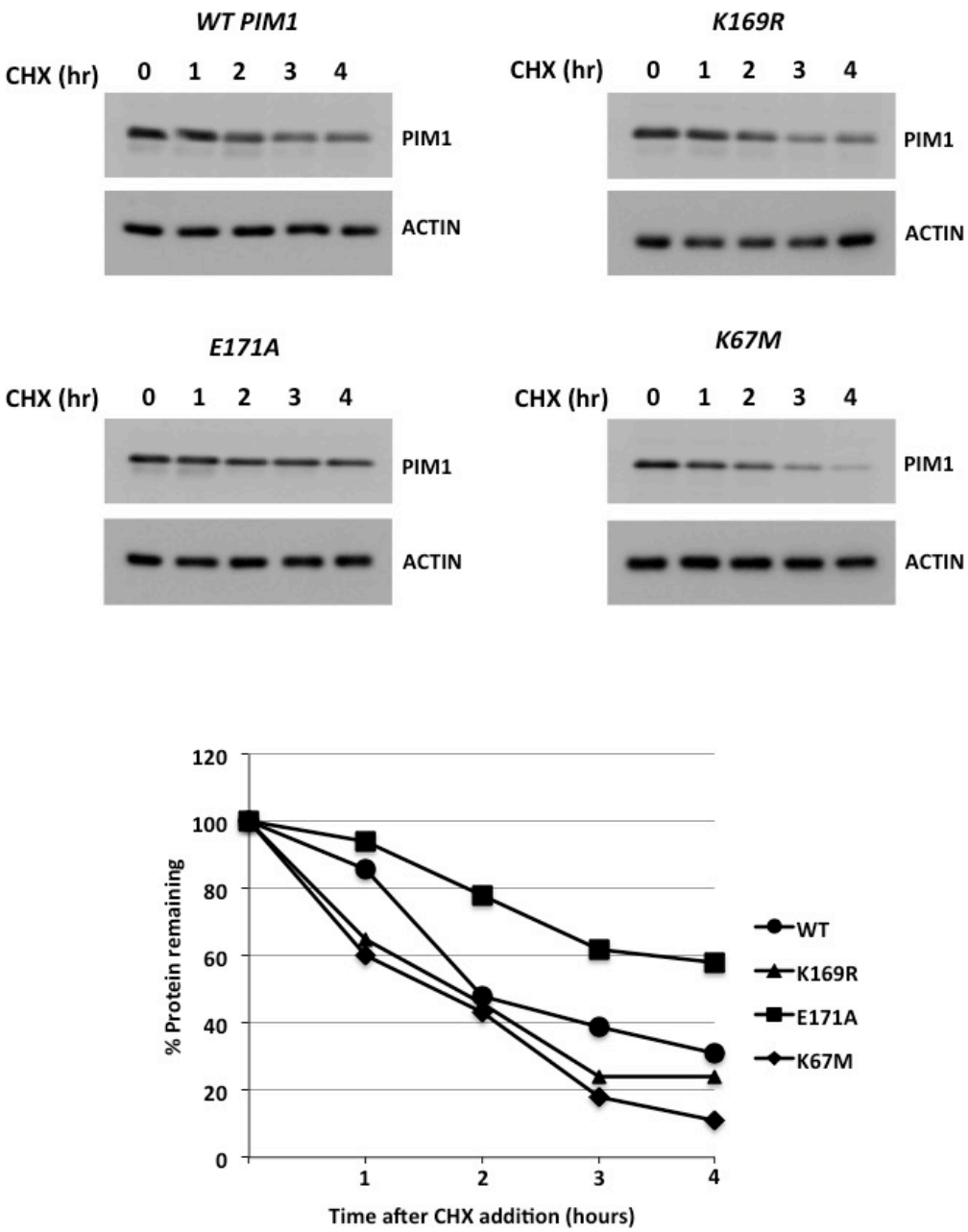

Figure 4.13 Cycloheximide chase of different PIM1 mutants in H1299 cells

Cells were transiently transfected with plasmids encoding MYC-tagged PIM1 and treated with cycloheximide (50 µg/ml) 24 hours post transfection. Cell lysates were harvested directly in 2X sample buffer at the indicated time points, followed by western blotting for PIM1. Actin was used a loading control. The band intensity in each case was quantified relative to the zero time point, which was set as 1, using Biorad ImageLab software, and plotted on a graph as percentage of protein remaining. The data shown here is representative of two independent experiments.

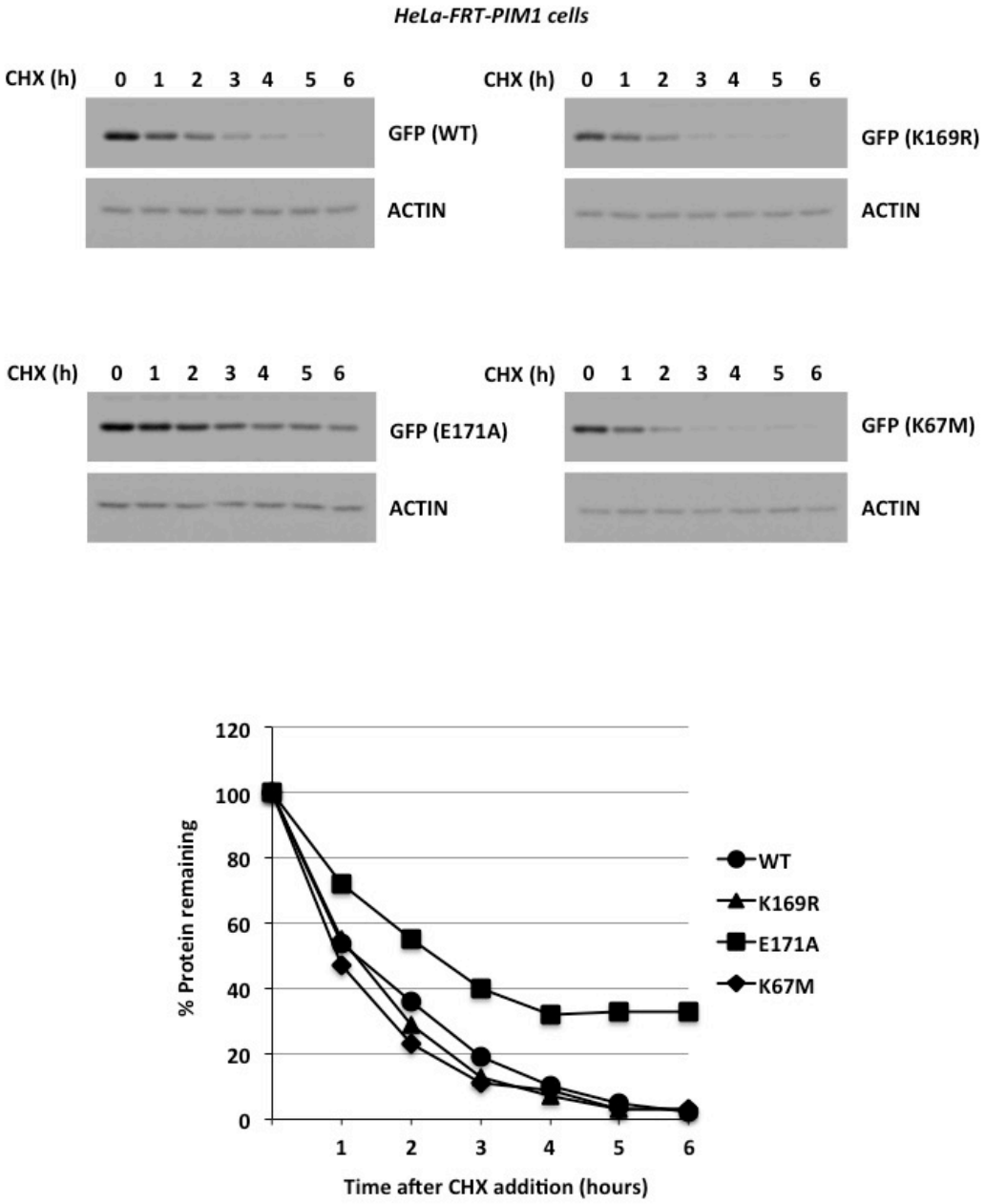

Figure 4.14 Cycloheximide chase of different PIM1 mutants in HeLa-FRT cells

HeLa-FRT cells stably expressing YFP-PIM1 were treated with 50 ng/ml doxycycline for 24 hours followed by addition of cycloheximide (50 µg/ml). Cell lysates were harvested directly in 2X sample buffer at the indicated time points, followed by western blotting for GFP (PIM1). Actin was used a loading control. The band intensity in each case was quantified relative to the zero time point, which was set as 1, using Biorad ImageLab software, and plotted on a graph as percentage of protein remaining. The data shown here is representative of two independent experiments.

4.10 SUMOylation of PIM1 promotes its ubiquitination

As mentioned in chapter-1, SUMOylation has been shown to either promote or inhibit ubiquitination of substrates. Since the PIM1 SUMO mutants showed a change in protein stability, I wanted to investigate if this was due to a change in their ability to undergo ubiquitination in cells. To answer this, I performed ubiquitination assays in H1299 cells. Cells were transfected with plasmids expressing 6Xhis-tagged ubiquitin with either WT PIM1, K169R, E171A or K67M mutants. Ubiquitinated proteins were pulled down using Ni^{2+}-NTA beads under denaturing conditions, and the elutions were subjected to SDS-PAGE, followed by western blotting for PIM1. As shown in figure 4.15, WT PIM1 was ubiquitinated as evidenced by the formation of higher molecular weight adducts. Interestingly, the pattern of ubiquitination observed was different from that of PIM1 SUMOylation, which usually runs as a doublet. Both K169R and K67M mutants were also ubiquitinated similar to WT PIM1 suggesting that mutation of these lysines does not affect PIM1 ubiquitination. This also indicates that K169 and K67 are probably not the major sites of ubiquitination. Although it cannot be ruled that, like SUMO, the sites of ubiquitination in PIM1 are also promiscuous. Conversely, the ubiquitination of the E171A mutant was significantly reduced, although not completely abolished, suggesting that SUMOylation of PIM1 might promote its ubiquitination. So far, mutation of a glutamic acid has not been shown to affect ubiquitination independently of SUMOylation, so it is plausible that this is a SUMO specific effect.

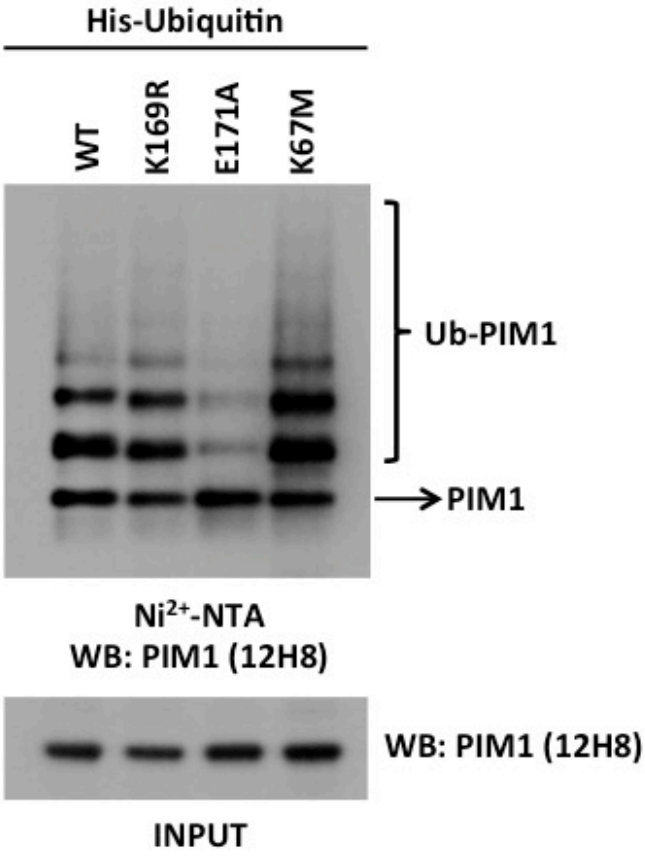

Figure 4.15 Ubiquitination assay of WT PIM1 and mutants

H1299 cells were transfected with plasmids expressing MYC-tagged WT PIM1, K169R, E171A and K67M with 6Xhis-ubiquitin. Forty-eight hours post transfection, ubiquitinated proteins were affinity purified under denaturing conditions using Ni^{2+}-NTA beads, as done previously for SUMOylation assays. Eluted proteins and whole cell lysate (input) were resolved by SDS-PAGE, and western blotting was performed using 12H8 (PIM1) antibody. The data shown here is representative of three independent experiments.

4.11 RNF4 mediates degradation of SUMOylated PIM1

Ubiquitination assay performed with the PIM1 SUMO-mutant, E171A, suggested that SUMOylation might enhance PIM1 ubiquitination. Interestingly, it was shown that polySUMO-modified proteins, such as PML, are specifically targeted for degradation by the SUMO-specific E3 ubiquitin ligase RNF4 (Tatham *et al.*, 2008). Therefore, I wanted to test if RNF4 could also mediate degradation of polySUMOylated PIM1. COS7 cells were transfected with plasmids encoding MYC-PIM1 together with or without 6Xhis-SUMO2 and HA-UBC9, in the presence of absence of WT or mutant RNF4. A Ni^{2+}-NTA pull-down experiment was performed as described previously, and the lysates were subjected to SDS-PAGE and western blotting.

As shown in figure 4.16, expression of SUMO2 and UBC9 with PIM1 led to the formation of polySUMOylated PIM1. Addition of RNF4 to the reaction caused a decrease in the levels of SUMOylated PIM1. This effect was most likely due to selective ubiquitin-mediated degradation of SUMOylated PIM1, as a mutant form of RNF4, where the RING domain is mutated (mRING), is unable to degrade SUMOylated PIM1. Furthermore, the RNF4 mSIM mutant, where the three SUMO interacting motifs were mutated, was also incapable of degrading SUMOylated PIM1 suggesting that recognition or binding of RNF4 to polySUMO chains on the substrate (PIM1) is equally important for its degradation.

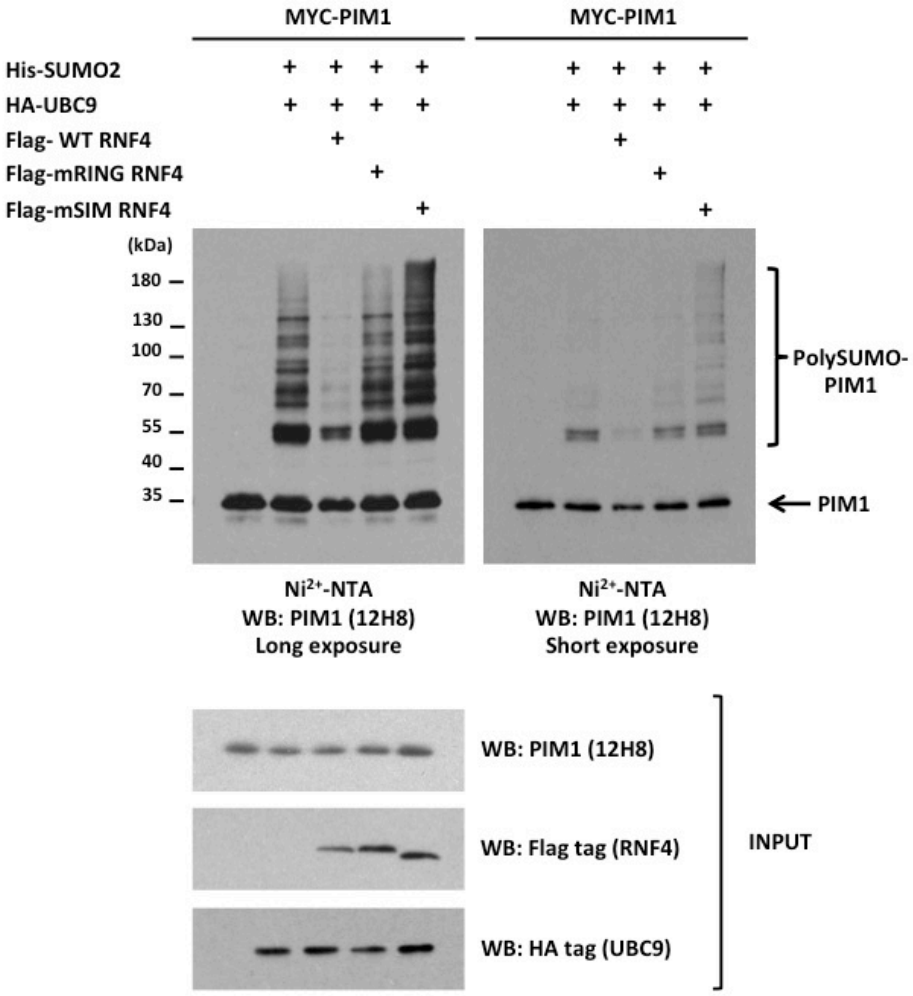

Figure 4.16 Degradation of SUMOylated PIM1 by RNF4

COS7 cells were transfected with plasmids expressing MYC-tagged PIM1 alone or with HA-UBC9 and 6Xhis-SUMO2 to stimulate PIM1 SUMOylation. Cells were additionally transfected with plasmids expressing WT RNF4 or RING finger mutant RNF4 (mRING) or SUMO-interaction motif mutant RNF4 (mSIM). Cells were lysed under denaturing condition after 48 hours, and SUMOylated proteins were captured on Ni^{2+}-NTA beads. Proteins bound to Ni^{2+}-NTA beads were resolved by SDS-PAGE followed by western blotting. Western blotting was also performed on whole cell lysate (input) to confirm expression of the transfected proteins. The data shown here is representative of two independent experiments.

4.12 Knockdown of UBC9 and RNF4 increase levels of endogenous PIM1

To show that SUMOylation regulates levels of endogenous PIM1 in cells, I first performed siRNA knockdown of the SUMO E2 enzyme UBC9 in H1299 and HeLa cells using the procedure described in chapter-2 (section 2.5.9). Cells were also transfected, in parallel, with a pool of non-targeting siRNA as a negative control, and harvested at the indicated time points. As shown in figure 4.17A, the expression of UBC9 was reduced by 90% in both cell lines. Reduction of UBC9 resulted in an increase in the levels of unconjugated or free SUMO2 in cells, as expected. Knockdown of UBC9 also resulted in an increase in levels of endogenous PIM1 at 48 and 72 hours compared to the control (siNS) in both cell lines, suggesting that inhibition of SUMOylation stabilises PIM1. However, this effect could also be indirect, as UBC9 knockdown will affect SUMOylation of hundreds of proteins simultaneously in the cells. Furthermore, to validate that RNF4 can act as an E3 ubiquitin ligase for PIM1 in cells, siRNA knockdown for RNF4 was also performed in H1299 cells. Figure 4.17B shows that RNF4 was efficiently knocked down in cells, which was accompanied with an increase in endogenous PIM1 after 72 and 96 hours post siRNA transfection. Taken together, these results support the hypothesis that SUMOylation negatively regulates PIM1 protein levels in cells.

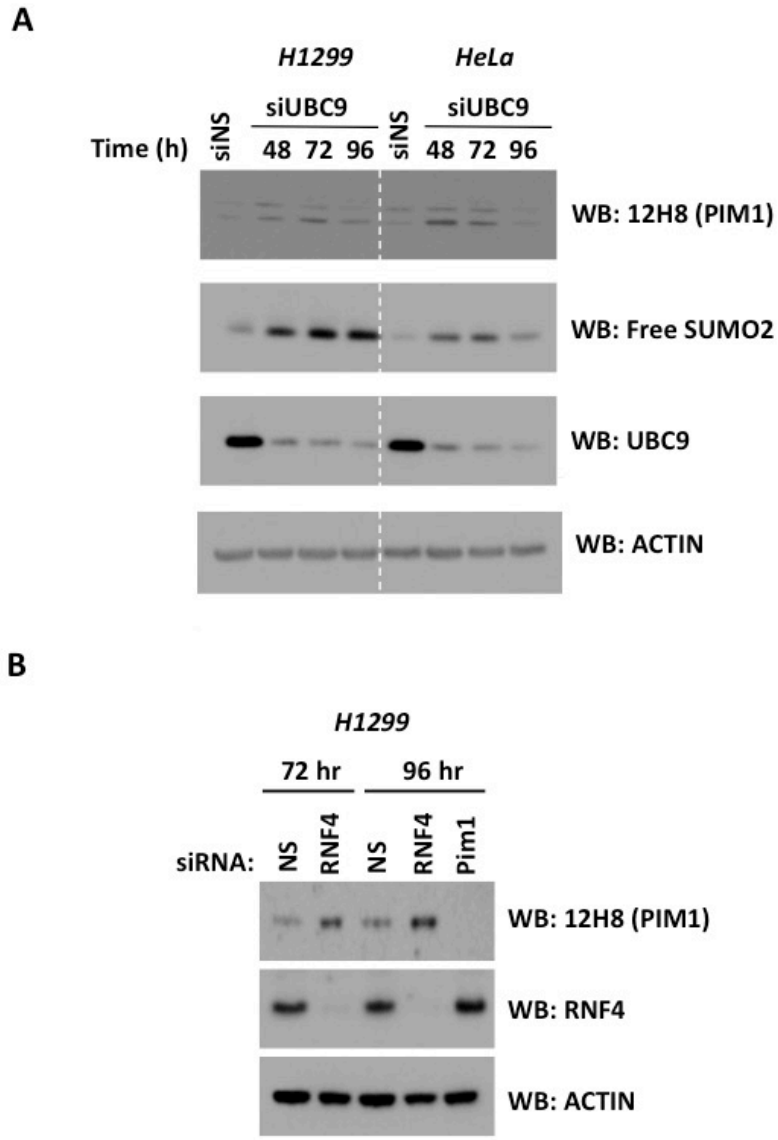

Figure 4.17 Effect of UBC9 and RNF4 siRNA on endogenous PIM1 levels

(A) H1299 or HeLa cells were transfected with a pool of siRNA targeting UBC9 (siUBC9), or non-targeting siRNA pool (siNS) as negative control. Lysates were harvested at the indicated time points, and western blotting was performed for endogenous PIM1 (using 12H8 antibody), SUMO2 and UBC9. **(B)** H1299 cells were transfected with a pool of siRNA targeting RNF4 (siRNF4), or non-targeting siRNA pool (siNS) as negative control. Lysates were harvested at the indicated time points, and western blotting was performed for endogenous PIM1 (using 12H8 antibody) and RNF4. Actin was used a loading control in each case. The data shown here is representative of two independent experiments.

4.13 SUMOylation has no effect on the cellular localisation of PIM1

PIM1 does not contain any obvious nuclear localisation signal (NLS) or nuclear export signal (NES), and has been reported to localise in the cytoplasm and the nucleus, depending on the cell type (Ishibashi *et al.*, 2001; Ionov *et al.*, 2003; Bachmann *et al.*, 2004). Since SUMOylation has been shown to regulate nuclear-cytoplasmic transport and/or sub-cellular localisation of various proteins such as RanGAP1 (Joseph *et al.*, 2002), KLF5 (Du *et al.*, 2008), PML (Zhong *et al.*, 2000) , TEL (Wood *et al.*, 2003), IGF1 receptor (Sehat *et al.*, 2010), I wanted to investigate if SUMOylation of PIM1 affects its sub-cellular localisation. To do this, plasmids encoding MYC-tagged WT PIM1, K169R, E171A or K67M were transiently transfected into H1299 cells, and nuclear-cytoplasmic fractionation experiment was performed as described in chapter-2 (section 2.5.13).

Figure 4.18A shows that the fractionation was successful as the cytoplasmic protein GAPDH was only detected in the cytoplasmic fraction, while the nuclear protein Histone H3 was only detected in the nuclear fraction. WT PIM1 localised to both the cytoplasm and the nucleus. No differences were observed in the localisation of the K169R, E171A mutants indicating that SUMOylation may not be involved in nuclear-cytoplasmic shuttling of PIM1. The K67M mutant was also localised in the nucleus and the cytoplasm, which also indicates that PIM1 localisation occurs independently of its kinase activity.

PIM1 localisation was also checked in DU145 cells stably expressing PIM1. Because of the difference in stability of different PIM1 mutants, the cells were treated with the proteasome inhibitor, MG132, prior to fractionation

to equalise protein levels. As shown in figure 4.18B, there was no difference in the localisation of the WT PIM1, K169R, E171A and K67M mutants. In each case, PIM1 was observed both in the cytoplasm and the nucleus, but relatively more was observed in the nucleus. Since we obtain 3.5X more cytoplasmic extract than the nuclear extract in these experiments (see section 2.5.13), the higher levels of PIM1 observed in the nucleus may be because of the higher concentration of nuclear extract resolved on the gel. This was further confirmed by confocal microscopy of DU145 under the same condition. The merged images from different cell lines further indicated that PIM1 was predominantly cytoplasmic in these cells with weak PIM1 staining in the nucleus (Fig 4.19) as expected. The DNA was stained using DAPI (shown in blue) and PIM1 was stained using the 12H8 antibody (shown in yellow).

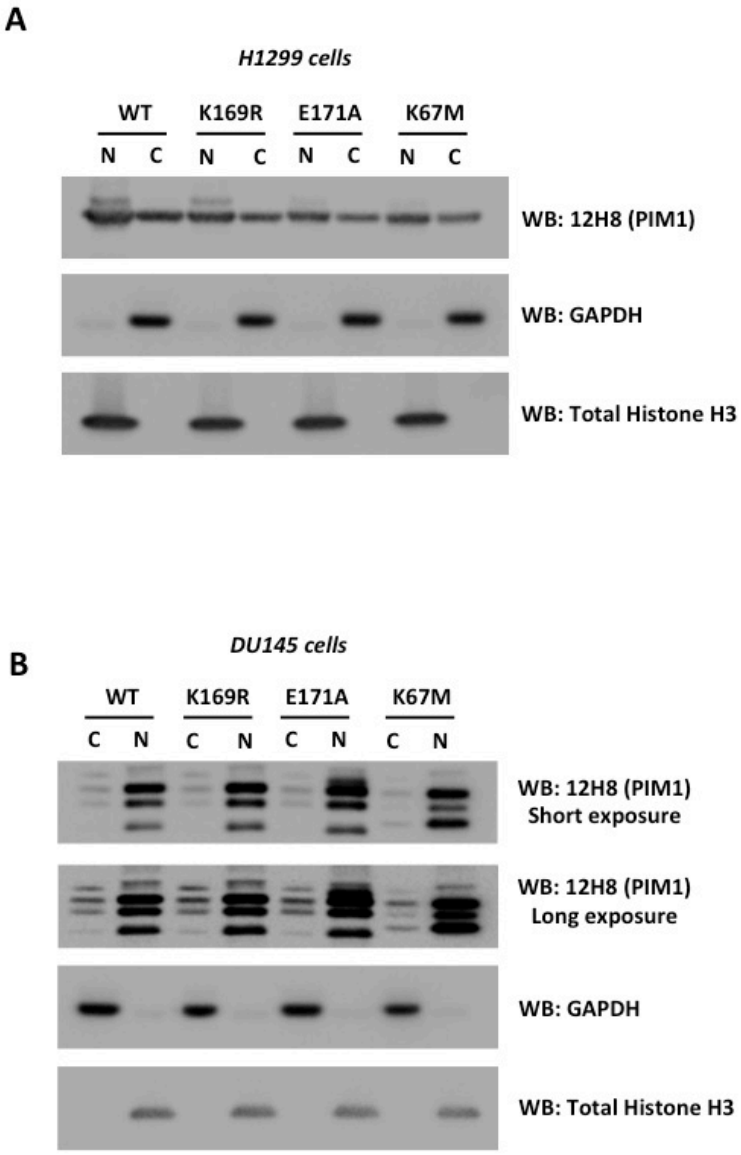

Figure 4.18 Nuclear-cytoplasmic fractionation of WT PIM1 and mutants

(A) H1299 cells were transiently transfected with plasmid expressing MYC-tagged WT PIM1 or mutants, and a nuclear-cytoplasmic fractionation was performed. Equal concentration of the nuclear and cytoplasmic fractions was resolved by SDS-PAGE and western blotting was performed using 12H8 (PIM1 antibody) **(B)** DU-145 cells stably expressing different PIM1 proteins were treated with MG132 (20 μM for 6 hours) to equalise protein levels, and subjected to nuclear-cytoplasmic fractionation. Equal concentration of the nuclear and cytoplasmic fractions was resolved by SDS-PAGE and western blotting was performed using 12H8 (PIM1 antibody). In both experiments, GAPDH was used a cytoplasmic marker and Histone H3 as a nuclear marker to check efficiency of fractionation. The data shown here is representative of two independent experiments.

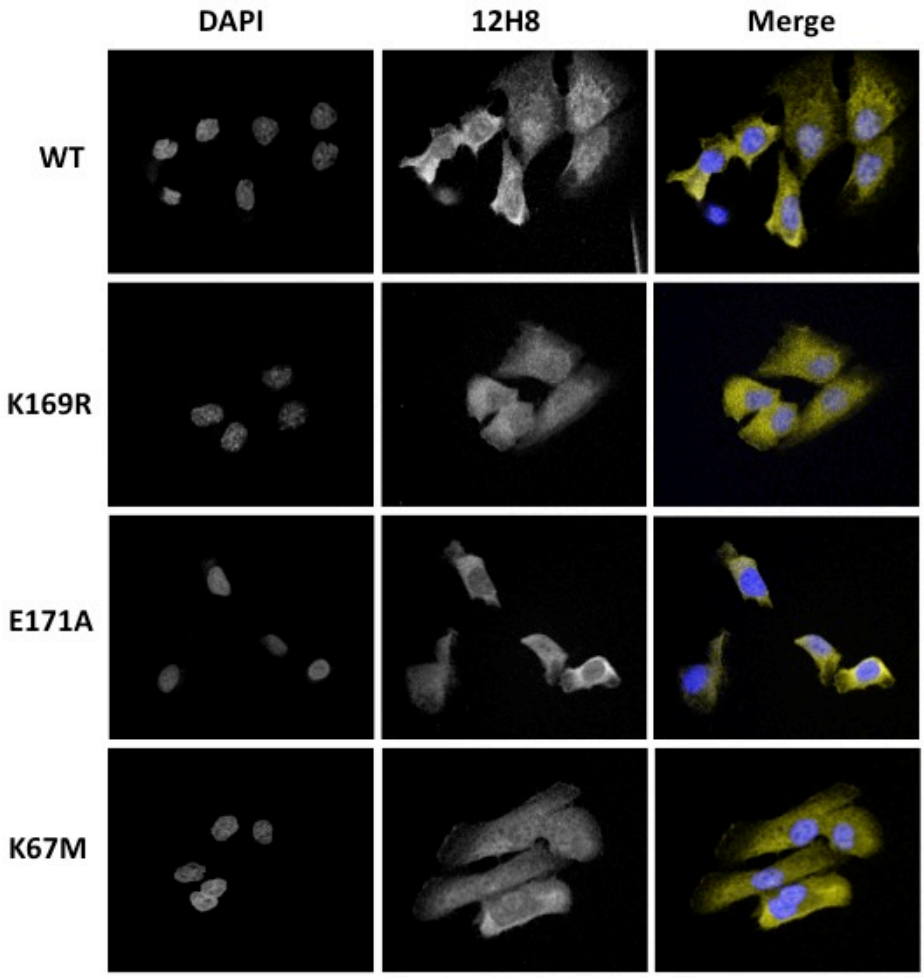

Figure 4.19 Cellular localisation of WT PIM1 and mutants in DU145 stable cell lines
DU145 cells stably expressing WT PIM1 or mutants were grown on coverslips, and stained with 12H8 (PIM1) antibody (shown in yellow) overnight, followed by incubation with a fluorescent-labelled secondary antibody. DAPI was used to stain DNA or nuclear (blue). Images were acquired using a 63X oil immersion objective lens of a Leica SP5 confocal microscope. Representative images of different fields of view have been shown here. The data shown here is representative of one experiment.

4.14 Soft agar colony formation assay

To explore the role of PIM1 in promoting tumorigenesis, I performed soft agar colony formation assays in DU145 cells stably expressing WT PIM1 or mutants. The experimental procedure has been described in chapter-2 (section 2.5.16). DU145 cells were chosen for this experiment as a previous study showed that overexpression of PIM1 in DU145 increased colony formation ability of these cells by 6-fold, as well as colony size (Kim, Roh and Abdulkadir, 2010). H1299 cells were used as a positive control as they readily form colonies in soft-agar within 2 weeks.

As shown in figure 4.20, H1299 cells formed colonies indicating the experimental set up was working as expected. Unfortunately, no colonies were formed in any of the DU145 stable cell lines in this assay, even after 6 weeks of incubation. The very fact that no colonies were observed in cells expressing WT PIM1 indicates that maybe higher PIM1 levels are required to induce colony formation in these cells. Another explanation is that the genetic composition of DU145 cells used by us maybe different from the ones used in the previous study. Due to time constraints, I was not able to create stable cell lines in other background such as H1299; however, this could be performed in the future.

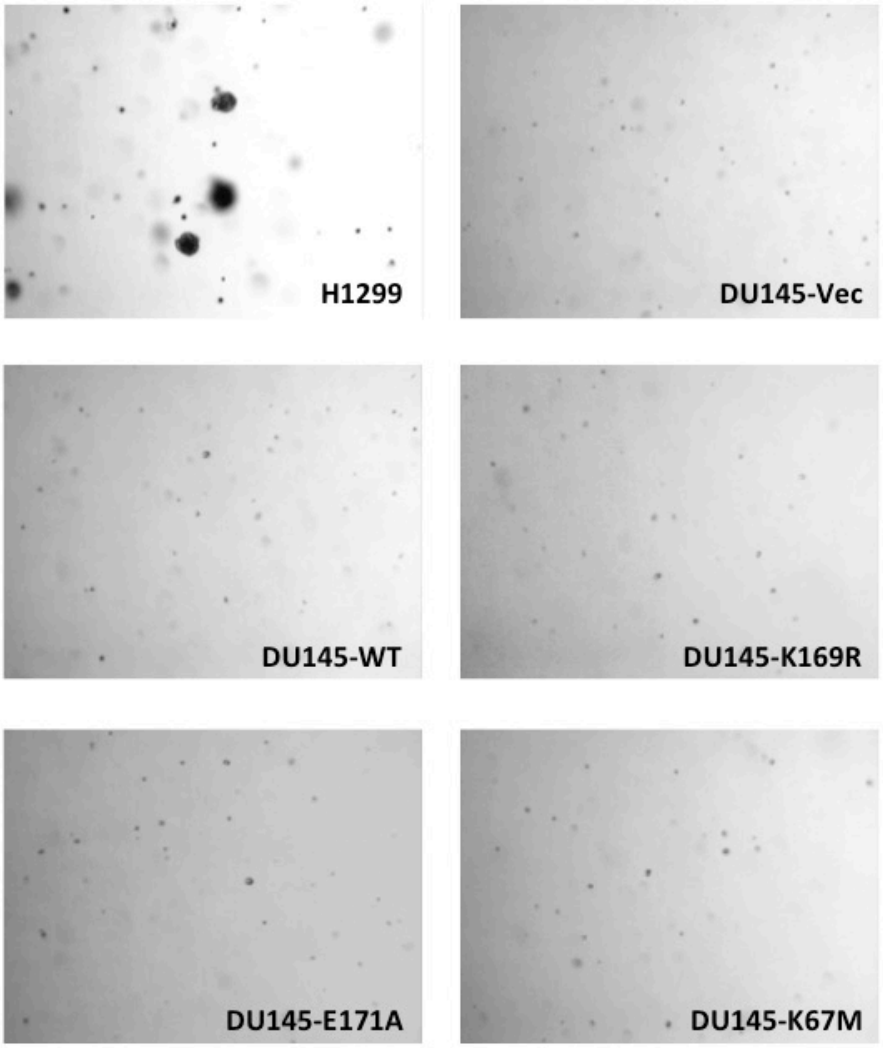

Figure 4.20 Soft-agar colony formation in DU145-PIM1 stable cell lines

DU145 cells stably expressing vector alone or WT PIM1 or PIM1 mutants (K169R, E171A, K67M) were grown in soft-agar for 6 weeks to check for their ability to form anchorage-independent colonies, following which images were acquired using a Motic AE31 inverted light microscope at 10X optical resolution. Representative images of different fields of view have been shown here. H1299 cells were used as a positive control. The data shown here is representative of two independent experiments.

4.15 Summary and Discussion

In this chapter, I explored the possible effects of SUMOylation on PIM1 activity, stability and localisation. The experiments were performed using the PIM1 SUMO mutants containing either a lysine to arginine (K169R) or glutamic acid to alanine (E171A) mutation. In the previous chapter, I showed that the K169R mutant is only SUMOylated at one site (other than K169), whereas the E171A mutant is incapable of undergoing SUMOylation at both sites in PIM1.

The use of single site substitutions, as performed in this study, to determine the effects of PTMs on a protein is commonplace in the scientific field, and can be very informative. However, the underlying assumption, when comparing a wild-type protein against a mutant one, is that 100% of wild-type protein is SUMOylated; when in reality only a small percentage of the total protein is modified at any given point. Therefore, the results obtained using the SUMO site mutants must be interpreted carefully. The results presented in this chapter have been summarised in Table. 4.1.

Table 4.1 Summary of results

PARAMETER	WT PIM1	K169R	E171A	K67M
SUMOylation	++	+	-	++
Autophosphorylation	+	-	+	-
***In vitro* Histone H3 Kinase activity**	++	++	++	-
***In vitro* c-MYC Kinase activity**	++	+	+	-
BAD phosphorylation in U2OS	+	-	-	-
Histone H3 phosphorylation in U2OS	+	+	+	-
Deactivation of AKT in U2OS	+	+	+	-
Activation of ERK1/2 in U2OS	+	-	-	-
Stability	++	+	+++	+
Ubiquitination	++	++	+	++
Localisation	No change	No change	No change	No change

Since the activity of many kinases is regulated by autophosphorylation, I first looked at autophosphorylation of bacterially purified recombinant WT PIM1, and mutants. I demonstrated that WT PIM1 was capable of undergoing autophosphorylation *in vitro*, but the kinase-dead K67M mutant was not. Surprisingly, only the E171A, but not the K169R, mutant could undergo autophosphorylation. The most plausible explanation as to why the K67M and K169R mutants are incapable of autophosphorylation can be derived from catalysis studies performed with other protein kinases such as PKCα (Hanks and Hunter, 1995). It is known that the lysine residues equivalent to the conserved PIM1 K67 and K169 in other Ser/Thr-kinases are required for efficient ATP binding and transfer of phosphate to the substrate. So, the mutation of these core kinase domain residues may be expected to negatively affect the kinase activity, and hence autophosphorylation. Another explanation is that a lysine to arginine substitution might alter the structure of the protein leading to changes in activity. It is quite difficult to say if SUMOylation has any effect on the autophosphorylation status of PIM1, as the K169 residue might be essential for the catalytic activity of the kinase. The E171A mutant, on the other hand, is only semi-conserved in protein kinases, and is still capable of tyrosine autophosphorylation. This suggests that the E171A mutant might be a better indicator of the effect SUMOylation has on PIM1 activity rather than the K169R mutant.

Next, I tested the ability of WT PIM1 and the mutants to phosphorylate previously reported PIM1 substrates in an *in vitro* kinase assay. From autophosphorylation studies one would expect the K169R mutant to be

catalytically inactive, however, I found that both K169R and E171A mutants were active *in vitro* and phosphorylated Histone H3.3 at Ser10, similar to WT PIM1. Intriguingly, both K169R and E171A were able to phosphorylate c-MYC at Ser62 *in vitro*, but their kinase activity was significantly reduced when compared to the WT. In both cases, the K67M mutant was completely inactive in phosphorylating substrates. These results would suggest two important things. First, despite the K169R and the E171A mutants displaying clear differences in autophosphorylation, their kinase activities seem to be unaffected, suggesting that overall autophosphorylation of PIM1 may not be required for its basal activity, at least *in vitro*. The exact sites of PIM1 autophosphorylation are unknown, so it was not possible to examine the contribution of individual sites towards PIM1 activity. Additionally, I was able to show that PIM1, although being a serine/threonine kinase, is also able to autophosphorylate on tyrosine residues, which supports a previously published study (Palaty *et al.*, 1997). Second, the ability of the PIM1 SUMO mutants to phosphorylate some substrate more efficiently than others *in vitro* would suggest that SUMOylation might regulate substrate specificity. Since the microenvironment in cells is completely different to that of an *in vitro* kinase assay, I expressed WT PIM1 or mutants in U2OS cells, and looked at phosphorylation of endogenous PIM1 substrates such as BAD, c-MYC and Histone H3. It was observed that WT PIM1 phosphorylated BAD up to 10 times higher than the no kinase control, but the SUMO mutants were incapable of phosphorylating BAD. Conversely, WT PIM1 and both the SUMO mutants were able to phosphorylate H3 and c-MYC. Intriguingly, WT PIM1 and both the K169 and the E171A mutants reduced AKT activation in

cells, whereas the K67M mutant did not. On the other hand, only WT PIM1 was able to increase phosphorylation of ERK1/2. These results broadly suggest that SUMOylation of PIM1 might promote activation of some pathways, or increase their activity towards proteins of a specific pathway. To the best of our knowledge, this is the first time the SUMOylation site mutants of a kinase have been shown to display differential kinase activity towards different substrates, indicating substrate specificity *in vitro* and in cells.

Unlike other kinases, PIM1 is constitutively active i.e. it does not have an ON or OFF state in cells, so it is unlikely that SUMOylation is required for activation of PIM1 kinase activity. Data obtained from *in vitro* kinase assays using the mutants suggest that the mutants are indeed active, but since the WT PIM1 used in these assays is not SUMOylated, it is hard to predict its exact function. Therefore, I attempted to purify SUMOylated PIM1 from *in vitro* SUMOylation reactions. It was difficult to completely isolate SUMOylated PIM1 because of technical reasons, but the kinase assays containing a mix of unmodified and SUMO modified PIM1 showed higher kinase activity when compared with unmodified PIM1 only. This would suggest that SUMO conjugation enhances PIM1 kinase activity, and gives rise to two interesting concepts. First, one can speculate that SUMO may enhance kinase-substrate interactions, or orient the substrate in a manner that increases the rate of reaction. Second, since the fraction of SUMOylated PIM1 in the reaction is very small compared to unmodified PIM1, this would suggest that SUMOylated PIM1 might form a complex with unmodified PIM1, which results in increased kinase activity.

Furthermore, I showed that both the kinase dead PIM1 K67M and the

K169R mutant were less stable than WT PIM1 in cells by cycloheximide chase assay, whereas the E171A mutant was considerably more stable than WT PIM1. From the kinase assays, we know that both K169R and E171A mutants are still active, but the K67M mutant is not. If one considers that PIM1 kinase activity and stability are directly related, then K67M should be the least stable. However, the K169R mutant is also less stable than WT PIM1, which would suggest that the ability to phosphorylate other substrates might not contribute to PIM1 stability in cells. Instead, going back to autophosphorylation studies, the observation that both K67M and K169R cannot autophosphorylate, and are relatively unstable than both WT PIM1 and E171A (both of which can autophosphorylate) would suggest that PIM1 autophosphorylation regulates its stability in cells. This is consistent with previous studies suggesting that the protein phosphatase PP2A reduces PIM1 stability by dephosphorylation (Losman *et al.*, 2003; Ma *et al.*, 2007). This also indicates that the change in stability of K169R may not be related to SUMOylation at K169, but is due to mutation of an important catalytic site in PIM1 that impairs its autophosphorylation. Conversely, mutation of E171 does not appear to affect its autophosphorylation and activity. So, the increase in stability of the E171A mutant would suggest that SUMOylation negatively affects PIM1 stability.

In support of these observations, when SUMOylation was reduced in cells by siRNA knockdown of the SUMO E2 enzyme, UBC9, an increase in levels of endogenous PIM1 was observed. This is consistent with the idea that abolishing SUMOylation would increase PIM1 stability in cells. However, it cannot be ruled that these effects are indirect, as knocking down UBC9

would have widespread changes in the activity and levels of other SUMOylated proteins inside the cell. Ubiquitination assays were also performed to investigate any changes in the levels of ubiquitination of the PIM1 mutants compared to the WT. Interestingly, while the K67M and the K169R mutants could still be efficiently ubiquitinated, ubiquitination of the E171A mutant was markedly reduced. This suggests that decreased levels of ubiquitination of E171A might contribute, in part, to its enhanced stability observed previously in the cycloheximide chase assay. SUMOylation has been shown to promote ubiquitin-proteasome mediated of substrates by recruiting SUMO-targeted ubiquitin ligases such as RNF4 (Geoffroy and Hay, 2009). Coexpression of polySUMOylated PIM1 with catalytically active RNF4, but not RNF4 mutants, led to proteasomal degradation of the SUMOylated pool of PIM1, demonstrating that SUMOylation can promote PIM1 ubiquitination via RNF4. Additionally, siRNA knockdown of RNF4 caused an increase in levels of endogenous PIM1, further suggesting that RNF4 might act as an E3 ubiquitin ligase for SUMOylated PIM1 in cells.

I also looked at the localisation of WT PIM1, the SUMO mutants and the kinase dead K67M mutants by ectopic expression or stable expression in cell lines. As previously reported, WT PIM1 localised to the nucleus and the cytoplasm in the cell lines used (Valdman *et al.*, 2004; Brault *et al.*, 2012). However, there was no change in the localisation of the K169R, the E171A and the K67M mutant, suggesting that localisation of PIM1 is independent of its activity, autophosphorylation status and SUMOylation. Unfortunately, I was not able to set up functional assays to study the effects of PIM1 SUMOylation on cells due to time constraints and technical difficulties.

Overall the results presented in this chapter identify SUMO as a novel regulator of PIM1 kinase activity and stability in cells. Further opportunities and challenges in studying PIM1 SUMOylation are discussed in the next chapter.

Chapter 5

Discussion & Future directions

5.1 Challenges in studying PIM1 SUMOylation

In general, studying protein SUMOylation is challenging, as at a given point only a very small proportion of the protein is SUMOylated (Gill, 2004; Johnson, 2004). This is because SUMOylated proteins are rapidly deconjugated by SUMO proteases. Another possibility is that only a small population of a protein that is structurally or functionally different from the main pool is SUMO modified in a cell. In case of PIM1, the study was further complicated by the lack of antibodies that could immunoprecipitate endogenous PIM1, which itself is expressed at low levels. In chapter-3, I demonstrated that ectopically expressed 6Xhis-PIM1 could be modified by endogenous SUMO2 and ubiquitin. This approach can be extended to endogenous PIM1 by the introduction of a 6Xhis tag at the 5' end of the endogenous *PIM1* gene locus using CRISPR technology. This should also circumvent the need of a PIM1 specific antibody as a His-tag antibody could be used instead.

Another challenge in studying protein SUMOylation is the identification of a physiological condition under which the endogenous protein is modified by SUMO. A good starting point would be to look at stress responses such as heat shock, oxidative stress and hypoxia since these induce global changes in protein SUMOylation (Saitoh and Hinchey, 2000; Nguyen *et al.*, 2006). Interestingly, both heat shock and hypoxia have been shown to stabilise PIM1 (Shay *et al.*, 2005; Chen *et al.*, 2009), therefore it would be interesting to test endogenous PIM1 SUMOylation under these conditions. A recent study showed that metabolic or energy stress can induce SUMOylation of LKB1 kinase, which is an upstream kinase of AMPK (Ritho

et al., 2015). In addition, SUMOylation of AKT was observed upon insulin treatment and heat shock (Li *et al.*, 2013; de la Cruz-Herrera *et al*., 2014a). These examples suggest that SUMOylation of a kinase can occur independently of conditions that affect global SUMOylation, and in doing so form an integral part of the signalling cascade. However, no such mechanisms have been reported for PIM1 in the literature so far. In fact, PIM1 kinase activity was shown to remain largely unaffected even when the cells were treated with insulin, forskolin, PMA, sorbitol, H_2O_2 and UV radiation (Macdonald *et al.*, 2006). It is currently unknown if cytokines and growth factors, that induce expression of PIM1 mRNA, also affect the activity of the pre-existing pool of PIM1 protein. If this is the case, then SUMOylation might be a mechanism that balances steady state levels of PIM1 in cells.

One could also expect PIM1 SUMOylation to occur during activation of the JAK-STAT signalling, since the E3 SUMO ligases, PIAS1 and PIAS3, are also activated under these conditions. As mentioned previously, PIM1 can negatively regulate the JAK-STAT pathway by a feedback mechanism that involves phosphorylation and activation of SOCS1 and SOCS3 (Peltola *et al.*, 2004). Activated SOCS bind to and inhibit the transcriptional activity of STATs, in a manner that is similar to PIAS1 and PIAS3. So, PIM1 SUMOylation by PIAS might be another feedback mechanism to control PIM1 levels or control the activity of the JAK-STAT pathway in cells, but this hypothesis warrants future investigation. Interestingly, both STAT1 and STAT3 have also been reported to undergo SUMOylation. Activation of STAT1 by IFNγ induces STAT1 SUMOylation at Lys703 by PIAS1, and has been suggested to negatively regulate STAT1 mediated target gene

activation (Ungureanu *et al.*, 2003, 2005). More recently, STAT3 was shown to be SUMOylated at Lys451, which enhances its interaction with the nuclear phosphatase TC45 through a SIM present in TC45 (Zhou *et al.*, 2016). Like STAT1, SUMOylation also negatively affects the transcriptional activity of STAT3. This would be consistent with the emerging concept of 'group SUMOylation' where multiple targets involved in the same biological process or pathway are SUMOylated simultaneously (Psakhye and Jentsch, 2012).

Other instances where proteins can be SUMOylated are during the specific stages of the cell cycle. For example, the kinase CDK6 is only modified by SUMO2 during the G1 phase and mitosis (Bellail *et al*., 2014), whereas Aurora B SUMOylation is only detected during mitosis (Fernández-Miranda *et al.*, 2010; Ban *et al*., 2011). Interestingly, PIM1 was one of the hundreds of proteins suggested to be modified by both SUMO and ubiquitin during mitosis in a protein microarray screen performed by Merbl and colleagues (Merbl *et al.*, 2013). In this study, active mitotic cell extracts from HeLa S3 cells were incubated on a protein microarray spotted with >9000 proteins (including PIM1). The resulting ubiquitin and ubiquitin-like modifications occurring on a target protein were then detected individually using ubiquitin or SUMO antibody. It should be noted that although the enzymes involved in ubiquitin or Ubl modification used in this screen were endogenous, the target proteins spotted on the microarray were not. In the present study, I did not investigate cell cycle specific changes in PIM1 activity and SUMOylation, which is something that can be followed up in the future.

5.2 Regulation of kinase activity by SUMO

Based on the amino acid sequence of PIM1, I identified the presence of a consensus SUMO modification site in PIM1 ($IK_{169}DE_{171}$). Various studies have reported the crystal structure of PIM1 in complex with small molecule inhibitors. Using these structures, we can visualise the exact position and nature of the residues involved in the SUMOylation of PIM1, and at the same time predict the outcome of having the SUMO polypeptide conjugated at this position. As shown previously in figure 3.1, PIM1 displays the conserved bi-lobe structure observed in most protein kinases. Here, the ATP-binding site is indicated by AMP-PNP (a non-hydrolysable analogue of ATP), while the substrate binding site is the indicated by the position of the consensus peptide substrate or PIMitide (KRRRHPS*, where * is the phosphorylated residue). The residues required for SUMOylation (IKDE) can be mapped directly to the substrate binding pocket, which raises two possibilities with regards to how SUMO can affect the activity of PIM1. First, the presence of SUMO at this position might block access to the substrate, and hence inhibit the activity of the kinase. Second, SUMO might act as a tether to bring the substrates close to PIM1 promoting protein-protein interaction, and hence enhance PIM1 kinase activity. The results presented in this thesis support the second hypothesis that PIM1 SUMOylation enhances its activity, and are consistent with the published literature on SUMOylation of other kinases.

SUMOylation of other kinases such as pancreatic Glucokinase (Aukrust *et al.*, 2013), AKT (Li *et al.*, 2013; de la Cruz-Herrera *et al.*, 2014a; Lin, Liu and Lee, 2016), AMPKβ2 (Rubio, Vernia and Sanz, 2013) and Protein kinase R (de la Cruz-Herrera *et al.*, 2014b) has been shown to

increase their kinase activity. There are also studies where SUMOylation has been shown to inhibit the kinase activity, such as in the case of MEK (Kubota *et al.*, 2011) and AMPKα1 (Yan *et al.*, 2015). Of note, most of these kinases are SUMOylated at a non-consensus site or outside the kinase domain, with the exception of AKT and Aurora B, which are SUMOylated at a conserved lysine similar to PIM1 in the kinase domain. Strikingly, K147 in CDK6 (which is equivalent to K169 in PIM1) is not a part of a consensus SUMO motif, and is ubiquitinated instead (Bellail *et al.*, 2014). More importantly, mutation of K147 also abolished CDK6 kinase activity. Unfortunately, a unifying mechanism to explain changes in the kinase activity by SUMOylation has not be identified so far, and every kinase appears to be affected by SUMO in a different way.

Studying the effect of SUMOylation on a kinase is particularly challenging when the modified lysine is present in the kinase domain. In this scenario, it becomes difficult to distinguish between the functions of the lysine residue associated with the intrinsic activity of the kinase and SUMOylation of the substrate. For example, the human Aurora B SUMO mutant, K202R, was found to be kinase dead in a study by Ban and colleagues. However, the authors did not observe any change in the kinase activity when WT Aurora B was coexpressed with SUMO2 and PIAS3 in the presence and absence of SENP2. Therefore, it was suggested that the K202R mutant was not appropriate to study effects of SUMOylation on Aurora B activity. Unfortunately, the authors did not test the activity of the E204A mutant in this study. Furthermore, the AKT SUMOylation mutant K276R was also found to be kinase dead, but still capable of

autophosphorylation (Li *et al.*, 2013). Similar effects were observed when the E278A mutant of AKT was used, which led the authors to conclude that the decrease in kinase activity was a SUMO-specific effect.

Although the K169R and the E171A SUMO mutant of PIM1 are identical in terms of their kinase activity, their ability to undergo SUMOylation status is different. To the best of my knowledge, this has not been reported in the literature so far. A major difference between the K169R and the E171A mutants was in their ability to autophosphorylate. As mentioned before, K169 is a conserved residue involved in catalysis; therefore the impaired autophosphorylation might reflect a change in the intrinsic activity of the kinase. On the other hand, the E171A mutant is only semi-conserved in protein kinases. It not only retained its ability to autophosphorylate but also abolished PIM1 SUMOylation at both sites, which makes its a better mutant to study the effect of SUMOylation on PIM1, in my opinion. A sequence alignment of this region in other kinases has been shown in figure 5.1.

One approach used in the literature to overcome the confounding effects observed with the Lys to Arg substitution is to fuse the substrate with WT UBC9, to mimic a constitutively SUMOylated protein (Jakobs *et al.*, 2007). The method has been used successfully to study effects of SUMOylation on MEK and TBK1 kinases (Kubota *et al.*, 2011; Saul *et al.*, 2015). Another method of mimicking a SUMOylation defective protein would be to fuse the substrate with the catalytic domain of SENP1. However, both approaches have limited potential since it involves creation of an artificial chimeric protein. Therefore, no single approach can be considered as optimal to study effects of SUMOylation on the target protein.

Figure 5.1 Sequence alignment of the catalytic loop of protein kinases

Protein sequence alignment showing the conserved residues (red) in the catalytic loop of some protein kinases. Note that the lysine residue present within the consensus SUMO motif is also conserved in other serine/threonine kinases. Kinases reported to be SUMOylated at the conserved lysine are shown in bold. The glutamic acid of PIM1 E171 (green) is also aligned with the equivalent residues in other kinases, which shows that E at this position is not strictly conserved (Adapted from Hanks and Hunter, 1995).

5.3 Regulation of kinase stability by SUMO and ubiquitin

Many activated protein kinases can be degraded by the ubiquitin proteasome system (UPS) or through the lysosomal pathway in cells. Many factors affect the protein stability of a kinase, but a study performed with Protein kinase C suggests that the active conformation of a kinase is necessary to elicit its degradation (Lu *et al.*, 1998; Kang *et al.*, 2000). In other words, prolonged activation of a kinase can automatically trigger its degradation. In another study activation of the receptor tyrosine kinase, EGFR, by EGF was shown to not only activate it kinase activity, but also trigger its degradation (Galcheva-Gargova *et al*., 1995; Huang *et al.*, 2006).

Although PIM1 is constitutively active, the idea that SUMOylation can further enhance its activity, and also result in its degradation is analogous to the above-mentioned examples. SUMOylation of AKT was also shown to increase its kinase activity in three separate studies (Li *et al.*, 2013; de la Cruz-Herrera *et al.*, 2014a; Lin, Liu and Lee, 2016). However, there are conflicting reports on its stability. Li and colleagues showed that SUMOylation does not affect its ubiquitination, whereas Lin and colleagues suggest that SUMOylation might stabilise AKT. The discrepancy is due to the different experimental techniques used in these studies. Li and colleagues used the K276R mutant in their ubiquitination assays with a reported E3 ligase for AKT called TRAF6. In contrast, Lin and colleagues used overexpression of SUMO2, UBC9 and PIAS1 in their cycloheximide assays. In the present study, both ubiquitination assay and CHX chase assays were performed with the E171A mutant, both of which support our hypothesis that SUMOylation destabilises PIM1 by the UPS.

Results presented in chapter-3 suggested that both PIAS1 and PIAS3 might catalyse formation of polySUMO chains on PIM1. Polymeric SUMO chains on PIM1 were observed upon proteasome treatment, even in the absence of an E3 ligase, suggesting that the UPS also degrades SUMOylated PIM1. The addition of an E3 ligase further enhanced this effect, notably PIAS1 mediated polySUMOylation was more clear when the cells were treated with MG132. It was also observed that PIAS3 was a more potent E3 SUMO ligase for PIM1 than PIAS1. Intriguingly, PIAS3 mediated SUMOylation seemed to increase the levels of total PIM1 (input). This raised the possibility that PIAS3 might stabilise PIM1, whereas PIAS1 might destabilise PIM1. However, this could be an artefact of overexpression as PIAS3 probably oversaturates the cells with polySUMO chains, leading to accumulation of SUMOylated PIM1 that can no longer be degraded, as the availability of either the proteasome or the ubiquitin ligases becomes limiting. This is also consistent with other studies showing that although PIAS1 promotes ubiquitination of PML, its expression alone does not lead to degradation (Rabellino *et al.*, 2012). A good experiment to do would be to measure PIM1 ubiquitination in the absence and presence of PIAS1 or PIAS3. Another approach would be to look at PIM1 protein levels following knockdown of all PIAS family members simultaneously, as knockdown of individual PIAS family members is not effective, most likely due to overlapping substrate specificity (Seifert *et al.*, 2015).

The SUMO targeted ubiquitin ligase RNF4 plays an important role in UPS mediated degradation of SUMOylated proteins. Knockdown of RNF4 increased endogenous protein levels of PIM1 suggesting that RNF4 can act

as an E3 ubiquitin ligase for PIM1. As mentioned before, RNF4 has also been shown to control the stability of PML in response to arsenic trioxide (Tatham *et al.*, 2008), HIF2α during hypoxia (van Hagen *et al.*, 2009) and TRIM28 during DNA damage (Kuo *et al.*, 2014) suggesting that RNF4 has specialised functions under stress conditions. However, I was able to observe increase in PIM1 protein under unstressed conditions, which raise two questions. Is SUMO mediated degradation of PIM1 by RNF4 a general housekeeping mechanism to regulate PIM1 levels? Or does RNF4 also regulate PIM1 stability upon stress conditions? Finding the answer to these questions could also inform us about the physiological relevance of PIM1 SUMOylation in cells.

5.4 Function of PIM1 SUMOylation

PIM1 is a weak oncogene, and as such overexpression of PIM1 alone is not sufficient to induce cellular transformation or promote proliferation of cells (Shirogane *et al.*, 1999; Kim, Roh and Abdulkadir, 2010). Only about 5-10% of mice overexpressing PIM1 develop lymphomas following a long period of latency (7-9 months) (van Lohuizen *et al.*, 1989). It has also been suggested that *in vivo* models are better suited to study the oncogenic activity of PIM1, as the same cells used for xenograft experiments show no obvious changes in proliferation or survival when grown in plastic dishes (Kim *et al*., 2010). It is also possible that PIM1 overexpression is superfluous in most cancer cells as they already express all three PIM kinases, in addition to AKT. Therefore, a CRISPR knockout of PIM1 alone might not be

sufficient, and would require knocking out PIM2, PIM3 and all the AKT isoforms simultaneously.

Based on the literature, mouse embryonic fibroblasts (MEF) from PIM triple knockout mice (PIM TKO) are probably the best system available to study the function of WT PIM1 and mutants. However, the only laboratory that still uses these MEF for their own studies was not willing to share them with us. Therefore, I created cell lines in HeLa and U2OS expressing PIM1 in a tetracycline-inducible manner, to study the effect of WT PIM1 and SUMO mutants on the phosphorylation of endogenous PIM1 substrates. The results from these cell lines have been discussed in the previous chapter. Although I was able to show phosphorylation of known PIM1 targets proteins under basal conditions, I was not able to follow up on functional assays due to time constraints. Nevertheless, it was surprising to find that the K169R and E171A mutants displayed substrate specificity *in vitro* and in cells, especially in their ability to decrease autophosphorylation of AKT at Ser473 similar to WT PIM1. This suggests the existence of a possible feedback mechanism between PIM and AKT kinases. It is likely that PIM1 indirectly activates a negative regulator of AKT, such as Protein kinase C (PKC) or PP2A, which decreases phosphorylation at Ser473 (Li *et al.*, 2006).

Intriguingly, expression of WT PIM1 but not the SUMO mutants enhanced phosphorylation of ERK1/2. However, it is unlikely that ERK1/2 is a direct target of PIM1, as the phosphorylated residues do not conform to PIM1 consensus phosphorylation motif. On that subject, it is worth mentioning that a recent study suggested that PIM1 might phosphorylate the upstream ERK kinase, MEK1/2 at Ser217/221, to support cell survival

(Blanco *et al.*, 2015). There is also evidence in CLL suggesting that PIM1 indirectly induces the MAPK pathway by phosphorylating the receptor tyrosine kinase CXCR4 at Ser339 (Decker *et al.*, 2014). It would be interesting to follow up on this aspect, as this would suggest that SUMOylation of PIM1 might specifically support activation of the ERK pathway. Additional experiments to study phosphorylation of PIM1 substrates in the absence and presence of enzymes involved in SUMO modification of PIM1 should also be performed. Furthermore, since phospho-BAD was increased in the presence of WT PIM, but not the mutants, it might be useful to perform apoptosis assays in these cell lines under different stress conditions or drug treatments.

5.5 Clinical relevance

The clinical implications of PIM1 SUMOylation may not be immediately apparent at the moment, but it is exciting to think of a drug that can induce SUMOylation of PIM1, causing its degradation. Drugs that rely on inducing SUMOylation of target proteins are already being used in the clinic. For example, Arsenic trioxide, used for the treatment of acute promyelocytic leukemia (APL), induces rapid SUMOylation and degradation of the oncogenic PML-RARα fusion protein by RNF4 (Lallemand-Breitenbach *et al.*, 2008). Another example is the anti-diabetic drug Rosiglitazone, which exerts its anti-inflammatory effects by inducing SUMOylation of PPARγ (Pascual *et al.*, 2005; Lu *et al.*, 2013).

PIM kinases have been described as one of the potent suppressors of MYC-induced apoptosis. The strong synergism between PIM and MYC is

evident from PIM1/MYC transgenic mice where 100% mice develop tumours in utero (Verbeek *et al.*, 1991). However, MYC has remained a difficult drug target, and therefore other approaches to indirectly target MYC activity have been proposed, such as inhibition of PIM kinases (Kirschner *et al.*, 2015). Interestingly, the SUMO pathway sustains the MYC transcriptional program, and inhibition of SAE1/2 was found to be synthetic lethal in breast cancer cells exhibiting high MYC activity (Kessler *et al.*, 2012). This is also true in case of B-cell lymphomas, where MYC induces a hyper SUMOylation state by upregulating gene expression of the components of the SUMO machinery (Hoellein *et al.*, 2014). Inhibition of the SUMO pathway resulted in a G2/M arrest and subsequent apoptosis of B-cell lymphomas. Knockdown of UBC9 in the present study caused an increase in PIM1 levels, which would suggest that PIM kinase inhibitors might be more effective following inhibition of SUMOylation. This hypothesis can be tested easily by treating cells with or without UBC9, and measuring their survival following PIM kinase inhibitor treatment.

A recent study identified 1 as a PIM1 target protein. PIM1 mediated phosphorylation of NOTCH1 enhances its activity, and the interaction itself was suggested to stabilise PIM1 (Santio *et al.*, 2016). NOTCH1 activation in breast cancer cells seems to reduce the levels of unconjugated SUMO by an undefined mechanism, which makes them highly sensitive to the inhibition of UBC9. However, like c-MYC, it is currently not possible to target NOTCH1, hence it might be interesting to test PIM inhibitors in NOTCH1 activated cells.

5.5 Proposed model

In brief, the data presented in this thesis identify a novel mechanism of regulation of PIM1 kinase activity, and protein levels by SUMO modification. There are at least two sites of modification in PIM1, but due to technical issues it was not possible to determine the site-specific effects of SUMOylation on PIM1. Overall, the results obtained suggest that SUMOylation of PIM1 can enhance its kinase activity *in vitro*, and also promote its degradation by the ubiquitin proteasome system. Although the exact sequence of events remains unclear, it is tempting to speculate a sequential modification model for PIM1 SUMOylation (Figure 5.2). In this model, stimuli such as growth factor or cellular stress induce PIM1 SUMOylation, and enhance its oncogenic potential as a kinase. Once phosphorylation of the substrate is achieved, PIM1 can be polySUMOylated and targeted for degradation by the E3 ubiquitin ligase RNF4. The deregulation of the SUMO pathway in cancers might contribute to the increased activity and/or stability of PIM1 observed in cancers. In this sense, further analysis of the PIM-SUMO interaction may provide avenues for rational co-targeting, which can be exploited therapeutically to improve the efficacy of either a SUMO or a PIM kinase inhibitor.

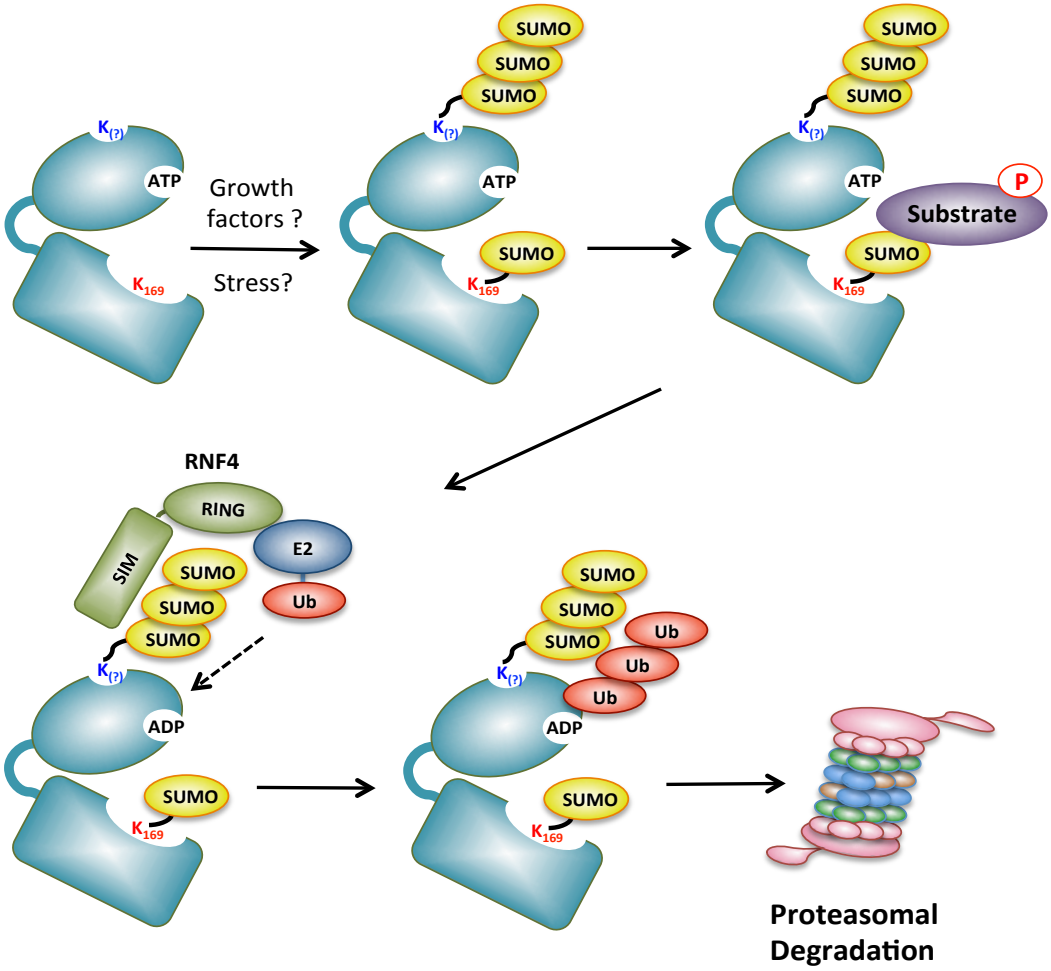

Figure 5.2 Model for regulation of PIM1 by SUMOylation

The bi-lobed structure of PIM1 kinase is shown in blue. The consensus SUMOylated lysine residue is located in the substrate binding pocket (K169 in red). For representation sake, the non-consensus lysine is shown in blue in the N-terminal domain. Stimulus such as growth factors or stress might induce SUMOylation of PIM1 under endogenous conditions. SUMOylated PIM1 can bind and phosphorylate substrates. Once this is achieved, a SUMO targeted ubiquitin ligase is recruited to polySUMOylated PIM1 leading to attachment of polyubiquitin chains on PIM1. The SUMOylated and ubiquitinated PIM1 is then targeted for degradation by the proteasome.

References

Agostinho, M., Santos, V., Ferreira, F., Costa, R., Cardoso, J., Pinheiro, I., Rino, J., Jaffray, E., Hay, R. T. and Ferreira, J. (2008) 'Conjugation of human topoisomerase 2 alpha with small ubiquitin-like modifiers 2/3 in response to topoisomerase inhibitors: Cell cycle stage and chromosome domain specificity', *Cancer Research*, 68(7), pp. 2409–2418. doi: 10.1158/0008-5472.CAN-07-2092.

Aho, T. L. T., Sandholm, J., Peltola, K. J., Mankonen, H. P., Lilly, M. and Koskinen, P. J. (2004) 'Pim-1 kinase promotes inactivation of the pro-apoptotic Bad protein by phosphorylating it on the Ser112 gatekeeper site', *FEBS Letters*, 571(1–3), pp. 43–49. doi: 10.1016/j.febslet.2004.06.050.

Al-Hakim, A. K., Zagorska, A., Chapman, L., Deak, M., Peggie, M. and Alessi, D. R. (2008) 'Control of AMPK-related kinases by USP9X and atypical Lys(29)/Lys(33)-linked polyubiquitin chains.', *The Biochemical journal*, 411(2), pp. 249–260. doi: 10.1042/BJ20080067.

Amson, R., Sigaux, F., Przedborski, S., Flandrin, G., Givol, D. and Telerman, a (1989) 'The human protooncogene product p33pim is expressed during fetal hematopoiesis and in diverse leukemias.', *Proceedings of the National Academy of Sciences of the United States of America*, 86(22), pp. 8857–61. doi: 10.1073/pnas.86.22.8857.

Aukrust, I., Bjorkhaug, L., Negahdar, M., Molnes, J., Johansson, B. B., Müller, Y., Haas, W., Gygi, S. P., Sovik, O., Flatmark, T., Kulkarni, R. N. and Njolstad, P. R. (2013) 'SUMOylation of pancreatic glucokinase regulates its cellular stability and activity', *Journal of Biological Chemistry*, 288(8), pp. 5951–5962. doi: 10.1074/jbc.M112.393769.

Ayaydin, F. and Dasso, M. (2004) 'Distinct in vivo dynamics of vertebrate SUMO paralogues.', *Molecular biology of the cell*, 15(12), pp. 5208–18. doi: 10.1091/mbc.E04-07-0589.

Bachmann, M., Hennemann, H., Pei, X. X., Hoffmann, I. and Möröy, T. (2004) 'The oncogenic serine/threonine kinase Pim-1 phosphorylates and inhibits the activity of Cdc25C-associated kinase 1 (C-TAK1): A Novel role for Pim-1 at the G2TM cell cycle checkpoint', *Journal of Biological Chemistry*, 279(46), pp. 48319–48328. doi: 10.1074/jbc.M404440200.

Bachmann, M., Kosan, C., Xing, P. X., Montenarh, M., Hoffmann, I. and Möröy, T. (2006) 'The oncogenic serine/threonine kinase Pim-1 directly phosphorylates and activates the G2/M specific phosphatase Cdc25C', *International Journal of Biochemistry and Cell Biology*, 38(3), pp. 430–443. doi: 10.1016/j.biocel.2005.10.010.

Ban, R., Nishida, T. and Urano, T. (2011) 'Mitotic kinase Aurora-B is regulated by SUMO-2/3 conjugation/deconjugation during mitosis', *Genes to Cells*, 16(6), pp. 652–669. doi: 10.1111/j.1365-2443.2011.01521.x.

Beharry, Z., Mahajan, S., Zemskova, M., Lin, Y.-W., Tholanikunnel, B. G., Xia, Z., Smith, C. D. and Kraft, A. S. (2010) 'The Pim protein kinases regulate energy metabolism and cell growth.', *Proceedings of the National Academy of Sciences of the United States of America*, 108(2), pp. 1–6. doi: 10.1073/pnas.1013214108.

Bellail, A. C., Olson, J. J. and Hao, C. (2014) 'SUMO1 modification stabilizes CDK6 protein and drives the cell cycle and glioblastoma progression.', *Nature communications*, 5, p. 4234. doi: 10.1038/ncomms5234.

Benson, M. D., Li, Q.-J., Kieckhafer, K., Dudek, D., Whorton, M. R., Sunahara, R. K., Iñiguez-Lluhí, J. a and Martens, J. R. (2007) 'SUMO modification regulates inactivation of the voltage-gated potassium channel Kv1.5.', *Proceedings of the National Academy of Sciences of the United States of America*, 104(6), pp. 1805–1810. doi: 10.1073/pnas.0606702104.

Bernier-Villamor, V., Sampson, D. A., Matunis, M. J. and Lima, C. D. (2002) 'Structural basis for E2-mediated SUMO conjugation revealed by a complex between ubiquitin-conjugating enzyme Ubc9 and RanGAP1', *Cell*, 108(3), pp. 345–356. doi: 10.1016/S0092-8674(02)00630-X.

Bhattacharya, N., Wang, Z., Davitt, C., McKenzie, I. F. C., Xing, P.-X. and Magnuson, N. S. (2002) 'Pim-1 associates with protein complexes necessary for mitosis.', *Chromosoma*, 111(2), pp. 80–95. doi: 10.1007/s00412-002-0192-6.

Blanco-Aparicio, C., Carnero, A., Li, Y. Y., Mukaida, N., Mondello, P., Cuzzocrea, S., Mian, M., Harris, F. and Pierpoint, L. (2014) 'Pim kinases in hematological malignancies: where are we now and where are we going?', *Medicinal Research Reviews*, 7(6), pp. 9392–9404. doi: 10.1002/med.

Blanco, F. F., Jimbo, M., Wulfkuhle, J., Gallagher, I., Deng, J., Enyenihi, L., Meisner-Kober, N., Londin, E., Rigoutsos, I., Sawicki, J. A., Risbud, M. V, Witkiewicz, A. K., McCue, P. A., Jiang, W., Rui, H., Yeo, C. J., Petricoin, E., Winter, J. M. and Brody, J. R. (2015) 'The mRNA-binding protein HuR promotes hypoxia-induced chemoresistance through posttranscriptional regulation of the proto-oncogene PIM1 in pancreatic cancer cells.', *Oncogene*, 35(19), pp. 2529–2541. doi: 10.1038/onc.2015.325.

Boggio, R., Colombo, R., Hay, R. T., Draetta, G. F. and Chiocca, S. (2004) 'A mechanism for inhibiting the SUMO pathway', *Molecular Cell*, 16(4), pp. 549–561. doi: 10.1016/j.molcel.2004.11.007.

Bossis, G., Malnou, C. E., Farras, R., Andermarcher, E., Hipskind, R., Rodriguez, M., Schmidt, D., Muller, S., Jariel-Encontre, I. and Piechaczyk, M. (2005) 'Down-regulation of c-Fos/c-Jun AP-1 dimer activity by sumoylation.', *Molecular and cellular biology*, 25(16), pp. 6964–79. doi: 10.1128/MCB.25.16.6964-6979.2005.

Bossis, G. and Melchior, F. (2006) 'Regulation of SUMOylation by reversible oxidation of SUMO conjugating enzymes', *Molecular Cell*, 21(3), pp. 349–357. doi: 10.1016/j.molcel.2005.12.019.

Bouras, T., Fu, M., Sauve, A. A., Wang, F., Quong, A. A., Perkins, N. D., Hay, R. T., Gu, W. and Pestell, R. G. (2005) 'SIRT1 deacetylation and repression of p300 involves lysine residues 1020/1024 within the cell cycle regulatory domain 1', *Journal of Biological Chemistry*, 280(11), pp. 10264–10276. doi: 10.1074/jbc.M408748200.

Brault, L., Gasser, C., Bracher, F., Huber, K., Knapp, S. and Schwaller, J. (2010) 'Pim serine/threonine kinases in the pathogenesis and therapy of hematologic malignancies and solid cancers', *Haematologica*, pp. 1004–1015. doi: 10.3324/haematol.2009.017079.

Brault, L., Menter, T., Obermann, E. C., Knapp, S., Thommen, S., Schwaller, J. and Tzankov, a (2012) 'PIM kinases are progression markers and emerging therapeutic targets in diffuse large B-cell lymphoma.', *British journal of cancer*, 107(3), pp. 491–500. doi: 10.1038/bjc.2012.272.

Breuer, M. L., Cuypers, H. T. and Berns, A. (1989) 'Evidence for the involvement of pim-2, a new common proviral insertion site, in progression of lymphomas.', *The EMBO journal*, 8(3), pp. 743–748.

Bullock, A. N., Debreczeni, J., Amos, A. L., Knapp, S. and Turk, B. E. (2005) 'Structure and substrate specificity of the Pim-1 kinase', *Journal of Biological Chemistry*, 280(50), pp. 41675–41682. doi: 10.1074/jbc.M510711200.

Cen, B., Mahajan, S., Wang, W. and Kraft, A. S. (2013) 'Elevation of receptor tyrosine kinases by small molecule AKT inhibitors in prostate cancer is mediated by Pim-1', *Cancer Research*, 73(11), pp. 3402–3411. doi: 10.1158/0008-5472.CAN-12-4619.

Cen, B., Mahajan, S., Zemskova, M., Beharry, Z., Lin, Y. W., Cramer, S. D., Lilly, M. B. and Kraft, A. S. (2010) 'Regulation of Skp2 levels by the Pim-1 protein kinase', *Journal of Biological Chemistry*, 285(38), pp. 29128–29137. doi: 10.1074/jbc.M110.137240.

Cen, B., Xiong, Y., Song, J. H., Mahajan, S., DuPont, R., McEachern, K., DeAngelo, D. J., Cortes, J. E., Minden, M. D., Ebens, A., Mims, A., LaRue, A. C. and Kraft, A. S. (2014) 'The Pim-1 protein kinase is an important regulator of MET receptor tyrosine kinase levels and signaling.', *Molecular and cellular biology*, 34(13), pp. 2517–32. doi: 10.1128/MCB.00147-14.

Chang, M., Kanwar, N., Feng, E., Siu, A., Liu, X., Ma, D. and Jongstra, J. (2010) 'PIM kinase inhibitors downregulate STAT3(Tyr705) phosphorylation.', *Mol. Cancer Ther.*, 9(9), pp. 2478–87. doi: 10.1158/1535-7163.MCT-10-0321.

Chau, V., Tobias, J. W., Bachmair, A., Marriott, D., Ecker, D. J., Gonda, D. K. and Varshavsky, A. (1989) 'A multiubiquitin chain is confined to specific lysine in a targeted short-lived protein', *Science*, 243(4898), pp. 1576–1583. doi: 10.1126/science.2538923.

Chen, J., Kobayashi, M., Darmanin, S., Qiao, Y., Gully, C., Zhao, R., Kondo, S., Wang, H., Wang, H., Yeung, S.-C. J. and Lee, M.-H. (2009a) 'Hypoxia-mediated up-regulation of Pim-1 contributes to solid tumor formation.', *The American journal of pathology*, 175(1), pp. 400–11. doi: 10.2353/ajpath.2009.080972.

Chen, J., Kobayashi, M., Darmanin, S., Qiao, Y., Gully, C., Zhao, R., Yeung, S. C. and Lee, M. H. (2009b) 'Pim-1 plays a pivotal role in hypoxia-induced chemoresistance.', *Oncogene*, 28(28), pp. 2581–92. doi: 10.1038/onc.2009.124.

Chen, L. S., Redkar, S., Bearss, D., Wierda, W. G. and Gandhi, V. (2009c) 'Pim kinase inhibitor, SGI-1776, induces apoptosis in chronic lymphocytic leukemia cells', *Blood*, 114(19), pp. 4150–4157. doi: 10.1182/blood-2009-03-212852.

Chen, X. P., Losman, J. a, Cowan, S., Donahue, E., Fay, S., Vuong, B. Q., Nawijn, M. C., Capece, D., Cohan, V. L. and Rothman, P. (2002) 'Pim serine/threonine kinases regulate the stability of Socs-1 protein.', *Proceedings of the National Academy of Sciences of the United States of America*, 99(4), pp. 2175–2180. doi: 10.1073/pnas.042035699.

Chen, Z. J. and Sun, L. J. (2009) 'Nonproteolytic Functions of Ubiquitin in Cell Signaling', *Molecular Cell*, pp. 275–286. doi: 10.1016/j.molcel.2009.01.014.

Cheng, J., Kang, X., Zhang, S. and Yeh, E. T. H. (2007) 'SUMO-Specific Protease 1 Is Essential for Stabilization of HIF1 alpha during Hypoxia', *Cell*, 131(3), pp. 584–595. doi: 10.1016/j.cell.2007.08.045.

Chu, Y. and Yang, X. (2011) 'SUMO E3 ligase activity of TRIM proteins.', *Oncogene*, 30(9), pp. 1108–1116. doi: 10.1038/onc.2010.462.

Chung, C. D., Liao, J., Liu, B., Rao, X., Jay, P., Berta, P. and Shuai, K. (1997) 'Specific inhibition of Stat3 signal transduction by PIAS3.', *Science*, 278(5344), pp. 1803–1805. doi: 10.1126/science.278.5344.1803.

Cimarosti, H. and Henley, J. M. (2008) 'Investigating the mechanisms underlying neuronal death in ischemia using in vitro oxygen-glucose deprivation: potential involvement of protein SUMOylation.', *The Neuroscientist : a review journal bringing neurobiology, neurology and psychiatry*, 14(6), pp. 626–36. doi: 10.1177/1073858408322677.

Culjkovic, B., Topisirovic, I., Skrabanek, L., Ruiz-Gutierrez, M. and Borden, K. L. B. (2006) 'eIF4E is a central node of an RNA regulon that governs cellular proliferation', *Journal of Cell Biology*, 175(3), pp. 415–426. doi: 10.1083/jcb.200607020.

Danielsen, J. M. R., Sylvestersen, K. B., Bekker-Jensen, S., Szklarczyk, D., Poulsen, J. W., Horn, H., Jensen, L. J., Mailand, N. and Nielsen, M. L. (2011) 'Mass spectrometric analysis of lysine ubiquitylation reveals promiscuity at site level.', *Molecular & cellular proteomics : MCP*, 10(3), p. M110.003590. doi: 10.1074/mcp.M110.003590.

Decker, S., Finter, J., Forde, A. J., Kissel, S., Schwaller, J., Mack, T. S., Kuhn, A., Gray, N., Follo, M., Jumaa, H., Burger, M., Zirlik, K., Pfeifer, D., Miduturu, C. V, Eibel, H., Veelken, H. and Dierks, C. (2014) 'PIM kinases are essential for chronic lymphocytic leukemia cell survival (PIM2/3) and CXCR4-mediated microenvironmental interactions (PIM1).', *Molecular cancer therapeutics*, 13(5), pp. 1231–45. doi: 10.1158/1535-7163.MCT-13-0575-T.

Deng, L., Wang, C., Spencer, E., Yang, L., Braun, A., You, J., Slaughter, C., Pickart, C. and Chen, Z. J. (2000) 'Activation of the IκB Kinase Complex by TRAF6 Requires a Dimeric Ubiquitin-Conjugating Enzyme Complex and a Unique Polyubiquitin Chain', *Cell*, 103(2), pp. 351–361. doi: 10.1016/S0092-8674(00)00126-4.

DeNicola, G. M., Karreth, F. A., Humpton, T. J., Gopinathan, A., Wei, C., Frese, K., Mangal, D., Yu, K. H., Yeo, C. J., Calhoun, E. S., Scrimieri, F., Winter, J. M., Hruban, R. H., Iacobuzio-Donahue, C., Kern, S. E., Blair, I. A. and Tuveson, D. A. (2011) 'Oncogene-induced Nrf2 transcription promotes ROS detoxification and tumorigenesis.', *Nature*, 475(7354), pp. 106–9. doi: 10.1038/nature10189.

Denuc, A. and Marfany, G. (2010) 'SUMO and ubiquitin paths converge.', *Biochemical Society transactions*, 38(Pt 1), pp. 34–39. doi: 10.1042/BST0380034.

Desterro, J. M. P., Rodriguez, M. S., Kemp, G. D. and Hay R. T. (1999) 'Identification of the enzyme required for activation of the small ubiquitin-like protein SUMO-1', *Journal of Biological Chemistry*, 274(15), pp. 10618–10624. doi: 10.1074/jbc.274.15.10618.

Desterro, J. M. P., Thomson, J. and Hay, R. T. (1997) 'Ubch9 conjugates SUMO but not ubiquitin', *FEBS Letters*, 417(3), pp. 297–300. doi: 10.1016/S0014-5793(97)01305-7.

Desterro, J. M., Rodriguez, M. S. and Hay, R. T. (1998) 'SUMO-1 modification of IkappaBalpha inhibits NF-kappaB activation.', *Molecular cell*, 2(2), pp. 233–239. doi: 10.1016/S1097-2765(00)80133-1.

Du, J. X., Bialkowska, A. B., McConnell, B. B. and Yang, V. W. (2008) 'SUMOylation regulates nuclear localization of Krüppel-like factor 5', *Journal of Biological Chemistry*, 283(46), pp. 31991–32002. doi: 10.1074/jbc.M803612200.

Duval, D., Duval, G., Kedinger, C., Poch, O. and Boeuf, H. (2003) 'The "PINIT" motif, of a newly identified conserved domain of the PIAS protein family, is essential for nuclear retention of PIAS3L', *FEBS Letters*, 554(1–2), pp. 111–118. doi: 10.1016/S0014-5793(03)01116-5.

Eiring, A. M., Harb, J. G., Neviani, P., Garton, C., Oaks, J. J., Spizzo, R., Liu, S., Schwind, S., Santhanam, R., Hickey, C. J., Becker, H., Chandler, J. C., Andino, R., Cortes, J., Hokland, P., Huettner, C. S., Bhatia, R., Roy, D. C., Liebhaber, S. A., Caligiuri, M. A., Marcucci, G., Garzon, R., Croce, C. M., Calin, G. A. and Perrotti, D. (2010) 'miR-328 Functions as an RNA Decoy to Modulate hnRNP E2 Regulation of mRNA Translation in Leukemic Blasts', *Cell*, 140(5), pp. 652–665. doi: 10.1016/j.cell.2010.01.007.

Eladad, S., Ye, T. Z., Hu, P., Leversha, M., Beresten, S., Matunis, M. J. and Ellis, N. A. (2005) 'Intra-nuclear trafficking of the BLM helicase to DNA damage-induced foci is regulated by SUMO modification', *Human Molecular Genetics*, 14(10), pp. 1351–1365. doi: 10.1093/hmg/ddi145.

Emmerich, C. H., Ordureau, A., Strickson, S., Arthur, J. S. C., Pedrioli, P. G. a, Komander, D. and Cohen, P. (2013) 'Activation of the canonical IKK complex by K63/M1-linked hybrid ubiquitin chains.', *Proceedings of the National Academy of Sciences of the United States of America*, 110(38), pp. 15247–52. doi: 10.1073/pnas.1314715110.

Enserink, J. M. (2015) 'Sumo and the cellular stress response', *Cell Division*, 10, p. 4. doi: 10.1186/s13008-015-0010-1 10 [pii].

Erker, Y., Neyret-Kahn, H., Seeler, J. S., Dejean, A., Atfi, A. and Levy, L. (2013) 'Arkadia, a novel SUMO-targeted ubiquitin ligase involved in PML degradation.', *Molecular and cellular biology*, 33(11), pp. 2163–77. doi: 10.1128/MCB.01019-12.

Evdokimov, E., Sharma, P., Lockett, S. J., Lualdi, M. and Kuehn, M. R. (2008) 'Loss of SUMO1 in mice affects RanGAP1 localization and formation of PML nuclear bodies, but is not lethal as it can be compensated by SUMO2 or SUMO3.', *Journal of cell science*, 121(Pt 24), pp. 4106–4113. doi: 10.1242/jcs.038570.

Everett, R. D., Boutell, C. and Hale, B. G. (2013) 'Interplay between viruses and host sumoylation pathways.', *Nature reviews. Microbiology*, 11(6), pp. 400–11. doi: 10.1038/nrmicro3015.

Feldman, J. D., Vician, L., Crispino, M., Tocco, G., Marcheselli, V. L., Bazan, N. G., Baudry, M. and Herschman, H. R. (1998) 'KID-1, a protein kinase induced by depolarization in brain', *Journal of Biological Chemistry*, 273(26), pp. 16535–16543. doi: 10.1074/jbc.273.26.16535.

Fernández-Miranda, G., Pérez de Castro, I., Carmena, M., Aguirre-Portolés, C., Ruchaud, S., Fant, X., Montoya, G., Earnshaw, W. C. and Malumbres, M. (2010) 'SUMOylation modulates the function of Aurora-B kinase.', *Journal Of Cell Science*, 123(Pt 16), pp. 2823–2833. doi: 10.1242/jcs.065565.

Forshell, L. P., Li, Y., Forshell, T. Z. P., Rudelius, M., Nilsson, L., Keller, U. and Nilsson, J. (2011) 'The direct Myc target Pim3 cooperates with other Pim kinases in supporting viability of Myc-induced B-cell lymphomas.', *Oncotarget*, 2(6), pp. 448–460. doi: 283 [pii].

Friedmann, M., Nissen, M. S., Hoover, D. S., Reeves, R. and Magnuson, N. S. (1992) 'Characterization of the proto-oncogene Pim-1: Kinase activity and substrate recognition sequence', *Archives of Biochemistry and Biophysics*, 298(2), pp. 594–601. doi: 10.1016/0003-9861(92)90454-5.

Galcheva-Gargova, Z., Theroux, S. J. and Davis, R. J. (1995) 'The epidermal growth factor receptor is covalently linked to ubiquitin.', *Oncogene*, 11(12), pp. 2649–55.

Garcia, P., Langowski, J. and Wang, Y. (2014) 'Pan-PIM Kinase Inhibition Provides a Novel Therapy for Treating Hematological Cancers', *Clinical Cancer Research*, pp. 1834–1845. doi: 10.1158/1078-0432.CCR-13-2062.

Gareau, J. R. and Lima, C. D. (2010) 'The SUMO pathway: emerging mechanisms that shape specificity, conjugation and recognition.', *Nature reviews. Molecular cell biology*, 11(12), pp. 861–71. doi: 10.1038/nrm3011.

Geisler, S., Holmström, K. M., Skujat, D., Fiesel, F. C., Rothfuss, O. C., Kahle, P. J. and Springer, W. (2010) 'PINK1/Parkin-mediated mitophagy is dependent on VDAC1 and p62/SQSTM1.', *Nature cell biology*, 12(2), pp. 119–131. doi: 10.1038/ncb2012.

Geoffroy, M.-C. and Hay, R. T. (2009) 'An additional role for SUMO in ubiquitin-mediated proteolysis.', *Nature reviews. Molecular cell biology*, 10(8), pp. 564–568. doi: 10.1038/nrm2707.

Gill, G. (2004) 'SUMO and ubiquitin in the nucleus: Different functions, similar mechanisms?', *Genes and Development*, pp. 2046–2059. doi: 10.1101/gad.1214604.

Golebiowski, F., Matic, I., Tatham, M. H., Cole, C., Yin, Y., Nakamura, A., Cox, J., Barton, G. J., Mann, M. and Hay, R. T. (2009) 'System-wide changes to SUMO modifications in response to heat shock.', *Science signaling*, 2(72), p. ra24. doi: 10.1126/scisignal.2000282.

Gong, L., Li, B., Millas, S. and Yeh, E. T. H. (1999) 'Molecular cloning and characterization of human AOS1 and UBA2, components of the sentrin-activating enzyme complex', *FEBS Letters*, 448(1), pp. 185–189. doi: 10.1016/S0014-5793(99)00367-1.

Gresko, E., Ritterhoff, S., Sevilla-Perez, J., Roscic, a, Fröbius, K., Kotevic, I., Vichalkovski, a, Hess, D., Hemmings, B. a and Schmitz, M. L. (2009) 'PML tumor suppressor is regulated by HIPK2-mediated phosphorylation in response to DNA damage.', *Oncogene*, 28(5), pp. 698–708. doi: 10.1038/onc.2008.420.

Gu, J. J., Wang, Z., Reeves, R. and Magnuson, N. S. (2009) 'PIM1 phosphorylates and negatively regulates ASK1-mediated apoptosis.', *Oncogene*, 28(48), pp. 4261–4271. doi: 10.1038/onc.2009.276.

Guo, B., Yang, S.-H., Witty, J. and Sharrocks, a D. (2007) 'Signalling pathways and the regulation of SUMO modification.', *Biochemical Society transactions*, 35(Pt 6), pp. 1414–1418. doi: 10.1042/BST0351414.

Guo, D., Han, J., Adam, B. L., Colburn, N. H., Wang, M. H., Dong, Z., Eizirik, D. L., She, J. X. and Wang, C. Y. (2005) 'Proteomic analysis of SUMO4 substrates in HEK293 cells under serum starvation-induced stress', *Biochemical and Biophysical Research Communications*, 337(4), pp. 1308–1318. doi: 10.1016/j.bbrc.2005.09.191.

Gupta, P., Ho, P.-C., Huq, M. M., Ha, S. G., Park, S. W., Khan, A. A., Tsai, N.-P. and Wei, L.-N. (2008) 'Retinoic acid-stimulated sequential phosphorylation, PML recruitment, and SUMOylation of nuclear receptor TR2 to suppress Oct4 expression.', *Proceedings of the National Academy of Sciences of the United States of America*, 105(32), pp. 11424–9. doi: 10.1073/pnas.0710561105.

Ha, S., Iqbal, N. J., Mita, P., Ruoff, R., Gerald, W. L., Lepor, H., Taneja, S. S., Lee, P., Melamed, J., Garabedian, M. J. and Logan, S. K. (2013) 'Phosphorylation of the androgen receptor by PIM1 in hormone refractory prostate cancer', *Oncogene*, (July), pp. 1–9. doi: 10.1038/onc.2012.412.

van Hagen, M., Overmeer, R. M., Abolvardi, S. S. and Vertegaal, A. C. O. (2009) 'RNF4 and VHL regulate the proteasomal degradation of SUMO-conjugated Hypoxia-Inducible Factor-2??', *Nucleic Acids Research*, 38(6), pp. 1922–1931. doi: 10.1093/nar/gkp1157.

Häkli, M., Karvonen, U., Jänne, O. A. and Palvimo, J. J. (2005) 'SUMO-1 promotes association of SNURF (RNF4) with PML nuclear bodies', *Experimental Cell Research*, 304(1), pp. 224–233. doi: 10.1016/j.yexcr.2004.10.029.

Hammerman, P. S., Fox, C. J., Birnbaum, M. J. and Thompson, C. B. (2005) 'Pim and Akt oncogenes are independent regulators of hematopoietic cell growth and survival', *Blood*, 105(11), pp. 4477–4483. doi: 10.1182/blood-2004-09-3706.

Hammerman, P. S., Fox, C. J., Cinalli, R. M., Xu, A., Wagner, J. D., Lindsten, T. and Thompson, C. B. (2004) 'Lymphocyte transformation by Pim-2 is dependent on nuclear factor-kappaB activation', *Cancer Research*, 64(22), pp. 8341–8348. doi: 10.1158/0008-5472.CAN-04-2284.

Hanks, S. K. and Hunter, T. (1995) 'Protein kinases 6. The eukaryotic protein kinase superfamily: kinase (catalytic) domain structure and classification.', *FASEB journal : official publication of the Federation of American Societies for Experimental Biology*, 9(8), pp. 576–96. doi: 7768349.

Hardeland, U., Steinacher, R., Jiricny, J. and Schär, P. (2002) 'Modification of the human thymine-DNA glycosylase by ubiquitin-like proteins facilitates enzymatic turnover', *EMBO Journal*, 21(6), pp. 1456–1464. doi: 10.1093/emboj/21.6.1456.

Hardie, D. G. (2007) 'AMP-activated/SNF1 protein kinases: conserved guardians of cellular energy.', *Nature reviews. Molecular cell biology*, 8(10), pp. 774–785. doi: 10.1038/nrm2249.

Hay, R. T. (2005) 'SUMO: A history of modification', *Molecular Cell*, pp. 1–12. doi: 10.1016/j.molcel.2005.03.012.

Heery, D. M., Kalkhoven, E., Hoare, S. and Parker, M. G. (1997) 'A signature motif in transcriptional co-activators mediates binding to nuclear receptors.', *Nature*, 387(6634), pp. 733–736. doi: 10.1038/42750.

Hendriks, I. A., D'Souza, R. C. J., Yang, B., Verlaan-de Vries, M., Mann, M. and Vertegaal, A. C. O. (2014) 'Uncovering global SUMOylation signaling networks in a site-specific manner', *Nature Structural & Molecular Biology*, 21(10), pp. 927–936. doi: 10.1038/nsmb.2890.

Hendriks, I. A., Schimmel, J., Eifler, K., Olsen, J. V. and Vertegaal, A. C. O. (2015) 'Ubiquitin-specific protease 11 (USP11) deubiquitinates hybrid small ubiquitin-like modifier (SUMO)-ubiquitin chains to counteract RING finger protein 4 (RNF4)', *Journal of Biological Chemistry*, 290(25), pp. 15526–15537. doi: 10.1074/jbc.M114.618132.

Heride, C., Urbé, S. and Clague, M. J. (2014) 'Ubiquitin code assembly and disassembly', *Current Biology*, 24(6). doi: 10.1016/j.cub.2014.02.002.

Hickey, C. M., Wilson, N. R. and Hochstrasser, M. (2012) 'Function and regulation of SUMO proteases.', *Nature reviews. Molecular cell biology*, 13(12), pp. 755–66. doi: 10.1038/nrm3478.

Hietakangas, V., Anckar, J., Blomster, H. A., Fujimoto, M., Palvimo, J. J., Nakai, A. and Sistonen, L. (2006) 'PDSM, a motif for phosphorylation-dependent SUMO modification.', *Proceedings of the National Academy of Sciences of the United States of America*, 103(1), pp. 45–50. doi: 10.1073/pnas.0503698102.

Hoellein, A., Fallahi, M., Schoeffmann, S., Steidle, S., Schaub, F. X., Rudelius, M., Laitinen, I., Nilsson, L., Goga, A., Peschel, C., Nilsson, J. A., Cleveland, J. L. and Keller, U. (2014) 'Myc-induced SUMOylation is a therapeutic vulnerability for B-cell lymphoma', *Blood*, 124(13), pp. 2081–2090. doi: 10.1182/blood-2014-06-584524.

Hogan, C., Hutchison, C., Marcar, L., Milne, D., Saville, M., Goodlad, J., Kernohan, N. and Meek, D. (2008) 'Elevated levels of oncogenic protein kinase Pim-1 induce the p53 pathway in cultured cells and correlate with increased Mdm2 in mantle cell lymphoma', *Journal of Biological Chemistry*, 283(26), pp. 18012–18023. doi: 10.1074/jbc.M709695200.

Hoover, D. S., Wingett, D. G., Zhang, J., Reeves, R. and Magnuson, N. S. (1997) 'Pim-1 protein expression is regulated by its 5'-untranslated region and translation initiation factor eIF-4E.', *Cell growth & differentiation : the molecular biology journal of the American Association for Cancer Research*, 8(12), pp. 1371–80.

Hornbeck, P. V., Chabra, I., Kornhauser, J. M., Skrzypek, E. and Zhang, B. (2004) 'PhosphoSite: A bioinformatics resource dedicated to physiological protein phosphorylation', *Proteomics*, 4(6), pp. 1551–1561. doi: 10.1002/pmic.200300772.

Hu, Y. L., Passegué, E., Fong, S., Largman, C. and Lawrence, H. J. (2007) 'Evidence that the Pim1 kinase gene is a direct target of HOXA9', *Blood*, 109(11), pp. 4732–4738. doi: 10.1182/blood-2006-08-043356.

Huang, C.-Y., Beliakoff, J., Li, X., Lee, J., Li, X., Sharma, M., Lim, B. and Sun, Z. (2005) 'hZimp7, a novel PIAS-like protein, enhances androgen receptor-mediated transcription and interacts with SWI/SNF-like BAF complexes.', *Molecular endocrinology (Baltimore, Md.)*, 19(12), pp. 2915–2929. doi: 10.1210/me.2005-0097.

Huang, F., Kirkpatrick, D., Jiang, X., Gygi, S. and Sorkin, A. (2006) 'Differential regulation of EGF receptor internalization and degradation by multiubiquitination within the kinase domain', *Molecular Cell*, 21(6), pp. 737–748. doi: 10.1016/j.molcel.2006.02.018.

Huang, T. T., Wuerzberger-Davis, S. M., Wu, Z.-H. and Miyamoto, S. (2003) 'Sequential modification of NEMO/IKKgamma by SUMO-1 and ubiquitin mediates NF-kappaB activation by genotoxic stress.', *Cell*, 115(5), pp. 565–576. doi: S009286740300895X [pii].

Ionov, Y., Le, X., Tunquist, B. J., Sweetenham, J., Sachs, T., Ryder, J., Johnson, T., Lilly, M. B. and Kraft, A. S. (2003) 'Pim-1 protein kinase is nuclear in Burkitt's lymphoma: Nuclear localization is necessary for its biologic effects', *Anticancer Research*, 23(1 A), pp. 167–178.

Isaac, M., Siu, A. and Jongstra, J. (2011) 'The oncogenic PIM kinase family regulates drug resistance through multiple mechanisms', *Drug Resistance Updates*, 14(4–5), pp. 203–211. doi: 10.1016/j.drup.2011.04.002.

Ishibashi, Y., Maita, H., Yano, M., Koike, N., Tamai, K., Ariga, H. and Iguchi-Ariga, S. M. M. (2001) 'Pim-1 translocates sorting nexin 6/TRAF4-associated factor 2 from cytoplasm to nucleus', *FEBS Letters*, 506(1), pp. 33–38. doi: 10.1016/S0014-5793(01)02881-2.

Jacobs, A-M. F., Nicol, S. M., Hislop, R. G., Jaffray, E. G., Hay, R. T. and Fuller-Pace, F. V (2007) 'SUMO modification of the DEAD box protein p68 modulates its transcriptional activity and promotes its interaction with HDAC1.', *Oncogene*, 26, pp. 5866–5876. doi: 10.1038/sj.onc.1210387.

Jacobs, M. D., Black, J., Futer, O., Swenson, L., Hare, B., Fleming, M. and Saxena, K. (2005) 'Pim-1 ligand-bound structures reveal the mechanism of serine/threonine kinase inhibition by LY294002', *Journal of Biological Chemistry*, 280(14), pp. 13728–13734. doi: 10.1074/jbc.M413155200.

Jakobs, A., Himstedt, F., Funk, M., Korn, B., Gaestel, M. and Niedenthal, R. (2007) 'Ubc9 fusion-directed SUMOylation identifies constitutive and inducible SUMOylation', *Nucleic Acids Research*, 35(17). doi: 10.1093/nar/gkm617.

Jentsch, S. and Psakhye, I. (2013) 'Control of nuclear activities by substrate-selective and protein-group SUMOylation.', *Annual review of genetics*, 47, pp. 167–86. doi: 10.1146/annurev-genet-111212-133453.

Jin, B., Wang, Y., Wu, C. L., Liu, K. Y., Chen, H. and Mao, Z. Bin (2014) 'PIM-1 modulates cellular senescence and links IL-6 signaling to heterochromatin formation', *Aging Cell*, 13(5), pp. 879–889. doi: 10.1111/acel.12249.

Jin, L., Williamson, A., Banerjee, S., Philipp, I. and Rape, M. (2008) 'Mechanism of Ubiquitin-Chain Formation by the Human Anaphase-Promoting Complex', *Cell*, 133(4), pp. 653–665. doi: 10.1016/j.cell.2008.04.012.

Johnson, E. S. (2004) 'Sumo', *Annual Review of Biochemistry*, 73(1), pp. 355–382. doi: 10.1146/annurev.biochem.73.011303.074118.

Johnson, E. S. and Gupta, A. A. (2001) 'An E3-like factor that promotes SUMO conjugation to the yeast septins', *Cell*, 106(6), pp. 735–744. doi: 10.1016/S0092-8674(01)00491-3.

Johnson, E. S., Schwienhorst, I., Dohmen, R. J. and Blobel, G. (1997) 'The ubiquitin-like protein Smt3p is activated for conjugation to other proteins by an Aos1p/Uba2p heterodimer', *EMBO Journal*, 16(18), pp. 5509–5519. doi: 10.1093/emboj/16.18.5509.

Joseph, J., Tan, S. H., Karpova, T. S., McNally, J. G. and Dasso, M. (2002) 'SUMO-1 targets RanGAP1 to kinetochores and mitotic spindles', *Journal of Cell Biology*, 156(4), pp. 595–602. doi: 10.1083/jcb.200110109.

Kang, B. S., French, O. G., Sando, J. J. and Hahn, C. S. (2000) 'Activation-dependent degradation of protein kinase C eta.', *Oncogene*, 19(37), pp. 4263–72. doi: 10.1038/sj.onc.1203779.

Keane, N. A., Reidy, M., Natoni, A., Raab, M. S. and O'Dwyer, M. (2015) 'Targeting the Pim kinases in multiple myeloma.', *Blood cancer journal*, 5(May), p. e325. doi: 10.1038/bcj.2015.46.

Keeton, E. K., McEachern, K., Dillman, K. S., Palakurthi, S., Cao, Y., Grondine, M. R., Kaur, S., Wang, S., Chen, Y., Wu, A., Shen, M., Gibbons, F. D., Lamb, M. L., Zheng, X., Stone, R. M., DeAngelo, D. J., Platanias, L. C., Dakin, L. A., Chen, H., Lyne, P. D. and Huszar, D. (2014) 'AZD1208, a potent and selective pan-Pim kinase inhibitor, demonstrates efficacy in preclinical models of acute myeloid leukemia', *Blood*, 123(6), pp. 905–913. doi: 10.1182/blood-2013-04-495366.

Kerscher, O., Felberbaum, R. and Hochstrasser, M. (2006) 'Modification of proteins by ubiquitin and ubiquitin-like proteins.', *Annual review of cell and developmental biology*, 22, pp. 159–80. doi: 10.1146/annurev.cellbio.22.010605.093503.

Kessler, J. D., Kahle, K. T., Sun, T., Meerbrey, K. L., Schlabach, M. R., Schmitt, E. M., Skinner, S. O., Xu, Q., Li, M. Z., Hartman, Z. C., Rao, M., Yu, P., Dominguez-Vidana, R., Liang, A. C., Solimini, N. L., Bernardi, R. J., Yu, B., Hsu, T., Golding, I., Luo, J., Osborne, C. K., Creighton, C. J., Hilsenbeck, S. G., Schiff, R., Shaw, C. A., Elledge, S. J. and Westbrook, T. F. (2012) 'A SUMOylation-dependent transcriptional subprogram is required for Myc-driven tumorigenesis.', *Science (New York, N.Y.)*, 335(6066), pp. 348–53. doi: 10.1126/science.1212728.

Kim, H. K., Kim, C. W., Vo, M. T., Lee, H. H., Lee, J. Y., Yoon, N. A., Lee, C. Y., Moon, C. H., Min, Y. J., Park, J. W. and Cho, W. J. (2012) 'Expression of proviral integration site for moloney murine leukemia virus 1 (Pim-1) is post-transcriptionally regulated by tristetraprolin in cancer cells', *Journal of Biological Chemistry*, 287(34), pp. 28770–28778. doi: 10.1074/jbc.M112.376483.

Kim, J., Roh, M. and Abdulkadir, S. A. (2010) 'Pim1 promotes human prostate cancer cell tumorigenicity and c-MYC transcriptional activity.', *BMC cancer*, 10, p. 248. doi: 10.1186/1471-2407-10-248.

Kim, K. T., Baird, K., Ahn, J. Y., Meltzer, P., Lilly, M., Levis, M. and Small, D. (2005) 'Pim-1 is up-regulated by constitutively activated FLT3 and plays a role in FLT3-mediated cell survival', *Blood*, 105(4), pp. 1759–1767. doi: 10.1182/blood-2004-05-2006.

Kim, O., Jiang, T., Xie, Y., Guo, Z., Chen, H. and Qiu, Y. (2004) 'Synergism of cytoplasmic kinases in IL6-induced ligand-independent activation of androgen receptor in prostate cancer cells.', *Oncogene*, 23(10), pp. 1838–44. doi: 10.1038/sj.onc.1207304.

Kirschner, A. N., Wang, J., Van Der Meer, R., Anderson, P. D., Franco-Coronel, O. E., Kushner, M. H., Everett, J. H., Hameed, O., Keeton, E. K., Ahdesmaki, M., Grosskurth, S. E., Huszar, D. and Abdulkadir, S. A. (2015) 'PIM kinase inhibitor AZD1208 for treatment of MYC-driven prostate cancer', *Journal of the National Cancer Institute*, 107(2), pp. 1–11. doi: 10.1093/jnci/dju407.

Komander, D. (2009) 'The emerging complexity of protein ubiquitination.', *Biochemical Society transactions*, 37(Pt 5), pp. 937–53. doi: 10.1042/BST0370937.

Komander, D. and Rape, M. (2012) 'The Ubiquitin Code', *Annual Review of Biochemistry*, 81(1), pp. 203–229. doi: 10.1146/annurev-biochem-060310-170328.

Kotaja, N., Karvonen, U., Jänne, O. a and Palvimo, J. J. (2002) 'PIAS proteins modulate transcription factors by functioning as SUMO-1 ligases.', *Molecular and cellular biology*, 22(14), pp. 5222–5234. doi: 10.1128/MCB.22.14.5222-5234.2002.

Kubota, Y., O'Grady, P., Saito, H. and Takekawa, M. (2011) 'Oncogenic Ras abrogates MEK SUMOylation that suppresses the ERK pathway and cell transformation.', *Nature cell biology*, 13(3), pp. 282–91. doi: 10.1038/ncb2169.

Kulathu, Y. and Komander, D. (2012) 'Atypical ubiquitylation — the unexplored world of polyubiquitin beyond Lys48 and Lys63 linkages', *Nature Reviews Molecular Cell Biology*, 13(8), pp. 508–523. doi: 10.1038/nrm3394.

Kumar, A., Mandiyan, V., Suzuki, Y., Zhang, C., Rice, J., Tsai, J., Artis, D. R., Ibrahim, P. and Bremer, R. (2005) 'Crystal structures of proto-oncogene kinase Pim1: A target of aberrant somatic hypermutations in diffuse large cell lymphoma', *Journal of Molecular Biology*, 348(1), pp. 183–193. doi: 10.1016/j.jmb.2005.02.039.

Kuo, C.-Y., Li, X., Kong, X.-Q., Luo, C., Chang, C.-C., Chung, Y., Shih, H.-M., Li, K. K. and Ann, D. K. (2014) 'An Arginine-rich Motif of Ring Finger Protein 4 (RNF4) Oversees the Recruitment and Degradation of the Phosphorylated and SUMOylated Krüppel-associated Box Domain-associated Protein 1 (KAP1)/TRIM28 Protein during Genotoxic Stress', *Journal of Biological Chemistry* , 289(30), pp. 20757–20772. doi: 10.1074/jbc.M114.555672.

de la Cruz-Herrera, C. F., Campagna, M., Garcia, M. a, Marcos-Villar, L., Lang, V., Baz-Martinez, M., Gutierrez, S., Vidal, A., Rodriguez, M. S., Esteban, M. and Rivas, C. (2014b) 'Activation of the Double-Stranded RNA-Dependent Protein Kinase PKR by Sumo.', *The Journal of biological chemistry*, p. M114.560961-. doi: 10.1074/jbc.M114.560961.

de la Cruz-Herrera, C. F., Campagna, M., Lang, V., Del Carmen González-Santamaría, J., Marcos-Villar, L., Rodríguez, M. S., Vidal, a, Collado, M. and Rivas, C. (2014a) 'SUMOylation regulates AKT1 activity.', *Oncogene*, (August 2013), pp. 1–9. doi: 10.1038/onc.2014.48.

Lallemand-Breitenbach, V., Jeanne, M., Benhenda, S., Nasr, R., Lei, M., Peres, L., Zhou, J., Zhu, J., Raught, B. and de Thé, H. (2008) 'Arsenic degrades PML or PML-RARalpha through a SUMO-triggered RNF4/ubiquitin-mediated pathway.', *Nature cell biology*, 10(5), pp. 547–555. doi: 10.1038/ncb1717.

Laplante, M. and Sabatini, D. M. (2009) 'mTOR signaling at a glance', *J Cell Sci*, 122(Pt 20), pp. 3589–3594. doi: 122/20/3589 [pii] 10.1242/jcs.051011.

Lee, J., Beliakoff, J. and Sun, Z. (2007) 'The novel PIAS-like protein hZimp10 is

a transcriptional co-activator of the p53 tumor suppressor', *Nucleic Acids Research*, 35(13), pp. 4523–4534. doi: 10.1093/nar/gkm476.

Lee, J., Lee, Y., Lee, M. J., Park, E., Kang, S. H., Chung, C. H., Lee, K. H. and Kim, K. (2008) 'Dual modification of BMAL1 by SUMO2/3 and ubiquitin promotes circadian activation of the CLOCK/BMAL1 complex.', *Molecular and cellular biology*, 28(19), pp. 6056–6065. doi: 10.1128/MCB.00583-08.

Levy, D., Davidovich, A., Zirkin, S., Frug, Y., Cohen, A. M., Shalom, S. and Don, J. (2012) 'Activation of cell cycle arrest and apoptosis by the proto-oncogene Pim-2', *PLoS ONE*, 7(4). doi: 10.1371/journal.pone.0034736.

Li, L., Sampat, K., Hu, N., Zakari, J. and Yuspa, S. H. (2006) 'Protein kinase C negatively regulates Akt activity and modifies UVC-induced apoptosis in mouse keratinocytes', *Journal of Biological Chemistry*, 281(6), pp. 3237–3243. doi: 10.1074/jbc.M512167200.

Li, R., Wei, J., Jiang, C., Liu, D., Deng, L., Zhang, K. and Wang, P. (2013) 'Akt SUMOylation regulates cell proliferation and tumorigenesis.', *Cancer research*, 73(18), pp. 5742–53. doi: 10.1158/0008-5472.CAN-13-0538.

Liang, Y.-C., Lee, C.-C., Yao, Y.-L., Lai, C.-C., Schmitz, M. L. and Yang, W.-M. (2016) 'SUMO5, a Novel Poly-SUMO Isoform, Regulates PML Nuclear Bodies', *Scientific Reports*. Nature Publishing Group, 6, p. 26509. doi: 10.1038/srep26509.

Lin, C. H., Liu, S. Y. and Lee, E. H. Y. (2016) 'SUMO modification of Akt regulates global SUMOylation and substrate SUMOylation specificity through Akt phosphorylation of Ubc9 and SUMO1.', *Oncogene*, 35(5), pp. 595–607. doi: 10.1038/onc.2015.115.

Lin, D., Tatham, M. H., Yu, B., Kim, S., Hay, R. T. and Yuan Chen, Y. (2002) 'Identification of a substrate recognition site on Ubc9', *Journal of Biological Chemistry*, 277(24), pp. 21740–21748. doi: 10.1074/jbc.M108418200.

Lin, D. Y., Huang, Y. S., Jeng, J. C., Kuo, H. Y., Chang, C. C., Chao, T. T., Ho, C. C., Chen, Y. C., Lin, T. P., Fang, H. I., Hung, C. C., Suen, C. S., Hwang, M. J., Chang, K. S., Maul, G. G. and Shih, H. M. (2006) 'Role of SUMO-Interacting Motif in Daxx SUMO Modification, Subnuclear Localization, and Repression of Sumoylated Transcription Factors', *Molecular Cell*, 24(3), pp. 341–354. doi:

10.1016/j.molcel.2006.10.019.

Lin, J. Y., Ohshima, T. and Shimotohno, K. (2004) ‘Association of Ubc9, an E2 ligase for SUMO conjugation, with p53 is regulated by phosphorylation of p53’, *FEBS Letters*, 573(1–3), pp. 15–18. doi: 10.1016/j.febslet.2004.07.059.

Liu, B., Liao, J., Rao, X., Kushner, S. A., Chung, C. D., Chang, D. D. and Shuai, K. (1998) ‘Inhibition of Stat1-mediated gene activation by PIAS1.’, *Proceedings of the National Academy of Sciences of the United States of America*, 95(18), pp. 10626–31. doi: 10.1073/pnas.95.18.10626.

van Lohuizen, M., Verbeek, S., Krimpenfort, P., Domen, J., Saris, C., Radaszkiewicz, T. and Berns, A. (1989) ‘Predisposition to lymphomagenesis in pim-1 transgenic mice: Cooperation with c-myc and N-myc in murine leukemia virus-induced tumors’, *Cell*. Elsevier, 56(4), pp. 673–682. doi: 10.1016/0092-8674(89)90589-8.

Lois, L. M. and Lima, C. D. (2005) ‘Structures of the SUMO E1 provide mechanistic insights into SUMO activation and E2 recruitment to E1.’, *The EMBO journal*, 24(3), pp. 439–51. doi: 10.1038/sj.emboj.7600552.

Losman, J. A., Chen, X. P., Vuong, B. Q., Fay, S. and Rothman, P. B. (2003) ‘Protein phosphatase 2A regulates the stability of Pim protein kinases’, *Journal of Biological Chemistry*, 278(7), pp. 4800–4805. doi: 10.1074/jbc.M208246200.

Lu, J., Zavorotinskaya, T., Dai, Y., Niu, X.-H., Castillo, J., Sim, J., Yu, J., Wang, Y., Langowski, J. L., Holash, J., Shannon, K. and Garcia, P. D. (2013) ‘Pim2 is required for maintaining multiple myeloma cell growth through modulating TSC2 phosphorylation.’, *Blood*, 122(9), pp. 1610–20. doi: 10.1182/blood-2013-01-481457.

Lu, Y., Zhou, Q., Shi, Y., Liu, J., Zhong, F., Hao, X., Li, C., Chen, N. and Wang, W. (2013) ‘SUMOylation of PPARγ by rosiglitazone prevents LPS-induced NCoR degradation mediating down regulation of chemokines expression in renal proximal tubular cells’, *PLoS ONE*, 8(11). doi: 10.1371/journal.pone.0079815.

Lu, Z., Liu, D., Hornia, a, Devonish, W., Pagano, M. and Foster, D. a (1998) ‘Activation of protein kinase C triggers its ubiquitination and degradation.’, *Molecular and cellular biology*, 18(2), pp. 839–45.

van der Lugt, N. M., Domen, J., Verhoeven, E., Linders, K., van der Gulden, H., Allen, J. and Berns, a (1995) 'Proviral tagging in E mu-myc transgenic mice lacking the Pim-1 proto-oncogene leads to compensatory activation of Pim-2.', *The EMBO journal*, 14(11), pp. 2536–2544.

Luo, K., Zhang, H., Wang, L., Yuan, J. and Lou, Z. (2012) 'Sumoylation of MDC1 is important for proper DNA damage response', *The EMBO Journal*, 31(13), pp. 3008–3019. doi: 10.1038/emboj.2012.158.

Ma, J., Arnold, H. K., Lilly, M. B., Sears, R. C. and Kraft, a S. (2007) 'Negative regulation of Pim-1 protein kinase levels by the B56beta subunit of PP2A.', *Oncogene*, 26(35), pp. 5145–5153. doi: 10.1038/sj.onc.1210323.

Macdonald, A., Campbell, D. G., Toth, R., McLauchlan, H., Hastie, C. J. and Arthur, J. S. C. (2006) 'Pim kinases phosphorylate multiple sites on Bad and promote 14-3-3 binding and dissociation from Bcl-XL.', *BMC cell biology*, 7, p. 1. doi: 10.1186/1471-2121-7-1.

Mahajan, R., Delphin, C., Guan, T., Gerace, L. and Melchior, F. (1997) 'A small ubiquitin-related polypeptide involved in targeting RanGAP1 to nuclear pore complex protein RanBP2.', *Cell*, 88(1), pp. 97–107. doi: 10.1016/S0092-8674(00)81862-0.

Mahat, D. B., Brennan-Laun, S. E., Fialcowitz-White, E. J., Kishor, A., Ross, C. R., Pozharskaya, T., Rawn, J. D., Blackshear, P. J., Hassel, B. A. and Wilson, G. M. (2012) 'Coordinated expression of tristetraprolin post-transcriptionally attenuates mitogenic induction of the oncogenic ser/thr kinase Pim-1', *PLoS ONE*, 7(3). doi: 10.1371/journal.pone.0033194.

Malinen, M., Jääskeläinen, T., Pelkonen, M., Heikkinen, S., Väisänen, S., Kosma, V. M., Nieminen, K., Mannermaa, A. and Palvimo, J. J. (2013) 'Proto-oncogene PIM-1 is a novel estrogen receptor target associating with high grade breast tumors', *Molecular and Cellular Endocrinology*. Elsevier Ireland Ltd, 365(2), pp. 270–276. doi: 10.1016/j.mce.2012.10.028.

Martin, N., Schwamborn, K., Schreiber, V., Werner, A., Guillier, C., Zhang, X.-D., Bischof, O., Seeler, J.-S. and Dejean, A. (2009) 'PARP-1 transcriptional activity

is regulated by sumoylation upon heat shock.', *The EMBO journal*, 28(22), pp. 3534–48. doi: 10.1038/emboj.2009.279.

Martin, S., Wilkinson, K. a, Nishimune, A. and Henley, J. M. (2007) 'Emerging extranuclear roles of protein SUMOylation in neuronal function and dysfunction.', *Nature reviews. Neuroscience*, 8(12), pp. 948–959. doi: 10.1038/nrn2276.

Matic, I., Schimmel, J., Hendriks, I. A., van Santen, M. A., van de Rijke, F., van Dam, H., Gnad, F., Mann, M. and Vertegaal, A. C. O. (2010) 'Site-Specific Identification of SUMO-2 Targets in Cells Reveals an Inverted SUMOylation Motif and a Hydrophobic Cluster SUMOylation Motif', *Molecular Cell*, 39(4), pp. 641–652. doi: 10.1016/j.molcel.2010.07.026.

Matsumoto, M. L., Wickliffe, K. E., Dong, K. C., Yu, C., Bosanac, I., Bustos, D., Phu, L., Kirkpatrick, D. S., Hymowitz, S. G., Rape, M., Kelley, R. F. and Dixit, V. M. (2010) 'K11-linked polyubiquitination in cell cycle control revealed by a K11 linkage-specific antibody', *Molecular Cell*, 39(3), pp. 477–484. doi: 10.1016/j.molcel.2010.07.001.

Matunis, M. J., Coutavas, E. and Blobel, G. (1996) 'A novel ubiquitin-like modification modulates the partitioning of the Ran-GTPase-activating protein RanGAP1 between the cytosol and the nuclear pore complex', *Journal of Cell Biology*, 135(6), pp. 1457–1470. doi: 10.1083/jcb.135.6.1457.

Van Der Meer, R., Song, H. Y., Park, S. H., Abdulkadir, S. A. and Roh, M. (2014) 'RNAi screen identifies a synthetic lethal interaction between PIM1 overexpression and PLK1 inhibition', *Clinical Cancer Research*, 20(12), pp. 3211–3221. doi: 10.1158/1078-0432.CCR-13-3116.

Meja, K., Stengel, C., Sellar, R., Huszar, D., Davies, B. R., Gale, R. E., Linch, D. C. and Khwaja, A. (2014) 'PIM and AKT kinase inhibitors show synergistic cytotoxicity in acute myeloid leukaemia that is associated with convergence on mTOR and MCL1 pathways', *British Journal of Haematology*, 167(1), pp. 69–79. doi: 10.1111/bjh.13013.

Melchior, F. (2000) 'SUMO--nonclassical ubiquitin.', *Annual review of cell and developmental biology*, 16, pp. 591–626. doi: 10.1146/annurev.cellbio.16.1.591.

Merbl, Y., Refour, P., Patel, H., Springer, M. and Kirschner, M. W. (2013) 'Profiling of ubiquitin-like modifications reveals features of mitotic control', *Cell*, 152(5), pp. 1160–1172. doi: 10.1016/j.cell.2013.02.007.

Mikkers, H., Allen, J., Knipscheer, P., Romeijn, L., Hart, A., Vink, E. and Berns,

A. (2002) ‘High-throughput retroviral tagging to identify components of specific signaling pathways in cancer.’, *Nature genetics*, 32(september), pp. 153–159. doi: 10.1038/ng950.

Mikkers, H., Nawijn, M., Allen, J., Brouwers, C., Verhoeven, E., Jonkers, J. and Berns, A. (2004) ‘Mice Deficient for All PIM Kinases Display Reduced Body Size and Impaired Responses to Hematopoietic Growth Factors’, *Molecular and Cellular Biology*, 24(13), pp. 6104–6115. doi: 10.1128/MCB.24.13.6104.

Min, M., Mevissen, T., Luca, M. De, Komander, D. and Lindon, C. (2015) ‘Efficient APC/C substrate degradation in cells undergoing mitotic exit depends on K11 ubiquitin linkages’, *bioRxiv*, p. 16139. doi: 10.1101/016139.

Mizuno, K., Shirogane, T., Shinohara, A., Iwamatsu, A., Hibi, M. and Hirano, T. (2001) ‘Regulation of Pim-1 by Hsp90’, *Biochem Biophys Res Commun*, 281(3), pp. 663–669. doi: 10.1006/bbrc.2001.4405.

Mochizuki, T., Kitanaka, C., Noguchi, K., Muramatsu, T., Asai, A. and Kuchino, Y. (1999) ‘Physical and functional interactions between pim-1 kinase and Cdc25A phosphatase. Implications for the Pim-1-mediated activation of the c-Myc signaling pathway’, *Journal of Biological Chemistry*, 274(26), pp. 18659–18666. doi: 10.1074/jbc.274.26.18659.

Moilanen, A. M., Poukka, H., Karvonen, U., Häkli, M., Jänne, O. A. and Palvimo, J. J. (1998) ‘Identification of a novel RING finger protein as a coregulator in steroid receptor-mediated gene transcription.’, *Molecular and cellular biology*, 18(9), pp. 5128–39.

Morishita, D., Katayama, R., Sekimizu, K., Tsuruo, T. and Fujita, N. (2008) ‘Pim kinases promote cell cycle progression by phosphorylating and down-regulating p27kip1 at the transcriptional and posttranscriptional levels’, *Cancer Research*, 68(13), pp. 5076–5085. doi: 10.1158/0008-5472.CAN-08-0634.

Muraski, J. a, Rota, M., Misao, Y., Fransioli, J., Cottage, C., Gude, N., Esposito, G., Delucchi, F., Arcarese, M., Alvarez, R., Siddiqi, S., Emmanuel, G. N., Wu, W., Fischer, K., Martindale, J. J., Glembotski, C. C., Leri, A., Kajstura, J., Magnuson, N., Berns, A., Beretta, R. M., Houser, S. R., Schaefer, E. M., Anversa, P. and Sussman, M. a (2007) ‘Pim-1 regulates cardiomyocyte survival downstream of Akt.’, *Nature medicine*, 13(12), pp. 1467–75. doi: 10.1038/nm1671.

Nasser, M. W., Datta, J., Nuovo, G., Kutay, H., Motiwala, T., Majumder, S., Wang, B., Suster, S., Jacob, S. T. and Ghoshal, K. (2008) 'Down-regulation of micro-RNA-1 (miR-1) in lung cancer: Suppression of tumorigenic property of lung cancer cells and their sensitization to doxorubicin-induced apoptosis by miR-1', *Journal of Biological Chemistry*, 283(48), pp. 33394–33405. doi: 10.1074/jbc.M804788200.

Natarajan, K., Xie, Y., Burcu, M., Linn, D. E., Qiu, Y. and Baer, M. R. (2013a) 'Pim-1 Kinase Phosphorylates and Stabilizes 130 kDa FLT3 and Promotes Aberrant STAT5 Signaling in Acute Myeloid Leukemia with FLT3 Internal Tandem Duplication', *PLoS ONE*, 8(9). doi: 10.1371/journal.pone.0074653.

Natarajan, K., Bhullar, J., Shukla, S., Burcu, M., Chen, Z. S., Ambudkar, S. V. and Baer, M. R. (2013b) 'The Pim kinase inhibitor SGI-1776 decreases cell surface expression of P-glycoprotein (ABCB1) and breast cancer resistance protein (ABCG2) and drug transport by Pim-1-dependent and -independent mechanisms', *Biochemical Pharmacology*, 85(4), pp. 514–524. doi: 10.1016/j.bcp.2012.12.006.

Nawijn, M. C., Alendar, A. and Berns, A. (2011) 'For better or for worse: the role of Pim oncogenes in tumorigenesis', *Nat Rev Cancer*, 11(1), pp. 23–34. doi: 10.1038/nrc2986.

Nguyen, H.-V., Chen, J.-L., Zhong, J., Kim, K.-J., Crandall, E. D., Borok, Z., Chen, Y. and Ann, D. K. (2006) 'SUMOylation attenuates sensitivity toward hypoxia- or desferroxamine-induced injury by modulating adaptive responses in salivary epithelial cells.', *The American journal of pathology*, 168(5), pp. 1452–1463. doi: 10.2353/ajpath.2006.050782.

Nieborowska-Skorska, M., Hoser, G., Kossev, P., Wasik, M. A. and Skorski, T. (2002) 'Complementary functions of the antiapoptotic protein A1 and serine/threonine kinase pim-1 in the BCR/ABL-mediated leukemogenesis', *Blood*, 99(12), pp. 4531–4539. doi: 10.1182/blood.V99.12.4531.

Nihira, K., Ando, Y., Yamaguchi, T., Kagami, Y., Miki, Y. and Yoshida, K. (2010) 'Pim-1 controls NF-kappaB signalling by stabilizing RelA/p65.', *Cell death and differentiation*, 17(4), pp. 689–98. doi: 10.1038/cdd.2009.174.

Okubo, S., Hara, F., Tsuchida, Y., Shimotakahara, S., Suzuki, S., Hatanaka, H., Yokoyama, S., Tanaka, H., Yasuda, H. and Shindo, H. (2004) 'NMR structure of the N-terminal domain of SUMO ligase PIAS1 and its interaction with tumor

suppressor p53 and A/T-rich DNA oligomers', *Journal of Biological Chemistry*, 279(30), pp. 31455–31461. doi: 10.1074/jbc.M403561200.

Olsen, S. K., Capili, A. D., Lu, X., Tan, D. S. and Lima, C. D. (2010) 'Active site remodelling accompanies thioester bond formation in the SUMO E1', *Nature*, 463(7283), pp. 906–912. doi: nature08765 [pii]\n10.1038/nature08765.

Owerbach, D., McKay, E. M., Yeh, E. T. H., Gabbay, K. H. and Bohren, K. M. (2005) 'A proline-90 residue unique to SUMO-4 prevents maturation and sumoylation', *Biochemical and Biophysical Research Communications*, 337(2), pp. 517–520. doi: 10.1016/j.bbrc.2005.09.090.

Padma, R. and Nagarajan, L. (1991) 'The human PIM-1 gene product is a protein serine kinase', *Cancer Research*, 51(9), pp. 2486–2489.

Palaty, C. K., Clark-lewis, I., Leung, D. and Pelech, S. L. (1997) 'Phosphorylation site substrate specificity determinants for the Pim-1 protooncogene-encoded protein kinase', *Biochemistry and Cell Biology*, 75(2), pp. 153–162. doi: 10.1139/o97-026.

Pang, W., Tian, X., Bai, F., Han, R., Wang, J., Shen, H., Zhang, X., Liu, Y., Yan, X., Jiang, F. and Xing, L. (2014) 'Pim-1 kinase is a target of miR-486-5p and eukaryotic translation initiation factor 4E, and plays a critical role in lung cancer.', *Molecular cancer*, 13(1), p. 240. doi: 10.1186/1476-4598-13-240.

Pascual, G., Fong, A. L., Ogawa, S., Gamliel, A., Li, A. C., Perissi, V., Rose, D. W., Willson, T. M., Rosenfeld, M. G. and Glass, C. K. (2005) 'A SUMOylation-dependent pathway mediates transrepression of inflammatory response genes by PPAR-γ', *Nature*, 437(7059), pp. 759–763. doi: 10.1038/nature03988.

Pasqualucci, L., Neumeister, P., Goossens, T., Nanjangud, G., Chaganti, R. S., Kuppers, R. and Dalla-Favera, R. (2001) 'Hypermutation of multiple proto-oncogenes in B-cell diffuse large-cell lymphomas', *Nature*, 412(6844), pp. 341–346. doi: 10.1038/35085588.

Peltola, K. J., Paukku, K., Aho, T. L. T., Ruuska, M., Silvennoinen, O. and Koskinen, P. J. (2004) 'Pim-1 kinase inhibits STAT5-dependent transcription via its interactions with SOCS1 and SOCS3', *Blood*, 103(10), pp. 3744–3750. doi:

10.1182/blood-2003-09-3126.

Pichler, A., Knipscheer, P., Oberhofer, E., van Dijk, W. J., Körner, R., Olsen, J. V., Jentsch, S., Melchior, F. and Sixma, T. K. (2005) 'SUMO modification of the ubiquitin-conjugating enzyme E2-25K.', *Nature structural & molecular biology*, 12(3), pp. 264–269. doi: 10.1038/nsmb903.

Pichler, A., Knipscheer, P., Saitoh, H., Sixma, T. K. and Melchior, F. (2004) 'The RanBP2 SUMO E3 ligase is neither HECT- nor RING-type', *Nature Structural & Molecular Biology*, 11(10), pp. 984–991. doi: 10.1038/nsmb834.

Potts, P. R. and Yu, H. (2005) 'Human MMS21/NSE2 is a SUMO ligase required for DNA repair.', *Molecular and cellular biology*, 25(16), pp. 7021–32. doi: 10.1128/MCB.25.16.7021-7032.2005.

Poukka, H., Aarnisalo, P., Santti, H., Jänne, O. A. and Palvimo, J. J. (2000) 'Coregulator small nuclear RING finger protein (SNURF) enhances Sp1- and steroid receptor-mediated transcription by different mechanisms', *Journal of Biological Chemistry*, 275(1), pp. 571–579. doi: 10.1074/jbc.275.1.571.

Poulsen, S. L., Hansen, R. K., Wagner, S. A., van Cuijk, L., van Belle, G. J., Streicher, W., Wikström, M., Choudhary, C., Houtsmuller, A. B., Marteijn, J. A., Bekker-Jensen, S. and Mailand, N. (2013) 'RNF111/Arkadia is a SUMO-targeted ubiquitin ligase that facilitates the DNA damage response.', *The Journal of cell biology*, 201(6), pp. 797–807. doi: 10.1083/jcb.201212075.

Prudden, J., Pebernard, S., Raffa, G., Slavin, D. A., Perry, J. J. P., Tainer, J. A., McGowan, C. H. and Boddy, M. N. (2007) 'SUMO-targeted ubiquitin ligases in genome stability.', *The EMBO journal*, 26(18), pp. 4089–101. doi: 10.1038/sj.emboj.7601838.

Psakhye, I. and Jentsch, S. (2012) 'Protein group modification and synergy in the SUMO pathway as exemplified in DNA repair', *Cell*, 151(4), pp. 807–820. doi: 10.1016/j.cell.2012.10.021.

Qian, K. C., Wang, L., Hickey, E. R., Studts, J., Barringer, K., Peng, C., Kronkaitis, A., Li, J., White, A., Mische, S. and Farmer, B. (2005) 'Structural basis of constitutive activity and a unique nucleotide binding mode of human Pim-1 kinase', *Journal of Biological Chemistry*, 280(7), pp. 6130–6137. doi:

10.1074/jbc.M409123200.

Qu, J., Liu, G. H., Wu, K., Han, P., Wang, P., Li, J., Zhang, X. and Chen, C. (2007) 'Nitric oxide destabilizes Pias3 and regulates sumoylation', *PLoS ONE*, 2(10). doi: 10.1371/journal.pone.0001085.

Rabellino, A., Carter, B., Konstantinidou, G., Wu, S. Y., Rimessi, A., Byers, L. A., Heymach, J. V., Girard, L., Chiang, C. M., Teruya-Feldstein, J. and Scaglioni, P. P. (2012) 'The SUMO E3-ligase PIAS1 regulates the tumor suppressor PML and its oncogenic counterpart PML-RARA', *Cancer Research*, 72(9), pp. 2275–2284. doi: 10.1158/0008-5472.CAN-11-3159.

Rahighi, S., Ikeda, F., Kawasaki, M., Akutsu, M., Suzuki, N., Kato, R., Kensche, T., Uejima, T., Bloor, S., Komander, D., Randow, F., Wakatsuki, S. and Dikic, I. (2009) 'Specific Recognition of Linear Ubiquitin Chains by NEMO Is Important for NF-κB Activation', *Cell*, 136(6), pp. 1098–1109. doi: 10.1016/j.cell.2009.03.007.

Ribet, D., Hamon, M., Gouin, E., Nahori, M.-A., Impens, F., Neyret-Kahn, H., Gevaert, K., Vandekerckhove, J., Dejean, A. and Cossart, P. (2010) 'Listeria monocytogenes impairs SUMOylation for efficient infection.', *Nature*, 464(April), pp. 1192–1195. doi: 10.1038/nature08963.

Ritho, J., Arold, S. T. and Yeh, E. T. H. (2015) 'A Critical SUMO1 Modification of LKB1 Regulates AMPK Activity during Energy Stress.', *Cell reports*, 12(5), pp. 734–42. doi: 10.1016/j.celrep.2015.07.002.

Rodriguez, M. S., Dargemont, C. and Hay, R. T. (2001) 'SUMO-1 Conjugation in Vivo Requires Both a Consensus Modification Motif and Nuclear Targeting', *Journal of Biological Chemistry*, 276(16), pp. 12654–12659. doi: 10.1074/jbc.M009476200.

Rubio, T., Vernia, S. and Sanz, P. (2013) 'Sumoylation of AMPKβ2 subunit enhances AMP-activated protein kinase activity.', *Molecular biology of the cell*, 24(11), pp. 1801–11, S1-4. doi: 10.1091/mbc.E12-11-0806.

Saitoh, H. and Hinchey, J. (2000) 'Functional heterogeneity of small ubiquitin-related protein modifiers SUMO-1 versus SUMO-2/3', *Journal of Biological Chemistry*, 275(9), pp. 6252–6258. doi: 10.1074/jbc.275.9.6252.

Santio, N. M., Landor, S. K. J., Vahtera, L., Ylä-Pelto, J., Paloniemi, E., Imanishi, S. Y., Corthals, G., Varjosalo, M., Babu Manoharan, G., Uri, A., Lendahl, U., Sahlgren, C. and Koskinen, P. J. (2016) 'Phosphorylation of Notch1 by Pim kinases promotes oncogenic signaling in breast and prostate cancer cells', *Oncotarget; Vol 7, No 28*.

Sapetschnig, A., Rischitor, G., Braun, H., Doll, A., Schergaut, M., Melchior, F. and Suske, G. (2002) 'Transcription factor Sp3 is silenced through SUMO modification by PIAS1', *EMBO Journal*, 21(19), pp. 5206–5215. doi: 10.1093/emboj/cdf510.

Saris, C. J., Domen, J. and Berns, A. (1991) 'The pim-1 oncogene encodes two related protein-serine/threonine kinases by alternative initiation at AUG and CUG.', *The EMBO journal*, 10(3), pp. 655–664.

Saul, V. V., Niedenthal, R., Pich, A., Weber, F. and Schmitz, M. L. (2015) 'SUMO modification of TBK1 at the adaptor-binding C-terminal coiled-coil domain contributes to its antiviral activity', *Biochimica et Biophysica Acta - Molecular Cell Research*, 1853(1), pp. 136–143. doi: 10.1016/j.bbamcr.2014.10.008.

Schatz, J. H., Oricchio, E., Wolfe, A. L., Jiang, M., Linkov, I., Maragulia, J., Shi, W., Zhang, Z., Rajasekhar, V. K., Pagano, N. C., Porco Jr., J. A., Teruya-Feldstein, J., Rosen, N., Zelenetz, A. D., Pelletier, J. and Wendel, H. G. (2011) 'Targeting cap-dependent translation blocks converging survival signals by AKT and PIM kinases in lymphoma', *J Exp Med*, 208(9), pp. 1799–1807. doi: 10.1084/jem.20110846.

Schulz, S., Chachami, G., Kozaczkiewicz, L., Winter, U., Stankovic-Valentin, N., Haas, P., Hofmann, K., Urlaub, H., Ovaa, H., Wittbrodt, J., Meulmeester, E. and Melchior, F. (2012) 'Ubiquitin-specific protease-like 1 (USPL1) is a SUMO isopeptidase with essential, non-catalytic functions.', *EMBO reports*, 13(10), pp. 930–8. doi: 10.1038/embor.2012.125.

Sehat, B., Tofigh, A., Lin, Y., Trocmé, E., Liljedahl, U., Lagergren, J. and Larsson, O. (2010) 'SUMOylation mediates the nuclear translocation and signaling of the IGF-1 receptor.', *Science signaling*, 3(108), p. ra10. doi: 10.1126/scisignal.2000628.

Seifert, A., Schofield, P., Barton, G. J. and Hay, R. T. (2015) 'Proteotoxic stress reprograms the chromatin landscape of SUMO modification.', *Science signaling*,

8(384), p. rs7. doi: 10.1126/scisignal.aaa2213.

Selten, G., Cuypers, H. T. and Berns, A. (1985) ‘Proviral activation of the putative oncogene Pim-1 in MuLV induced T-cell lymphomas.’, *The EMBO journal*, 4(7), pp. 1793–8.

Seufert, W., Futcher, B. and Jentsch, S. (1995) ‘Role of a ubiquitin-conjugating enzyme in degradation of S- and M-phase cyclins.’, *Nature*, pp. 78–81. doi: 10.1038/373078a0.

Shay, K. P., Wang, Z., Xing, P.-X., McKenzie, I. F. C. and Magnuson, N. S. (2005) ‘Pim-1 kinase stability is regulated by heat shock proteins and the ubiquitin-proteasome pathway.’, *Molecular cancer research : MCR*, 3(3), pp. 170–181. doi: 10.1158/1541-7786.MCR-04-0192.

Shen, L. N., Dong, C., Liu, H., Naismith, J. H. and Hay, R. T. (2006) ‘The structure of SENP1-SUMO-2 complex suggests a structural basis for discrimination between SUMO paralogues during processing.’, *The Biochemical journal*, 397(2), pp. 279–288. doi: 10.1042/BJ20052030.

Shen, Z., Pardington-Purtymun, P. E., Comeaux, J. C., Moyzis, R. K. and Chen, D. J. (1996a) ‘Associations of UBE2I with RAD52, UBL1, p53, and RAD51 proteins in a yeast two-hybrid system.’, *Genomics*, pp. 183–6. doi: 10.1006/geno.1996.0540.

Shen, Z., Pardington-Purtymun, P. E., Comeaux, J. C., Moyzis, R. K. and Chen, D. J. (1996b) ‘UBL1, a human ubiquitin-like protein associating with human RAD51/RAD52 proteins.’, *Genomics*, 36(2), pp. 271–279. doi: 10.1006/geno.1996.0462.

Shin, E. J., Shin, H. M., Nam, E., Kim, W. S., Kim, J.-H., Oh, B.-H. and Yun, Y. (2012) ‘DeSUMOylating isopeptidase: a second class of SUMO protease.’, *EMBO reports*, 13(4), pp. 339–46. doi: 10.1038/embor.2012.3.

Shirogane, T., Fukada, T., Muller, J. M., Shima, D. T., Hibi, M. and Hirano, T. (1999) ‘Synergistic roles for Pim-1 and c-Myc in STAT3-mediated cell cycle progression and antiapoptosis.’, *Immunity*, 11(6), pp. 709–719. doi: 10.1016/S1074-7613(00)80145-4.

Song, J. H., Padi, S. K. R., Luevano, L. A., Minden, M. D., DeAngelo, D. J., Hardiman, G., Ball, L. E., Warfel, N. A. and Kraft, A. S. (2016) ‘Insulin receptor

substrate 1 is a substrate of the Pim protein kinases', *Oncotarget; Vol 7, No 15*.

Song, J. H., An, N., Chatterjee, S., Kistner-Griffin, E., Mahajan, S., Mehrotra, S. and Kraft, A. S. (2014) 'Deletion of Pim kinases elevates the cellular levels of reactive oxygen species and sensitizes to K-Ras-induced cell killing', *Oncogene*, 34(28), pp. 3728–3736. doi: 10.1038/onc.2014.306.

Song, J. H. and Kraft, A. S. (2012) 'Pim kinase inhibitors sensitize prostate cancer cells to apoptosis triggered by Bcl-2 family inhibitor ABT-737', *Cancer Research*, 72(1), pp. 294–303. doi: 10.1158/0008-5472.CAN-11-3240.

Steinacher, R. and Schär, P. (2005) 'Functionality of human thymine DNA glycosylase requires SUMO-regulated changes in protein conformation', *Current Biology*, 15(7), pp. 616–623. doi: 10.1016/j.cub.2005.02.054.

Stindt, M. H., Carter, S., Vigneron, A. M., Ryan, K. M. and Vousden, K. H. (2011) 'MDM2 promotes SUMO-2/3 modification of p53 to modulate transcriptional activity', *Cell Cycle*, 10(18), pp. 3176–3188. doi: 10.4161/cc.10.18.17436.

Sun, H. and Hunter, T. (2012) 'Poly-small ubiquitin-like modifier (PolySUMO)-binding proteins identified through a string search', *Journal of Biological Chemistry*, 287(50), pp. 42071–42083. doi: 10.1074/jbc.M112.410985.

Tammsalu, T., Matic, I., Jaffray, E. G., Ibrahim, A. F. M., Tatham, M. H. and Hay, R. T. (2014) 'Proteome-wide identification of SUMO2 modification sites.', *Science signaling*, 7(323), p. rs2. doi: 10.1126/scisignal.2005146.

Tatham, M. H., Geoffroy, M.-C., Shen, L., Plechanovova, A., Hattersley, N., Jaffray, E. G., Palvimo, J. J. and Hay, R. T. (2008) 'RNF4 is a poly-SUMO-specific E3 ubiquitin ligase required for arsenic-induced PML degradation.', *Nature cell biology*, 10(5), pp. 538–546. doi: 10.1038/ncb1716.

Tatham, M. H., Jaffray, E., Vaughan, O. A., Desterro, J. M. P., Botting, C. H., Naismith, J. H. and Hay, R. T. (2001) 'Polymeric Chains of SUMO-2 and SUMO-3 are Conjugated to Protein Substrates by SAE1/SAE2 and Ubc9', *Journal of Biological Chemistry*, 276(38), pp. 35368–35374. doi: 10.1074/jbc.M104214200.

Tatham, M. H., Rodriguez, M. S., Xirodimas, D. P. and Hay, R. T. (2009) 'Detection of protein SUMOylation in vivo.', *Nature protocols*, 4(9), pp. 1363–1371. doi: 10.1038/nprot.2009.128.

Telerman, a, Amson, R., Zakut-Houri, R. and Givol, D. (1988) 'Identification of the human pim-1 gene product as a 33-kilodalton cytoplasmic protein with tyrosine kinase activity.', *Molecular and cellular biology*, 8(4), pp. 1498–503. doi: 10.1128/MCB.8.4.1498.

Theo Cuypers, H., Selten, G., Quint, W., Zijlstra, M., Maandag, E. R., Boelens, W., van Wezenbeek, P., Melief, C. and Berns, A. (1984) 'Murine leukemia virus-induced T-cell lymphomagenesis: Integration of proviruses in a distinct chromosomal region', *Cell*, 37(1), pp. 141–150. doi: 10.1016/0092-8674(84)90309-X.

Thomas, M., Lange-Grunweller, K., Weirauch, U., Gutsch, D., Aigner, A., Grunweller, A. and Hartmann, R. K. (2012) 'The proto-oncogene Pim-1 is a target of miR-33a', *Oncogene*, 31(7), pp. 918–928. doi: 10.1038/onc.2011.278.

Thrower, J. S., Hoffman, L., Rechsteiner, M. and Pickart, C. M. (2000) 'Recognition of the polyubiquitin proteolytic signal.', *The EMBO journal*, 19(1), pp. 94–102. doi: 10.1093/emboj/19.1.94.

Uchimura, Y., Ichimura, T., Uwada, J., Tachibana, T., Sugahara, S., Nakao, M. and Saitoh, H. (2006) 'Involvement of SUMO modification in MBD1- and MCAF1-mediated heterochromatin formation', *Journal of Biological Chemistry*, 281(32), pp. 23180–23190. doi: 10.1074/jbc.M602280200.

Ulrich, H. D. (2009) 'Regulating post-translational modifications of the eukaryotic replication clamp PCNA', *DNA Repair*, pp. 461–469. doi: 10.1016/j.dnarep.2009.01.006.

Ullmann, R., Chien, C. D., Avantaggiati, M. L. and Muller, S. (2012) 'An Acetylation Switch Regulates SUMO-Dependent Protein Interaction Networks', *Molecular Cell*, 46(6), pp. 759–770. doi: 10.1016/j.molcel.2012.04.006.

Ungureanu, D., Vanhatupa, S., Grönholm, J., Palvimo, J. J. and Silvennoinen, O. (2005) 'SUMO-1 conjugation selectively modulates STAT1-mediated gene responses', *Blood*, 106(1), pp. 224–226. doi: 10.1182/blood-2004-11-4514.

Ungureanu, D., Vanhatupa, S., Kotaja, N., Yang, J., Aittomaki, S., Jänne, O. A., Palvimo, J. J. and Silvennoinen, O. (2003) 'PIAS proteins promote SUMO-1 conjugation to STAT1', *Blood*, 102(9), pp. 3311–3313. doi: 10.1182/blood-2002-12-3816.

Valdman, A., Fang, X., Pang, S.-T., Ekman, P. and Egevad, L. (2004) 'Pim-1 expression in prostatic intraepithelial neoplasia and human prostate cancer.', *The Prostate*, 60(4), pp. 367–371. doi: 10.1002/pros.20064.

Verbeek, S., van Lohuizen, M., van der Valk, M., Domen, J., Kraal, G. and Berns, A. (1991) 'Mice bearing the E mu-myc and E mu-pim-1 transgenes develop pre-B-cell leukemia prenatally', *Mol Cell Biol*, 11(2), pp. 1176–1179.

Vertegaal, A. C. O., Andersen, J. S., Ogg, S. C., Hay, R. T., Mann, M. and Lamond, A. I. (2006) 'Distinct and overlapping sets of SUMO-1 and SUMO-2 target proteins revealed by quantitative proteomics.', *Molecular & cellular proteomics : MCP*, 5(12), pp. 2298–2310. doi: 10.1074/mcp.M600212-MCP200.

Wang, C., Deng, L., Hong, M., Akkaraju, G. R., Inoue, J. and Chen, Z. J. (2001) 'TAK1 is a ubiquitin-dependent kinase of MKK and IKK.', *Nature*, 412(6844), pp. 346–51. doi: 10.1038/35085597.

Wang, H., Wang, L., Erdjument-Bromage, H., Vidal, M., Tempst, P., Jones, R. S. and Zhang, Y. (2004) 'Role of histone H2A ubiquitination in Polycomb silencing', *Nature*, 431(7010), pp. 862–868. doi: 10.1038/nature02926.

Wang, J., Anderson, P. D., Luo, W., Gius, D., Roh, M. and Abdulkadir, S. a (2012) 'Pim1 kinase is required to maintain tumorigenicity in MYC-expressing prostate cancer cells.', *Oncogene*, 31(14), pp. 1794–803. doi: 10.1038/onc.2011.371.

Wang, Z., Bhattacharya, N., Mixter, P. F., Wei, W., Sedivy, J. and Magnuson, N. S. (2002) 'Phosphorylation of the cell cycle inhibitor p21Cip1/WAF1 by Pim-1 kinase', *Biochimica et Biophysica Acta - Molecular Cell Research*, 1593(1), pp. 45–55. doi: 10.1016/S0167-4889(02)00347-6.

Warfel, N. A., Sainz, A. G., Song, J. H. and Kraft, A. S. (2016) 'PIM Kinase Inhibitors Kill Hypoxic Tumor Cells by Reducing Nrf2 Signaling and Increasing Reactive Oxygen Species', *Molecular Cancer Therapeutics*, 15(7), p. 1637 LP-1647.

Weger, S., Hammer, E. and Heilbronn, R. (2005) 'Topors acts as a SUMO-1 E3 ligase for p53 in vitro and in vivo', *FEBS Letters*, 579(22), pp. 5007–5012. doi: 10.1016/j.febslet.2005.07.088.

Wei, W., Yang, P., Pang, J., Zhang, S., Wang, Y., Wang, M. H., Dong, Z., She, J. X. and Wang, C. Y. (2008) 'A stress-dependent SUMO4 sumoylation of its substrate proteins', *Biochemical and Biophysical Research Communications*, 375(3), pp. 454–459. doi: 10.1016/j.bbrc.2008.08.028.

Weinberg, F., Hamanaka, R., Wheaton, W. W., Weinberg, S., Joseph, J., Lopez, M., Kalyanaraman, B., Mutlu, G. M., Budinger, G. R. S. and Chandel, N. S. (2010) 'Mitochondrial metabolism and ROS generation are essential for Kras-mediated tumorigenicity.', *Proceedings of the National Academy of Sciences of the United States of America*, 107(19), pp. 8788–93. doi: 10.1073/pnas.1003428107.

Wilkinson, K. a. and Henley, J. M. (2010) 'Mechanisms, regulation and consequences of protein SUMOylation.', *Biochemical Journal*, 428(2), pp. 133–145. doi: 10.1042/BJ20100158.

Wingett, D., Reeves, R. and Magnuson, N. S. (1991) 'Stability changes in pim-1 proto-oncogene mRNA after mitogen stimulation of normal lymphocytes', *J Immunol*, 147(10), p. 3653–9.

Wood, L. D., Irvin, B. J., Nucifora, G., Luce, K. S. and Hiebert, S. W. (2003) 'Small ubiquitin-like modifier conjugation regulates nuclear export of TEL, a putative tumor suppressor.', *Proceedings of the National Academy of Sciences of the United States of America*, 100(6), pp. 3257–62. doi: 10.1073/pnas.0637114100.

Wu-Baer, F., Ludwig, T. and Baer, R. (2010) 'The UBXN1 protein associates with autoubiquitinated forms of the BRCA1 tumor suppressor and inhibits its enzymatic function.', *Molecular and cellular biology*, 30(11), pp. 2787–98. doi: 10.1128/MCB.01056-09.

Wu, K., Yamoah, K., Dolios, G., Gan-Erdene, T., Tan, P., Chen, A., Lee, C. G., Wei, N., Wilkinson, K. D., Wang, R. and Pan, Z. Q. (2003) 'DEN1 is a dual function protease capable of processing the c terminus of Nedd8 and deconjugating hyper-neddylated CUL1', *Journal of Biological Chemistry*, 278(31), pp. 28882–28891. doi: 10.1074/jbc.M302888200.

Xie, Y., Burcu, M., Linn, D. E., Qiu, Y. and Baer, M. R. (2010) 'Pim-1 kinase protects P-glycoprotein from degradation and enables its glycosylation and cell surface expression.', *Molecular pharmacology*, 78(2), pp. 310–8. doi: 10.1124/mol.109.061713.

Xie, Y., Xu, K., Dai, B., Guo, Z., Jiang, T., Chen, H. and Qiu, Y. (2006) 'The 44 kDa Pim-1 kinase directly interacts with tyrosine kinase Etk/BMX and protects human prostate cancer cells from apoptosis induced by chemotherapeutic drugs.', *Oncogene*, 25(1), pp. 70–78. doi: 10.1038/sj.onc.1209058.

Xie, Y., Xu, K., Linn, D. E., Yang, X., Guo, Z., Shimelis, H., Nakanishi, T., Ross, D. D., Chen, H., Fazli, L., Gleave, M. E. and Qiu, Y. (2008) 'The 44-kDa Pim-1 kinase phosphorylates BCRP/ABCG2 and thereby promotes its multimerization and drug-resistant activity in human prostate cancer cells', *Journal of Biological Chemistry*, 283(6), pp. 3349–3356. doi: 10.1074/jbc.M707773200.

Xu, D., Allsop, S. A., Witherspoon, S. M., Snider, J. L., Yeh, J. J., Fiordalisi, J. J., White, C. D., Williams, D., Cox, A. D. and Baines, A. T. (2011) 'The oncogenic kinase Pim-1 is modulated by K-Ras signaling and mediates transformed growth and radioresistance in human pancreatic ductal adenocarcinoma cells', *Carcinogenesis*, 32(4), pp. 488–495. doi: 10.1093/carcin/bgr007.

Yan, B., Zemskova, M., Holder, S., Chin, V., Kraft, A., Koskinen, P. J. and Lilly, M. (2003) 'The PIM-2 Kinase Phosphorylates BAD on Serine 112 and Reverses BAD-induced Cell Death', *Journal of Biological Chemistry*, 278(46), pp. 45358–45367. doi: 10.1074/jbc.M307933200.

Yan, Y., Ollila, S., Wong, I. P. L., Vallenius, T., Palvimo, J. J., Vaahtomeri, K. and Mäkelä, T. P. (2015) 'SUMOylation of AMPKα1 by PIAS4 specifically regulates mTORC1 signalling.', *Nature communications*, 6, p. 8979. doi: 10.1038/ncomms9979.

Yang, H., Wang, Y., Qian, H., Zhang, P. and Huang, C. (2011) 'Pim protein kinase-3 is regulated by TNF-alpha and promotes endothelial cell sprouting', *Molecules and Cells*, 32(3), pp. 235–241. doi: 10.1007/s10059-011-1026-z.

Yang, Q., Chen, L. S., Neelapu, S. S., Miranda, R. N., Medeiros, L. J. and Gandhi, V. (2012) 'Transcription and translation are primary targets of Pim kinase inhibitor SGI-1776 in mantle cell lymphoma', *Blood*, 120(17), pp. 3491–3500. doi: 10.1182/blood-2012-02-412643.

Yang, S.-H., Galanis, A., Witty, J. and Sharrocks, A. D. (2006) 'An extended consensus motif enhances the specificity of substrate modification by SUMO.', *The EMBO journal*, 25(21), pp. 5083–93. doi: 10.1038/sj.emboj.7601383.

Yang, S. H., Jaffray, E., Senthinathan, B., Hay, R. T. and Sharrocks, A. D. (2003) 'SUMO and transcriptional repression: dynamic interactions between the MAP kinase and SUMO pathways.', *Cell cycle (Georgetown, Tex.)*, pp. 528–530. doi: 10.4161/cc.2.6.597.

Yeh, E. T. H. (2009) 'SUMOylation and De-SUMOylation: Wrestling with life's processes', *Journal of Biological Chemistry*, pp. 8223–8227. doi: 10.1074/jbc.R800050200.

Yunus, A. A. and Lima, C. D. (2009) 'Structure of the Siz/PIAS SUMO E3 Ligase Siz1 and Determinants Required for SUMO Modification of PCNA', *Molecular Cell*, 35(5), pp. 669–682. doi: 10.1016/j.molcel.2009.07.013.

Zemskova, M., Lilly, M. B., Lin, Y.-W., Song, J. H. and Kraft, A. S. (2010) 'p53-dependent induction of prostate cancer cell senescence by the PIM1 protein kinase.', *Molecular cancer research : MCR*, 8(8), pp. 1126–41. doi: 10.1158/1541-7786.MCR-10-0174.

Zhang, F.-P., Mikkonen, L., Toppari, J., Palvimo, J. J., Thesleff, I. and Jänne, O. a (2008b) 'Sumo-1 function is dispensable in normal mouse development', *Molecular and cellular biology*, 28(17), pp. 5381–5390. doi: 10.1128/MCB.00651-08.

Zhang, F., Beharry, Z. M., Harris, T. E., Lilly, M. B., Smith, C. D., Mahajan, S. and Kraft, A. S. (2009) 'PIM1 protein kinase regulates PRAS40 phosphorylation and mTOR activity in FDCP1 cells', *Cancer Biology and Therapy*, 8(9), pp. 846–853. doi: 10.4161/cbt.8.9.8210.

Zhang, Y., Lei, W., Yan, W., Li, X., Wang, X., Zhao, Z., Hui, J., Shen, Z. and Yang, J. (2016) 'microRNA-206 is involved in survival of hypoxia preconditioned mesenchymal stem cells through targeting Pim-1 kinase', *Stem Cell Research & Therapy*, 7(1), pp. 1–10. doi: 10.1186/s13287-016-0318-z.

Zhang, Y., Wang, Z., Li, X. and Magnuson, N. S. (2008a) 'Pim kinase-dependent inhibition of c-Myc degradation.', *Oncogene*, 27(35), pp. 4809–4819. doi: 10.1038/onc.2008.123.

Zhang, Y., Wang, Z. and Magnuson, N. S. (2007) 'Pim-1 Kinase-Dependent Phosphorylation of p21Cip1/WAF1 Regulates Its Stability and Cellular Localization in H1299 Cells', *Molecular Cancer Research*, 5(9), p. 909 LP-922.

Zhao, Y., Hamza, M. S., Leong, H. S., Lim, C.-B., Pan, Y.-F., Cheung, E., Soo, K.-C. and Iyer, N. G. (2008) 'Kruppel-like factor 5 modulates p53-independent apoptosis through Pim1 survival kinase in cancer cells.', *Oncogene*, 27(1), pp. 1–8. doi: 10.1038/sj.onc.1210625.

Zhong, S., Müller, S., Ronchetti, S., Freemont, P. S., Dejean, A. and Pandolfi, P. P. (2000) 'Role of SUMO-1-modified PML in nuclear body formation.', *Blood*, 95(9), pp. 2748–52.

Zhou, Z., Wang, M., Li, J., Xiao, M., Chin, Y. E., Cheng, J., Yeh, E. T. H., Yang, J. and Yi, J. (2016) 'SUMOylation and SENP3 regulate STAT3 activation in head and neck cancer', *Oncogene*. Macmillan Publishers Limited. Available at: http://dx.doi.org/10.1038/onc.2016.124.

Zhu, J., Zhu, S., Guzzo, C. M., Ellis, N. A., Ki, S. S., Cheol, Y. C. and Matunis, M. J. (2008) 'Small ubiquitin-related modifier (SUMO) binding determines substrate recognition and paralog-selective SUMO modification', *Journal of Biological Chemistry*, 283(43), pp. 29405–29415. doi: 10.1074/jbc.M803632200.

Zhu, N., Ramirez, L. M., Lee, R. L., Magnuson, N. S., Bishop, G. a and Gold, M. R. (2002) 'CD40 signaling in B cells regulates the expression of the Pim-1 kinase via the NF-kappa B pathway.', *Journal of immunology (Baltimore, Md. : 1950)*, 168(2), pp. 744–754. doi: 10.4049/jimmunol.168.2.744.

Zippo, A., De Robertis, A., Serafini, R. and Oliviero, S. (2007) 'PIM1-dependent phosphorylation of histone H3 at serine 10 is required for MYC-dependent transcriptional activation and oncogenic transformation.', *Nature cell biology*, 9(8), pp. 932–944. doi: 10.1038/ncb1618.

Zippo, A., Serafini, R., Rocchigiani, M., Pennacchini, S., Krepelova, A. and Oliviero, S. (2009) 'Histone Crosstalk between H3S10ph and H4K16ac Generates a Histone Code that Mediates Transcription Elongation', *Cell*, 138(6), pp. 1122–1136. doi: 10.1016/j.cell.2009.07.031.

Appendix

A1. CXR1002

CXR1002, an ammonium salt of perfluorooctanoic acid, was identified by CXR Biosciences as a potential anti-cancer agent, and tested in Phase I clinical trials. It is cytotoxic to cancer cells in culture and in xenograft models. Various mechanisms of action of this drug have been proposed. It primarily acts as a lipid mimetic, and causes endoplasmic reticulum (ER) stress in cells. Additionally, it was also shown to inhibit PIM kinases in a panel of 50 kinases tested *in vitro*. The drug is unique in that it is not metabolised at all in the human body and gets accumulated to a certain level, following which it is excreted intact. Hence, inter-patient variability observed with other drugs, due to differences in their ability to metabolise the drug, is thought not to be a problem with CXR1002, which makes it an attractive drug.

The data presented here were performed as a part of validation of CXR1002 as a bonafide PIM kinase inhibitor. The main goal of the project was to perform a synthetic lethal screen with PIM kinase inhibitors, including CXR1002. But soon after the start of this project, a study was published identifying PIM1 and PLK1 (Polo-like kinase 1) as synthetic lethal targets in prostate cancer (Van Der Meer *et al*., 2014, advance online publication Jan 2013). Since various studies in the literature had already tested AKT and mTOR inhibitors in combination with PIM1 inhibitors (Blanco-Aparicio and Carnero, 2013), we decided to take an alternative approach and focus on studying regulation of PIM1. In doing so, I identified SUMOylation as a novel mechanism affecting PIM1 function, which could impact PIM kinase inhibitors in the future.

A2. Experimental methods

Methods not described previously in Chapter-2 have been included here.

a) Cell lines

PC3, LNCaP and K562 cells were grown in RPMI1640 media supplemented with 10% FBS and 2 mM L-glutamine, in a 37 ^{0}C humidified CO_2 incubator.

b) Cell viability assay

Cell viability or cytotoxicity was measured using CellTiter 96 Aqueous One Solution Proliferation assay (MTS) kit from Promega. 100 µl of PC3 and LNCaP cells were seeded at a density of 10,000 cells per well, and 50 µl of K562 at 5000 cells per well in a 96-well plate in triplicate for 24 hours. The following day, the media on PC3 and LNCaP was replaced with 100 µl fresh media containing 0.1% DMSO as control, or the desired concentrations of either SGI-1776 or CXR1002. In the case of K562, 50 µl of fresh media containing 2X of final desired drug concentration was added directly to the wells, for a final volume of 100 µl and 1X drug concentration. 20 µl of MTS reagent was added to the cells after 24 or 72 hours of drug treatment, and cell viability was measured by reading absorbance at 490 nm.

c) Kinase assays by western blotting

PIM1 kinase assays were carried out using purified recombinant GST-PIM1 with histone H3.3 (NEB, UK) as substrate. Reactions were carried out in a total volume of 20 µl containing 50 mM Tris-HCl pH 7.5, 10 mM $MgCl_2$, 0.2 mM ATP, 0.5 µg substrate and approximately 0.2 µg PIM1 kinase.

Appropriate negative control reactions without any substrate or kinase were also set up simultaneously. Reactions were incubated in a 30 ^{0}C water bath for 30 min, and terminated by addition of 2X SDS sample buffer (with DTT). The reactions were boiled for 5 min followed by either coomassie staining of the gel or SDS-PAGE and western blotting using a phospho-specific antibody against Ser10 of Histone H3.3.

d) Kinase assays using ADP-Glo kinase luminescent assay (Promega)

Non-radioactive *in vitro* kinase assays were carried out in 25 µl reaction volume containing 200 ng GST-PIM1, 500 ng Histone H3.3 (substrate), 100 µM ATP (supplied in the Kinase Glo kit), 10 mM $MgCl_2$, 50 mM Tris pH 7.5 and 100 µM DTT, with or without desired drug concentration in a 96 well white-bottom plate. The plate was incubated at 30 ^{0}C for 30 min, followed by addition of 25 µl ADP-Glo reagent and further incubated for 40 min at RT. Next, 50 µl of Kinase detection reagent was added to each well, and incubated for 1 hour at RT, following which luminescence was measured using Promega GloMax luminometer.

A3. Effect of SGI-1776 and CXR1002 on cell viability

Since PIM kinases are overexpressed in prostate cancer and haematological malignancies, I chose two prostate cancer cell lines (PC3 and LNCaP) and one CML line (K562) to test the efficacy of CXR1002. I also used a commercially available inhibitor of SGI-1776 as a control, and for comparison with CXR1002. MTS assays were carried out to measure cell viability after 24 and 72 hours of drug treatment. The cells were treated with increasing doses of either SGI-1776 or CXR1002 to determine half maximal inhibitory concentration (IC50). As shown in figure 1 and 2, both SGI-1776 and CXR1002 decreased cell viability in a dose dependent manner in all three cell lines tested at 24 and 72 hours. However, SGI-1776 was clearly more potent than CXR-1002, which was used at high micromolar concentrations in this assay to observe an effect. The average IC50 values for SGI-1776 and CXR1002 in these cell lines was around 7 μM and 350 μM respectively.

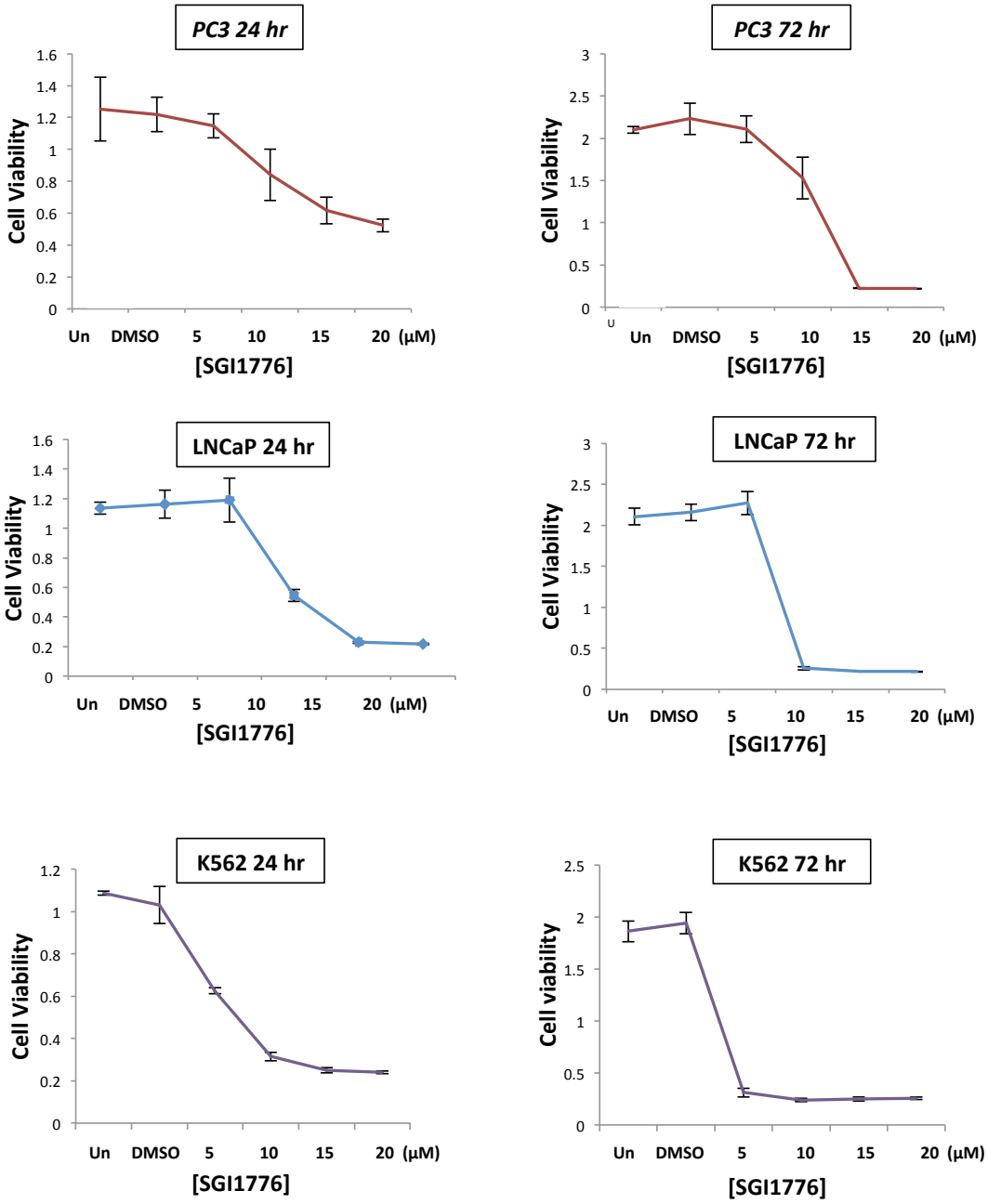

Figure 1 Cell viability following SGI-1776 treatment

LNCaP, PC3 and K562 cells were plated in 96 well plates for 24 hours prior to addition of the indicated drug concentrations for 24 or 72 hours. Cell viability was measured using MTS assay kit from Promega as per manufacturer's instructions. The optical density, which is directly proportional to cell viability, was measured at 490 nm and plotted on a graph.

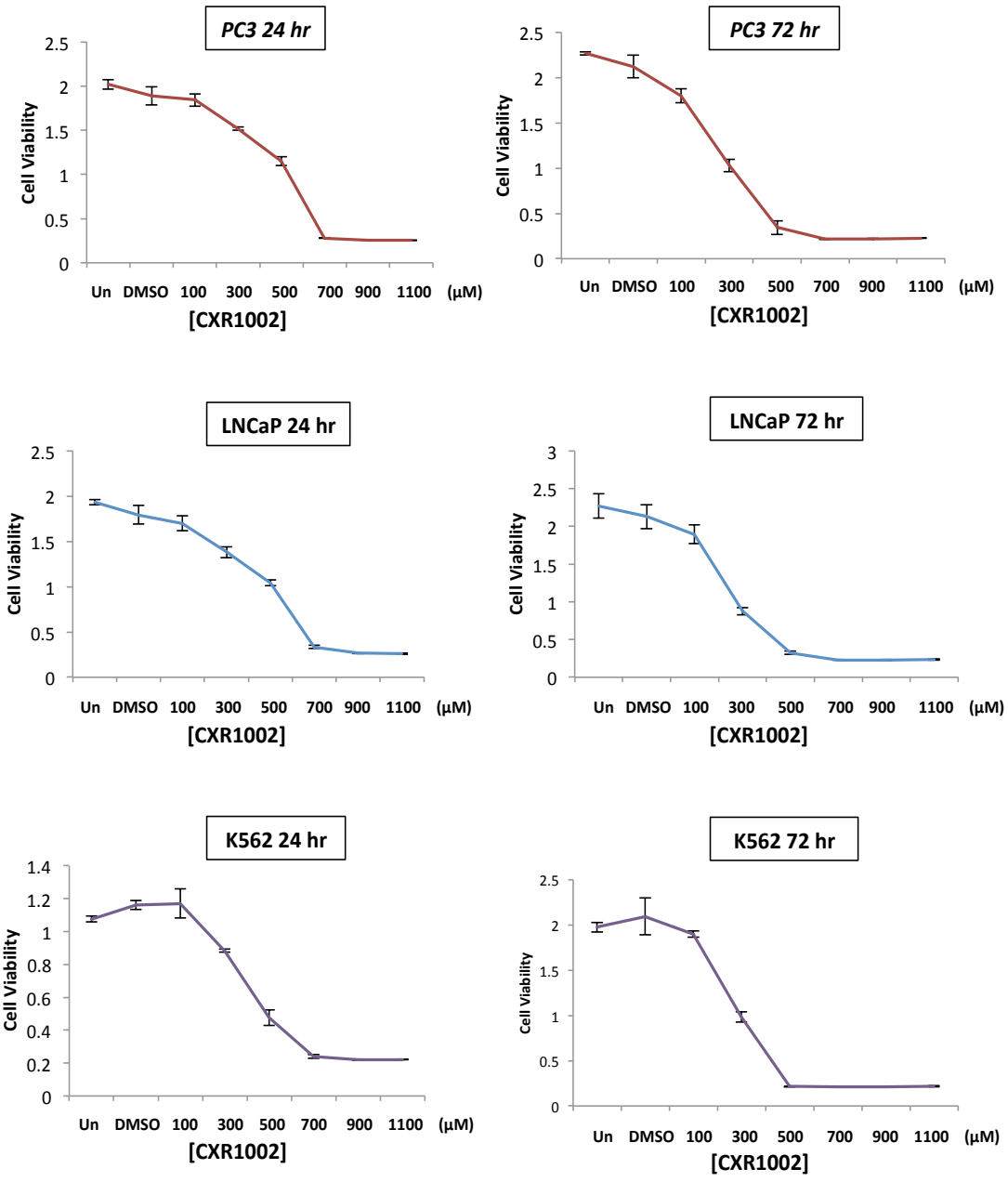

Figure 2 Cell viability following CXR1002 treatment

LNCaP, PC3 and K562 cells were plated in 96 well plates for 24 hours prior to addition of the indicated drug concentrations for 24 or 72 hours. Cell viability was measured using MTS assay kit from Promega as per manufacturer's instructions. The optical density, which is directly proportional to cell viability, was measured at 490 nm and plotted on a graph.

A3. Inhibition of PIM1 kinase *in vitro*

As a proof of concept, *in vitro* kinase assays were performed to test direct inhibition of PIM1 by CXR1002 and SGI-1776. Kinase assays were carried out using recombinant Histone H3.3 as a substrate, and phosphorylation of H3.3 at Ser10 was used as a read-out for PIM1 kinase activity by western blotting. Negative control reactions containing no kinase or no substrate, and appropriate DMSO controls were also set up. Based on the killing curves, I chose two arbitrary concentrations of SGI-1776 and CXR1002 in the assay. As shown in figure 3A, Histone H3.3 phosphorylation was observed only in the presence of WT PIM1, and not in its absence. SGI-1776, a known ATP-competitive inhibitor of PIM1, decreased phosphorylation of Histone H3.3 at both 10 μM and 20 μM final concentration. Phosphorylation was decreased at 320 μM CXR1002, but completely abolished at 700 μM.

Since the assay worked as expected, I adapted it into a more quantitative 96-well plate based assay, and measured PIM1 activity in response to increasing drug concentrations *in vitro*. For this I used the ADP-Glo kinase assay (Promega), which is explained in figure 4. The procedure has been described in section A2 experimental methods, and the results are shown in figure 3B (SGI-1776) and 3C (CXR-1002). The concentration of SGI-1776 used in this assay was in the range of 0.625 μM to 5 μM, and that of CXR1002 was in the range of 1.36 μM to 350 μM. Both drugs showed a dose dependent decrease in kinase assays. Again, SGI-1776 was significantly more potent than CXR1002.

Since the ADP-Glo kinase assay is designed to test small molecular inhibitors, I wanted to test if CXR1002 affected the components of this assay. To do this, different ratios of ATP and ADP (supplied in the kit) were incubated with or without 350 μM CXR1002, and the assay was performed as described. The results shown in figure 5 indicate that CXR1002 does not significantly affect the assay, and therefore the results obtained in figure 3C were a true representation of the inhibition of PIM1 by CXR1002.

The results presented here indicate that while CXR1002 can indeed inhibit activity of PIM1 *in vitro,* the use of such high concentrations of CXR1002 even in *in vitro* assays would suggest that it not a very specific inhibitor of PIM kinases. Also, the mode of inhibition may be different to that of SGI-1776 (ATP competitive).

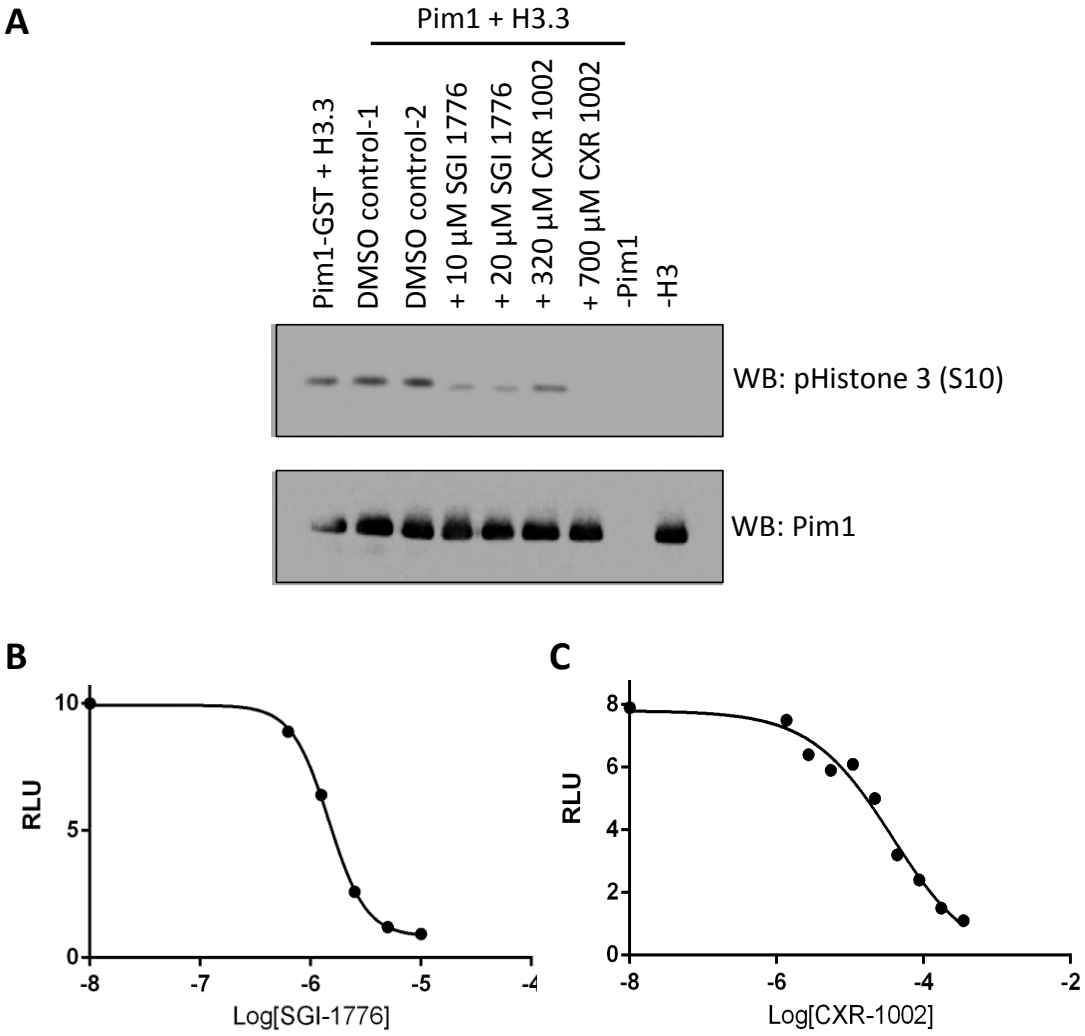

Figure 3 Inhibition of PIM1 kinase activity

(A) *In vitro* kinase assays were carried out using Histone H3.3 as substrate and GST-PIM1, in the absence or presence of SGI-1776 and CXR1002. After completion the reactions were resolved by SDS-PAGE and western blotting was performed using phospho Ser10 Histone H3 antibody as a read out for PIM kinase activity. **(B)** ADP-Glo kinase assay was performed to measure inhibition of PIM1 kinase activity in response to increasing concentrations of SGI-1776 or **(C)** CXR1002.

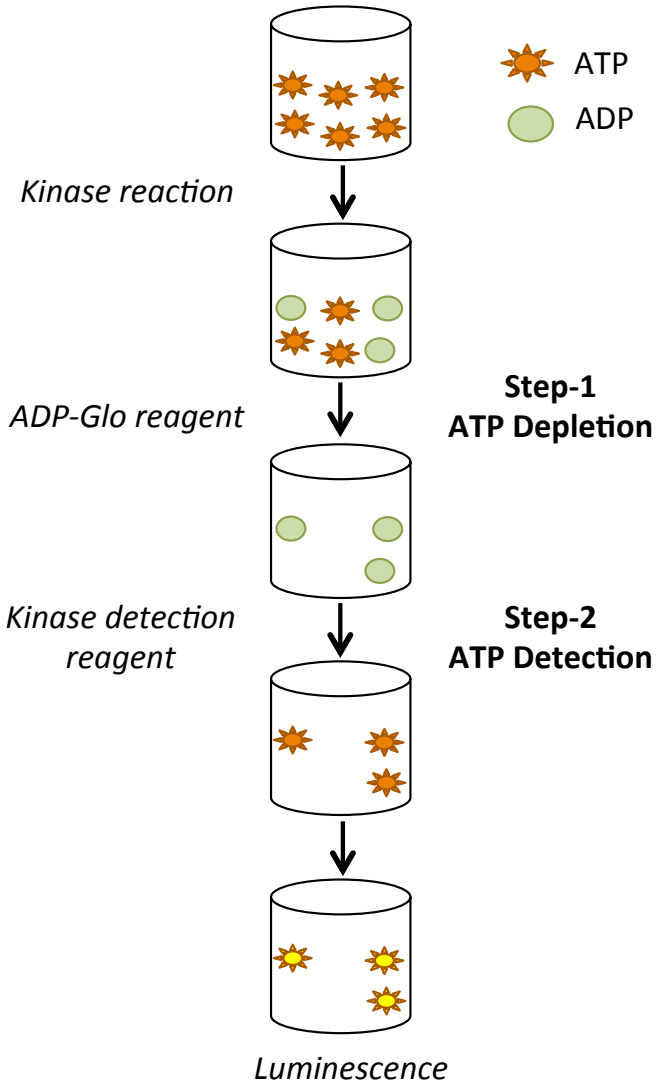

Figure 4 Principle of ADP-Glo kinase assay (Adapted from ADP-Glo kinase assay manual, Promega)

Kinase assays are set up in 96-well white-bottom plates using ATP supplied with the kit. After the kinase reaction has occurred, the ADP-Glo reagent is added to terminate the reaction, and to deplete the remaining ATP. In the second step, the Kinase detection reagent is added to convert the ADP to ATP, and allow the newly synthesises ATP to be measured using a luciferase/luciferin reaction. The light generated (in the form of luminescence) correlates to the amount to ADP generated in the kinase reaction, which is indicative of kinase activity.

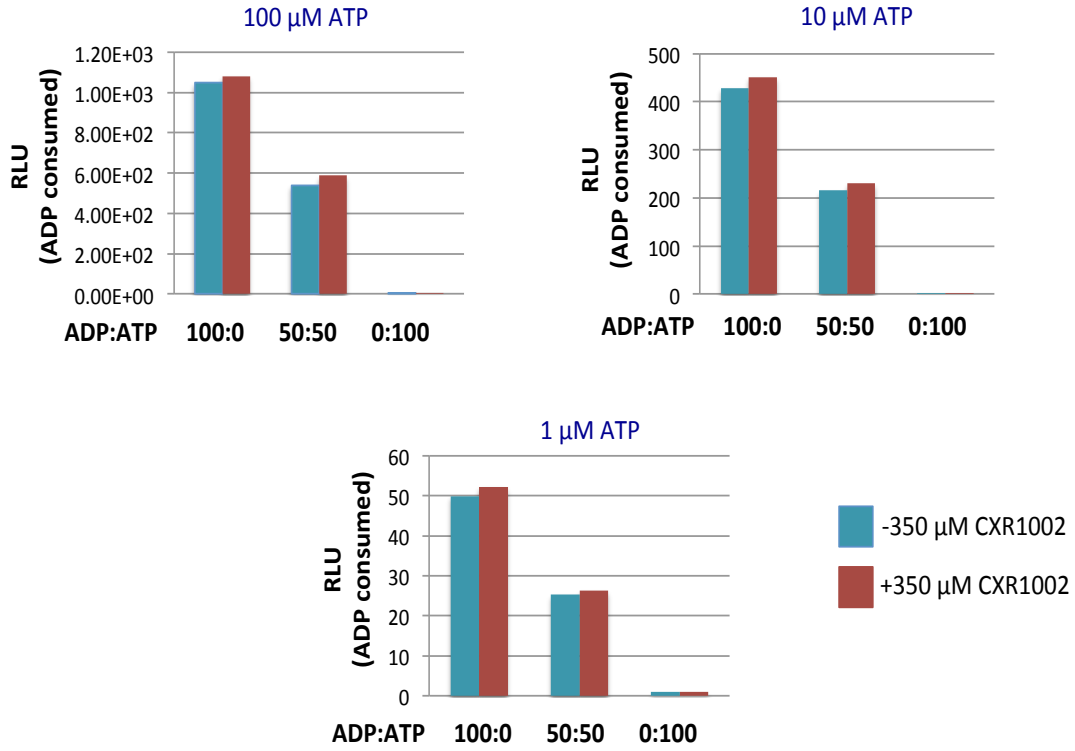

Figure 5 CXR1002 does not affect the components of the ADP-Glo kinase assay

ATP and ADP were combined in the indicated ratios at 1, 10 and 100 µM concentrations, with or without CXR1002. ADP-Glo kinase assay was performed as per manufacturer's instructions, and luminescence was measured using a luminometer.